UNIVERSITY OF NOTTINGHAM

SCHOOL OF CIVIL ENGINEERING

LINEAR AND NON-LINEAR VISCOELASTIC BEHAVIOUR OF BINDERS AND ASPHALTS

By

Behzad Rahimzadeh, BSc, MSc, MIAT, MIHT

Thesis submitted to the University of Nottingham

For the degree of Doctor of Philosophy

March 2002

To Mana

ACKNOWLEDGEMENTS

I would like to acknowledge my sincere thanks for all those who have supported, advised and assisted me in developing my knowledge and understanding on the subject that I was researching.

I would like to express my gratitude to my supervisor Dr G.D. Airey for his friendly, encouraging and expert guidance throughout my research wok. Thanks are also due to my co-supervisor Dr A.C. Collop for his constructive criticism and technical advice. Special thanks are due to Professor S.F. Brown, my co-supervisor and the leader of the Pavements and Geotechnics group, for his technical advice and encouragement.

A particular dept of gratitude is due to Mr. Barry Brodrick for his remarkable assistance in the experimental work. Thanks are also due to all those technicians who helped me in experimental work; in particular, the names of Shane Malkin, Andy Leyko and Mick Winfield should be mentioned.

I would like to thank all who have assisted me in some way but have not been specially mentioned above.

Finally, I would like to thank my wife for her unending patience and support throughout the period of my study at the University of Nottingham.

DECLARATION

The research described in this thesis was conducted at the University of Nottingham, School of Civil Engineering between January 1999 and March 2002. I declare that this dissertation is the result of my own original work and no part of the work has been, or is currently being submitted for any degree, diploma or other qualifications.

B Rahimzadeh
University of Nottingham
March 2002

ABSTRACT

In order to predict the engineering performance of a material, it is necessary to understand its stress/strain behaviour. This is usually accomplished by means of laboratory tests under controlled stress or controlled strain conditions. As bituminous materials are viscoelastic in nature, their performance must be characterised with test methods and analytical techniques that account for time (or rate) of loading and temperature. In addition, it is usually advisable to confine the characterisation of a bitumen to its linear viscoelastic (LVE) response (small strains) to simplify the mathematical modelling of the material, as non-linear response, particularly for viscoelastic materials, is extremely difficult to characterise in the laboratory and model in practical engineering problems.

This thesis describes research into the linearity limits of various unmodified (penetration grade) and modified (both process modification and polymer modification) bitumens as well as the linearity limits of asphalt mixtures incorporating these binders. The linearity limits for the binders have been determined by means of stress sweeps at various temperatures and frequencies using a dynamic shear rheometer (DSR). The linearity limits and dynamic mechanical properties of the conventional and modified asphalt mixtures have been determined by means of a purpose built dynamic, direct tension-compression, servo-hydraulic testing apparatus.

The linearity results show that for sensibly engineered modified binders (softer base bitumens with higher modifier contents) there is no significant narrowing of the linear range. The process modified, plastomeric (EVA PMB) and conventional binders show a strain dependent LVE criterion between 2% and 6% at low temperatures (high stiffness and intermediate to low phase angles) as well as a stress dependent LVE criterion between 1.5 and 7 kPa at high temperatures (low stiffness and high phase angles). The thermoplastic rubbers (SBS PMBs) show, in addition to the low temperature strain criterion, a high temperature (low stiffness) polymeric-based strain dependent LVE criterion between 50% and 150%.

The asphalt mixtures studied in this thesis consisted of dense bitumen macadam (DBM), hot rolled asphalt (HRA) and HRA mortar mixtures with conventional 50 pen bitumen, radial and linear SBS PMBs, EVA PMB and multigrade bitumen. Cylindrical specimens of the mixtures were subjected to sinusoidal loading conditions at temperatures between 10 and 40°C under stress sweep conditions. The results indicate that the linearity limits of behaviour for the asphalt mixtures are strain dependent and found to be between 20 and 100 microstrain for the DBM and HRA mixtures and between 50 and 150 microstrain for the HRA mortars.

Additionally, upon establishing the LVE limit, the viscoelastic properties of the bitumens and asphalt mixtures, in their linear region, were evaluated by means of frequency sweep tests at various temperatures and frequencies. The results show that, in the low frequency region (high temperatures), the rheological behaviour of the SBS PMBs differs from that of the other bitumens. The DBM and HRA mixtures all show very similar rheological characteristics over the temperature and frequency range used in this study. With regard to the HRA mortars, due to their higher binder and air void volumetric proportions, their stiffness values tend to be approximately half that of the DBM and HRA mixtures.

Finally, the relationship between binder and mixture stiffness was investigated in the linear viscoelastic region, for different unmodified and modified binders and asphalt mixtures. Measured asphalt mixture stiffness was compared with selected empirical and theoretical mixture stiffness prediction methods. In general, the bitumen to mixture complex modulus relationship was independent of temperature. However, although a straight line could be established for the EVA PMB and linear SBS PMB binders, the results show that the binder to mixture stiffness relationship exhibits temperature dependence for mixtures produced with these two binders. The results show that there are large differences between the stiffness predicted by the empirical and theoretical methods and those measured experimentally.

TABLE OF CONTENTS

LIST OF FIGURES

LIST OF TABLES

Chapter 1

INTRODUCTION

1.1 Background

Domination of road transport over other forms of land transport due to the flexibility to collect and deliver at low costs has led to a great upsurge in traffic volumes and road building activities both in the UK and abroad. In addition, due to increasing weights, volumes of traffic using the roads and the complex gear configurations of trucks, it has become necessary to pay more attention to the methods of design and use a more realistic and rational assessment of pavement material behaviour, particularly in terms of dynamic stress-strain responses.

The application of a pavement design approach depends upon the knowledge of three factors:

- The stresses and strains, which exist in the structure under working conditions,
- A knowledge of the behaviour of the construction materials, and
- The design criteria, such as design life, failure mechanisms of the pavement, etc.

Considerable research is currently being performed on the three aspects mentioned above. However, understanding of the stress-strain behaviour of road materials is an important factor, which aids engineers in the design of roads.

Bitumen is widely used as a binder in the construction of pavements in the UK and throughout the world. Bitumen is a viscoelastic material, meaning that its response under a given condition of stress or strain depends not only upon the current state of stress or strain, but also upon its loading history. In more practical terms, this also means that the mechanical response of viscoelastic materials is both time and temperature dependent. Therefore bitumen performance must be characterised with test methods and analytical techniques that account for time (or rate) of loading and temperature.

Bitumen is used primarily in the production of asphalt paving mixtures. Asphalt is the natural and artificial mixture of bitumen and mineral matter. Natural asphalt is formed once the unstable components of crude oils have evaporated upon nearing the ground surface, with the residue seeping through the splits of the porous rock and being mixed with mineral matter. The term “asphalt mixture” is used for artificial mixtures made of bitumen and mineral matter, e.g., sand asphalt, asphalt concrete, sheet asphalt, asphalt macadam and mastic asphalt. The relationship between bitumen and asphalt is similar to that found between cement and concrete [110]. As asphalt mixtures are viscoelastic materials like bitumen, their response under load also depends on the rate of loading and temperature. Although the bitumen is the component having the lowest concentration in an asphalt paving mixture, its characteristics are those which predominantly influence the properties and the performance of the mixture as a whole.

A variety of experimental methods exist for characterising viscoelastic materials such as bitumens and asphalt mixtures. One of the most common techniques is dynamic mechanical analysis (DMA), which involves the application of a sinusoidal stress or strain and the measurements and analysis of the resulting response. Instruments for making such measurements are becoming increasingly practical for use in routine characterisation and even for specification testing of bitumens and related materials. DMA began to be commonly used as a research tool for evaluating viscoelastic materials in the 1960’s. Several researchers presented papers in the late 1960’s and early 1970’s on the DMA of asphalt mixtures [43, 44, 63]. This technique represents a great improvement over traditional, empirical tests in terms of both the quality and quantity of information gathered.

1.2 Linear Viscoelastic Limits of Bituminous Materials

Calculating the critical stresses and strains in the various layers of a pavement is one of the most important components of asphalt pavement design as this ensures that stresses and strains do not exceed permissible values for the material being used. Asphalt pavements have traditionally been designed using elastic theories of pavement behaviour as this is the simplest and easiest form of analysis. However it is desirable to use viscoelastic methods of analysis to assist in the design of asphalt

pavements. In keeping with the desire for simplicity, it would seem appropriate to define the limits of the applicability of linear viscoelastic theory to design before adding the complication of non-linear theory. In general, bituminous materials display non-linear stress/strain behaviour with a decrease in stiffness modulus with increasing stress amplitude. The non-linearity generally becomes negligible at small strains where the behaviour can be approximated as linear. In addition, it is usually advisable to confine the characterisation of a bitumen to its linear viscoelastic response (small strains) to simplify the mathematical modelling of the material, as non-linear response, particularly for viscoelastic materials, is extremely difficult to characterise in the laboratory and model in practical engineering problems. However, conditional to understanding the applicability of linear theory to pavement design is the knowledge of the extent of the linear viscoelastic domain of asphalt mixtures [71].

There are three important reasons why the linear viscoelastic regions of bitumen and asphalt mixtures need to be defined. Firstly, in keeping with the desire for simplicity, it would seem appropriate to define the limits of applicability of linear viscoelastic theory to the design of asphalt mixtures before adding the complications of a non-linear theory. Secondly, in order to find correlations between bitumen and asphalt mixture rheology it is necessary to study both bitumens and asphalt mixtures in the same domain. Finally, as the viscoelastic parameters of complex modulus, phase angle, storage modulus and loss modulus are all defined under linear viscoelastic (LVE) conditions, it is vital that rheological measurements are undertaken within the LVE region of response. Within the LVE region, the relationship between stress and strain is influenced only by temperature and loading time (frequency) and not by the magnitude of the stress or strain [47]. In addition, methods of characterisation and analysis, such as the generation of master curves by means of the time-temperature superposition principle (TTSP), rely on the linearity of the rheological viscoelastic data [26].

1.3 Objectives of the Research

This research is concerned with the use of dynamic mechanical testing to investigate the linear and non-linear viscoelastic behaviour of unmodified and modified binders and asphalt mixtures. The main objectives are to:

- Define the linear limits of various unmodified (penetration grade) and modified (both process modification and polymer modification) bitumens under various temperature and loading time conditions.
- Investigate the linearity limits of different conventional and modified asphalt mixtures at different rate of loading and temperature. This part of the research involves the development of a dynamic, direct tension-compression, servo-hydraulic testing apparatus in order to carry out uniaxial tension-compression testing of asphalt mixtures.
- Evaluate the rheological properties of the conventional and modified bitumens and asphalt mixtures at intermediate and high temperatures in their linear viscoelastic region over a wide range of frequencies.
- Investigate the relationship between the measured stiffnesses of binders and asphalt mixtures in their linear region.
- Review selected empirical and theoretical binder to mixture stiffness relationships and compare the mixture stiffness predicted by these models to mixture stiffness measured by experimental methods.

1.4 Scope

The experimental work undertaken in this research has been divided into two main parts: bitumen testing and asphalt mixture testing.

Five different unmodified and modified bituminous binders were selected for this investigation. The bitumens was tested in both their unaged and short term aged conditions. As oxidative ageing and loss of volatiles occurs during asphalt mixture preparation and since one of the objectives of this research was to study the relationship between the rheological properties of bitumen and asphalt mixtures, it was decided to test all bitumens after subjecting them to short-term ageing. To simulate short-term ageing, all the binders were aged using the Rolling Thin Film Oven Test (RTFOT). In addition, the 50 pen bitumen and radial SBS PMB were studied in both their unaged and aged conditions to compare the results for these two situations. Dynamic mechanical tests were performed using a Bohlin stress controlled Dynamic Shear Rheometer (DSR) with parallel plate configuration in an oscillatory shear mode. Tests were conducted in two stages:

- Stress sweep tests, and
- Frequency sweep tests.

Prior to performing frequency sweeps, stress sweep tests were performed to establish the linear viscoelastic range of bitumens. To establish the linear range, stress sweeps were performed at different temperatures and frequencies. After completing the stress sweep tests and establishing the target stresses for the linear region, frequency sweeps for a range of temperatures and frequencies were performed on all the samples.

The asphalt mixture experimental phase consisted of testing five DBM, two HRA and two HRA mortar mixtures. In order to study the effects of different bitumen types on asphalt mixture behaviour, asphalt mixtures were produced using different unmodified and modified bitumens. The goal of these tests was to determine the viscoelastic linear region and the rheological parameters of these mixtures at different temperatures and frequencies. The test procedure consisted of mounting the test specimens in a temperature controlled room and allowing them to stand for at least eight hours at the required temperature. At the end of this period, specimens were subjected to axial sinusoidal stresses at a range of amplitudes at different temperatures and frequencies, whilst monitoring the resulting axial strains for the calculation of complex modulus and phase angle. In a similar manner to bitumen testing, tests were conducted in two stages:

- Stress sweep tests, and
- Frequency sweep tests.

To establish the linear range for each asphalt mixture, stress sweep tests were performed at different temperatures and frequencies. After completing the stress sweep testing and establishing the target stresses for the linear region, frequency sweep tests at different temperatures and frequencies were performed on all the samples.

1.5 Organisation of Thesis

This thesis is comprised of eight chapters as demonstrated in Figure 1.1. These chapters have been arranged and are presented in the following order:

Justification of the need for more attention to the methods of design and material characterisation used in road construction, the development of bituminous materials and mechanical properties of bitumens and asphalt mixtures, the objectives and scope of thesis are presented in Chapter One.

Chapter Two consists of an extensive literature review, which is comprised of five parts. The first part concerns a review of the behaviour of viscoelastic materials and an overview of linear viscoelastic theory. Bitumen rheology, different test methods for studying the rheological properties of bitumens, and the contribution of bitumen in resisting pavement failures are explained in the second part of this chapter. The third part of this chapter describes the properties of modified bitumens, specifically different kinds of modifiers especially polymers. The rheology of asphalt mixtures, dynamic characterisation of asphalt mixtures and factors affecting the dynamic modulus of asphalt mixtures are evaluated in the fourth part of this chapter. The fifth part explains the different empirical and theoretical binder to mixture stiffness relationships. The linear and non-linear limits of the viscoelastic behaviour of bitumen and asphalt mixtures and the relationship between bitumen and asphalt mixture rheology are described in the last part of this chapter.

The stress/strain DSR limitations and sample preparation methods are described in Chapter Three. The first part is aimed at studying the limitations of the DSR. A large number of tests at different strain levels and temperatures were carried out to accurately define the limitations of this machine. The second part is concerned with the influence of different sample preparation methods on the rheological parameters measured with the DSR, particularly the repeatability of the results.

Chapter Four deals with the bitumen testing process and analysis of results. This chapter consists of three main parts. The first part deals with the material investigation and testing procedure. The investigation of the linear limit of the different unmodified

and modified bitumens is presented in the second part of this chapter. The last part details the frequency sweep testing in the linear region to detect the rheological properties of the different bitumens in their linear region.

The asphalt mixture testing process and analysis of results are presented in Chapter Five. This chapter consists of four main parts. The first part describes the material investigation, manufacturing of specimens and testing procedures. The development of a hydraulic testing equipment for dynamic tension-compression testing is presented in second part. The investigation of the linear viscoelastic limits of different unmodified and modified asphalt mixtures is explained in the third part of this chapter. The last part is concerned with frequency sweep testing of mixtures in their linear region to evaluate the rheological behaviour of different mixtures in their linear region.

Chapter Six concerns the relationship between the dynamic testing parameters of bitumens and asphalt mixtures. This chapter aims to investigate the relationship between the rheological properties of different unmodified and modified binders and asphalt mixtures.

Chapter Seven describes different models used to determine the relationship between the stiffness of bitumen and asphalt mixtures as well as a comparison of their predicted stiffnesses with experimental results.

The main significant findings of this research and recommendations for future work are presented in Chapter Eight.

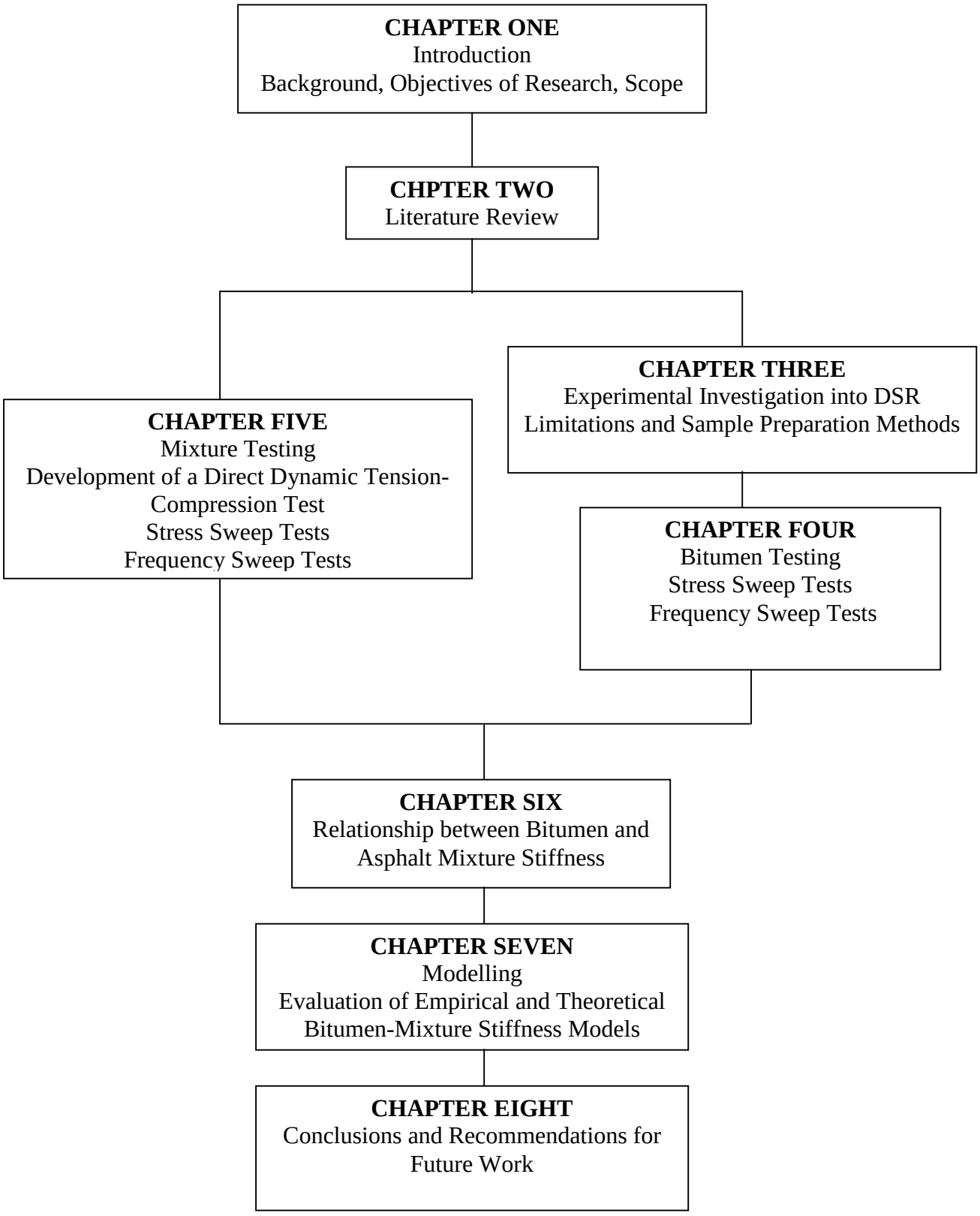

Figure 1.1: Schematic of the Organisation of the Thesis

Chapter 2

LITERATURE REVIEW

2.1 Introduction

This chapter summarises the principal findings from a review of selected literature concerning the rheological characteristics of bitumen and asphalt mixtures. This literature review comprises five sections. The first section is concerned with bitumen rheology with regard to its definition and the different methods of measurement. In order to understand the behaviour of viscoelastic materials such as bitumen, an overview of linear viscoelastic theory is also presented in this section. The review gives a brief description of stress relaxation, creep and dynamic response of viscoelastic materials. In addition, the most commonly used conventional tests, such as penetration and softening point, and new physical properties tests, such as the dynamic shear rheometer (DSR) and the bending beam rheometer (BBR) for the measurement of bitumen rheology, are described in this section. Different data presentation methods, such as isothermal and isochronal plots, the contribution of bitumens in resisting pavement failures, such as rutting, fatigue cracking and thermal cracking, and bitumen ageing are also included.

The second section of the literature review deals with bitumen modification. This section aims to describe the reasons for modification, introduce different types of modified bitumens, especially polymer modified bitumens (PMBs), and describe the stability of modified bitumens.

The rheological behaviour of asphalt mixtures is described in the third section. The review gives a brief description of the dynamic characterisation of asphalt mixtures with particular emphasis on the dynamic modulus of mixtures. The fundamentals of the complex modulus test and factors affecting the dynamic modulus of asphalt mixtures are explained in this section.

The fourth section of this review deals with the evaluation of the relationship between bitumen and asphalt mixture stiffness. Selected empirical and theoretical relationships between binder and mixture stiffness are reviewed and evaluated in this section.

The final section discusses the linear and non-linear viscoelastic behaviour of bitumen and asphalt mixtures. The review gives a brief description of non-linear behaviour and the importance of finding the linear viscoelastic region of these materials. Also, the different methods of defining the linear viscoelastic limit (LVE) and determining this limit are explained in this section.

2.2 Bitumen Rheology

Rheology is the study of material flow and deformation characteristics. In other words, rheology is the study of the relationship between stress and strain of materials. If a load is applied to a purely elastic material, the deformation produced will return to zero immediately after the removal of the stress. For a purely viscous material deformation increases as long as a stress is applied but this deformation remains at its maximum after removing the stress. However, for a viscoelastic material such as bitumen, part of the deformation is recovered while part remains after removing the stress. The viscoelastic properties of bitumen are therefore a combination of those found for purely elastic and purely viscous materials. Prior to any attempt to characterise the behaviour of the bitumen, a thorough understanding of the structure and properties of its components is necessary.

2.2.1 Origin of Bitumen

Many thousand of years before crude oil exploration and its industrial processing began, the numerous advantages of bitumen had already been recognised. The production of this material started with the use of natural deposits of bitumen. Examples of natural deposits are the Trinidad Lake deposits on the Island of Trinidad, Bermudas Lake deposits and the tar sands throughout western Canada [89]. In the middle of the 19th century, the importance of natural bitumen consumption increased, for example, attempts were made to utilise rock asphalt from European deposits for road surfacing [110]. At the end of the 19th century major uses of bitumen were

introduced in different parts of the industry, e.g. road construction [110]. Consequently, there was a dramatic increase in bitumen demand with the result that natural deposits could not provide enough bitumen. Hence, the manufacture of bitumen from crude oil developed.

Bitumen is the residue of certain crude oils after the removal of the volatile components [114]. The formation of natural bitumen and that produced by the distillation of crude oil are similar. However, the production of bitumen obtained by distillation is quicker, although it requires higher production temperatures. Nowadays, bitumen used in road construction is generally manufactured from refined crude oil. There are about 1500 different crude oils produced throughout the world but only a few of these are suitable for the manufacture of bitumen [110]. The main sources of crude oil are the United States, the Middle East, the countries around the Caribbean and the countries of the former Soviet Union [110].

2.2.2 Bitumen Constitution

Because of the different constitutions of crude oils, bitumen obtained from them contains various hydrocarbons and hydrocarbon groups in different proportions. This is influenced, even in the case of a given crude oil, by the bitumen production methods [114].

Bitumen is basically composed of hydrocarbon molecules, along with small percentages of sulphur, nitrogen and oxygen. The last three elements are called heteroatoms and may have considerable effect on bitumen properties. In addition to heteroatoms, some heavy metals such as nickel and vanadium may exist in very small amounts [57].

Bitumen consists of a large variety of molecular structures. Therefore, a thorough identification and classification of all these structures is an extremely difficult task. As an alternative, the bitumen constituents can be classified on polarity and solubility. On this basis, bitumen is comprised of three fractions:

- Asphaltenes,

- Resins, and
- Oils (aromatics and saturates).

Asphaltenes are highly polar, high molecular weight hydrocarbons surrounded by moderately polar aromatic molecules and dispersed in a continuous non-polar oily phase. Resins are semi-solid fractions acting as a peptising agent, which keep the asphaltene molecules from coagulation [66]. The proportion of resins to asphaltenes governs to a degree the solution (SOL) or gelatinous (GEL) type character of the bitumen (see Figure 2.1). Aromatics, which consist of the lowest molecular weight naphthenic aromatic compounds in the bitumen, present the major proportion of the dispersion medium for the peptised asphaltenes [110]. They consist of non-polar carbon chains in which unsaturated ring systems dominate, and they have a high dissolving ability for other high molecular weight hydrocarbons. Saturates comprise straight and branch-chain aliphatic hydrocarbons, together with alkylnaphthenes and some alkyl-aromatics. They are non-polar viscous oils, which are white in colour [110]. A schematic representation of the molecular structure of the different bitumen components is shown in Figure 2.2.

To conclude, asphaltenes constitute the body of the bitumen, aromatics affect the adhesive and ductile properties, and saturates and resins influence the viscosity and flow [57].

2.2.3 Models of Bitumen Microstructure

The colloidal model is a traditional model of bitumen behaviour, which was first proposed by Nellensteyn in the 1920's [77], and later elaborated upon by Pfeiffer and others [86]. The basic premise of this model is that colloidal micelles, consisting of moderately polar molecules surrounding highly polar asphaltenes, are dispersed throughout a continuous, non-polar phase [19]. In this model, the asphaltenes, which are the highest molecular weight components, are dispersed in the lower molecular weight maltenes (i.e. aromatics, saturates, resins). According to this model, the rheology of bitumen can be greatly affected by the degree of effectiveness to which the resins can keep the asphaltene fraction dispersed in the maltene oil fraction. Bitumens containing highly peptised asphaltenes generally exhibit Newtonian

behaviour, while non-Newtonian flow is usually the characteristic of bitumens with lower amounts of dispersed asphaltenes [89]. Furthermore, the physical properties of bitumen are a function of the relative proportion of these fractions. In general, the colloidal construction of bitumen depends on the following factors [114]:

- Chemical nature and percentage quantity of the asphaltenes,
- Chemical character and percentage quantity of the maltenes, and
- Temperature of the system.

As mentioned previously, bitumen can be classified as SOL bitumens (fluid type) and GEL bitumens (structured type) on the basis of the extent of micelle dissolution. Figure 2.1 shows the schematic of these two colloidal types. If the maltenes contain a sufficient amount of aromatics/resins relative to the quantity and quality of the asphaltenes, a SOL structure will be formed, whereas with a low aromatic/resin content a GEL structure will result. Thus the colloidal constitution of bitumen does not only depend on the quantity of the asphaltenes.

Temperature affects the degree to which the asphaltenes are dissolved in the oily maltene medium. Increasing the temperature results in a greater dissolution with the GEL structure being changed into a SOL structure, whereas decreasing the temperature results in the opposite rheological properties becoming dominant. Therefore, it can be concluded that the colloidal constitution determines the rheological properties of the bitumen to a great extent. The colloidal constitution also causes bitumens, which are solid at room temperature to become liquid at high temperatures.

It is known that liquids, which obey Newton’s Law are termed Newtonian or normal liquids [114]. For normal liquids the rate of deformation as a consequence of the force of gravity remains constant. However, this correlation is not valid for non-Newtonian liquids. Most bitumens exhibit these non-Newtonian material properties at room temperature because of their colloidal structure. However, at higher temperatures bitumen also behaves as a Newtonian liquid.

Another model for bitumen microstructure which, has recently been suggested [19], is the dispersed polar fluid (DPF) model, which accounts for some important features of the viscoelastic behaviour of bitumen. According to this model, molecules of varying size and polar functionality are continuously distributed in a fluid phase. Interaction of the molecules through various levels and types of bonding is considered to be the source of the viscoelastic nature of bitumen.

2.2.4 The Viscoelastic Nature of Bitumens

Bitumens are viscoelastic materials. Behaviour of these materials therefore combines two parts: elastic behaviour and viscous behaviour. Materials with elastic behaviour return to their initial state after removal of the applied loads, whereas permanent deformations remain under applied loads under viscous behaviour. Several factors affect the behaviour of viscoelastic materials in terms of their elastic and viscous behaviour. Temperature is the most critical of these parameters. Viscoelastic materials have more elastic behaviour at low temperatures, whereas they behave more viscously at high temperatures. The second parameter, which has an effect on viscoelastic materials, is loading time or rate of loading. Bitumen behaves like an elastic solid at high rates of loading, whereas it behaves as a viscous liquid at long times of loading. Therefore, to conclude, at a fixed temperature, long times of loading correspond to high temperature behaviour (more viscous) and at short loading times the response shifts to low temperature behaviour (more elastic). Bitumen, therefore, exhibits high stiffness and brittleness at short times of loading, whereas it is linked with high ductility and exhibits low stiffness at long loading times [63].

The two most commonly used methods of determining viscoelastic properties are:

- Transient methods, e.g. creep loading, stress relaxation, and constant rate of loading, and
- Dynamic (oscillatory) test methods.

Dynamic (oscillatory) testing is generally considered the more appropriate technique as it covers a wide range of loading in a relatively short testing time to give a wide range of properties [22].

Based on standard creep testing, the viscoelastic behaviour of bitumen is represented in Figure 2.3. It can be seen from this figure that bitumen has three regions of behaviour: elastic, delayed elastic and viscous. There are non-recoverable deformations after loading in the viscous portion of the response. The elastic response dominates at low temperatures or short loading times, whereas at long loading times or high temperatures the viscous response dominates. However, at intermediate loading times and temperatures, the delayed elastic response dominates. It should be noted that because of changes in the relative magnitude of these three components, the shape of the creep curve (see Figure 2.3) changes at different loading times and test temperatures [19].

2.2.5 Overview of Linear Viscoelastic Theory

The response of a linear elastic material is not time dependent. In other words, if a constant load is suddenly applied to it, it will deform immediately, maintain a constant deformation and return to its initial shape after the removal of the load. However, in a viscous material, according to Newton's law, stress is time dependent and is directly proportional to the rate of strain but independent of strain itself [47].

The behaviour of linear viscoelastic materials combine both linear elastic and linear viscous behaviour. If a constant strain is applied to this material, the stress, which is required to maintain this deformation, decreases gradually or relaxes. Also, when a constant stress is applied, deformation increases slowly with time or creeps. Under oscillatory testing, the stress in a viscoelastic material is not exactly in phase with strain (pure elastic solid), and also not 90° out of phase with strain (pure viscous fluid) but is between these two extremes. The difference between linear viscoelastic and non-linear viscoelastic materials is that in linear viscoelastic materials the ratio of stress and strain is a function of time (or frequency) and temperature but not of stress magnitude.

A cubical element of linear viscoelastic material, which deforms under simple shear, is shown in Figure 2.4. The shear stress at time t can be calculated from the following equation [47]:

$$\tau_{21}(t)=\int_{-\infty}^{t} G(t-t')\dot{\gamma}_{21}(t')dt' \quad \textbf{(2.1)}$$

Where: G (t) = relaxation modulus

$\dot{\gamma}_{21}$ = the rate of strain (shear rate)

$= \partial\gamma_{21} / \partial t$

This integration is performed from time t' to current time *t*.

The following equation can also be used for calculating strain in terms of stress [47]:

$$\gamma_{21}(t) = \int_{-\infty}^{t} J(t-t')\dot{\tau}_{21}(t')dt' \quad \textbf{(2.2)}$$

Where: $\tau^{\bullet}_{21}$ = rate of stress

$= d\tau_{21} / dt$

J(t) = creep compliance

As mentioned previously, the viscoelastic behaviour of bitumen can be characterised by transient or dynamic response. Stress relaxation and creep are two important types of transient response.

2.2.5.1 Stress Relaxation

Stress relaxation can be explained by sudden strain being applied to bitumen over a very short period of time λ. As shown in Figure 2.5, shear strain and stress reach a maximum value after the loading time of λ but while the strain remains constant, shear stress begins to decrease. Shear stress can be calculated from the following equation:

$$\tau(t) = \gamma \times G(t) \quad \textbf{(2.3)}$$

Where G(t) is the relaxation modulus. The relaxation modulus is a time-dependence parameter in the linear region but it is a function of both time and stress magnitude, G (t,τ), in the non-linear range of response.

2.2.5.2 Creep Response

Creep can be explained by a sudden stress being applied to bitumen. Creep after sudden stress is the opposite of stress relaxation after sudden strain [47]. In a stress relaxation test, stress decreases for constant strain, whereas in creep, strain increases at constant stress (Figure 2.6). Shear strain, which is a function of time, can be calculated from the following equation:

$$\gamma(t)=\tau\times J(t) \qquad \textbf{(2.4)}$$

Where J(t) is the creep compliance, which is a function of time. In the non-linear range of response, the creep compliance is a function of both time and stress magnitude, i.e., J = J (t,τ). For a purely elastic solid J = 1/G but for a viscoelastic material J(t) ≠ 1/G(t) because there is a phase difference between stress and strain in these materials [47].

2.2.5.3 Dynamic Response

Dynamic mechanical analysis is the most widely used method for characterising viscoelastic behaviour. Dynamic (oscillatory) tests may be performed in stress controlled or strain controlled modes. In stress controlled testing, a sinusoidal stress is applied to the sample and the resultant strain is monitored with time, whereas in strain controlled testing a sinusoidal strain is applied to the sample and the resultant stress is monitored with time. When considering tests in the controlled strain mode, applied strain is calculated according to the following equation:

$$\gamma = \gamma_{\max} \sin \omega t \qquad \textbf{(2.5)}$$

Where: $\omega = 2\pi f$,

f = the frequency of the sinusoidal strain (Hz), and

γ_{max} = the amplitude of strain.

Differentiating equation 2.5 results in the following equation:

$$\dot{\gamma} = \omega \gamma_{max} \cos \omega t \quad \textbf{(2.6)}$$

Stress can be calculated from Equation 2.1 by replacing $t–t'$ by s. Therefore we have:

$$\tau(t) = \int_0^\infty G(s)\omega\gamma_{max} \cos[\omega(t-s)]ds \quad \textbf{(2.7)}$$

$$=\gamma_{max}[\omega\int_0^\infty G(s)\sin\omega s \quad ds]\sin\omega t+\gamma_{max}[\omega\int_0^\infty G(s)\cos\omega s ds]\cos\omega t \quad \textbf{(2.8)}$$

Replacing first bracket with $G'(\omega)$ and second bracket with $G''(\omega)$ we have:

$$\tau=\gamma_{max}(G'(\omega)\sin\omega t+G''(\omega)\cos\omega t) \quad \textbf{(2.9)}$$

$G'(\omega)$ and $G''(\omega)$ are two frequency dependent functions, termed the shear storage modulus and the shear loss modulus respectively.

As mentioned previously, the behaviour of viscoelastic materials, such as bitumen, falls between ideal elastic solid behaviour and ideal viscous fluid response. Therefore, the maximum stress, which is a function of ω, has a phase difference, δ, between 0° and 90° ahead of the peak applied strain (see Figure 2.7). Therefore, the resultant stress is calculated using the following equation:

$$\tau=\tau_{max}\sin(\omega t+\delta)=\tau_{max}\cos\delta\sin\omega t+\tau_{max}\sin\delta\cos\omega t \quad \textbf{(2.10)}$$

By combining equations 2.9 and 2.10, we obtain:

$$G'(\omega)=(\tau_{max}/\gamma_{max})\cos\delta \quad \textbf{(2.11)}$$

$$G''(\omega) = (\tau_{max}/\gamma_{max})\sin\delta \quad \textbf{(2.12)}$$

Stress can also be expressed as a complex quantity with modulus being expressed according to the following formula:

$$\tau^*/\gamma^* = G^*(\omega) = G' + iG'' \quad \textbf{(2.13)}$$

Where: τ^* = dynamic oscillatory shear stress,

γ^* = dynamic oscillatory shear strain, and

$G^*(\omega)$ = complex shear modulus.

Comparison of equations 2.11, 2.12, and 2.13 shows that:

$$G^* = G' + iG'' = \tau_{\max}/\gamma_{\max}\cos\delta + i\tau_{\max}/\gamma_{\max}\sin\delta = \tau_{\max}/\gamma_{\max}e^{i\delta} \quad \textbf{(2.14)}$$

Furthermore, the absolute value of complex modulus can be computed as follows:

$$\left|G^*(\omega)\right| = \tau_{\max}/\gamma_{\max} = \sqrt{(G')^2 + (G'')^2} \quad \textbf{(2.15)}$$

Comparison of equations 2.11, 2.12, and 2.15 shows that:

$$G' = \left|G^*\right|\cos\delta \quad \textbf{(2.16)}$$

$$G'' = \left|G^*\right|\sin\delta \quad \textbf{(2.17)}$$

Therefore, it can be concluded that the shear storage modulus is the in-phase component of $\left|G^*\right|$ and the shear loss modulus is the out-of-phase component of $\left|G^*\right|$.

If the same equations are expressed for complex compliance, the following equations are derived [47]:

$$J^*(\omega) = \gamma^*/\tau^* = J' - iJ'' \quad \textbf{(2.18)}$$

$$\left|J^*(\omega)\right| = \gamma_{max}/\tau_{max} = \sqrt{(J')^2 + (J'')^2} \quad \textbf{(2.19)}$$

Where: J* = the complex compliance,

J′ = the storage compliance, and

J″ = the loss compliance.

The relationship between these parameters is shown in Figure 2.8.

2.2.6 Conversion of Viscoelastic Functions

The ability to convert a viscoelastic function from one form to another is extremely useful. The following approximate equation is one of the simplest equations, which can be used to convert shear modulus to an uniaxial modulus for bitumen. This equation is based on the assumption that the Poisson's ratio is 0.5 [40].

$$E^*(\omega) = 3G^*(\omega) \quad \textbf{(2.20)}$$

Where: E*(ω) = the uniaxial complex modulus, and

G*(ω) = the shear complex modulus.

The same equation can be used for calculating the uniaxial creep compliance, D (t), from the shear creep compliance, J (t) [40].

$$D(t) = J(t)/3 \quad \textbf{(2.21)}$$

Other important conversions are the equations, which are used for converting creep stiffness parameters to dynamic complex modulus parameters. Van der Poel [104] defined the following equation for direct conversion between creep compliance and dynamic complex modulus:

$$G^*(\omega) \approx 1/J(t) \qquad t \rightarrow 1/\omega \quad \textbf{(2.22)}$$

This means that the dynamic complex modulus at a frequency of 1/t equals the inverse of the creep compliance at time t.

The following equations can be used for direct conversion between the storage/loss compliance and the storage/loss modulus [47]:

$$J' = \frac{G'}{(G'^2 + G''^2)} = \frac{1/G'}{1 + \tan^2 \delta} \quad \textbf{(2.23)}$$

$$J'' = \frac{G''}{(G'^2 + G''^2)} = \frac{1/G''}{1 + (\tan^2 \delta)^{-1}} \quad \textbf{(2.24)}$$

$$G' = \frac{J'}{(J'^2 + J''^2)} = \frac{1/J'}{1 + \tan^2 \delta} \quad \textbf{(2.25)}$$

$$G'' = \frac{J''}{(J'^2 + J''^2)} = \frac{1/J''}{1 + (\tan^2 \delta)^{-1}} \quad \textbf{(2.26)}$$

In these equations, $\tan\delta = G''/G' = J''/J'$, is termed the loss tangent, which can be expressed as the ratio of energy lost to energy stored in a deformation cycle. To conclude, these methods of converting are approximate, however in most cases they are accurate enough for engineering calculations.

2.2.7 Conventional Bitumen Physical Property Tests

There are several conventional tests, which have been developed for the quality evaluation of manufactured bitumens. These test methods are standardised in individual countries, e.g., UK, USA and Germany. However, the methods commonly used to evaluate bitumens are practically identical, with negligible differences. Consistency tests are one of the main types of conventional tests.

2.2.7.1 Consistency Tests

Consistency describes the degree of fluidity of bitumen at any particular temperature. Since bitumen is a thermoplastic material, its consistency varies with temperature. Therefore, if comparisons are to be made for different bitumens, it is necessary to measure the consistency of bitumen at the same temperature and shear loading condition [89].

A strictly empirical measure of consistency of bitumen is the penetration test. According to BS 2000 Part 49 [5], penetration is defined as the distance a standard needle loaded with a 100 g weight will penetrate into a bitumen sample for 5 seconds. The test is usually performed at 25ºC, however, other temperatures with different needle loads and penetration times may be used as well.

The absolute or dynamic viscosity is another consistency test, which is measured in accordance with ASTM D 2171 [3], using a U-shaped capillary tube viscometer. Bitumen at a temperature of 60ºC is poured into the large tube of the viscometer and rises in the capillary tube under application of a vacuum. The measured time of flow between two successive timing marks on the capillary tube is multiplied by the calibration factor of the viscometer to yield the viscosity of bitumen in units of poises (1 Pa.s = 10 P). Absolute viscosity provides the basis for a widely used bitumen grading system. Based on the viscosity grading system, paving grade bitumens are classified into six groups of AC-2.5, AC-5, AC-10, AC-20, AC-30 and AC-40, where the numbers refer to the viscosity of the original binder in units of 100 poises.

Another consistency test is the kinematic viscosity test. According to ASTM D 2170 [2], the kinematic viscosity test is performed at 135ºC. A cross-armed viscometer is used and bitumen flows in the capillary tube due to gravity rather than vacuum application. Other than this, the procedure is similar to the absolute viscosity test. Kinematic viscosity is usually defined in units of centistoke (1 mm^2/s = 1 centistoke).

Softening point is also an empirical test, which is performed in accordance with BS 2000 part 58 [6]. It measures a temperature at which the bitumen phase changes from

semi-solid to liquid. At the softening point temperature, the bitumen sample placed in a brass ring, can no longer support the weight of a steel ball, and consequently flows.

2.2.7.2 Problems of Conventional Bitumen Characterisation

The viscoelastic behaviour of bitumen is too complicated to be described by simple traditional measures of consistency such as penetration and softening point. For example, although viscosity at 60ºC and 135ºC is a fundamental rheological parameter, it is not capable of characterising the response with respect to varying shear rates, loading times and temperatures. Therefore, nowadays new methods, such as dynamic mechanical analysis, are needed to provide rheological data on bitumens.

The need for complete characterisation of bitumen has long been recognised. However, since bitumen is a complicated material in comparison with other viscoelastic materials used for construction purposes, study of the rheological properties of bitumen is not an easy task. Furthermore, the use of rheological test equipment is expensive and complicated. With respect to these difficulties many bitumen researchers have tried to find simple methods of measuring bitumen properties. Therefore, a large number of properties and parameters have been discovered and related to different indications of pavement performance. These properties, or parameters, may be divided into three main groups [23]:

- Empirical single point measurements,
- Viscosity measures, and
- Susceptibility parameters.

Penetration, ductility and softening point are three important empirical single point measurements, which have been used to evaluate bitumen properties and relate them to pavement performance. However these parameters can be misleading because of the following reasons:

Firstly, the empirical nature of these parameters means that they cannot be expressed in terms of engineering units and therefore, the complete rheological characteristics of bitumen cannot be directly related to these parameters. Secondly, they do not give an

indication of the viscoelastic nature of the bitumen at the test temperature or its time dependency. Finally, these measurements do not have the flexibility to be undertaken at different loading modes, at different loading rates and even different temperatures [23].

As mentioned above, another conventional parameter is absolute viscosity. The coefficient of viscosity is the ratio of shear stress to shear rate. This parameter is a fundamental measure of Newtonian fluids whose properties are independent of strain rate or stress level. Although, bitumens exhibit Newtonian behaviour at high temperatures (generally above their softening point temperatures) or at very low shear rates, they are non-Newtonian at lower temperatures (in-service temperatures) or short loading times (traffic loading times). Therefore, bitumen cannot be described at low temperatures or short loading times by the absolute viscosity parameter [23]. Moreover, this parameter is not suitable for describing the rheological characteristics of PMBs as their behaviour is generally non-Newtonian.

Many researchers have proposed viscoelastic parameters that may, in some ways, describe a range of properties within the time-temperature domain [23]. Susceptibility parameters are one group of these parameters. One particular susceptibility parameter is temperature susceptibility. There are several temperature susceptibility parameters, which are different in terms of the type of consistency measurement used and the range of temperatures covered [36]. Changing of penetration with temperature is one of these parameters, which has been used to calculate different temperature susceptibilities, for example, the temperature which is required to change penetration by a certain amount and the slope of the logarithmic plot of penetration versus temperature [23]. Changing of viscosity as a function of temperature is the second parameter, which has been used to calculate temperature susceptibility, for example, the logarithmic change of viscosity with temperature or logarithm of temperature. Other parameters, which have been used to describe temperature susceptibility, are combinations of different empirical measurements for example, penetration, softening point, and viscosity. Two well known parameters of this type are the penetration-viscosity number (PVN) [72], and the penetration index (PI) [104]. Although, these parameters give an indication of temperature susceptibility, they may be misleading. The reason for this is that they are calculated from empirical measurements and

therefore, have the same problems referred to above of not including time dependency. This can have a significant effect on the reliability of these parameters as the rheological properties of bitumen depend on both time and temperature.

In short, these problems have resulted in new rheological parameters being introduced, which have been shown to be fundamentally sound and able to represent bitumen rheological behaviour [23].

2.2.8 Moving from Conventional to Fundamental Tests

In the past, refineries used the direct distillation method in one or two stages to manufacture bitumen from crude oil. The crude oil supply was consistent and consequently, the chemical composition of bitumen, which affects the properties and performance of bitumen, did not change much. This meant that traditional test methods gave a reasonable indication of performance of the bitumen in service. However, with increasing variation of crude sources, variety of processes used in different refineries, increasing numbers of refineries and the use of additives and modifiers, the properties of bitumen are affected by other factors other than the crude oil source and its chemical composition. Therefore to predict performance, the use of tests which are directly related to the stress and deformation of asphalt in service are necessary.

There are two ways to achieve this aim: direct tests and indirect tests. A simulative test such as Wheel Tracking is used as a direct test. The weakness of direct tests is the difficulty to scale all the factors, which have an effect on performance. In indirect tests, a number of fundamental properties are measured and then related to the required performance aspect by a combination of theory and practice. An advantage of the fundamental approach is the separation of the problems of measurement techniques from the problem of relating measurements to performance, with the possibility of up-grading both aspects [58].

2.2.9 New Test Methods for Studying the Rheological Properties of Bitumens

The study of the physical properties of bitumens, which are related to pavement performance, and the methods to reliably measure these properties have been one of the main objectives of bitumen researchers. However, there is still significant uncertainty regarding bitumen properties and which of these properties can more reliably be related to pavement performance. This uncertainty is because of the complex behaviour of bitumen and the empirical nature of the test methods used for measuring bitumen properties. Therefore, new test methods were introduced to measure more fundamental properties, which can be related to pavement performance. These test methods can be divided into two parts [19]:

- New physical properties tests that are fundamental in nature and can be related to the critical distress mechanisms and field performance through rational models. These new test methods include the DSR, the BBR and the direct tension test (DTT).
- Ageing tests, which can produce aged materials with hardness and rheological characteristics similar to that of field-aged material. These test methods include short and long-term ageing.

These new test methods produce new parameters, which are more related to the fundamental properties of bitumens, for example, complex shear modulus (G*), phase angle (δ), creep stiffness S(t), logarithmic creep rate m(t), and failure strain ε_f.

2.2.10 Dynamic Shear Rheometer Testing

Dynamic shear rheometers are used to study the dynamic characterisation of the rheological behaviour of bitumen. In this test, bitumen is sandwiched between two parallel plates, which can be rotated at different frequencies (Figure 2.9) [53]. Since, the DSR only takes two measurements, namely torque and angular rotation, all the results (e.g. strain, G* and η*) are calculated from these measurements. The following equations are used for calculating strain and stress in this instrument [17, 54]:

$$\gamma = \frac{\theta R}{h} \quad \textbf{(2.27)}$$

Where: γ = strain

θ = angular rotation

R = radius of plate (mm)

h = gap between plates (mm)

$$\tau = \frac{2T}{\pi R^3} \quad \textbf{(2.28)}$$

Where: τ = stress

T = torque value measured by equipment

Therefore, from the calculation of strain and stress, the absolute complex modulus can be calculated according to the following formula:

$$\left|G^*(\omega)\right| = \frac{\tau_{\max}}{\gamma_{\max}} \quad \textbf{(2.29)}$$

DSR testing can be conducted in several modes, such as [58]:

- constant stress mode,
- stress viscometry mode,
- stress sweep mode, and
- oscillatory mode.

The oscillatory mode is the most useful mode for studying the dynamic characteristics of bitumens. In this mode of testing, the parallel plates are rotated in a sinusoidal manner with respect to each other. This test can be done in stress-controlled or strain-controlled mode. In the stress-controlled mode, the sinusoidal stress with constant amplitude is applied to the sample, whereas in the strain-controlled mode the

amplitude of sinusoidal strain applied to sample is constant. Dynamic (oscillatory) shear measurements with DSR testing are shown in Figure 2.9.

Dynamic shear tests offer the advantage that measurements can be made at different frequencies and temperatures. Therefore, as a large amount of data is generated, presentation of these results is very important. For this purpose different plots, which may contain one or more parameters, can be generated, for example, stiffness modulus or phase angle versus temperature or frequency.

2.2.10.1 Isochronal Plots

An isochronal plot is simply a plot of some viscoelastic function, such as complex modulus, versus temperature at a constant frequency or loading time. Therefore, viscoelastic data can be presented over a range of temperatures at a given frequency using an isochronal plot. The simplest benefit of isochronal plots is the comparison of complex modulus or phase angle at different temperatures. Moreover, several properties of bitumens, such as temperature susceptibility, can be interpreted from this type of plot.

Temperature susceptibility, which is often a major performance criterion for bitumens, may be defined as the change in consistency, stiffness or viscosity, as a function of temperature. Temperature susceptibility should be based on measurements at different temperatures but similar loading times as the rheological properties of bitumens are a function of both time and temperature. The general shape of an isochronal plot at a constant frequency is shown in Figure 2.10.

2.2.10.2 Isothermal Plots and Master Curves

An isothermal plot is simply a plot of some viscoelastic function, such as complex modulus or phase angle, versus loading time or frequency (see Figure 2.11). In this plot, viscoelastic data, at a given temperature, is plotted over a range of frequencies or loading times. Therefore, this plot can be used to compare different viscoelastic functions at different loading times at a constant temperature. In addition, it can be used to study the time dependency of materials. However, the rheological properties of bitumen cannot be presented over an extremely wide range of loading times or

frequencies because DSR testing is usually only undertaken over a limited frequency range. Therefore, master curves are used to extend the data over a wider range of loading times. Master curves allow the representation of rheological measurements such as complex modulus or phase angle at frequencies or temperatures, which cannot be attained by the test instrument. Master curves therefore reflect the time dependency of bitumen over a wide range of loading times, e.g. values of complex modulus or phase angle at a few thousandths of a second or several years of loading time. Time-temperature superposition is used over a range of temperatures and frequencies in the construction of a master curve [19, 40, 58]. At first, a reference temperature is selected and then the data at all other temperatures is shifted horizontally with respect to time to produce a single smooth curve. The shifting is done by using the shift factor, a(T), which varies for each test temperature. Master curves can be constructed manually using a graph-drawing program or spreadsheet. The construction of a master curve using shift factors is shown in Figure 2.12.

As shown in Figure 2.13, four parameters can be calculated from the master curve [19, 40]:

- The glassy modulus, G_g, which is the value of complex modulus at very high frequencies (short loading times) or low temperatures and for most bitumens in shear loading is very near to 1 GPa. The glassy modulus can also be calculated by plotting the complex modulus versus phase angle. The modulus at which phase angle is zero (found by extrapolation) is the glassy modulus.
- The steady-state viscosity, $\eta^*(\omega)$, which is approximately the dynamic viscosity as the phase angle approaches 90°.
- The crossover frequency, $\omega_\circ$, which is defined as a frequency at a given temperature where the storage modulus equals the loss modulus ($\tan \delta = 1$). As shown in Figure 2.13, it can be approximately defined using the master curve as the point at which the viscous asymptote crosses the glassy modulus.
- The rheological index, R, as shown at Figure 2.13, is the difference between the glassy modulus and the dynamic complex modulus at the crossover frequency.

According to Figure 2.13, the linear viscoelastic response of a bitumen can be classified into three zones of behaviour:

- Low temperatures or short loading times (high frequencies), where bitumen behaves as an elastic solid and shear stiffness approaches 1 GPa (glassy region),
- Intermediate temperatures or loading times, where bitumen gradually changes from elastic behaviour to fluid behaviour. Within this transition region, behaviour of bitumen is composed of both elastic and viscous responses, and
- High temperatures or long loading times (low frequencies), where bitumen behaves as a viscous fluid.

2.2.10.3 Mathematical Models for Shift Factors

The temperature dependency of the viscoelastic behaviour of bitumens can be indicated by shift factors, a(T) [19, 44]. Two equation are used for representing shift factors:

- The Williams-Landel-Ferry (WLF) equation [112]
- An Arrhenius function [19, 40]

The WLF function, which has been widely used for bitumens, is defined as follows:

$$\log a(T) = \frac{-C_1(T - T_d)}{(C_2 + T - T_d)} \qquad \textbf{(2.30)}$$

Where: a(T) = horizontal shift factor

T = the select temperature, °C

T_d = the defining temperature, °C

C_1, C_2 = empirical constants

The difficulty in using the above equation is to find the defining temperature. Schmidt et al [95] proposed that the defining temperature can be related to the glass transition temperature, T_g. However, Anderson et al [19] state that the use of the glass transition

temperature should be avoided because it is often associated with a dilatometric measurement.

Williams et al [112] proposed that if the defining temperature, T_d is suitably chosen for each material then C_1 and C_2 could be allotted universal values of 8.86 and 101.6 respectively. However, according to the analysis of shift factors for the SHRP bitumens by Anderson et al [19, 40], the constants C_1 and C_2 were found to be -19 and 92.

The shift factor can also be determined using the following Arrhenius function:

$$\log a(T) = \frac{\Delta H_a}{2.303R}\left(\frac{1}{T} - \frac{1}{T_d}\right) \qquad \textbf{(2.31)}$$

Where: a(T) = horizontal shift factor

ΔH = activation energy, typically 250 kJ/mol

R = the ideal gas constant, 8.34 J/°K-mol

T = the select temperature, °K

T_d = the defined temperature, °K

2.2.10.4 Black Diagrams

A black diagram is simply a plot of complex modulus versus phase angle obtained from a dynamic test [9, 58]. Therefore, viscoelastic data is plotted over wide range of temperatures and frequencies using the black diagram. Measurement errors, changes in composition, or variations in bitumen structure can cause deviations within the black diagram. This plot is therefore very useful for presenting the effect of ageing or modification of bitumens.

2.2.10.5 Factors Affecting Results of DSR Testing

Although, the DSR is a good instrument to determine the rheological properties of bitumens, many factors may affect the accuracy of the results. These factors can be divided into three parts [37]:

- Factors related to the instrument, e.g., temperature control system and calibration,
- Factors related to test performance, e.g., sample geometry, sample preparation and operator training, and
- Factors related to the properties of bitumen, e.g., non-linear viscoelastic properties of bitumen.

The temperature control system is one of the most important factors, which affects the accuracy of the results. The reason for this is that bitumen is highly temperature susceptible and small changes in temperature cause significant changes in the results. Therefore, the temperature of the sample must be accurately controlled and also the temperature of whole sample should be constant during testing. Using a circulating fluid can provide these conditions. In this temperature control system, the sample, top plate and bottom plate are immersed in a fluid, e.g., water, which is circulated by a pump.

Calibration of temperature and torque in the DSR at regular intervals is essential to maintain reasonable repeatability and reproducibility of rheological data [101]. The major source of error in the results from DSR tests is due to differences in rheometers, such as, model, manufacture, stress or strain control, and the medium used for temperature control (i.e., fluid or air) [45]. The difference in instruments leads to differences in calibration procedures and verification standards. Therefore, it is necessary to use a standard fluid for verifying the calibration of rheometers. Most DSR manufacturers carry out measurements of displacement and applied torque and confirm such calibrations with measurements in steady shear on a standard fluid [37]. The problem with using this standard liquid is that it has low viscosity in comparison with bitumen. Therefore, it can be misleading when measuring high bitumen stiffness.

Sample geometry is another factor, which affects the testing results of the DSR. Plate diameter and gap setting are two factors, which affect sample geometry. Carswell et al [37] showed that increasing the gap (sample height) reduces the problem of gap setting but the effect is still significant, causing lower than expected complex modulus values as phase angles tend to zero. Also reducing the diameter of the plate to 8 mm improves the results but, even with a combination of reduced plate diameter and

increased sample height (1 mm), it does not appear possible to measure the limiting elastic stiffness of 10^9 Pa [37].

Non-linear properties of bitumen can affect the test results at high levels of strain. Although, rheological measurements are independent of strain at low levels of strain, rheological parameters are a function of strain at high levels of strain, for example, complex modulus reduces with increasing strain within the non-linear region.

2.2.11 Bending Beam Rheometer Testing

The BBR is used for direct measurements of the rheological properties of bitumen at the lowest pavement temperatures. Rheological properties of bitumens play a major role in controlling low temperature thermal cracking of bitumens. The basic requirements for studying the properties of bitumens at low temperatures are the ability to measure response as a function of loading time at the lowest range of pavement temperatures between -50°C and 0°C [22].

As mentioned previously, loading time dependency of bitumens can be measured in several modes but is classified into two main types: dynamic (oscillatory) and transient. Creep loading, stress relaxation and constant rate of loading are some examples of the transient type. The BBR is used in the creep mode. In this mode, the operation of the rheometer is simple, practical and less expensive than oscillation type testing.

Three loading modes can be used for the creep mode including: shear, extensional (tension or compression) or bending. Shear mode was excluded because it is not similar to the loading mode found in the field that leads to thermal cracking and also bitumens are too stiff at low temperatures to be directly sheared in relatively thin films. The extensional mode requires gripping of binder specimens, which is difficult because of the tendency of binders to flow. However, the bending mode does not require handling and samples are free of any fixtures.

Fluid circulating baths have been used for temperature control in the BBR test because they provide faster thermal conduction than air to ensure thermal stability and uniformity.

2.2.11.1 Components and Operation of the BBR

The BBR has three main components (see Figure 2.14):

- Testing frame unit,
- Temperature-controlled bath, and
- Circulator and data acquisition system using a personal computer.

According to Figure 2.14, the components of the testing frame include: a loading frame, specimen supports, an air bearing-pneumatic piston loading unit and a loading shaft. One load cell and a linear variable differential transformer (LVDT), which have been connected to a data acquisition system, are used for measuring load and displacement. Using the air bearing system, load is applied to a supported beam specimen, submerged in the fluid (alcohol).

A rectangular bitumen specimen is used as the test sample in this test. The dimensions of this specimen are 127 mm long, 12.7 mm wide and 6.3 mm thick with a testing span of 102 mm. This specimen requires approximately 15 grams of bitumen. As shown in Figure 2.15 aluminium moulds made of three stock bars are generally used for making the specimen. Polyethylene strips (0.1 mm thick) are used to cover the inner sides of the mould to isolate the bitumen from the aluminium bars. Two rubber O-rings are used at the two ends to assemble the mould.

Elementary bending theory is used to calculate the creep stiffness. Maximum deflection of a beam with loading in the centre of the span can be calculated according to the following process:

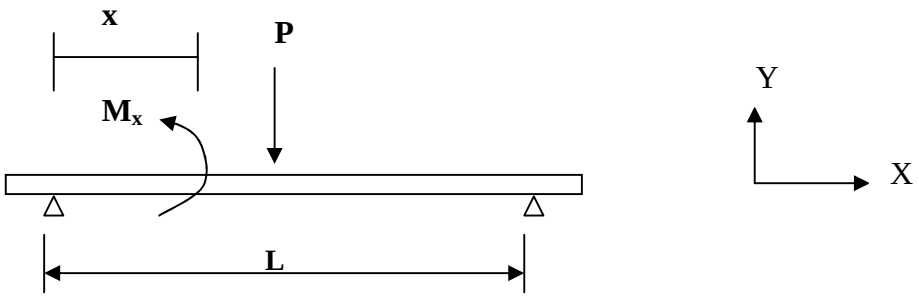

We have: $$EIy''=M_x=\frac{p}{2}x \quad \textbf{(2.32)}$$

$$EIy''=\frac{P}{2}x\Rightarrow EIy'=\frac{Px^2}{4}+C_1\Rightarrow EIy=\frac{Px^3}{12}+C_1x+C_2 \quad \textbf{(2.33)}$$

Where:

$$at \quad x=0 \quad y=0 \quad and \quad at \quad x=l/2 \quad y'=0 \quad \textbf{(2.34)}$$

Therefore:

$$C_2 = 0 \qquad \text{and} \qquad C_1 = -Pl^2/16 \quad \textbf{(2.35)}$$

And:

$$EIy=\frac{Px^3}{12}-\frac{Pl^2x}{16} \quad \textbf{(2.36)}$$

The maximum deflection is in the middle of beam therefore:

$$at \quad x=l/2 \quad y_{\max}=\frac{Pl^3}{96EI}-\frac{Pl^3}{48EI} \quad \textbf{(2.37)}$$

Therefore:

$$\delta=-\frac{Pl^3}{48EI} \quad \textbf{(2.38)}$$

In this formula, E is the modulus of elasticity and I is the moment of inertia of the section which is calculated according to following formula:

$$I = \frac{bh^3}{12} \quad \textbf{(2.39)}$$

Where: b = width of beam
h = depth of beam

According to the elastic-viscoelastic correspondence principle, it can be assumed that if a viscoelastic beam is subject to loads that are all applied simultaneously at time t = 0 and held constant, the stress distribution is the same as that in an elastic beam under the same load [48]. The strain and displacement depend on loading time and can be calculated from equation 2.38 by replacing the modulus of elasticity (E) with the creep stiffness (S(t)) and δ with δ(t) (time dependent displacement). Therefore the time dependent flexural creep stiffness is calculated from the following equation:

$$S(t) = \frac{Pl^3}{4bh^3\delta(t)} \quad \textbf{(2.40)}$$

Where: S(t) = creep stiffness at t
δ(t) = measured deflection at t
P = applied load at midspan

2.2.11.2 Factors Affecting Results of BBR Testing

There are three critical factors, which affect low temperature measurements using the BBR:

- Time and temperature dependency,
- Physical hardening at low temperatures, and
- Load level.

The effects of time and temperature on deflection are shown in Figure 2.16. It can be seen from this figure that deflection increases dramatically with increased temperature and loading time. The best loading time, which was selected for BBR testing, is 240 seconds [22]. This time gives enough data for the time-temperature superposition procedure.

Bitumens, at low temperatures, exhibit a hardening phenomenon similar to that termed physical ageing for polymers and other types of amorphous solids. The phenomenon is caused by delayed volume shrinkage and driven by the metastable structural state, which results in significant time-dependent hardening [22]. This phenomenon, which is different from oxidative ageing, is called physical hardening [22]. Physical hardening is the increase in S(t) and decrease of creep rate, m(t), as a result of time-dependent volume shrinkage of bitumen. The influence of physical hardening on flexural creep deflection is shown in Figure 2.17. In this figure, samples from one kind of bitumen have been tested at the same temperature but each sample has been held at this temperature for different times. It can be seen from this figure that deflection decreases dramatically with increasing isothermal age. This is because of the physical hardening of bitumen at low temperatures.

The load level, which is applied to the bitumen, is another important factor in BBR testing. The applied load should be within the linear viscoelastic region of the bitumen as the rheological characterisation with the BBR is based on the assumption of linear behaviour of the bitumen. The creep stiffness is independent of the stress level in the linear region. In this region stress and strain at the mid-span can be calculated according to following equations:

$$\sigma_{(t)} = \frac{3Pl}{2bh^2} \qquad \textbf{(2.41)}$$

$$\varepsilon_{(t)} = \frac{6\delta_{(t)}h}{l^2} \qquad \textbf{(2.42)}$$

Inputting the dimensions of the sample and the span length of 102 mm, stress and strain can be calculated from the following equations:

$$\sigma_{(t)} = 297.6P \quad \textbf{(2.43)}$$

$$\varepsilon_{(t)} = 0.003691\delta_{(t)} \quad \textbf{(2.44)}$$

Using these equations, stress and strain can be calculated for different load levels and the linear limit can be found by plotting stress against strain. Bahia and Anderson [22] showed that the load level is not a critical factor within the LVE region of bitumen behaviour. Considering other factors such as the weight of the loading shaft, the resolution of typical low cost load cells, and possible experimental variability, a load of 100 g was selected as a standard testing load [22].

2.2.12 Contribution of Bitumens to Resist Pavement Failures

Three failure modes were identified as critical pavement distress modes in which bitumen plays an important role: rutting, fatigue cracking, and thermal cracking [23]. The aim of the new measurements of bitumen properties using new test methods, such as the rotational viscometer, the DSR, the BBR and the direct tension test, is to address these distress modes.

2.2.12.1 Contribution of Bitumens to Permanent Deformation Resistance

Permanent deformation of flexible pavements is a result of accumulated plastic deformation, which is caused by repeated application of loads [18, 23, 96]. Rutting occurs primarily at intermediate and high temperatures, where bitumen behaviour is more viscous resulting in non-recoverable deformation. Although, the aggregate properties have an important role in rutting resistance, the contribution of the bituminous binder cannot be ignored.

Rutting can be investigated by considering the energy dissipated as plastic deformation occurs during each cycle of loading under stress-controlled conditions. Therefore, the energy dissipated should be minimised for minimum rutting. The energy dissipated can be calculated from the following equation [23, 96]:

$$W_c = \pi.\tau_\circ.\varepsilon_\circ.\sin\delta \qquad \textbf{(2.45)}$$

Where: W_c = energy dissipated

$\tau_\circ$ = maximum stress amplitude

$\varepsilon_\circ$ = maximum strain amplitude

δ = phase angle

Strain can be calculated from the following equation in the stress-controlled mode:

$$\varepsilon_\circ = \frac{\tau_\circ}{G^*} \qquad \textbf{(2.46)}$$

Comparing equations 2.45 and 2.46, we have:

$$W_c = \pi\tau_\circ{}^2\left[\frac{1}{G^*/\sin(\delta)}\right] \qquad \textbf{(2.47)}$$

It can be seen from this formula that if $G^*/\sin(\delta)$ increases, energy dissipation decreases. In the other words, rutting decreases with increasing $G^*/\sin(\delta)$.

Bouldin [31] related loss compliance to the total accumulated deformation by the following equation:

$$\frac{1}{J''} = \frac{\tau_\circ}{y_{acc}} = \frac{G^*}{\sin(\delta)} \qquad \textbf{(2.48)}$$

Where: y_{acc} = accumulated strain

J'' = loss compliance

As shown in this equation, increasing $G^*/\sin(\delta)$ results in a decrease in loss compliance.

2.2.12.2 Contribution of Bitumens to Fatigue Cracking Resistance

Fatigue cracking relates to fracture of the pavement, which occurs under repeated traffic loading with magnitudes far less than the materials fracture strength [96]. Fatigue cracking can occur in thick pavement layers, which can be modelled by a controlled-stress condition or it can occur in thin pavement layers, which can be modelled by a controlled-strain condition [25]. The current criterion for fatigue cracking in the Superpave binder specification is based on a measure of total dissipated energy, which is energy expended in propagating cracks in the pavement [91]. The dissipated energy or work per cycle for controlled-strain cyclic loading can be calculated according to the following equation [18, 23, 96]:

$$W_c = \pi.\tau_\circ.\varepsilon_\circ.\sin(\delta) \qquad \textbf{(2.49)}$$

Where: W_c = energy dissipated

$\tau_\circ$ = maximum stress amplitude

$\varepsilon_\circ$ = maximum strain amplitude

δ = phase angle

Stress, strain and complex modulus are related together by the following equation:

$$\tau_\circ = \varepsilon_\circ G^* \qquad \textbf{(2.50)}$$

Combining equations 2.49 and 2.50, we have:

$$W_c = \pi.\varepsilon_\circ^{\,2}.[G^* \times \sin(\delta)] \qquad \textbf{(2.51)}$$

According to this formula, energy dissipation decreases with decreasing loss modulus ($G^* \times \sin(\delta)$) with a subsequent decrease in fatigue cracking. According to the final version of the specification as developed by Strategic Highway Research Program (SHRP) the loss modulus at 10 rad/s (1.59 Hz) must be less than 5 MPa at the intermediate pavement design temperature [18].

2.2.12.3 Contribution of Bitumens to Thermal Cracking Resistance

Thermal cracking in pavements is the result of stress developed due to thermal shrinkage caused by a drop in environmental temperature [23]. Two factors are important for resistance to thermal cracking: the stiffness or resistance to deformation and the ability to relax stresses by dissipating energy. In the Superpave method, the BBR test is used to evaluate low temperature cracking. The stiffness of bitumen as a function of time, can be measured at low temperatures by using the BBR. In addition, the ability of the bitumen to relax stresses can be measured by measuring the logarithmic creep rate, m, according to the following equation (see Figure 2.18):

$$m(t) = \frac{d\log(S(t))}{d\log(t)} \qquad \textbf{(2.52)}$$

Where: S (t) = the flexural creep stiffness

t = the loading time

The maximum stiffness of 300 MPa and a minimum "m" value of 0.3 at a loading time of 60 s are selected as the Superpave specification criteria for thermal cracking [22].

2.2.13 Implication of Bitumen Ageing

Ageing is the change of the chemical and physical properties of bitumens due to volatilisation and oxidation. Ageing of bitumens occurs in two stages [1, 87]:

- The first stage occurs during road construction, i.e. mixing and paving, where the stiffness of bitumen increases because of rapid oxidation and volatilisation as a result of high temperatures used during construction, and
- The second stage occurs after construction during the in-service life of the pavement. This stage is a much slower process than the first stage as oxidation occurs at much lower temperatures with a reduced supply of oxygen.

Several factors affect the rate and magnitude of bitumen ageing, i.e., chemical composition of the bitumen, climatic conditions, mixture type, aggregate gradation, air-void content and distribution in the mixture [87].

2.2.13.1 Short Term Ageing

As mentioned previously, this ageing occurs because of volatilisation and oxidation at high temperatures during construction. There are two test methods for simulating short term ageing of bitumens: the thin film oven test (TFOT) method (ASTM D-1754) [1], and the rolling thin film oven test (RTFOT) method (ASTM D-2872) [4].

In the TFOT ageing test, 50 grams of bitumen is placed in a cylindrical flat-bottom pan at approximately 3.2 mm thickness. The pan is then placed on a shelf in a ventilated oven for 5 hours at 163°C while the shelf, which can carry four pans, rotates at 5 to 6 rpm.

In the RTFOT ageing test, 35 grams of bitumen is placed into a bottle. The bottle is then placed into one of the holes of a circular carriage, which is placed into an electrically heated convection oven. Air is blown into each sample by means of an air jet at the lowest position of the carriage as the carriage rotates. The samples are heated at 163°C for 85 minutes.

2.2.13.2 Long Term Ageing

Long term ageing, which occurs after construction of a pavement, continues as a result of oxidation at moderate temperatures [87]. The Pressure Ageing Vessel (PAV) [24, 87] was developed by the SHRP team to simulate long-term ageing of bitumens. In this method, 50 grams of aged bitumen, by the TFOT or RTFOT method, is placed on one of 10 stainless steel plates, which are placed into the pressure vessel. The bitumen is then aged under a pressure of 2.07 MPa at temperatures between 90 and 110°C for 20 hours. After this time the pressure is slowly released over a time period of 8 to 10 minutes. Finally, to remove any contained air, the samples are placed in an oven at 150°C for 30 minutes.

2.3 Modified Bitumens

During the last two decades, increased deterioration of pavements due to increased traffic volumes and loads has been observed in many countries. There is no doubt that bitumen is one of the main influences on pavement behaviour and selecting a suitable bitumen for specific conditions such as climate, traffic and pavement structure is one of the aims of a pavement engineer. However, when bitumen does not meet the requirements, modification of the bitumen with an additive can be an effective engineering solution.

There has been a steady increase in the use of bitumen modifiers in the paving industry during the last decade as it has been found that they can improve performance [21]. However, the selection of modifiers to meet the requirements is not an easy task. Conventional testing methods, such as viscosity or penetration, have been used to help with the selection of modifiers. However, these test methods, cannot measure fundamental properties that are related to pavement performance. Consequently, new testing methods, such as the DSR, which address this problem, have been introduced following research undertaken during SHRP [19].

This section of the literature review aims to describe bitumen modification and to introduce different kinds of modified binders especially PMBs. The effect of modification on the rheology and failure properties of bitumen is briefly discussed and finally, the stability of modified bitumens is evaluated.

2.3.1 Objectives of Using Modified Bitumen

Improving one or more of the basic properties of bitumen related to one or more pavement distress modes (rutting, fatigue cracking and thermal cracking) is generally the aim of using modified bitumens [21]. The basic properties of bitumens, which can be improved by modification, can be classified into four main groups: rigidity, elasticity, brittleness and durability.

- Rigidity: modification can reduce the rigidity of bitumen at intermediate and low temperatures or at intermediate and short loading times. This results in increased

resistance of the pavement to fatigue and thermal cracking. Modification can also increase resistance of the pavement to rutting by increasing the rigidity of bitumen at high temperatures or long loading times. Rigidity can be measured as the complex modulus (G*) under dynamic loading, and creep stiffness (S(t)) under static loading.

- Elasticity: modification can decrease the elasticity of the bitumen at low temperatures in order to increase resistance to low temperature cracking. It can also increase elasticity at intermediate and high temperatures and so improves the resistance of the bitumen to rutting and fatigue cracking. Elasticity can be measured as phase angle (δ) under dynamic loading and the logarithmic creep rate (m) under static loading.
- Brittleness: modification can increase the ductility of the bitumen to improve resistance to fatigue and thermal cracking. Modification can decrease failure at low strain by increasing strain tolerance.
- Durability: modification can improve the durability of bitumens in terms of resistance to ageing and oxidation.

2.3.2 Different Kinds of Modifiers

Bitumen modifiers can be classified on the basis of the mechanism by which the modifier alters the bitumen properties, the composition and physical nature of the modifier and the target bitumen property that must be modified [27]. A large number of bitumen modifiers are used in paving applications. These materials have been classified into different groups by different researchers or institutes. For example, SHRP has classified modifiers in eight categories [76, 92]: thermoplastics, antistripping agents, mineral fillers, antioxidants, fibers, extenders, recycling agents and oxidants. Different kinds of modifiers are shown in Table 2.1 [27]. This study will focus only on polymers.

Table 2.1: Different types of bitumen modifiers used for pavement applications

Type of modifier	Class
Fillers	Carbon black Mineral: Hydrated lime Fly ash Portland cement Baghouse fines
Extenders	Sulphur Wood lignin
Polymers-Elastomers	Styrene butadiene diblock (SB) Styrene butadiene triblock/radial block (SBS) Styrene isoprene (SIS) Styrene ethylbutylene (SEBS) Styrene butadiene rubber latex (SBR) Polychloroprene latex
Polymers-Plastomers	Ethylene vinyl acetate (EVA) Ethylene propylene diene monomers (EDPM) Polyisobutylene Polyethylene Polypropylene
Crumb rubber	Different sizes, treatments and processes
Oxidants	Manganese compounds
Hydrocarbons	Aromatics Napthenics Paraffinics/wax Vacuum gas oil Asphaltenes: ROSE process resins SDA asphaltenes Tall oil Natural bitumens: Trinidad Gilsonite
Antistrips	Amines: Amidoamines Polyamines Hydrated lime Organo-metallics
Fibres	Polypropylene Polyester Reinforcement Natural: Cellulose Mineral
Antioxidants	Carbamates: Lead Zinc Carbon black Hydrated lime Phenols Amines

2.3.3 Polymers

The use of polymers in binders can be traced back to the early 1950s in Europe [89]. Gregg and Alcocke [55] published the earliest research available on polymer-modified asphalt in 1954. They studied bitumen modified with the polymer styrene butadiene and found the addition of polymers to bitumens improved or reduced temperature susceptibility. Thompson [102] in 1964 concluded that modification of bitumen with neoprene improved the toughness and ageing characteristics of bitumens.

Polymers are large chain-like molecules formed by the conjunction of small chemical units, called monomers. There are two stages in classifying various groups of polymeric materials [70].

- Classification based on the overall composition of the polymers, i.e. if the polymer contains only one type of unit or monomer then it is known as a homopolymer, whereas if more than one unit is present then it is known as a copolymer.
- Classification based on structural considerations, i.e. from knowledge of how the individual components of the polymers fit together. Polymers have three main structures: linear, branched and block polymers. The structure of the homopolymers is solely linear and branched, whereas the copolymers can be found in various forms, e.g. linear-random and linear-block (Figure 2.19) [108].

Polymers can also be classified in two general categories:

- Elastomers, and
- Plastomers.

The mechanism of resistance to deformation is different between elastomeric and plastomeric polymers. The load-deformation behaviour of elastomers is similar to rubbers, i.e. increasing tensile strength with increased elongation and ability to recover to the initial state after removal of load. Under a given load, elastomers deform faster than plastomers and recover early strength but are less flexible and more prone to fracture under large strains compared to plastomers [69].

2.3.3.1 Plastomeric (Thermoplastic) Polymers

Major plastomeric polymers used for paving applications are ethylene vinyl acetate (EVA), ethylene propylene diene monomer (EPDM), polyisobutylene, polyethylene, polyvinylchloride (PVC) and polypropylene [27]. These polymers are characterised by softening on heating and hardening on cooling [110]. One of the advantages of thermoplastic polymers is that the viscosity and the stiffness of the bitumen modified by these polymers increases at ambient temperature. However, most of the thermoplastic polymers can separate when heated and do not significantly improve the elastic properties of bitumen [62, 110].

One of the most popular thermoplastic polymers, which has been widely used as a polymer modifier in asphalt in European countries, is EVA. These copolymers have a random structure derived from the copolymerisation of ethylene and vinyl acetate [110]. The molecular weight, in terms of melt flow index (MFI), and vinyl acetate content governs the properties of EVA copolymers, i.e. if MFI is 150 g/10 min and the vinyl acetate content is 19%, the grade of EVA will be 150/19. The higher the MFI value, the lower the molecular weight and viscosity [110]. A schematic of the structure of EVA is shown in Figure 2.20. It can be seen from this figure that the structure of EVA consists of two parts [110]:

- The polyethylene segments, which are packed closely together and form the crystalline region, and
- The massive vinyl acetate groups, which produce the non-crystalline or amorphous rubbery region.

The crystalline regions, which are stiff, provide the strength of EVA while the amorphous regions have rubbery properties. Therefore, the higher vinyl acetate content causes a higher proportion of rubbery regions and a lower proportion of the crystalline regions [110].

EVA has been shown to improve the workability of asphalt as it is slightly softer than bitumen and is also more susceptible to shear. However, asphalt workability drops rapidly when using EVA in asphalt at cold ambient conditions. This is because of the

hardening of the EVA modified bitumen as a result of EVA polymer crystallisation [110].

2.3.3.2 Elastomeric Polymers (Thermoplastic Rubbers)

Elastomeric polymers or thermoplastic rubbers (TR) are the most important group of thermoplastic elastomers used for paving applications [110]. Examples of these polymers are styrene butadiene diblock (SB), styrene butadiene triblock/radial block (SBS), styrene isoprene (SIS), styrene ethylbutylene (SEBS), styrene butadiene rubber latex (SBR) and polypropylene [27]. Several benefits have been found when elastomeric polymers are added to bitumens. First, these materials have increased softening point, ductility, adhesion to aggregate and resistance to the effects of motor fuels. In addition they improve the resistance to ageing and the elastic recovery of bitumens [116]. Finally because of their high elastic response, they resist permanent deformation by stretching and recovering their initial shape [17]. As shown in Figure 2.21 elastomeric polymers have a linear or branched structure [110]. Of the thermoplastic elastomers, the best known group is the block copolymer, styrene butadiene styrene (SBS). They are characterised by their styrene content, their molecular weight and their configuration (linear or star shaped) [103]. SBS elastomers consist of polystyrene endblocks and polybutadiene midblocks with a star (tetrabranched) or linear structure (Figure 2.22) [103, 110]. Star shaped SBS elastomers have high viscosity, a high softening point and better low temperature flexibility of the compound, whereas linear SBS elastomers have low viscosity, a low softening point and increased toughness [103].

2.3.4 Stability of Modified Bitumens

Modified bitumens have multiphase systems in which the modifiers are dispersed into the bitumen phase [27]. Therefore, modifiers and base bitumens should be compatible. However, various factors influence the degree of compatibility. There are three mechanisms that can cause separation of modifiers and bitumens:

- Physical separation,
- Thermal effects, and
- Chemical effects.

The difference in density between a modifier and a bitumen is an important factor for physical separation. Decreasing the size of the modifier particle, increasing the viscosity of the bitumen and using additives such as thixotropic or thickening agents and fine inorganic fillers can prevent physical separation [27].

Cooling rate and temperatures at which modified bitumens are handled have an important effect on the thermal stability of modified bitumens. Therefore, laboratory testing conditions should be the same as the thermal treatment in the preparation of the polymer modified bitumen.

Chemical stability of modified bitumens may be affected by reaction of the modifiers with some materials such as salts and acid rain. Oxidation of modifiers can also cause a significant decrease in the modified bitumen stability.

2.4 Rheology of Asphalt Mixtures

Because of the increased load, volume of traffic and complex gear configurations of trucks and aeroplanes, there has been a strong demand for a more realistic and rational assessment of pavement material behaviour; particularly in terms of their true dynamic stress-strain responses. Since material behaviour is fundamentally governed by Young's modulus, significant research has been undertaken to develop reliable procedures to predict this property. However, Young's modulus is not a fixed or constant parameter for most pavement materials. Several different designations have been used for the elastic modulus, such as: Resilient Modulus, Flexural Stiffness, Complex Modulus, etc [68]. However, since pavement structures are generally subjected to dynamic pulse loading rather than static loading, the study of the dynamic modulus of asphalt mixtures is very important. Dynamic modulus can be found by using a dynamic test and subjecting asphalt samples to sinusoidal loading.

There are many factors, which affect the stress-strain response of asphalt mixtures, e.g. temperature, rate of loading, viscosity and ageing. Temperature is considered the most significant environmental factor affecting the stress-strain response of asphalt mixtures. At very low temperatures, stiffness modulus values are very high and the asphalt mixture behaves as though it was a very stiff material such as concrete. In

contrast, for very high temperatures, stiffness modulus values are very low. Also, the frequency of the repetitive loading affects the stress-strain response of asphalt mixtures, i.e. long loading times (which corresponds to low load frequency or low loading speed) lead to lower stiffness modulus values. Among the different mixture properties influencing the stiffness modulus value of an asphalt mixture, the bitumen viscosity (hardness) plays an important role. Besides being affected by temperature, the viscosity of bituminous materials is also subject to ageing effects. Age hardening is an important factor, which affects the stress-strain response of asphalt mixtures. Short-term ageing, which is brought about by hardening of the bitumen during the mixing process, and long-term ageing, which is due to environmental oxidation with time, lead to increases in the dynamic stress-strain response of asphalt mixtures with time. The overall impact of ageing processes is that the stiffness (dynamic modulus) of the asphalt mixture will increase affecting the pavement performance. This may be beneficial since stiffer mixtures provide for improved load distribution properties and are more resistant to permanent deformation. However, as the asphalt mixture becomes stiffer, its susceptibility to cracking and fracture increases.

2.4.1 Dynamic Characterisation of Asphalt Mixtures

An asphalt mixture is a rheological material whose response under load depends upon the rate of loading and the temperature. Stiffness is one of the most important properties of asphalt mixtures in pavement design and analysis.

There are various tests for measuring the stiffness of asphalt mixtures in the laboratory, which is commonly used as material input to structural analysis models to predict pavement responses under load. These test methods can be divided into two categories [104]:

- Static tests, e.g. static creep and relaxation test, and
- Dynamic tests.

Pavement structures are subjected to dynamic pulse loading rather than static loading and asphalt mixtures respond to dynamic loading with a higher modulus value. There

are several tests used to study the dynamic characteristics of asphalt mixtures of which the most important are [68]:

- Complex Modulus Test (dynamic modulus and phase angle),
- Indirect Tensile Resilient Modulus Test,
- Flexural Stiffness Modulus Test, and
- Dynamic Modulus measured with the Impact Resonance Test.

The dynamic modulus is generally expressed by the ratio of the peak induced dynamic stress ($\sigma_\circ$) to the peak recoverable strain ($\varepsilon_\circ$) [104]:

$$E=\frac{\sigma_\circ}{\varepsilon_\circ} \tag{2.53}$$

Dynamic modulus tests can be carried out at various loading frequencies. Therefore, dynamic modulus can be determined at a frequency close to what is expected under field loading conditions, which is important for accurately predicting the pavement response using multi-layered elastic solutions.

2.4.2 The (Complex) Dynamic Modulus Test

The complex modulus test was developed to measure the linear viscoelastic and elastic properties of pavement materials [68, 104]. By definition, the complex modulus (E*) is a complex number that relates stress to strain for viscoelastic materials subjected to continuously applied sinusoidal loading over a frequency domain.

In this test, a sinusoidal load is applied to a sample, which results in a displacement being measured (Figure 2.23) and the peak stress and peak strain determined. The ratio of the peak stress to the peak strain is the absolute value of the modulus, referred to as the norm of the complex modulus.

$$\left|E^*\right| = \frac{\sigma_\circ}{\varepsilon_\circ} \tag{2.54}$$

By definition, the complex modulus E* is represented by the storage modulus (real portion) and the loss modulus (imaginary portion) in the following relationship:

$$E^* = E' + iE'' \qquad \textbf{(2.55)}$$

Where: E* = Complex modulus

E' = Storage modulus

E'' = Loss modulus, and

$i = (-1)^{1/2}$

The relationship between complex modulus and the norm of the complex modulus is defined using the following polar form:

$$E^* = |E^*| e^{i\phi} \qquad \textbf{(2.56)}$$

Where: $e^{i\phi} = \cos(\phi) + i\sin(\phi)$

ϕ = phase angle

Therefore:

$$E^* = |E^*|\cos(\phi) + i|E^*|\sin(\phi) \qquad \textbf{(2.57)}$$

Comparison of equations 2.55 and 2.57 shows that:

$$E' = |E^*|\cos(\phi)$$
$$E'' = |E^*|\sin(\phi) \qquad \textbf{(2.58)}$$

And phase angle can be calculated from the following equation:

$$\phi = \tan^{-1}\left(\frac{E''}{E'}\right) \qquad \textbf{(2.59)}$$

The phase angle is simply the angle at which the harmonic oscillating strain (deformation) response lags behind the sinusoidal stress (load) input or equivalently:

$$\phi = \frac{t_i}{t_p}(360°) \qquad \textbf{(2.60)}$$

Where: t_i = time lag between the peak sinusoidal stress and strain, and

t_p = time for a complete stress cycle.

The value of phase angle is dependent on the balance of elastic and viscous response of materials. Phase angles have values between 0 and 90 degrees. For an elastic material, $\phi = 0°$ and for a viscous material, $\phi = 90°$. Therefore for a viscoelastic material the phase angle is between 0 and 90 degrees.

2.4.3 Factors Affecting the Dynamic Modulus of Asphalt Mixtures

There are several important factors, which influence the stress-strain response of asphalt mixtures. These factors can be summarised into five major groups [97, 104]:

- Temperature,
- Time of loading or frequency;
- Type of applied load,
- Physical properties of asphalt mixture, and
- Type of test.

Temperature

The influence of temperature on stiffness will be reflected in the temperature susceptibility of the bitumen. In other words, a change in the stiffness of the bitumen leads to a change in mixture stiffness. Temperature is the most significant variable influencing the dynamic modulus of asphalt mixtures. For example, Van der Poel [104] stated that the binder stiffness may vary by a factor of 2 for a temperature difference of 2°C. Since asphalt layers are subjected to local environmental changes

of temperature that may vary over a wide range in one single day, temperature should be considered as an extremely important factor when studying the dynamic modulus of an asphalt mixture.

Rate of Loading or Frequency

The influence of rate of loading or frequency on stiffness of asphalt mixtures will be reflected in the time dependency of the bitumen. Increasing rates of loading lead to increasing stiffness, whereas decreasing rates of loading lead to decreasing stiffness [104]. A moving vehicle on the pavement can be simulated by the rate of loading. As the vehicle velocity increases, the rate of loading or frequency increases and the dynamic modulus increases. Therefore, it can be concluded that the dynamic response of an asphalt mixture is a function of the rate of loading or, in other words, the vehicle speed.

Type of Applied Load

There are two major types of laboratory waveform loads, which are used for dynamic testing (Figure 2.24):

- Continuous wave, e.g. sinusoidal, and
- Pulse load, e.g. half sine.

As can be seen from Figure 2.24, the load time (t_l) is the time for one complete cycle for the continuous (sinusoidal) waveform. Therefore frequency can be simply calculated from the following equation:

$$f = \frac{1}{t_l} \qquad \textbf{(2.61)}$$

Pulse load forms are characterised by two separate time variables: loading time (t_l) and rest time (t_d) (Figure 2.24). The pseudo pulse frequency can be defined according to the following equation [113]:

$$f' = \frac{1}{(t_l + t_d)} \qquad \textbf{(2.62)}$$

However, the true frequency is calculated from the following equation:

$$f = \frac{1}{t_l} \qquad \textbf{(2.63)}$$

Physical Properties of Asphalt Mixtures

Physical properties of asphalt mixtures can be influenced by three factors:

- Bitumen type,
- Characteristic of the aggregate, and
- Characteristic of the asphalt mixture.

It is fairly certain that the stiffness of an asphalt mixture is influenced by the stiffness of the bitumen. As the stiffness of the bitumen increases, the stiffness of the asphalt mixture increases. Several researchers attempted to relate mixture stiffness to bitumen stiffness. Heukelom and Klomp [60] derived a semi-empirical equation, which relates mixture stiffness to bitumen stiffness. Van der Poel [104] developed graphs, which make it possible to obtain the stiffness of bitumen at different temperatures. From these graphs, the stiffness of bitumen is determined using the penetration and softening point of the bitumen.

In terms of the effect of aggregate characteristics on the dynamic modulus of asphalt mixtures, aggregate gradation and aggregate type are most important [80]. Well-graded aggregate mixtures result in more stable mixtures and higher dynamic modulus as compared to poorly graded aggregate mixtures.

Mixture characteristics, which affect the dynamic modulus of asphalt mixtures, can be divided into two parts:

- Weight components, e.g. density, and
- Volumetric components e.g. void content.

Type of Test

Although, different types of tests should ideally give similar dynamic modulus values, several researchers have shown that different test procedures give different results [64, 68]. Therefore, the dynamic modulus is a function of test method and the subsequent way in which dynamic (and/or static) stress states are applied.

The major type of test methods, which are used for finding dynamic modulus of asphalt mixtures are [68]:

- Direct tests (compression, tension and tension-compression),
- Indirect tension tests, e.g. Nottingham Asphalt Tester (NAT), and
- Impact resonance tests.

Figure 2.25 shows a schematic representation of a dynamic stiffness modulus test, which is a direct test. As can be seen from this figure, the tension, compression or tension-compression load is applied to the sample and the stress and strain as a function of time are monitored.

Kallas [64] conducted several tension, compression and tension-compression tests at different frequencies and temperatures and stated the following conclusions:

There are insignificant or relatively small differences between the dynamic tension or tension-compression modulus and the dynamic compression modulus for temperatures between 5°C and 20°C and frequencies between 1 and 16 Hz. However, there are significant differences between the dynamic tension or tension-compression modulus and the dynamic compression modulus for temperatures between 20°C and 40°C at a frequency of 1 Hz.

In indirect tests, a load pulse is applied along the vertical diameter of a cylindrical specimen and the resultant peak transient deformation along the horizontal diameter is measured (Figure 2.26). Dynamic stiffness can be calculated as a function of load, deformation, specimen dimensions and Poisson's ratio [34]. The British Standard

assumes 0.35 for Poisson's ratio but values of 0.25 at 10°C and below, 0.35 at 20°C and 0.45 at 30°C have been recommended [12].

The impact resonance method described in ASTM C215 was developed to determine the elastic properties of Portland cement concrete based on the resonance vibration response of a concrete specimen due to an impact load [68, 111]. Whitmoyer et al [111] stated that this method, which is a truly non-destructive testing method, produces very repetitive, consistent results for asphalt mixtures.

2.4.4 Ageing Study of Asphalt Mixtures

The majority of the previous work has investigated the ageing effects of bitumens rather than asphalt mixtures. However, ageing can have major effects on the properties of asphalt mixtures. Ageing of asphalt mixtures is associated with the phenomenon of hardening [29]. Many factors, such as the chemical composition of the bitumen, the type and grading of the aggregate, the interaction between bitumen and aggregate particles and climate, affect the durability of asphalt mixtures [34].

The ageing process of asphalt mixtures occurs in two stages: short term and long term. The short term ageing, which occurs during the construction phase, is primarily attributable to the loss of volatile components and oxidation while the mixture is hot, whereas the long term ageing is primarily attributable to the progressive oxidation of the asphalt mixture while in service [29]. Numerous laboratory tests have been developed to assess the durability of asphalt mixtures. One of the weaknesses of these tests is that a majority of the ageing procedures involve the testing of neat bitumen, which neglects the effect of the aggregate [34].

The short term ageing methods involve conditioning loose asphalt mixtures [29]. One method used for short term ageing of asphalt mixtures is forced-draft oven ageing (SHRP No. 1025 procedures) [15]. In this method, the loose asphalt mixture, which is placed in a baking pan and spread to an even thickness that produced about 21 kg/m^2, is placed in a forced draft oven for a period of 4 hours at a temperature of 135°C. Required specimens are then made by compacting the loose asphalt mixture.

The long term ageing methods involve conditioning of compacted asphalt mixtures [29]. SHRP No. 1030 procedure [14] presents a method for long term ageing of asphalt mixtures. In this method, the procedure consists of placing the compacted specimens, made with short term aged asphalt material, on a rack in a forced-draft oven for 120 hours at a temperature of 85°C. This procedure was designed to simulate the ageing that the compacted asphalt pavement undergoes during 5 to 10 years of service life [65].

The study of ageing effects on asphalt mixtures involves determining the same physical properties, such as stiffness, of the mixture before and after ageing. Therefore, ageing of asphalt mixtures can be studied by using the ratio between the dynamic stiffness modulus of aged (E_{aged}) and unaged (E_{unaged}) asphalt mixtures [34]. The stiffness modulus ageing ratio can be defined by the following equation:

$$\text{Ageing Ratio} = \frac{E_{aged}}{E_{unaged}} \qquad \textbf{(2.64)}$$

2.5 Relationship between Bitumen and Asphalt Mixture Rheology

Dynamic Mechanical Analysis (DMA) can be used to study the relationship between bitumen and asphalt mixture properties. This can be done by measuring the rheological properties of bitumens and asphalt mixtures, such as, complex modulus. Goodrich [52] studied the relationship of bitumens and asphalt mixtures. He found that the ratio between loss and storage modulus of bitumens, referred to as the loss tangent, correlates well with the performance of dense graded asphalt mixtures. The loss tangent represents the ratio between the energy lost to the energy stored in a cyclic deformation:

$$\text{Loss tangent} = \tan\delta = \frac{G''}{G'} \qquad \textbf{(2.65)}$$

Goodrich [53] used DMA to examine how the rheological properties of bitumens correlate to asphalt mixtures. He also characterised the influence of both the aggregate and the bitumen on asphalt mixtures. He conducted DMA testing on unmodified and

modified bitumen and asphalt mixtures and stated that the relationship between the rheology of the bitumen and the rheology of asphalt mixtures can be explained for three different temperature ranges [53]:

- At low temperatures below 10°C, the rheology of the mixture largely reflects the rheology of the bitumen. Bitumens with higher loss tangents yield mixtures with higher loss tangents. Although asphalt mixture rheology is predominantly influenced by bitumen, it is also affected by the asphalt mixture aggregate combination.
- At intermediate temperatures between 10°C and 50°C, both the bitumen and the aggregate influence asphalt mixture rheology. However, the unique properties of the bitumens are seen within this range of temperatures. Differences in bitumens, from Newtonian types to highly elastic types, are noticeable in asphalt mixtures at intermediate temperature. Therefore, bitumen properties (e.g. modified bitumens) are expected to have their best chance at improving the intermediate properties of asphalt mixtures.
- At high temperatures, above 50°C, the rheology of asphalt mixtures is predominantly influenced by the aggregate and it does not seem that the mechanical properties of asphalt mixtures are influenced by differences in bitumens.

2.6 Relationship between Bitumen and Asphalt Mixture Stiffness

Several factors, such as binder stiffness, the volume concentrations of the mixture components (i.e. the percent aggregate, bitumen, and air by volume), aggregate type and gradation have an influence on mixture stiffness. Several researchers have studied the influence of these factors on mixture stiffness. Van der Poel [105] assumed that the stiffness of the mixture is a function only of the stiffness of the bitumen and the volume fraction of the aggregate. Heukelom and Klomp [60] in 1964 attempted to relate mixture stiffness to bitumen stiffness. They reported that due to the complicated geometry of mixtures, the ratio of mixture stiffness to bitumen stiffness, S_{mix}/S_{bit}, cannot be exactly computed. However, they derived a semi-empirical model, which calculated mixture stiffness as a function of bitumen stiffness and the volume concentration of the aggregate. Work reported by Pagen and Ku [80] in 1965, using a

creep test, suggested that bitumen type, aggregate gradation and aggregate type all have some influence on the stiffness modulus of a mixture.

Mixture stiffness, not withstanding the different factors mentioned above, is primarily controlled through the selection of the binder. Even though other factors such as the void contents of the mixture, bitumen content, stiffness of aggregate and aggregate gradation have an effect on mixture stiffness, their influence is less significant than binder stiffness and the pavement engineer has much less freedom to modify these factors once the initial volumetric design is established.

This section of the literature review was conducted to review selected empirical and theoretical binder-to-mixture stiffness relationships.

2.6.1 Empirical Models of Binder-to-Mixture Stiffness Relationships

Empirical studies generally involve the fitting of various functions to measured binder and mixture stiffness, often considering the volume concentration of the aggregate, bitumen, and air as variables. The models of Heukelom and Klomp [60], Brown [33] and Bonnaure [30] were selected for evaluation because of their relatively widespread use.

Heukelom and Klomp presented a semi-empirical equation that could be used to obtain the stiffness of asphalt mixtures from stiffness of binder and the volume concentration, C_v, of the aggregate as given in Equation 2.66:

$$\frac{S_{mix}}{S_{bit}} = \left[1 + \left(\frac{2.5}{n}\right)\left(\frac{C_v}{1 - C_v}\right)\right]^n \qquad \textbf{(2.66)}$$

Where:

$$n = 0.83 \log\left[\frac{4 \times 10^{10}}{S_b}\right]$$

$$C_v = \frac{\text{Volume of aggregate}}{\text{Volume of (aggregate + binder)}}$$

S_m = Stiffness of mixture (Pa)

S_b = Stiffness of binder (Pa)

These equations were used for mixtures having C_v values between 0.7 and 0.9 and air voids less than or equal to 3%. Van Draat and Sommer [106] recommended the term C_v' instead of C_v for mixtures having air voids greater than 3%. C_v' can be calculated from following equation:

$$C_v' = \frac{C_v}{1+H} \quad \textbf{(2.67)}$$

Where: $H = (P_{av}/100)-0.03$

P_{av} = Percent air voids in the mixture

This equation is only valid for mixtures, which satisfy the following equation:

$$C_B \leq \frac{2}{3}(1-C_v') \quad \textbf{(2.68)}$$

$$C_B = \frac{\text{Volume of binder}}{\text{Volume of aggregate} + \text{binder}}$$

The relationship between stiffness modulus of mixtures and those of bituminous binders at various volume concentrations of aggregate and about 3% air voids from Heukelom and Klomp's work are shown in Figure 2.27. It can be seen from this figure that there is a strong correlation between asphalt mixture stiffness and bitumen stiffness for the various mixture compositions considered. As would be expected, for a given binder stiffness, mixture stiffness increases with increasing C_v. In addition, it can be seen from this figure that the curves have a tendency to converge at high bitumen stiffness.

Brown [33] presented a model, which is a modification of the Heukelom and Klomp model. In this model stiffness of asphalt mixtures could be obtained from stiffness of binder and percentage of voids in mixed aggregate (VMA), as given in equation 2.69:

$$S_{mix} = S_{bit}\left[1 + \frac{257.5 - 2.5VMA}{n(VMA - 3)}\right]^{n} \quad \textbf{(2.69)}$$

Where: $$n = 0.83\log\left[\frac{4\times10^{10}}{S_b(Pa)}\right]$$

VMA = Percentage of air voids in mixed aggregate

S_{mix} = Stiffness of mixture (Pa)

S_{bit} = Stiffness of binder (Pa)

These equations were presented for mixtures having VMA values between 12 and 30% and $S_{bit} \geq 5$ MPa. The limitation of binder stiffness for this model is due to the minimum value of binder stiffness for elastic behaviour, which is 5 MPa [30]. Above this, the mixture stiffness only depends on binder stiffness and volumetric proportions but below it, a large number of parameters, related to the properties of the aggregate, become significant as the binder influence decreases. This situation is illustrated in Figure 2.28 in which the mixture stiffness is shown as a function of binder stiffness [33].

Another model for estimating mixture stiffness from binder stiffness and volumetric proportions was developed by Bonnaure [30]. This model was based on studying twelve field and laboratory mixtures with different compositions, as given in equations 2.70 and 2.71.

For $5*10^6$ Pa< S_b < 10^9 Pa

$$\log S_m = \frac{\beta_4 + \beta_3}{2}(\log S_b - 8) + \frac{\beta_4 - \beta_3}{2}\left|\log S_b - 8\right| + \beta_2 \quad \textbf{(2.70)}$$

For 10^9 Pa< S_b < $3*10^9$ Pa

$$\log S_m = \beta_2 + \beta_4 + 2.0959(\beta_1 - \beta_2 - \beta_4)(\log S_b - 9) \quad \textbf{(2.71)}$$

Where:

$$\beta_1 = 10.82 - \frac{1.342(100 - V_g)}{V_g + V_b}$$

$$\beta_2 = 8.0 + 0.00568V_g + 0.0002135{V_g}^2$$

$$\beta_3 = 0.6\log\left(\frac{1.37{V_b}^2 - 1}{1.33V_b - 1}\right)$$

$$\beta_4 = 0.7582(\beta_1 - \beta_2)$$

and:

S_b = Binder stiffness, Pa

V_g = Percent of aggregate by volume

V_b = Percent of binder by volume

This model is valid only for binder stiffness greater than or equal to 5 MPa. Therefore, this model does not apply to mixtures containing softer binders (S_b < 5 MPa) [30].

Other researchers such as Saunier in 1967, Verstraeten in 1971 and Francken in 1975 [30] developed different models for estimating mixture stiffness from binder stiffness. All these methods were based on experimental results obtained over a wide range of mixtures.

2.6.2 Theoretical Models of Binder to Mixture Stiffness Relationship

The use of theoretical methods to estimate mechanical characteristics of asphalt mixtures from characteristics of each of its components are not as common as empirical methods. In theoretical methods, mixture stiffness can be computed from binder stiffness and volumetric proportions of mixture through micromechanical analysis. Micromechanics is a method by which properties of composite materials, such as the stiffness modulus, can be obtained from known properties of the constituents that make up the composite. Micromechanical methods have been widely used in the study of solid rocket propellants, metals, and fibre-reinforced ceramics but use of this method in asphalt mixture has been very limited [35]. This part of the literature review aims at introducing some micromechanical models, which can be used to predict mixture stiffness.

I) Paul Equation and the Law of Mixtures

Paul was the first person, who introduced bounds for the effective elastic modulus of two phase, irregular geometry composite materials [82]. Those bounds were derived based on the extremum principles of minimum potential and minimum complimentary energy, and are given in equations 2.72 and 2.73.

$$\frac{1}{\frac{c_1}{K_1}+\frac{c_2}{K_2}} \le K^* \le K_1 c_1 \le K_2 c_2 \qquad \textbf{(2.72)}$$

$$\frac{1}{\frac{c_1}{G_1}+\frac{c_2}{G_2}} \le G^* \le G_1 c_1 \le G_2 c_2 \qquad \textbf{(2.73)}$$

where: K*, G* = Effective bulk and shear modulus of the composite

K_1, K_2 = Bulk modulus of phase 1 and 2

G_1, G_2 = Shear modulus of phase 1 and 2

c_1, c_2 = Volume fractions of phase 1 and 2

The right hand sides of equations 2.72 and 2.73 are often referred to as the law of mixtures. However, it should be pointed out that these bounds are only useful when the difference in modulus of the two phases is very small.

In addition, Young's modulus (E) and shear modulus of composites can be calculated from shear and bulk modulus as given in equations 2.74 and 2.75.

$$E = \frac{1}{\frac{1}{3G}+\frac{1}{9K}} \qquad \textbf{(2.74)}$$

$$G = \frac{E}{3(1+\nu)} \qquad \textbf{(2.75)}$$

II) Hasin and Shtrikman's Model

Hasin and Shtrikman [56] presented a model for the derivation of bounds for the effective elastic modulus of quasi-isotropic and quasi-homogeneous multiphase

materials. In this model the bounds, based on two phase composites can be calculated from the following equations:

$$K_1^* = K_1 + \frac{c_2}{\frac{1}{K_2 - K_1} + \frac{3c_1}{3K_1 + 4G_1}} \quad \textbf{(2.76)}$$

$$K_2^* = K_2 + \frac{c_1}{\frac{1}{K_1 - K_2} + \frac{3c_2}{3K_2 + 4G_2}} \quad \textbf{(2.77)}$$

$$G_1^* = G_1 + \frac{c_2}{\frac{1}{G_2 - G_1} + \frac{6(K_1 + 2G_1)c_1}{5G_1(3K_1 + 4G_1)}} \quad \textbf{(2.78)}$$

$$G_2^* = G_2 + \frac{c_1}{\frac{1}{G_1 - G_2} + \frac{6(K_2 + 2G_2)c_2}{5G_2(3K_2 + 4G_2)}} \quad \textbf{(2.79)}$$

where: K_1^*, K_2^* = Effective bulk modulus of lower and upper bounds

G_1^*, G_2^* = Effective shear modulus of lower and upper bounds

K_1, K_2 = Bulk modulus of phase 1 and 2

G_1, G_2 = Shear modulus of phase 1 and 2

c_1, c_2 = Volume fractions of phase 1 and 2

In addition, the bulk and shear modulus of phase two should be bigger than phase one ($K_2 > K_1$ and $G_2 > G_1$).

It is obvious that the effective bulk and shear modulus of composites should be between the lower and upper bounds. ($K_1^* \le K^* \le K_2^*$ and $G_1^* \le G^* \le G_2^*$).

III) Christensen and Lo Model

The Christeson and Lo [41] model is based on the Kerner [67] model. This model is a three phase model or “core-shell” system developed in particular by Hervé and Zaoui

[59], which consists of a single composite sphere embelded in a infinite medium of unknown effective properties (Figure 2.29).

The bulk modulus of composite materials (e.g. bituminous mixtures) is given by the following equation:

$$K^* = K_m{}^* + \frac{c\left(K_i - K_m{}^*\right)}{1+(1-c)\left(K_i - K_m{}^*\right)/\left(K_m{}^* + (4/3)\mu_m{}^*\right)} \qquad \textbf{(2.80)}$$

The complex shear modulus determined by Christensen and Lo is the solution of the following quadratic equation:

$$A\left[\frac{\mu^*}{\mu_m{}^*}\right]^2 + 2B\left[\frac{\mu^*}{\mu_m{}^*}\right] + C = 0 \qquad \textbf{(2.81)}$$

A, B and C are lengthy functions of the elastic constants, given in the following equations:

$$\begin{aligned} A = {} & 8\left[\frac{\mu_i}{\mu_m}-1\right](4-5\nu_m)\eta_1 c^{\frac{10}{3}} - 2\left[63\left(\frac{\mu_i}{\mu_m}-1\right)\eta_2 + 2\eta_1\eta_3\right]c^{\frac{7}{3}} + 252\left[\frac{\mu_i}{\mu_m}-1\right]\eta_2 c^{\frac{5}{3}} \\ & - 50\left[\frac{\mu_i}{\mu_m}-1\right]\left(7-12\nu_m+8\nu_m{}^2\right)\eta_2 c + 4(7-10\nu_m)\eta_2\eta_3 \end{aligned} \qquad \textbf{(2.82)}$$

$$\begin{aligned} B = {} & -4\left[\frac{\mu_i}{\mu_m}-1\right](1-5\nu_m)\eta_1 c^{\frac{10}{3}} + 4\left[63\left(\frac{\mu_i}{\mu_m}-1\right)\eta_2 + 2\eta_1\eta_2\right]c^{\frac{7}{3}} - 504\left[\frac{\mu_i}{\mu_m}-1\right]\eta_2 c^{\frac{5}{3}} \\ & + 150\left[\frac{\mu_i}{\mu_m}-1\right]\eta_2 c^{\frac{5}{3}} + 150\left[\frac{\mu_i}{\mu_m}-1\right](3-\nu_m)\nu_m\eta_2 c + 3(15\nu_m+7)\eta_2\eta_3 \end{aligned} \qquad \textbf{(2.83)}$$

$$\begin{aligned} C = {} & 4\left[\frac{\mu_i}{\mu_m}-1\right](5\nu_m-7)\eta_1 c^{\frac{10}{3}} - 2\left[63\left(\frac{\mu_i}{\mu_m}-1\right)\eta_2 + 2\eta_1\eta_3\right]c^{\frac{7}{3}} + 252\left[\frac{\mu_i}{\mu_m}-1\right]\eta_2 c^{\frac{5}{3}} \\ & + 25\left[\frac{\mu_i}{\mu_m}-1\right]\left(\nu_m{}^2-7\right)\eta_2 c - (7+5\nu_m)\eta_2\eta_3 \end{aligned} \qquad \textbf{(2.84)}$$

where:

$$\eta_1 = \left[\frac{\mu_i}{\mu_m} - 1\right](49 - 50\nu_i\nu_m) + 35\left(\frac{\mu_i}{\mu_m}\right)(\nu_i - 2\nu_m) + 35(2\nu_i + \nu_m)$$

$$\eta_2 = 5\nu_i\left[\frac{\mu_i}{\mu_m} - 8\right] - 7\left[\frac{\mu_i}{\mu_m} + 4\right]$$

$$\eta_3 = \left(\frac{\mu_i}{\mu_m}\right)(8 - 10\nu_m) + (7 - 5\nu_m)$$

where: ν_i, ν_m = Poisson's ratio of the inclusion and matrix phase

μ_i, μ_m = Shear modulus of inclusion and matrix phase

$c = (a/b)^3$ (a and b are shown in Figure 2.29)

The mixture stiffness modulus can be calculated from equation 2.74 based on results of bulk and shear modulus.

A major source of error of the above models was their inability to accurately model materials having high concentrations of interacting inclusions. For example, the upper and lower bounds of the Paul model can be represented by springs in parallel and series as shown in Figure 2.30. In this model the upper bound is represent by columns of aggregates and binder loaded in parallel, where the aggregate dominates the response (maximum aggregate interlock), and the lower bound is represent by a column of aggregate and binder in series, where the binder dictates the response of the mixture (absence of aggregate interlock). However, neither of these bounds represents the actual response of asphalt mixtures as asphalt mixture response lies somewhere in between these bounds where an intermediate level of aggregate interaction occurs [35].

IV) Weng Model

Weng [109] developed a model, where an elastic sphere is isotropically dispersed in an elastic matrix, based on the Mori-Tanaka theory [75]. The effective bulk and shear modulus of composite materials can be calculated from the following equations:

$$K^* = K_m + \frac{c(K_i - K_m)K_m}{(1-c)(K_i - K_m)\alpha_1 + K_m} \quad \textbf{(2.85)}$$

$$\mu^* = \mu_m + \frac{c(\mu_i - \mu_m)\mu_m}{(1-c)(\mu_i - \mu_m)\beta_1 + \mu_m} \quad \textbf{(2.86)}$$

where:

$$\alpha_1 = \frac{3K_i}{3K_i + 4\mu_i}$$

$$\beta_1 = \frac{6(K_m + 2\mu_m)}{5(3K_m + 4\mu_m)}$$

Where all the variables are as defined before. In addition, the mixture stiffness modulus can be calculated from Equation 2.74 based on results of bulk and shear modulus.

2.7 Linear and Non-linear Viscoelasticity

Linear elasticity (Hooke's law) is the simplest model for a material. In this model stress is proportional to strain. However, at large strains, the response of bituminous materials is non-linear (Figure 2.31) and cannot be adequately modelled by a LVE approximation [73, 74, 79, 81]. Therefore, when analysing a viscoelastic material such as bitumen or asphalt mixtures by dynamic testing, two behaviour domains appear: the linear domain and the non-linear domain [32]. Generally the non-linearity responses of bitumen and asphalt mixtures become negligible at strain amplitudes smaller than a certain limit (depending on the considered material), and the material behaviour can then be considered to be linear. In most conditions, bitumen and asphalt mixture behaviour is non-linear and finding this linear limit forms an important part of the rheological study of these materials. Three important reasons can be mentioned for defining the linear viscoelastic region of bitumen and asphalt mixtures. Firstly, in keeping with the desire for simplicity, it would seem appropriate to limit procedure design to the linear region of behaviour before adding the complications of a non-linear theory. Secondly, in order to find correlations between bitumen and asphalt mixture rheology it is necessary to study both bitumen and asphalt mixtures in the

same domain. Finally, as time-temperature dependency is only valid in the linear region of behaviour, finding the linear limit is necessary in order to use a time-temperature superposition principle.

The linear and non-linear domains of asphalt mixtures are presented in Figure 2.32 [32]. This figure shows the dynamic response of asphalt mixtures in a log-log plane of strain amplitude versus number of loading cycles. It can be seen from this figure that strain amplitude and number of loading cycles affect the linear and non-linear domains of asphalt mixtures. Asphalt mixtures have linear behaviour at very low strain amplitudes and number of loading cycles. Therefore, it can be concluded that asphalt mixtures exhibit non-linear behaviour under most strain amplitudes and repetitive loading conditions.

Linear viscoelasticity can be defined in several ways. One definition is related to the creep compliance and relaxation modulus of a material. A material can be defined as linear if the value of its compliance in a series of creep tests or of its modulus in a series of relaxation tests is independent of the value of stress or strain at any given time. In addition, the viscosity of the material is independent of stress level in the linear region and decreases in value in the non-linear region. A second definition of linear viscoelasticity is related to dynamic repeated loading tests. In a repeated sinusoidal loading test, a material can be defined as acting linearly if, for a given frequency of loading, the complex modulus and phase angle remain constant with a change in the amplitude of strain or stress.

In a repeated sinusoidal loading test, non-linear behaviour generally becomes negligible at strain amplitudes smaller than a certain limit dependent on the material. Therefore, a linear region may be defined at small strain values where the shear modulus is relatively independent of shear stress and strain.

The linear region can be found from a stress sweep test, in which the applied stress is increased during the test, or a strain sweep test, in which the applied strain is increased during the test. Therefore the linear region can be found by plotting complex modulus versus shear strain. According to SHRP, the linear region can be

defined as the point beyond which the measured value of complex modulus decreases to 95% of its maximum value [85] (Figure 2.33).

2.8 Summary

Behaviour of bitumen combines two parts: elastic behaviour and viscous behaviour. Materials, such as bitumen, are known as viscoelastic materials, having elastic behaviour at low temperatures and high rates of loading, and viscous behaviour at high temperatures and low rates of loading. Bitumens exhibit different proportions of elastic, viscous and delayed elastic response depending upon the specific loading conditions and material properties.

New test methods have been introduced to measure more fundamental properties of bitumens, which can be related to pavement performance. These test methods can be divided into two parts. Firstly, new physical properties tests such as, DSR, BBR and DTT, which are fundamental in nature and can be related to the critical distress mechanisms and field performance through rational models. Secondly, ageing tests, which can produce aged materials with stiffness and rheological characteristics similar to that of field-aged material. Dynamic (oscillatory) testing generally is considered the most appropriate technique to determine the viscoelastic properties of bitumens as it covers a wide range of loading conditions to give a wide range of properties.

In analysing viscoelastic data in the linear region, time temperature superposition is used over a range of temperatures and frequencies to construct a master curve. Time temperature superposition involves shifting data horizontally with respect to time to produce a single smooth curve. The amount of shifting required in this process is quantified by the shift factor, a(T).

There is no doubt that bitumen is one of the main influences on pavement behaviour and selecting a suitable bitumen for specific conditions such as climate, traffic and pavement structure is one of the aims of a pavement engineer. However, when bitumen does not meet the requirements, modification of the bitumen with an additive can be an effective engineering solution. A large number of bitumen modifiers are

used in paving applications. These materials have been classified into different groups by different researchers or institutes. For example, SHRP has classified modifiers in eight categories: thermoplastics, antistripping agents, mineral fillers, antioxidants, fibers, extenders, recycling agents and oxidants.

Several different designations have been used for the elastic modulus of asphalt mixtures, such as: Resilient Modulus, Flexural Stiffness, Complex Modulus, etc. However, since pavement structures are generally subjected to dynamic pulse loading rather than static loading, the study of the dynamic modulus of asphalt mixtures is advisable. Dynamic modulus can be found by using a dynamic test and subjecting asphalt samples to sinusoidal loading.

Dynamic Mechanical Analysis (DMA) can be used to study the relationship between bitumen and asphalt mixture properties. This can be done by measuring the rheological properties of bitumens and asphalt mixtures, such as complex modulus. The use of theoretical methods to estimate the mechanical characteristics of asphalt mixtures from the characteristics of each of its components are not as common as empirical methods. In theoretical methods, mixture stiffness can be computed from binder stiffness and volumetric proportions of the mixture through micromechanical analysis. Micromechanics is a method by which properties of composite materials, such as the stiffness modulus, can be obtained from known properties of the constituents that make up the composite. Micromechanical methods have been widely used in the study of solid rocket propellants, metals and fibre-reinforced ceramics but use of this method in asphalt mixture has been very limited.

In a repeated sinusoidal loading test, non-linear behaviour generally becomes negligible at strain amplitudes smaller than a certain limit dependent on the material. Therefore, a linear region may be defined at small strain values where the shear modulus is relatively independent of shear stress. The linear region can be found from a stress sweep test, in which the applied stress is increased during the test, or a strain sweep test, in which the applied strain is increased during the test.

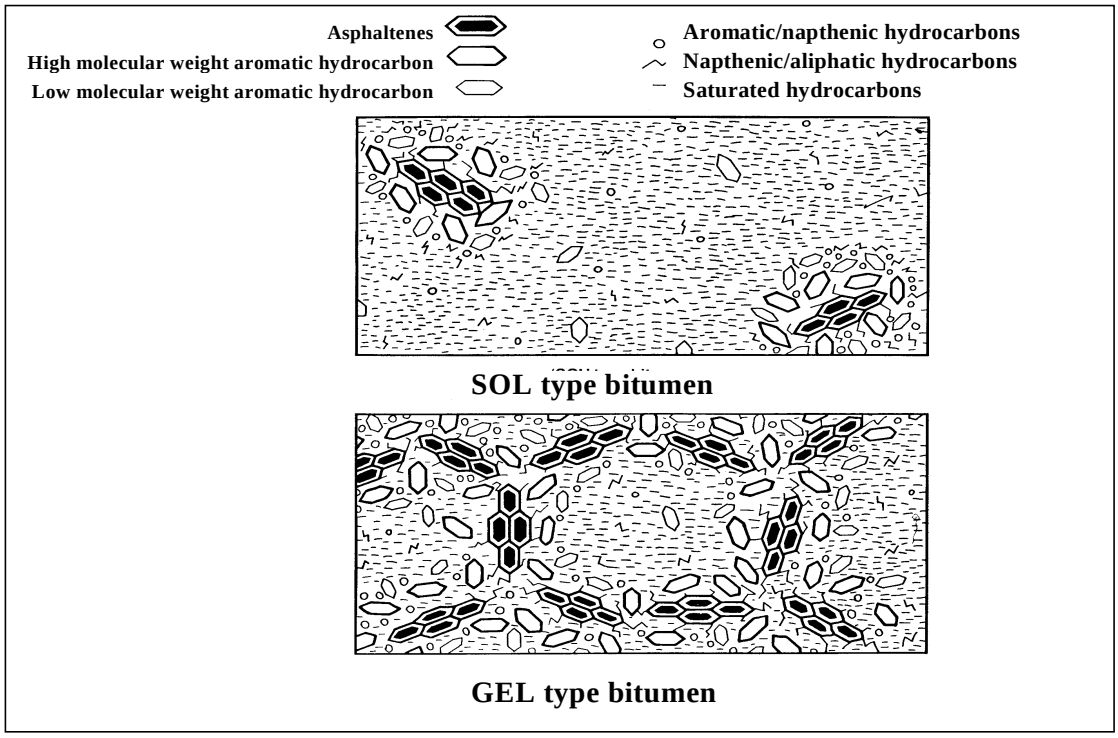

Figure 2.1:Schematic representation of SOL and GEL type bitumens [110]

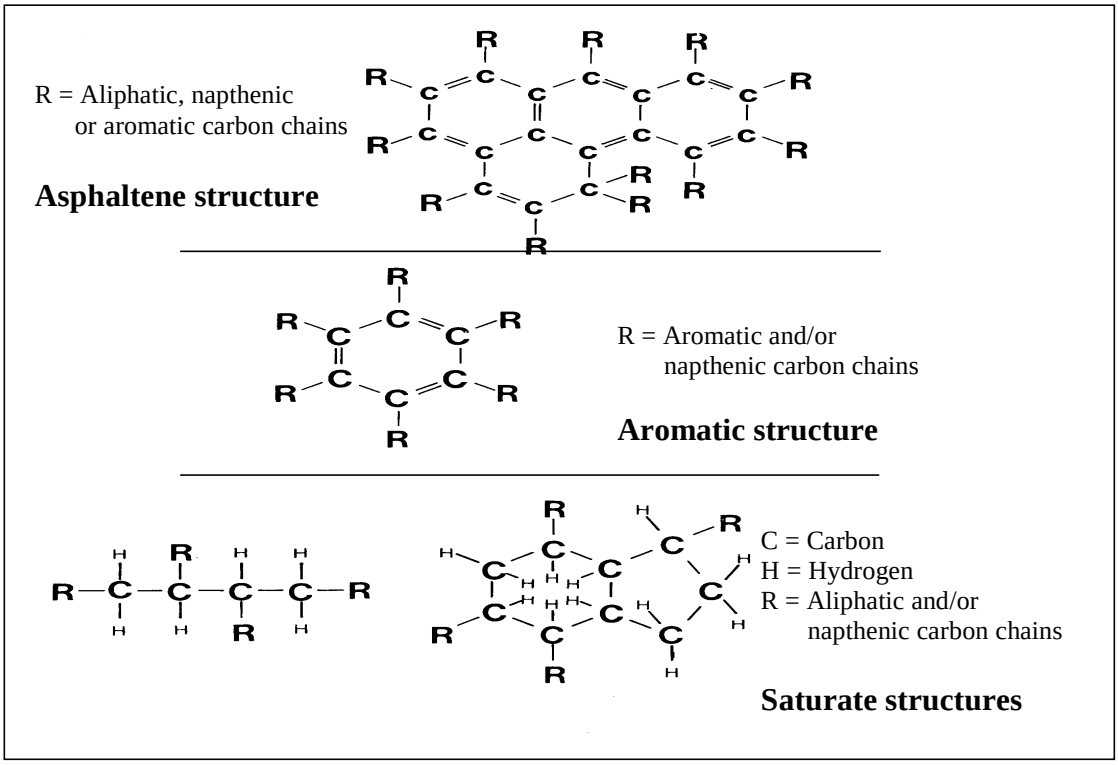

Figure 2.2: Schematic representation of the molecular structure of the different components of bitumens [110]

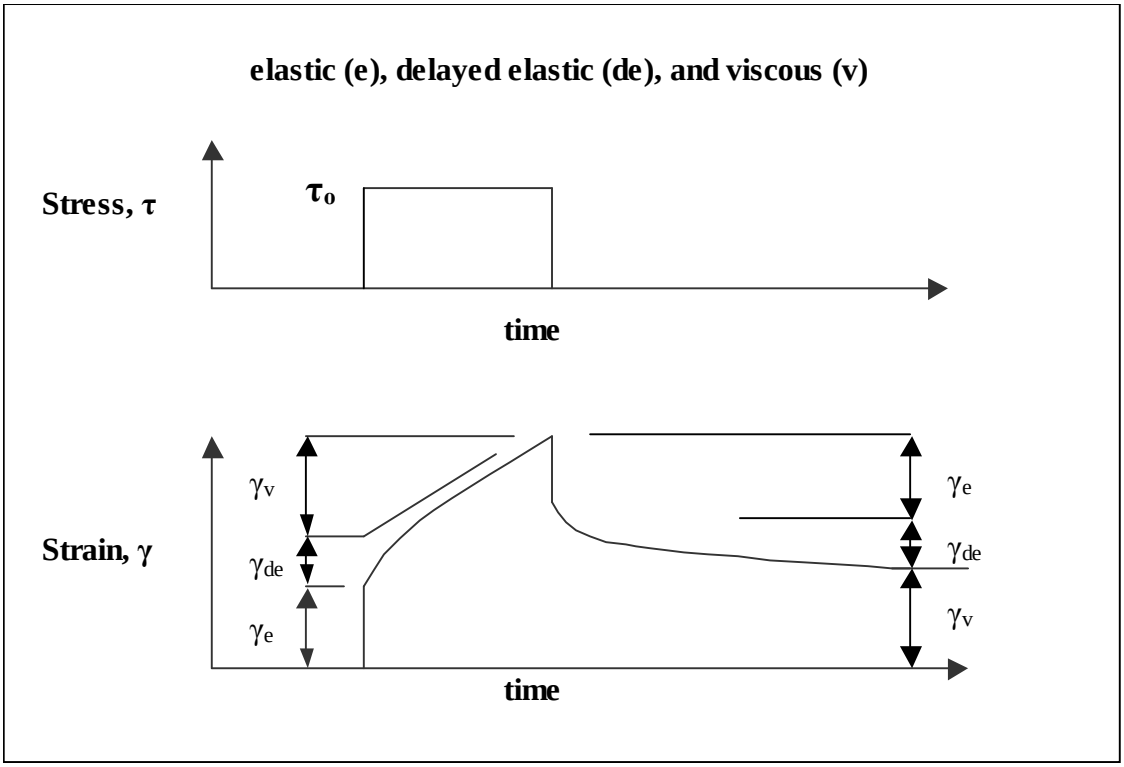

Figure 2.3: Representation of viscoelastic response of bitumen under static loading

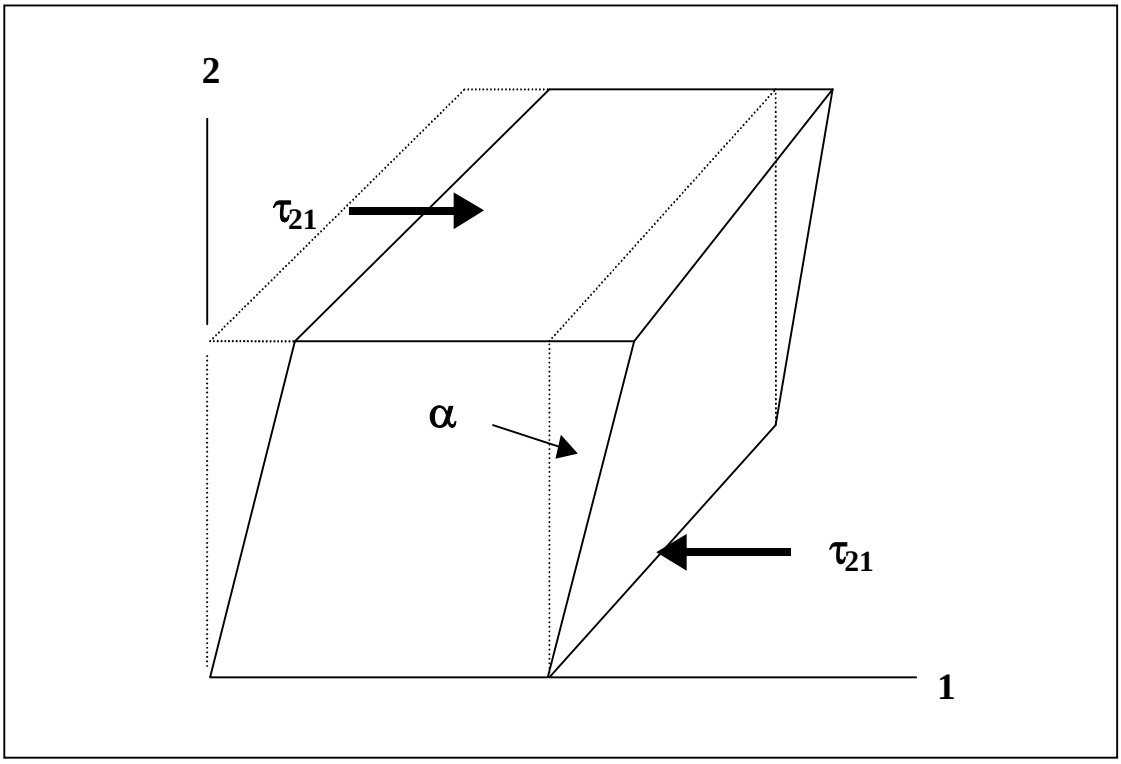

Figure 2.4: Effect of simple shear on a cubical element

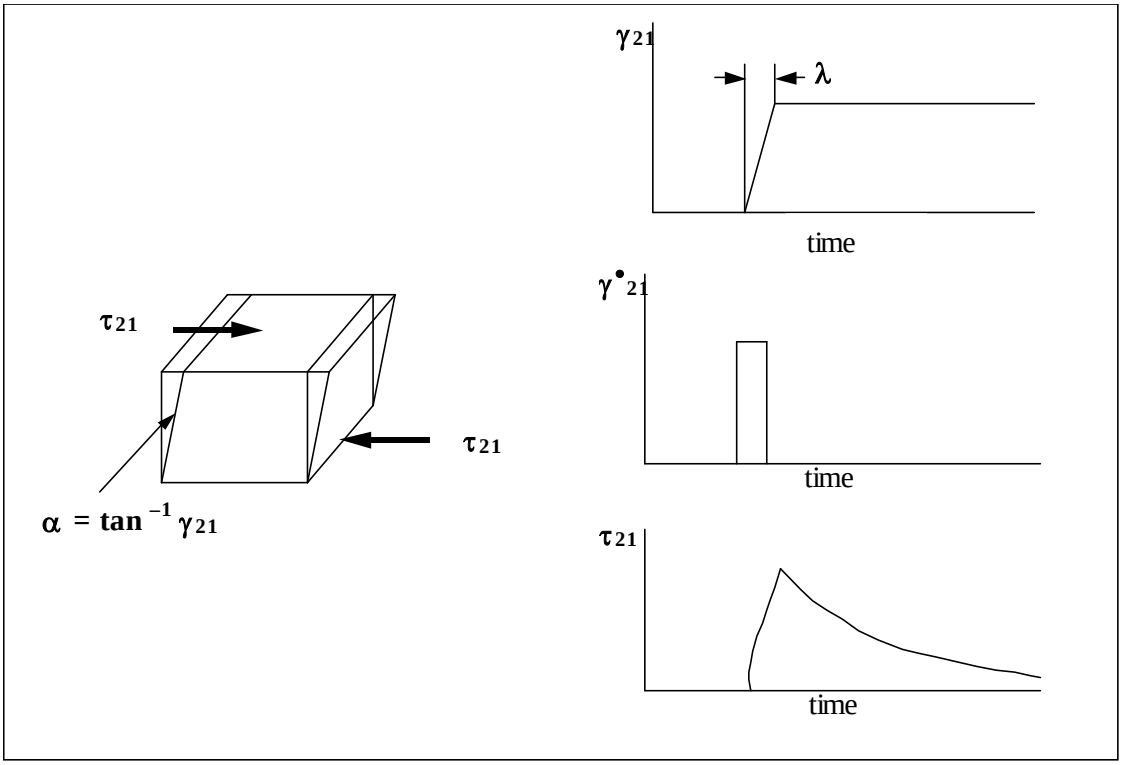

Figure 2.5: Shear stress relaxation following sudden strain

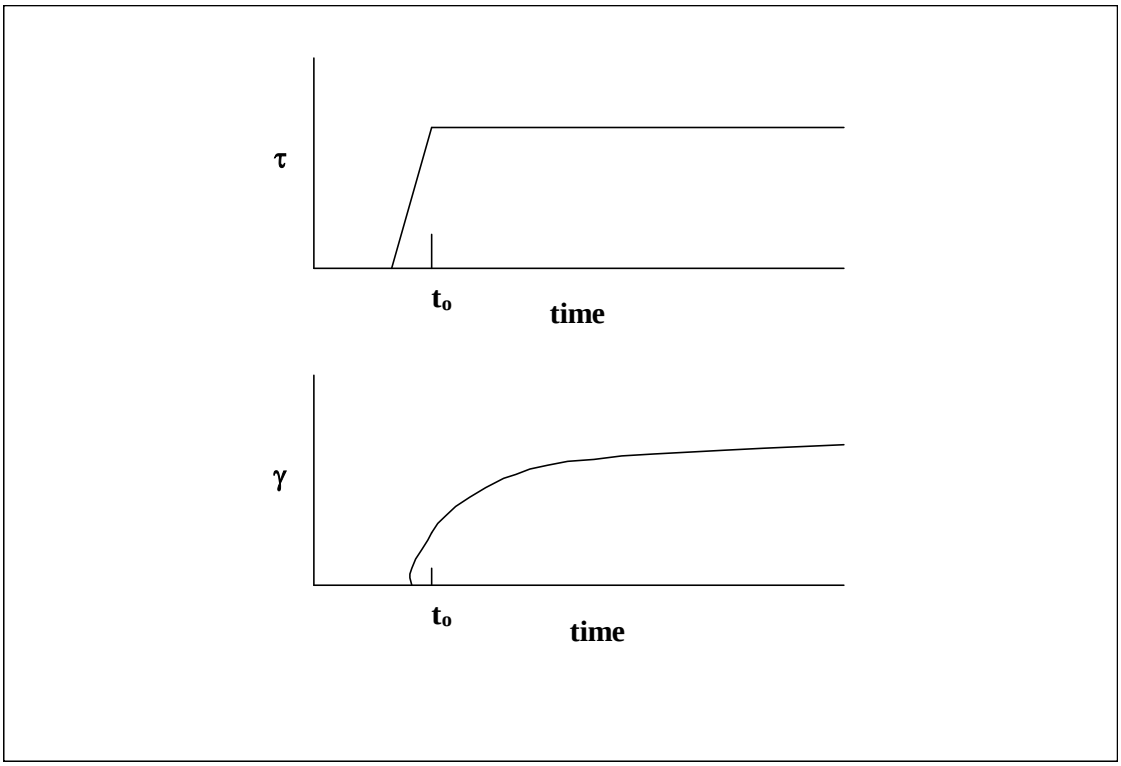

Figure 2.6: Stress and strain graphs for shear creep test

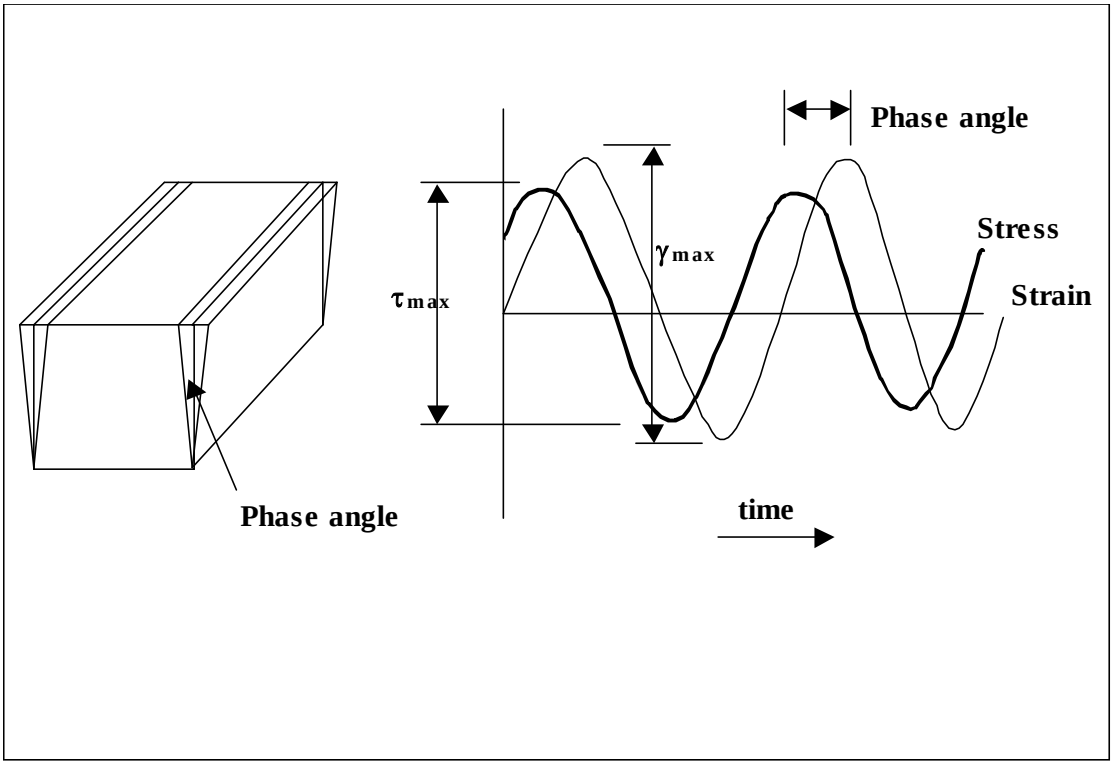

Figure 2.7: Stress-strain relationship with sinusoidally varying shear

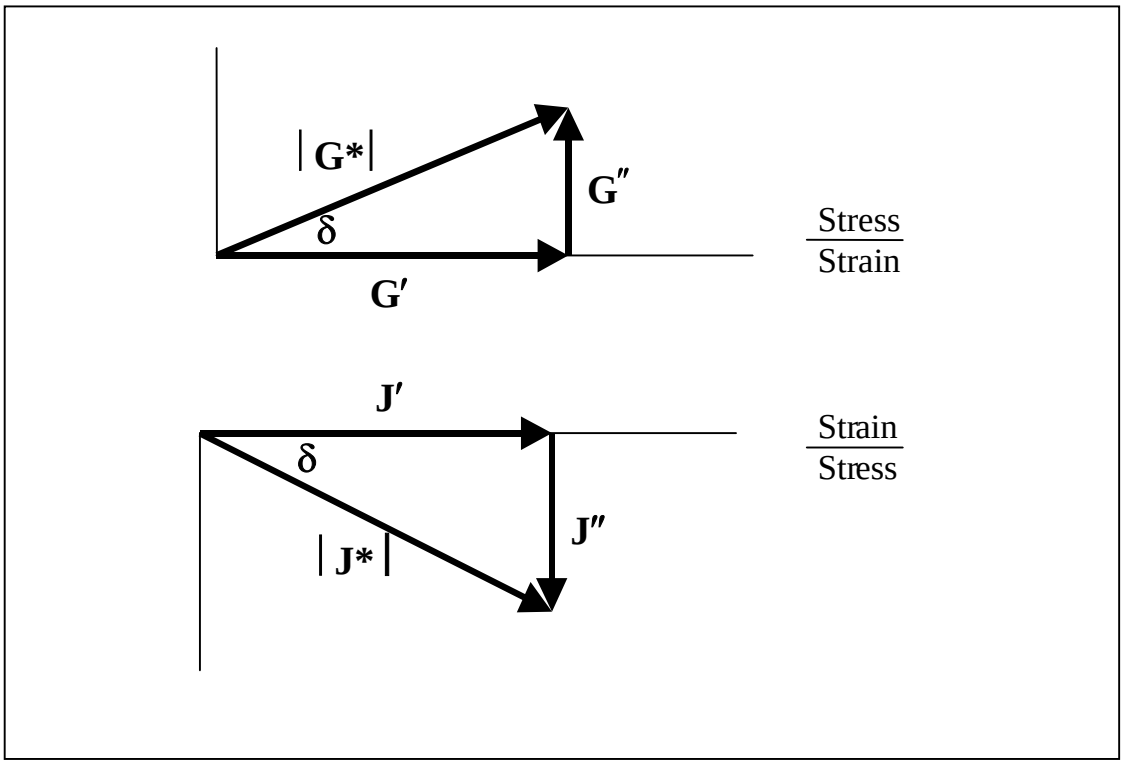

Figure 2.8: Components of complex modulus and compliance in sinusoidal shear deformation

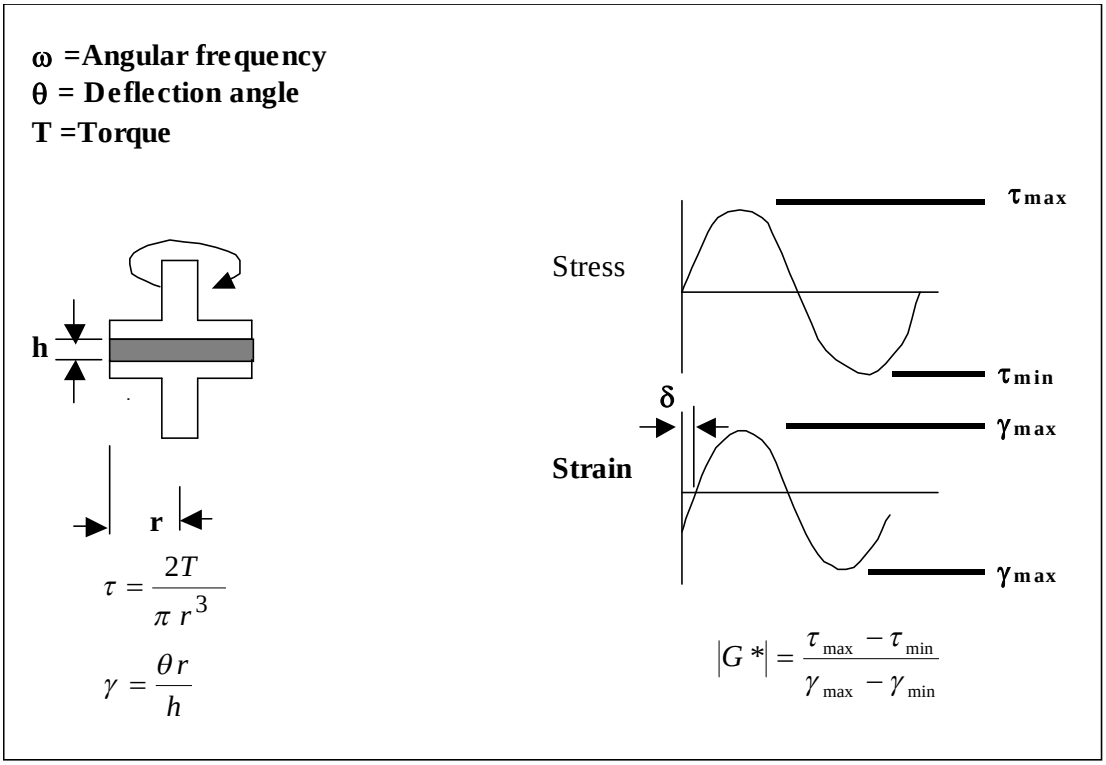

Figure 2.9: Dynamic shear measurements using parallel plate geometry

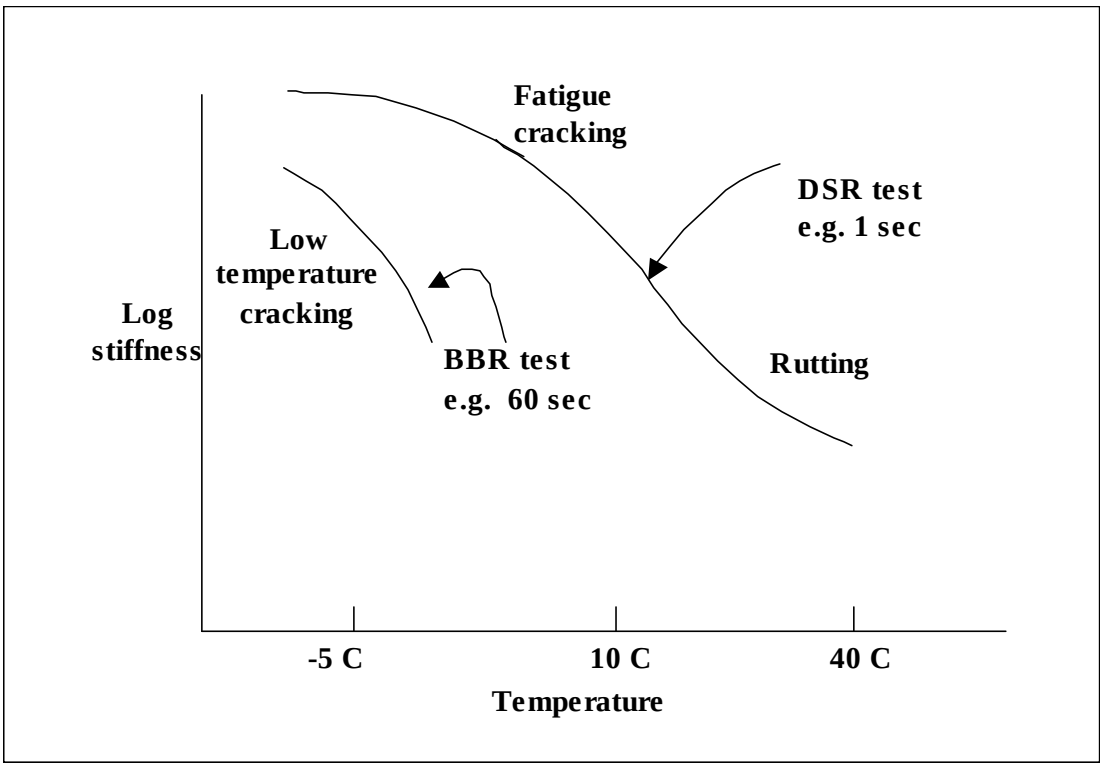

Figure 2.10: General shape of an isochronal plot

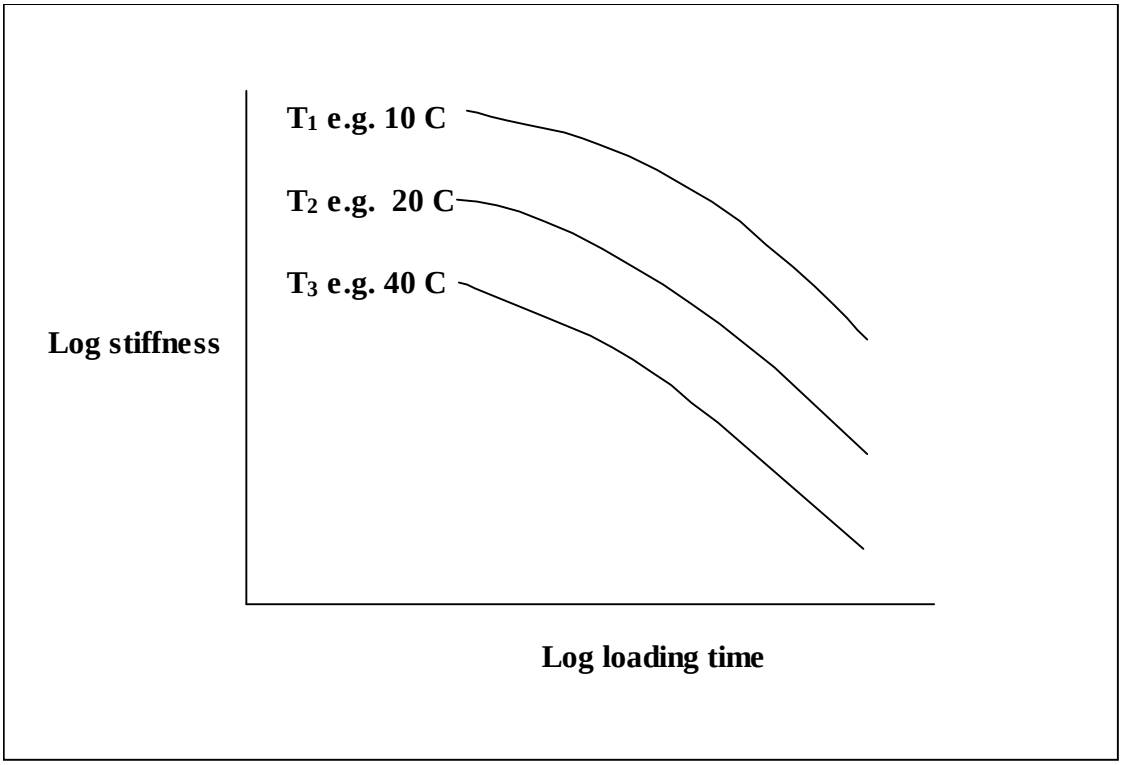

Figure 2.11: General shape of an isothermal plot

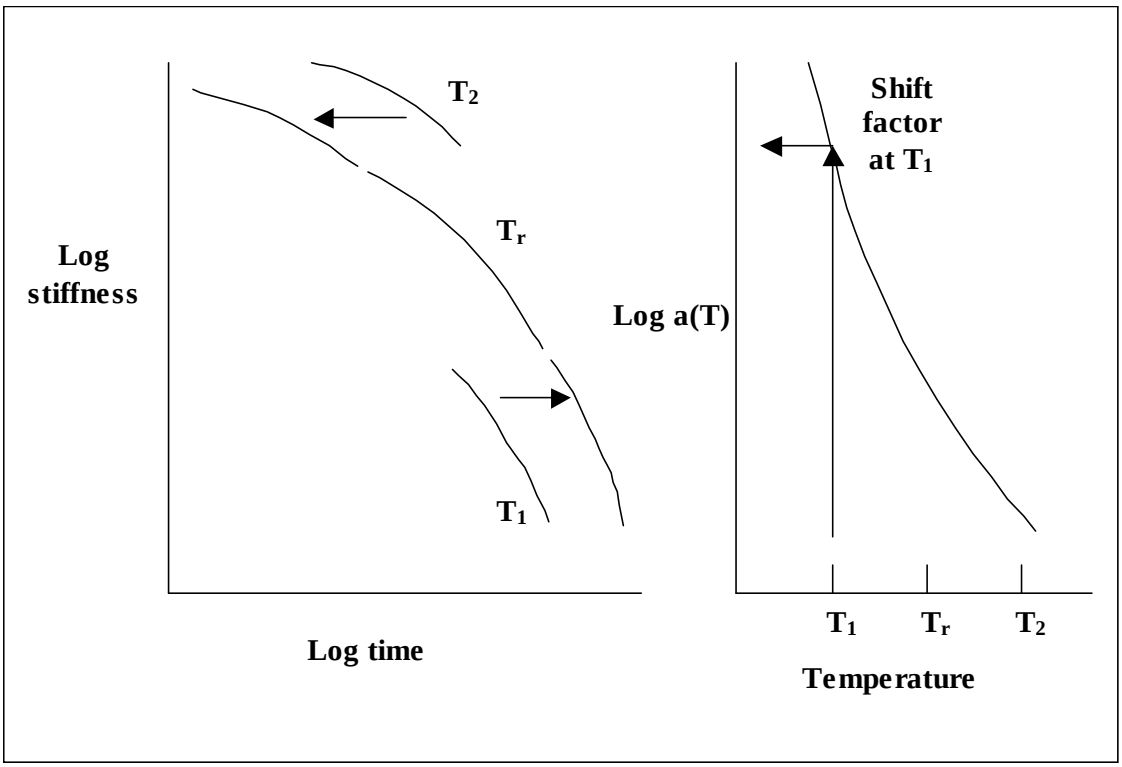

Figure 2.12: Schematic presentation of the construction of a master curve using time temperature superposition

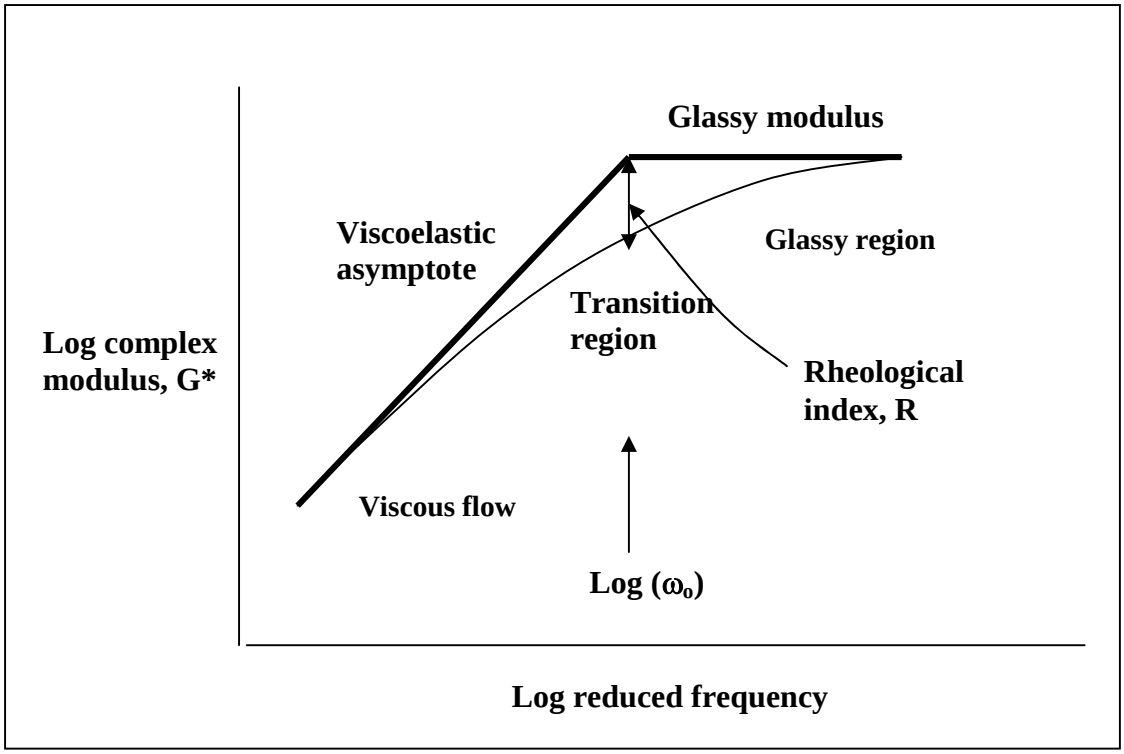

Figure 2.13: Construction of a master curve with dynamic parameters

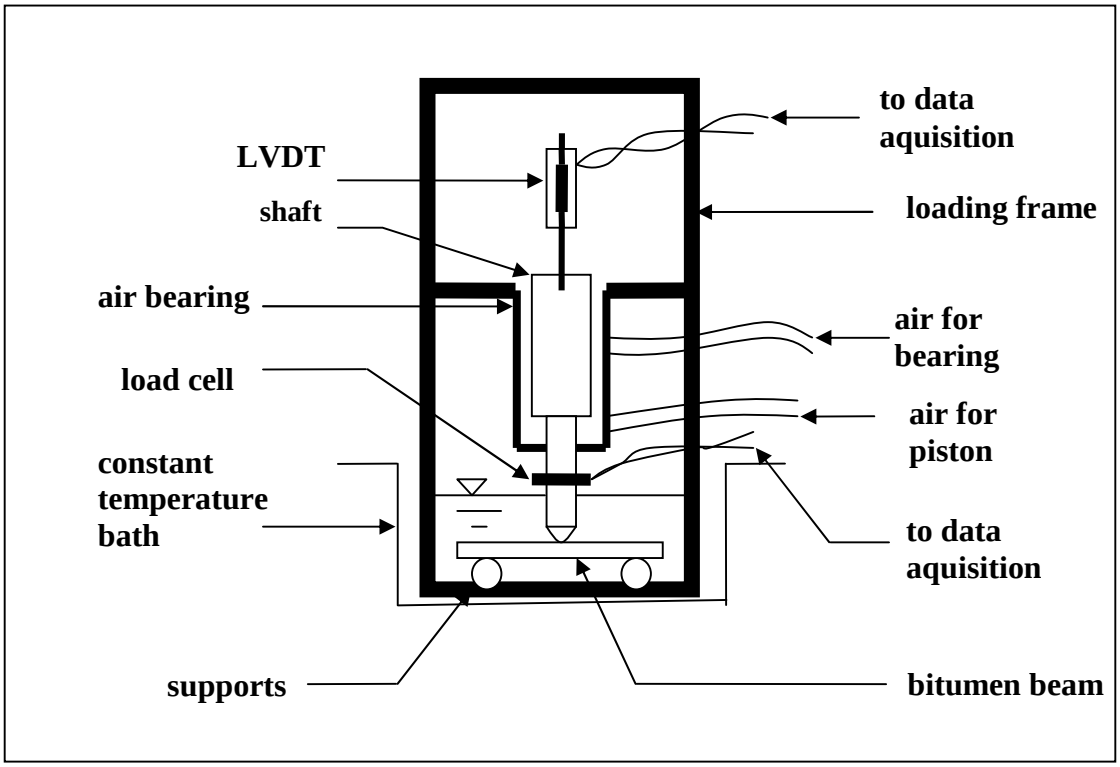

Figure 2.14: Schematic of the Bending Beam Rheometer (BBR)

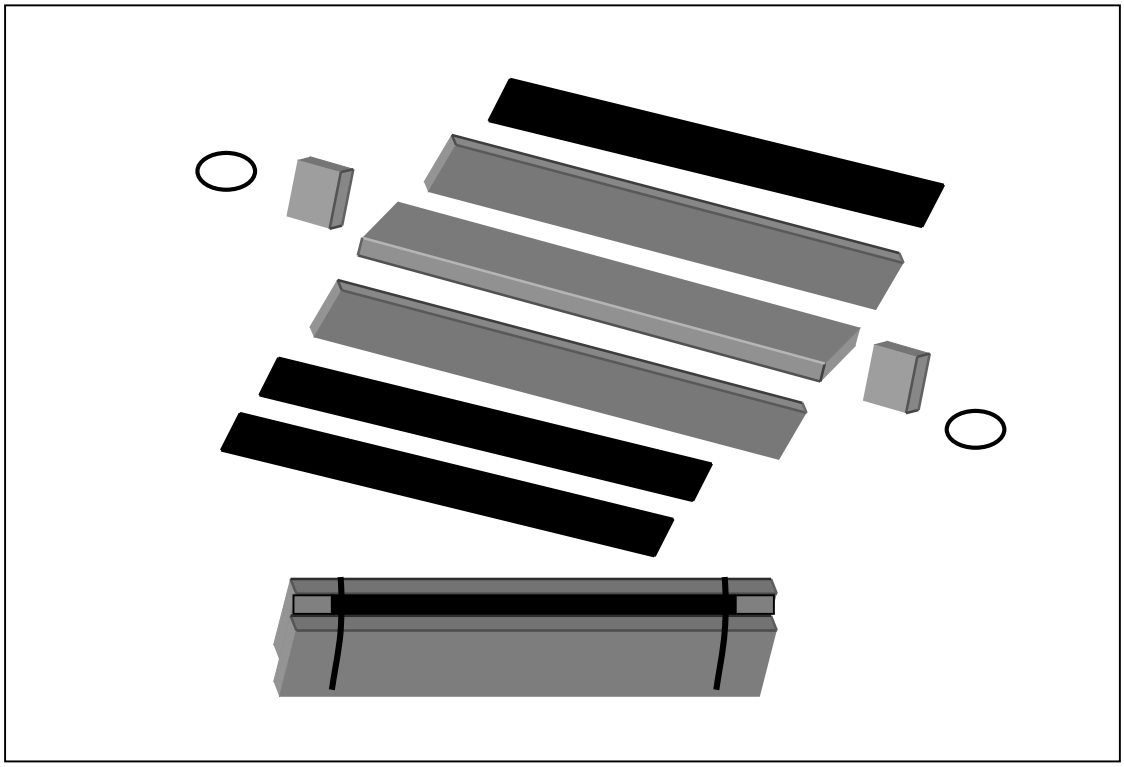

Figure 2.15: Mould used for preparing BBR specimen

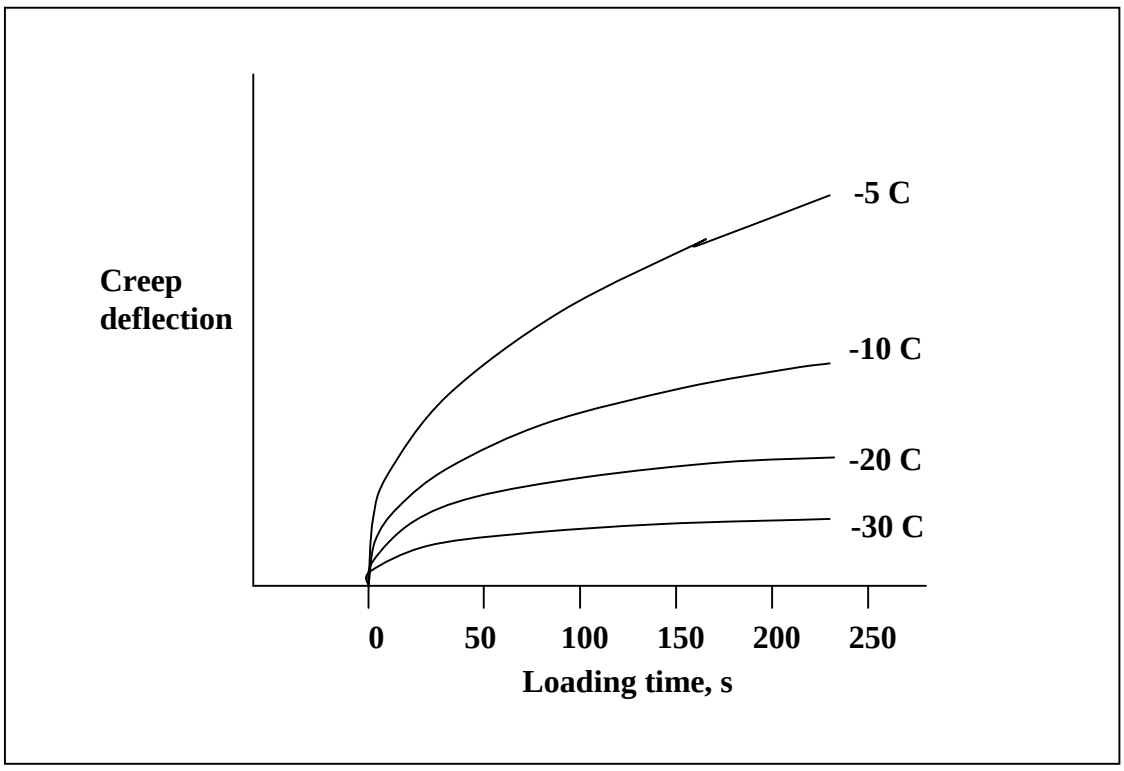

Figure 2.16: Effect of time and temperature on bitumen for the BBR test

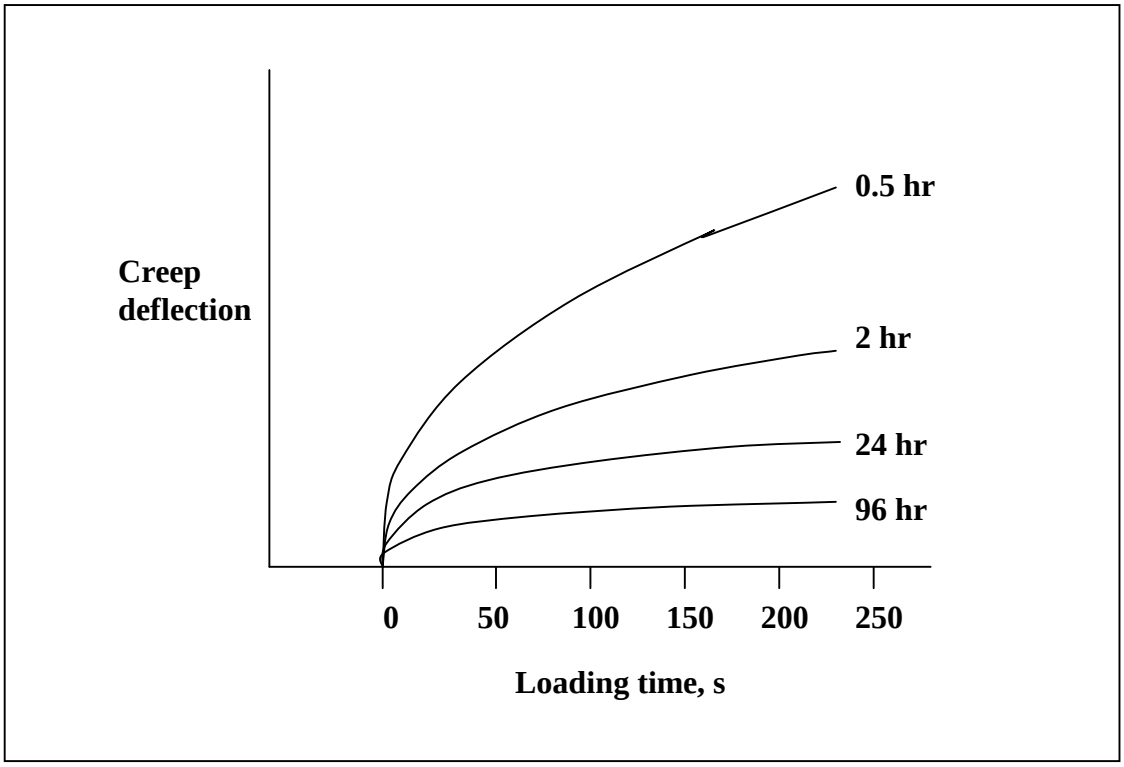

Figure 2.17: Effect of physical hardening on bitumen for the BBR test

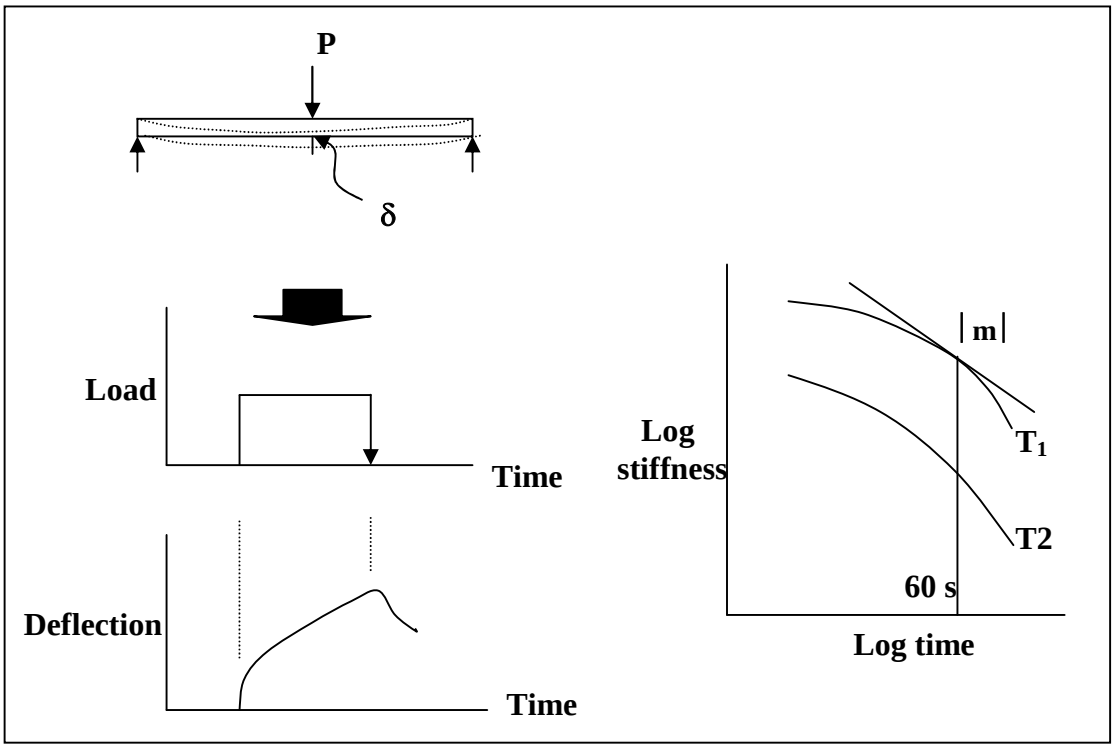

Figure 2.18: Analysis of BBR test results for determining m value

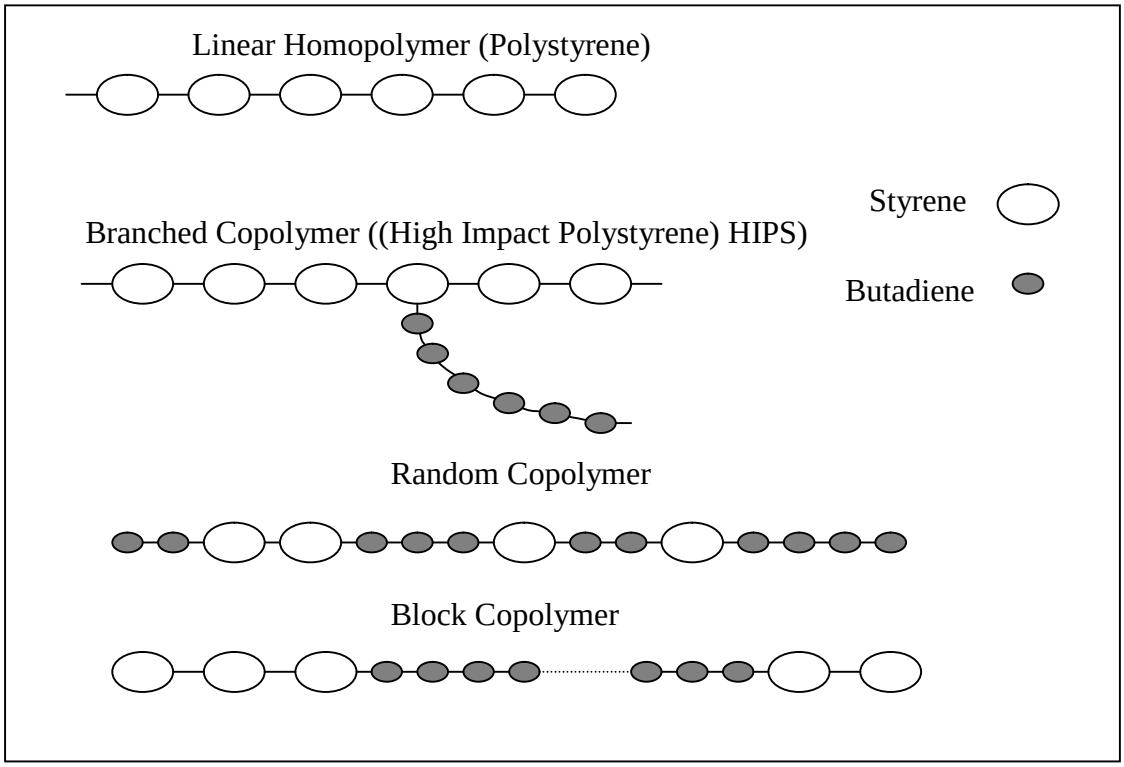

Figure 2.19: Schematic of different structures of polymers [108]

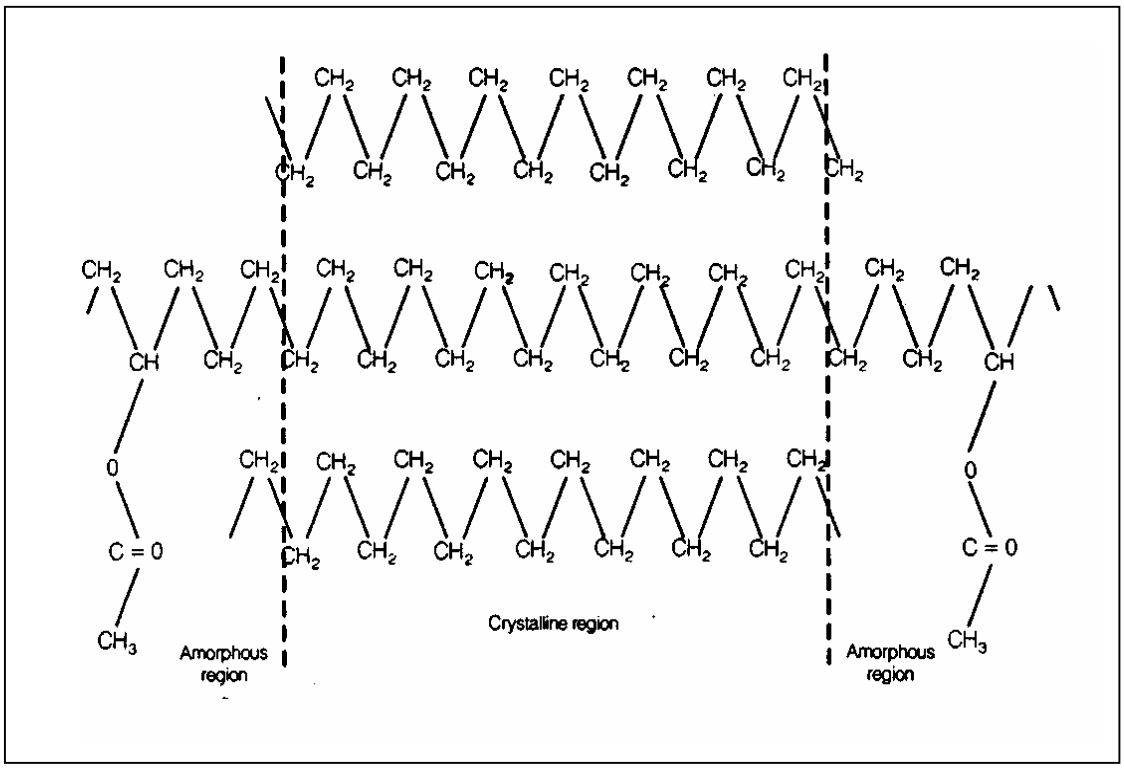

Figure 2.20: Schematic of molecular structure of EVA [110]

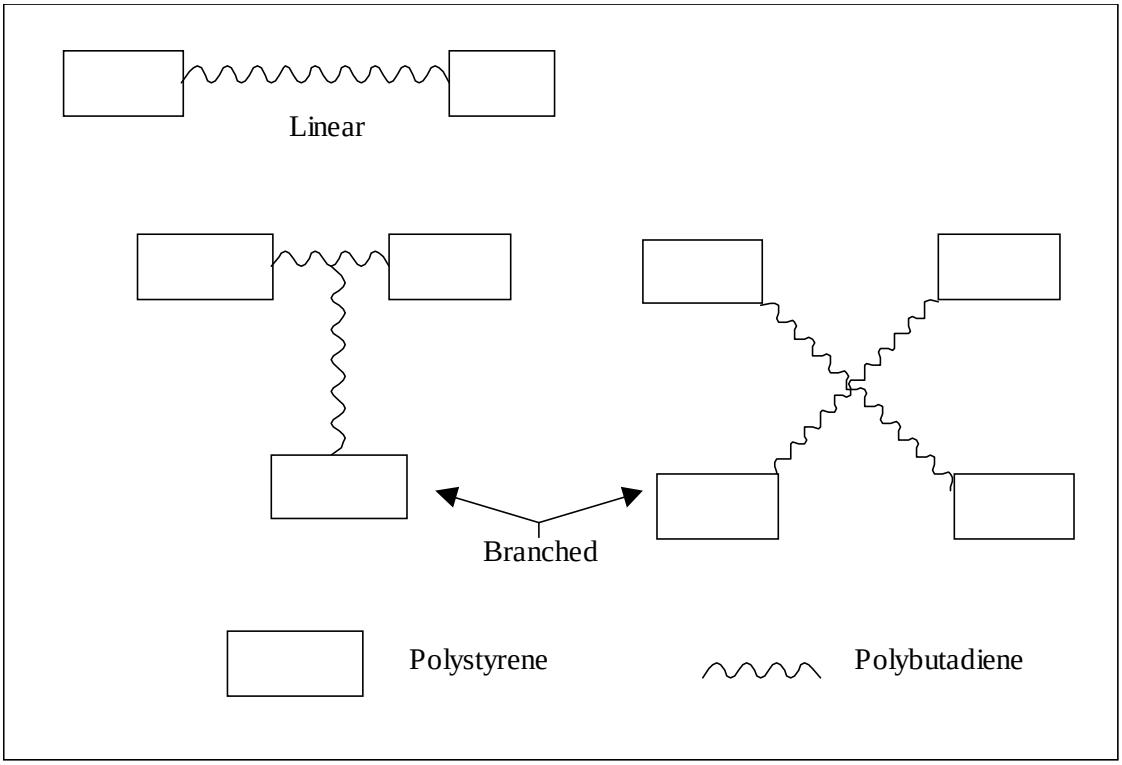

Figure 2.21: Linear and branched structure of elastomeric polymers [110]

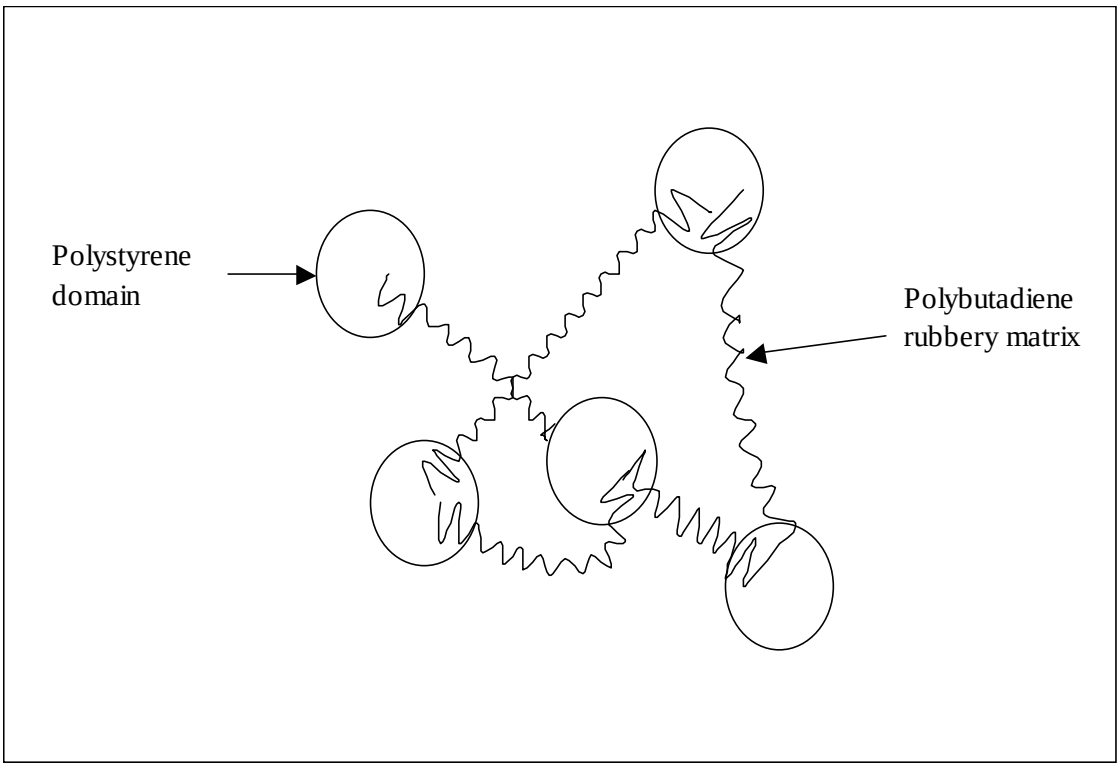

Figure 2.22: Schematic of the structure of SBS elastomers [110]

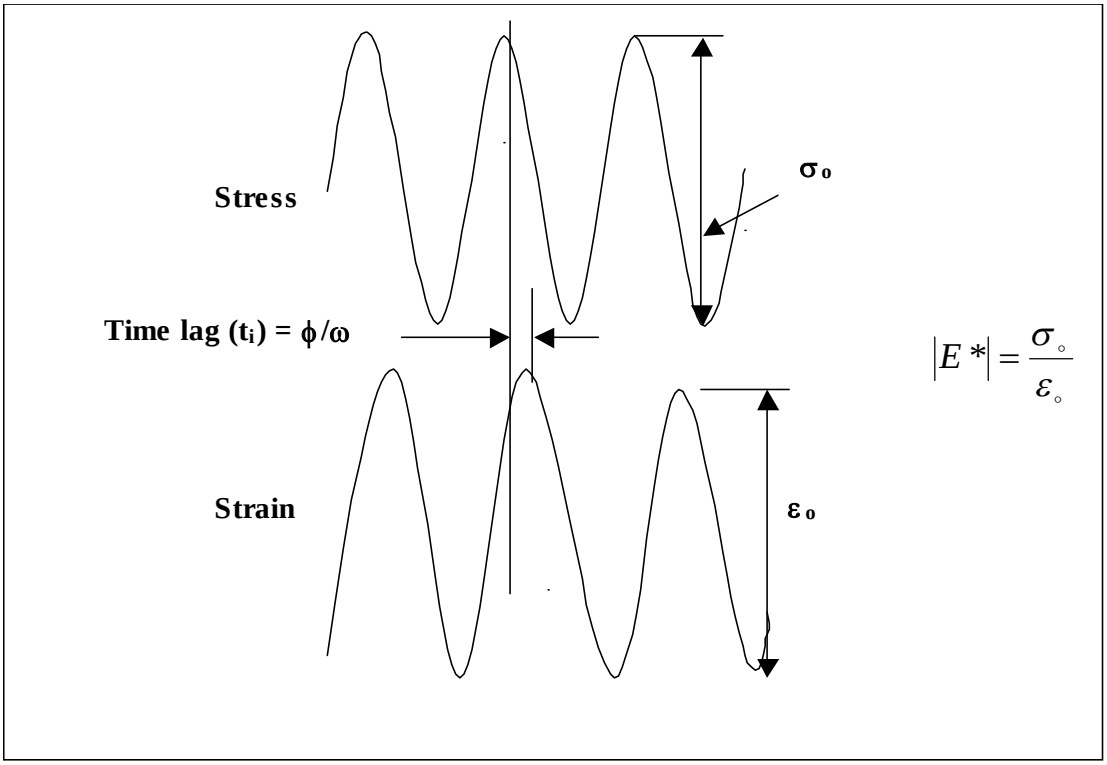

Figure 2.23: Typical plot of stress and strain versus time for a dynamic modulus test

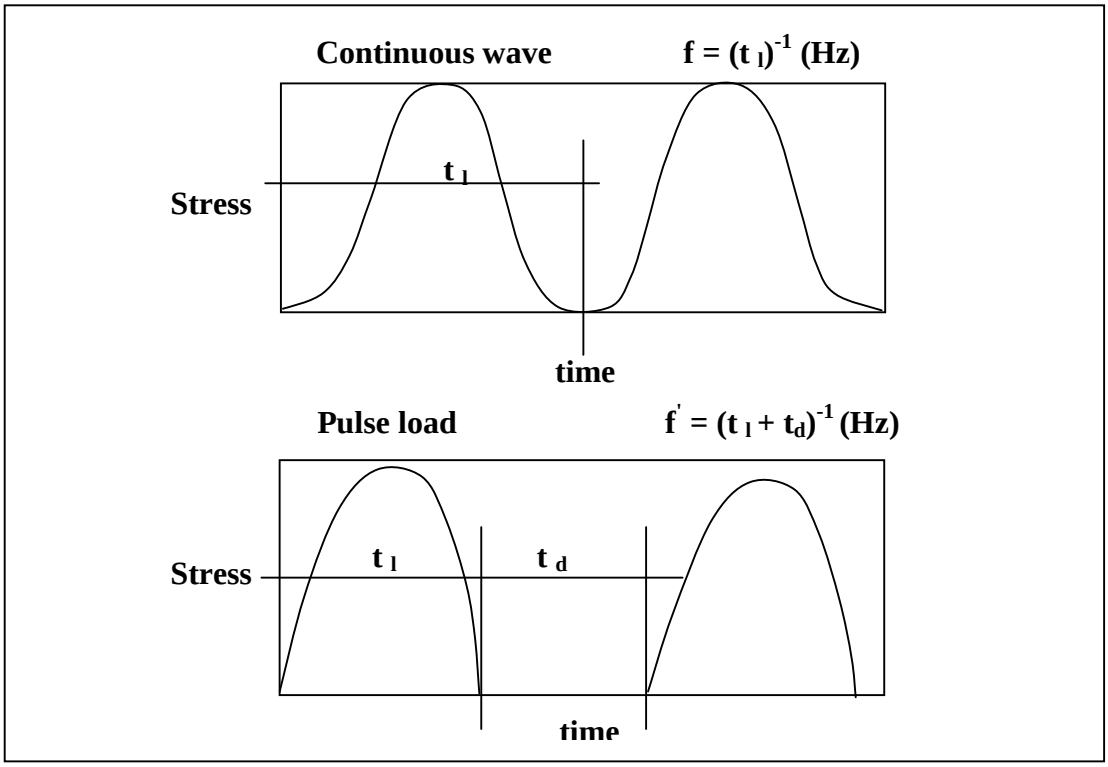

Figure 2.24: Pulse and continuous wave forms used in dynamic testing [113]

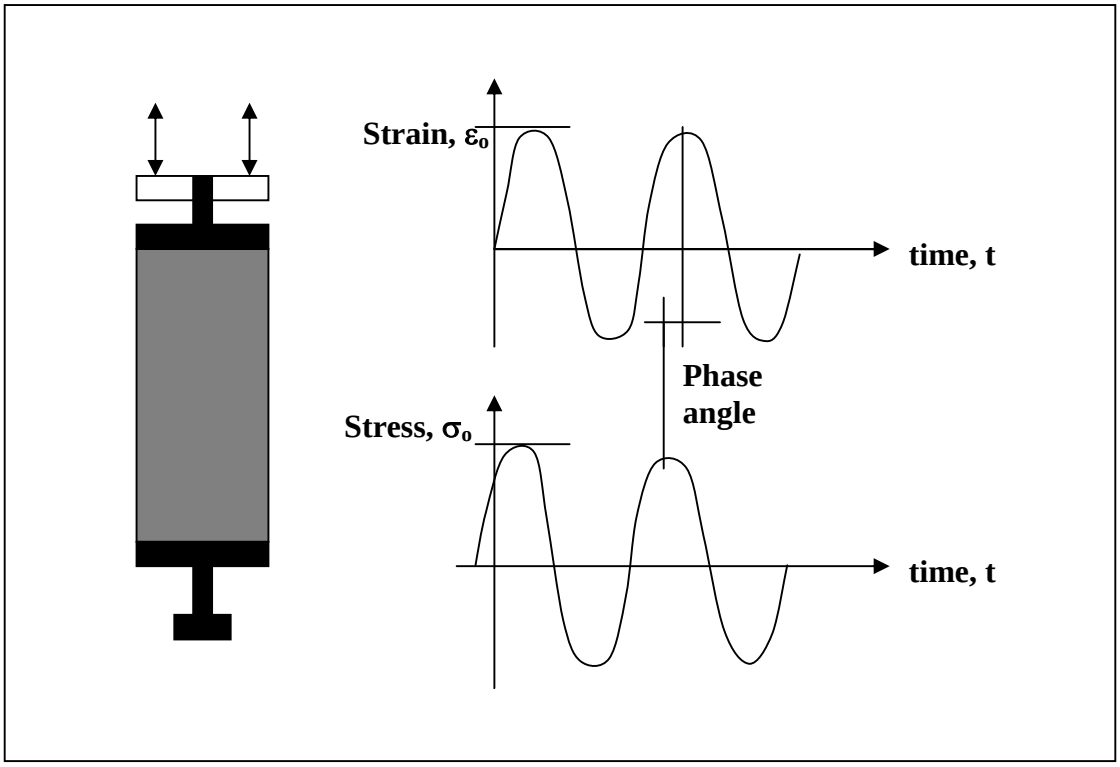

Figure 2.25: Schematic representation of dynamic stiffness modulus test (direct test)

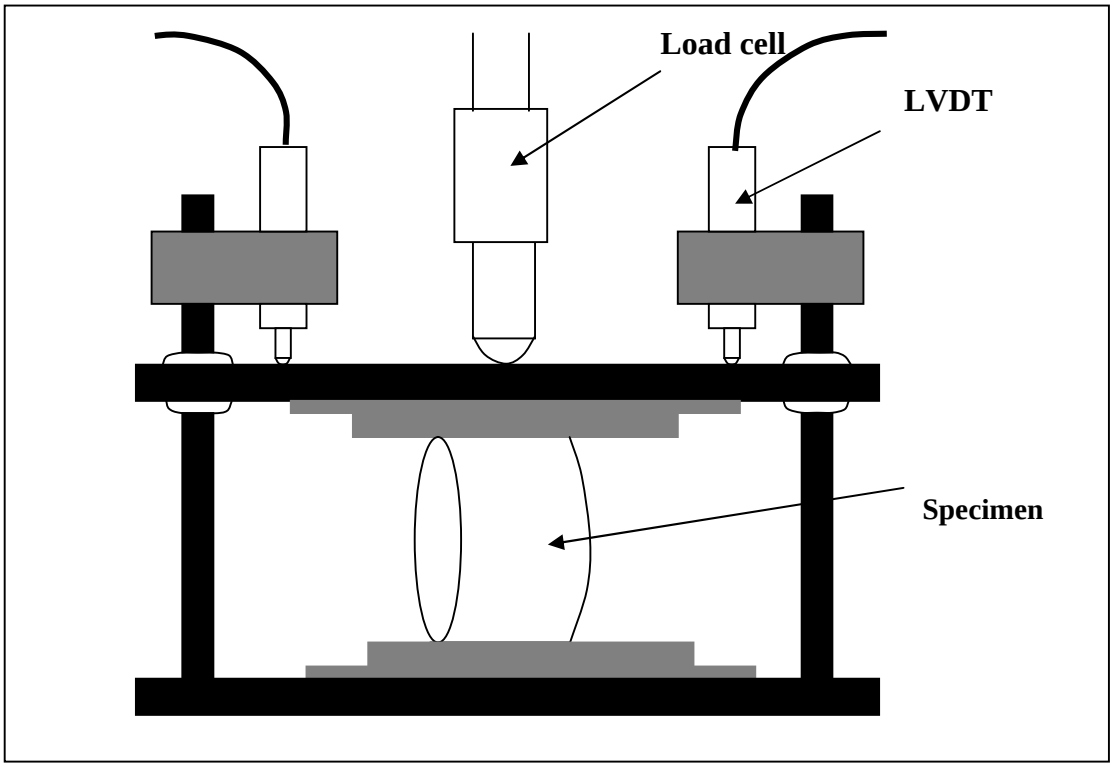

Figure 2.26: NAT indirect tension test

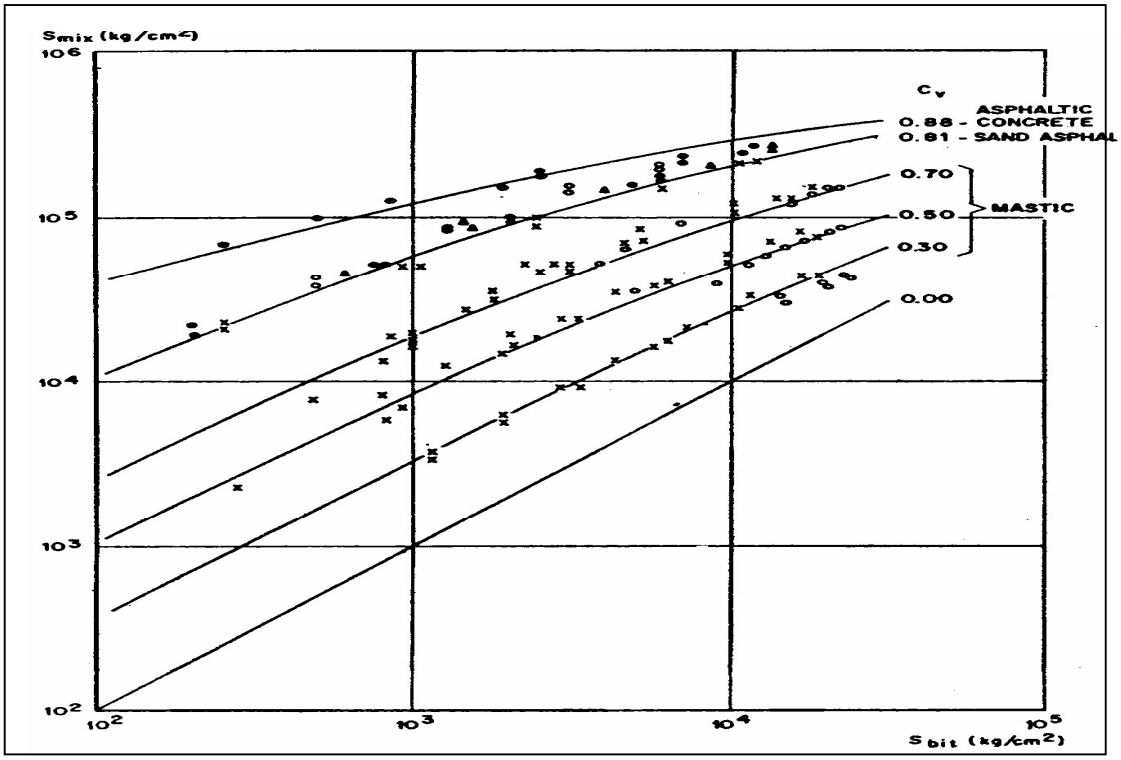

Figure 2.27: Relationship between the stiffness modulus of mixtures and those of the bituminous binder at various volume concentrations of aggregate (Cv) and about 3% air voids [60]

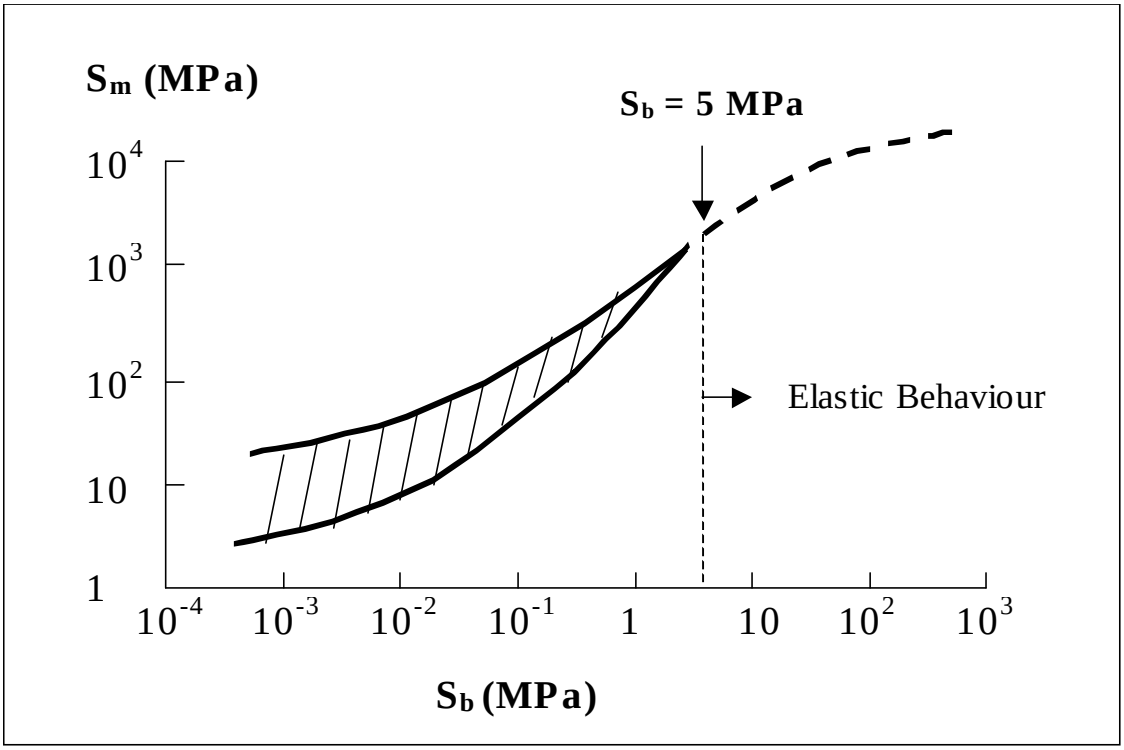

Figure 2.28: The relationship between mixture stiffness and binder stiffness

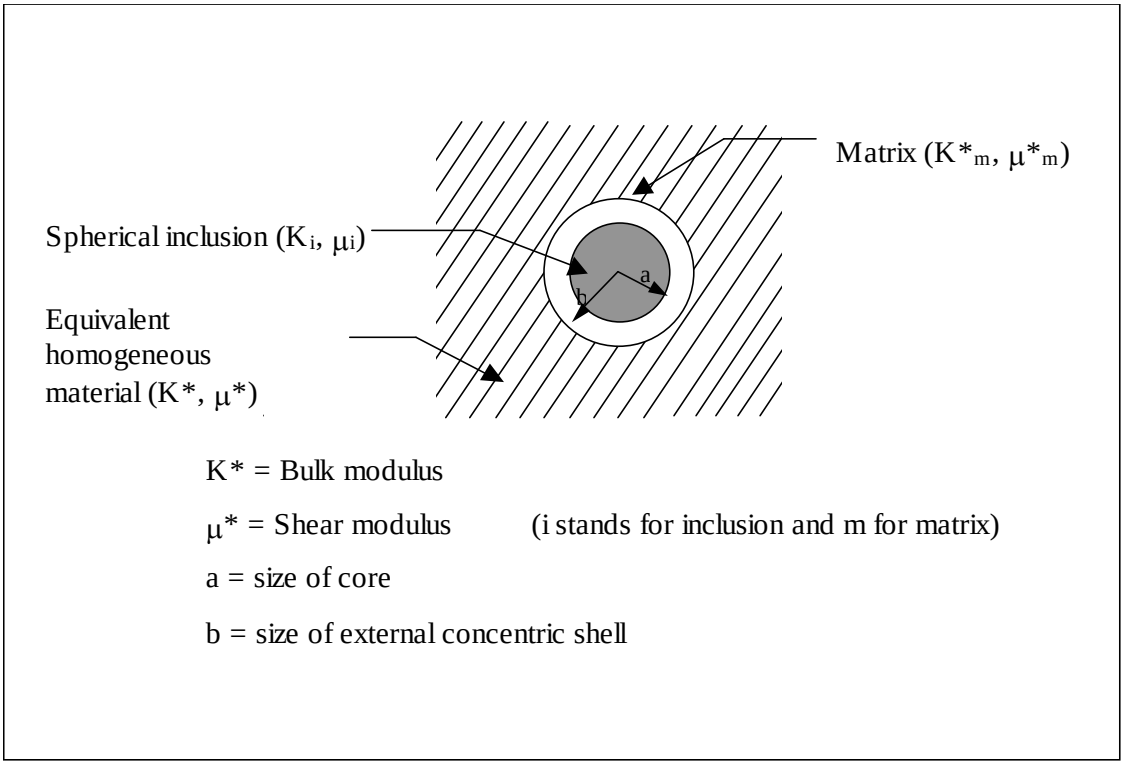

Figure 2.29: Spherical core-concentric shell model

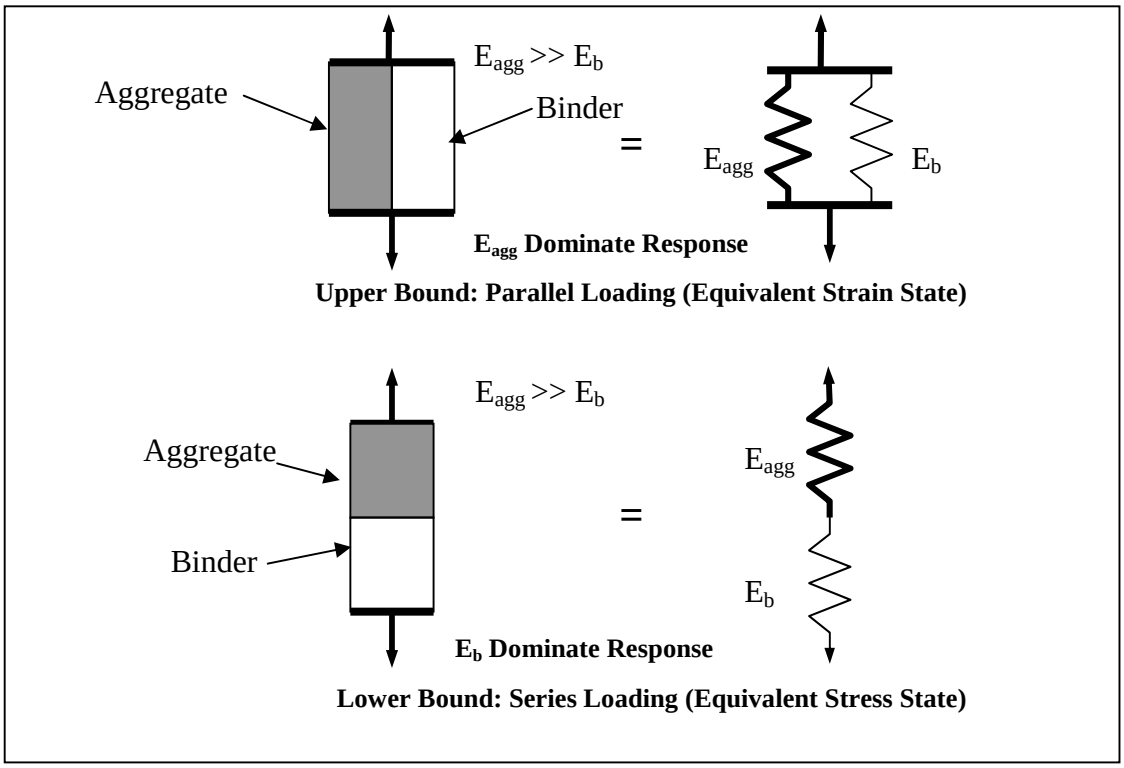

Figure 2.30: Physical representation of bounding relations in the Paul model

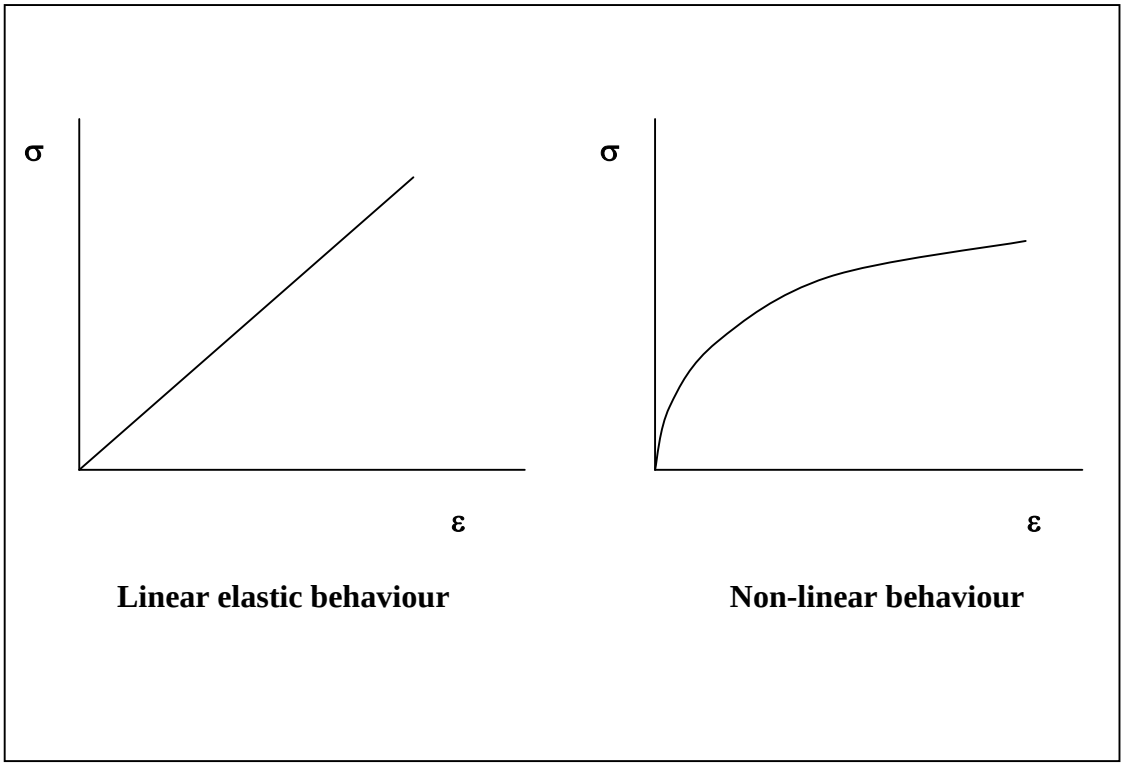

Figure 2.31: Schematic of strain-stress relationships for linear and non-linear behaviour of materials

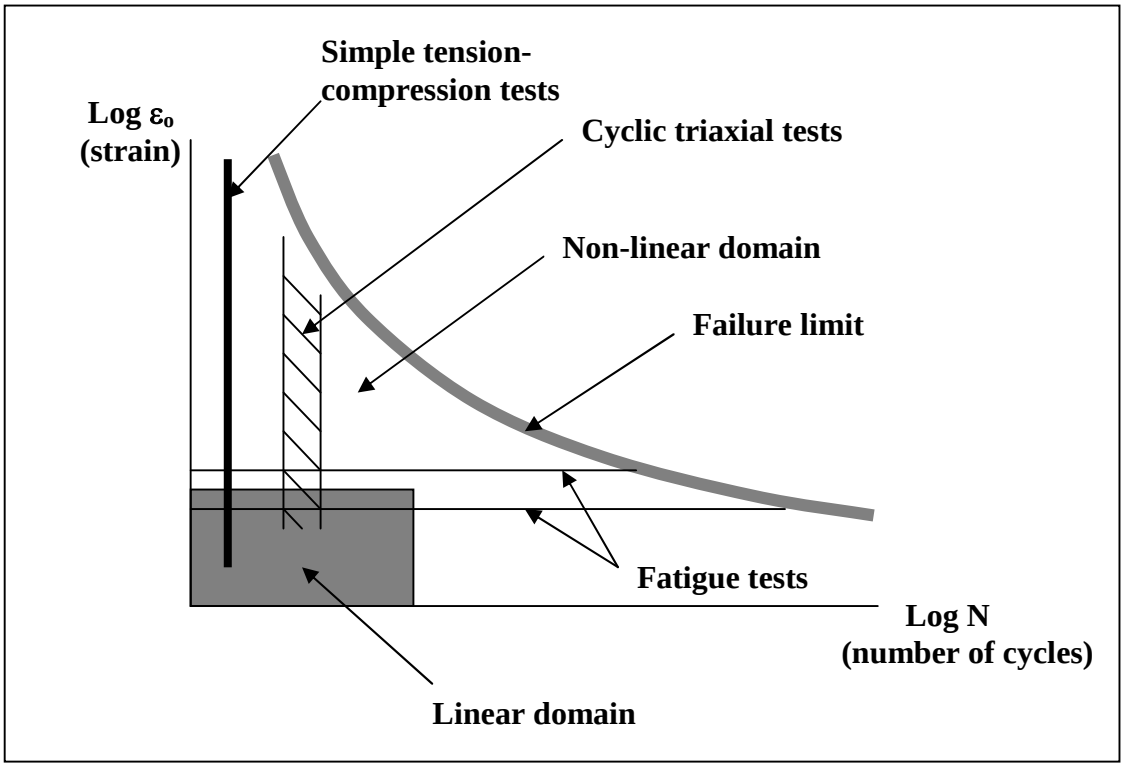

Figure 2.32: Schematic presentation of linear and non-linear behaviour of asphalt mixtures

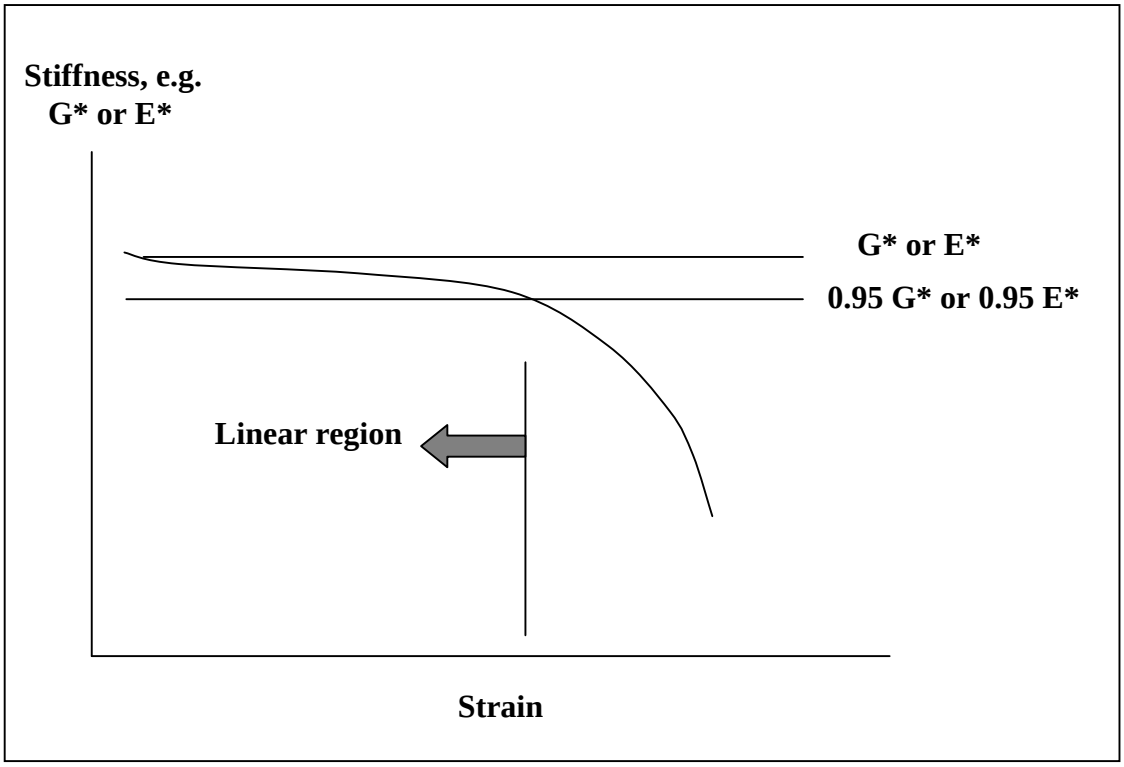

Figure 2.33: Determining the linear region using strain sweeps

Chapter 3

STRESS-STRAIN DSR LIMITATIONS AND SAMPLE PREPARATION METHODS

3.1 Introduction

The viscoelastic behaviour of bitumen is far too complex to be described by simple traditional measures of consistency such as the penetration and softening point tests. Therefore, new test instruments such as the Dynamic Shear Rheometer (DSR) and Bending Beam Rheometer (BBR) have been developed to provide rheological data on bitumen over a wide range of environmental conditions. The DSR can be considered to be the most complex and powerful instrument for characterising the flow properties of bitumen. However, DSRs, like any other testing instrument, have their design and operational limitations and the instrument operator must be aware of these limitations and must select operating conditions that will provide reliable and repeatable results.

One of the most important factors, which can have a significant effect on DSR test results, is the sample preparation method. In order to obtain accurate and repeatable results, it is important to select a reliable and robust sample preparation method, that can be used for both unmodified and modified bitumens.

The experimental work explained in this chapter has been divided into two main areas. The first area of study describes the operational limitations of the DSR in terms of applied stress levels and recoverable strain levels. A large number of tests at different target strain levels and temperatures were undertaken and the stress/strain limitations of the apparatus were determined. The second area of study investigated the influence of different sample preparation methods on the rheological parameters measured with the DSR, particularly the repeatability of the test results.

3.2 Stress-Strain Limitations of the DSR

3.2.1 Testing Programme

A large number of rheometers are currently commercially available, ranging in capability and price. Nonetheless, the basic rheological principles are the same. The rotational oscillatory rheometer, which is used in this investigation, is the Bohlin DSR. In order to study the stress-strain limitations of this instrument, DSR tests were performed on conventional 50 pen bitumen under the following test conditions:

- Mode of loading: Controlled-strain,
- Temperatures: 10, 25, 40 and 75°C,
- Frequencies: 0.01, 0.05, 0.1, 0.2, 0.3, 0.5, 1, 2, 3, 5, 10 and 15 Hz,
- Strain amplitude: 0.05 to 20%.

Parallel plate geometries with diameters of 8 mm and 25 mm were used for the temperature ranges of 10 to 40°C and 40 to 75°C, respectively. At the beginning of each test, the DSR plates were heated to 60˚C. The bitumen, which was heated to its softening point plus 100˚C, was then placed on the bottom plate in sufficient quantities to cover the entire surface. The top plate was then lowered to a preset gap (1 mm for the 25 mm diameter spindle and 2 mm for the 8 mm diameter spindle) to establish contact with the bitumen and the excess bitumen was trimmed around the circumference of the parallel plates. Tests were performed in an oscillatory mode and sinusoidal stresses and strains were measured.

Frequency sweep tests were performed in the controlled strain mode, over the entire range of temperatures and strain levels as described above. Prior to any measurements, the test specimen in the DSR was allowed to equilibrate at testing temperature for approximately 10 minutes.

3.2.2 Results and Discussions

The DSR, like every other instrument, has some operational limitations and it is important for the operator to understand these limitations. These limitations usually relate to the upper and lower limits of torque or angular deflection. Since the DSR records only two measurements, i.e. torque and angular rotation, all other results (e.g., strain and G*) are calculated from these two measurements. Therefore, it is essential that the limits for these measurements are carefully monitored. To study these limitations, the complex modulus, phase angle, strain and stress were measured under different conditions of temperature, frequency and strain level. The values of complex modulus, phase angle, strain and stress versus frequency were then plotted in the form of isothermal plots. As an example, a plot of strain versus frequency is shown in Figure 3.1. It can be seen from this graph that with the exception of a few points, the strain amplitude remains constant during controlled strain testing for a wide range of strain and frequency values.

The plot of stress versus frequency at 40°C is shown in Figure 3.2. This graph shows that a stress plateau exists at low frequencies and strain levels, (0.1% strain with 25 mm pp and 0.05% and 0.1% strain with 8 mm pp).

The reasons for this behaviour can be explained with the aid of the following equations, which are used to calculate stress and strain during the DSR testing.

$$\tau = \frac{2T}{\pi \times r^3} \qquad \textbf{(3.1)}$$

$$\gamma = \frac{\theta \times r}{h} \qquad \textbf{(3.2)}$$

$$\tau = G \times \gamma \qquad \textbf{(3.3)}$$

Where: τ = stress

T = torque

r = spindle radius

γ = strain

θ = rotational angle of spindle

h = bitumen thickness

G = shear modulus

Equation 3.3 states that there is a linear relationship between stress and strain. In other words, at a certain value of complex modulus the DSR needs to apply a lower stress level to achieve a lower strain level. There also exists a linear relationship between the torque applied by the DSR and stress according to Equation 3.1. This means that the torque applied by the instrument should be low in order to produce a low stress level. However, because of the limitations of instrument, the DSR cannot apply torque values below the minimum torque level of the instrument. With increasing frequency, the complex modulus of bitumen increases and the DSR needs to apply higher stress levels to achieve the constant strain level. Consequently, the torque applied by the instrument also needs to increase and once this value becomes larger than the minimum torque, stress begins to increase. As stress is indirectly related to the radius of spindle as shown in Equation 3.1, lower stress levels can be achieved with the 25 mm spindle than the 8 mm spindle. In other words, using 25 mm spindle for testing at lower strain levels is better than using the 8 mm spindle.

The DSR also has testing limitations at high stress levels. As shown in Figure 3.2, there is a plateau region of stress for the high strain levels at high frequencies (corresponding to high complex modulus values). The reason for such behaviour is similar to the reasons given for the low stress limitations, and can be explained by Equations 3.1 to 3.3. Equation 3.3 states that the DSR needs to apply higher stress levels to achieve higher strain levels at a certain value of complex modulus. Equation 3.1 also shows that there is a linear relationship between applied torque and stress and therefore the torque applied by the instrument should be higher to produce a high stress level. However, as the DSR cannot apply torque values above the maximum torque level, the stress remains constant (decrease in strain).

Once the DSR stress and strain limitations have been identified they can be easily accommodated and Table 3.1 summarizes the solutions to these problems by changing either the plate diameter or the target percentage strain amplitude.

Table 3.1: Solutions for DSR Torque Limitations

Problem	Solution
Maximum Torque Limit Exceeded	Reduce Plate Diameter Reduce Strain Amplitude
Minimum Torque Limit Exceeded	Increase Plate Diameter Increase Strain Amplitude

3.3 Sample Preparation

3.3.1 Sample Preparation Methods

The increased interest in fundamental rheological measurements, as a result of the research undertaken during SHRP, has lead to the generation of a large number of new DSR testing specifications, standards and protocols [8, 11, 13, 85]. Based on these documents, a number of sample preparation methods were identified, namely:

- Methods A, B and C as described in Clause 928 of the UK Specification for Highway Works [11],
- Methods 1, 2 and 3 as described in the SHRP DSR Protocol [85],
- Alternatives 1 and 2 as described in the AASHTO Standard Method of Test [13] based on the work of the SHRP asphalt research programme,
- Methods A and B as described in the Institute of Petroleum (IP) Standard [8],
- The method employed by Scott Wilson Pavement Engineering [58], and
- The method described in the University of Nottingham's DSR Testing Protocol [16].

Broadly speaking, all these sample preparation methods can be reduced to three main methods, described as:

- The Hot Pour Method,
- The Silicone Mould Method, and
- The Weighing (Mass) Method.

Prior to evaluating these three sample preparation methods, bulk quantities of the two bitumens were heated to a temperature approximating the bitumen's softening point temperature (see Table 3.2) plus 100°C (as recommended in the IP Standard [8]). The bitumen was then stirred to ensure homogeneity (especially important for PMBs) and then either poured into approximately 10 ml vials, which were then sealed and stored for later testing, or used immediately in one of the sample preparation methods.

Table 3.2: Standard specification parameters of the two bitumens

Bituminous Binder	Penetration (dmm)	Softening Point (°C)
50 pen bitumen	49	52.0
Radial SBS PMB	61	73.0

3.3.1.1 Hot Pour Method

The hot pour method is based on Method A of the Specification for Highway Works [11], Method A of the IP Standard [8], Methods 1 and 3 of the SHRP DSR Protocol [85], Alternative 1 of the AASHTO Standard [13] and the University of Nottingham's DSR Protocol [16].

The method consists of setting the gap between the upper and lower spindles to a height of 50 μm plus the require testing gap, either at the proposed testing temperature or at the mid-point of an expected testing temperature range. Once the gap has been set, a sufficient quantity of hot bitumen (typically 100°C to 150°C) is poured onto the bottom (lower) plate of the DSR to ensure a slight excess of material appropriate to the chosen testing geometry. The upper plate of the DSR is then gradually lowered to the required nominal testing gap plus 50 μm. The bitumen that has been squeezed out between the plates is then trimmed flush to the edge of the plates using a hot spatula or blade. After trimming, the gap is closed by a further 50 μm to achieve the required testing gap as well as a slight bulge around the circumference of the testing geometry (periphery of the test specimen).

3.3.1.2 Silicone Mould Method

The silicon mould method is based on Method B of the Specification for Highway Works [11], Method B of the IP Standard [8], Method 2 of the SHRP DSR Protocol [85] and Alternative 2 of the AASHTO Standard [13].

The method consists of pouring hot bitumen (typically 100°C to 150°C) into either a 8 mm or 25 mm diameter silicone mould of height approximately 1.5 times the recommended testing gap for the two geometries, namely 3 mm and 1.5 mm for the 8 mm and 25 mm geometries respectively. As with the hot pour method, the testing gap is set at a height of 50 μm plus 1 mm or 2 mm. Once the bitumen has cooled, either by means of short-term refrigeration or natural cooling, the bitumen disc (typically at ambient temperatures) is removed from the mould and centred on the lower plate of the DSR. The upper plate is then lowered to the required gap plus 50 μm, the excess bitumen trimmed with a hot spatula and the gap further closed to its final testing height.

The methods described in the Specification for Highway Works [11] and the IP Standard [8] do not prescribe any trimming of the specimen thereby implying that the specimens are either moulded to the required testing gap or cut to size before being mounted in the DSR. This will inevitably increase the variability associated with this method resulting from inaccurate centring of the specimen and possible lack of adhesion between the plates and the bitumen.

3.3.1.3 Weighing (Mass) Method

The weighing method is based on Method C of the Specification for Highway Works [11], Method B of the IP Standard [8] and the method employed by Scott Wilson Pavement Engineering [58].

For the weighing method the testing gap is set at exactly 1 mm or 2 mm for the 25 mm and 8 mm diameter spindles respectively. A pre-calculated amount (mass) of hot bitumen (typically 100°C to 150°C) is then poured directly onto the upper plate of the rheometer, which has been removed from the DSR and placed in a supporting assembly on an electronic balance (scale) with a resolution of 1 mg. The mass of

bitumen is calculated from a knowledge of the volume required and the specific gravity of the binder (taken to be approximately 1). The upper plate is then replaced in the DSR and the plates closed to their final testing gap. As the exact sample volume is placed between the plates, no trimming of the sample is required and no bulge is evident.

As with the silicone mould method, described in the Specification for Highway Works [11] and the IP Standard [8], the weighing method relies on the operator positioning the bitumen sample centrally on the upper plate. Any eccentricity will ultimately result in an overflow of bitumen on one side and a shortfall on the opposing side with the consequential loss of repeatability and generation of erroneous results.

3.3.2 Sample Preparation Testing Programme

3.3.2.1 Repeatability Study

The aim of the first series of tests was to determine the repeatability of the three sample preparation methods using the following testing regime:

- Two binders - Conventional 50 penetration grade bitumen (Venezuelan crude source) and intermediate polymer content (4%) radial SBS PMB,
- Sample preparation and testing @ 40°C, 8 mm spindle geometry,
- Sample preparation and testing @ 40°C, 25 mm spindle geometry,
- Sample preparation and testing @ 75°C, 25 mm spindle geometry,
- Temperature equilibrium time of 600 seconds,
- Frequency sweep from 0.1 to 10 Hz at 20 logarithmic intervals, and
- Ten samples per preparation method and test parameters.

The rationale for selecting the two binders was that the 50 penetration grade bitumen and the radial SBS PMB provided the two extremes in terms of ease of handling and subsequent sample preparation. Both standard testing geometries were included at temperatures above and below the softening point temperature of the binders (see Table 3.2). The temperature equilibrium time was based on the minimum recommended time of 10 minutes taken from the SHRP Protocol and AASHTO

Standard [13, 85], which is a third shorter than the recommended time of 15 minutes found in Clause 928 and the IP Standard [8, 11].

The suitability of the temperature equilibrium time was verified by continuously monitoring alterations in G* with time for 1000 seconds after ramping the temperature from 20°C to 80°C and vice versa. The fluctuations in complex modulus versus time for five test specimens at 80°C are shown in Figure 3.3. The results indicate that equilibrium is reached after approximately 5 minutes, which compares favourably with the recommended equilibrium times of 10 and 15 minutes mentioned in the DSR testing standards.

One tabular and one graphical method were used to assess the repeatability of each sample preparation method. For the tabular method the coefficient of variation, CoV, (standard deviation/average value) of the DSR parameters for each of the testing combinations was calculated at frequencies of 0.1, 1.13 and 10 Hz. The results for the three sample preparation methods are presented in Tables 3.3 to 3.5. The results include the CoV values for δ (see Table 3.4), which were found to be significantly lower than those for G* (see Table 3.3) for all combinations of sample preparation method and binder and therefore the investigation of repeatability was limited to G*. The hot pour method was found to be the most repeatable method (lowest CoV values) for all frequencies, temperatures, spindle configurations and bituminous binders.

Table 3.3: Coefficient of variation of complex modulus, G*, for SBS PMB (Radial)

DSR Testing Frequency (Hz)	Coefficient of Variation (CoV)								
	Hot Pour Method			Silicone Mould Method			Weighing (Mass) Method		
	40°C/ 8 mm	40°C/ 25 mm	75°C/ 25 mm	40°C/ 8 mm	40°C/ 25 mm	75°C/ 25 mm	40°C/ 8 mm	40°C/ 25 mm	75°C/ 25 mm
0.1	4.73%	4.14%	9.36%	19.06%	10.46%	11.66%	20.81%	12.88%	13.24%
1.13	6.70%	4.58%	6.01%	10.27%	6.87%	7.39%	20.37%	7.43%	10.21%
10	6.04%	4.33%	5.71%	9.24%	7.97%	6.95%	21.23%	6.84%	9.86%

Table 3.4: Coefficient of variation of phase angle, δ, for SBS PMB (Radial)

DSR Testing Frequency (Hz)	Coefficient of Variation (CoV)		
	Hot Pour Method	Silicone Mould Method	Weighing (Mass) Method
0.1	1.42%	3.51%	1.88%
1.13	0.15%	0.33%	0.51%
10	0.19%	0.80%	0.60%

Sample prepared and tested @ 40°C with 25 mm diameter spindle and 1 mm gap height.

Table 3.5: Coefficient of variation of complex modulus, G*, for 50 penetration grade bitumen

DSR Testing Frequency (Hz)	Coefficient of Variation (CoV)		
	Hot Pour Method	Silicone Mould Method	Weighing (Mass) Method
0.1	3.51%	4.00%	9.31%
1.13	2.66%	3.60%	10.08%
10	4.24%	7.18%	11.76%

Sample prepared and tested @ 40°C with 25 mm diameter spindle and 1 mm gap height.

For the graphical methods, the rheological data obtained for the ten bitumen samples were plotted, either on a logarithmic complex modulus versus logarithmic frequency scale or a normal versus logarithmic scale, and trend lines fitted to the data. The coefficient of correlation (R^2), used as an indicator of the accuracy of the fit, was determined for each of the trend lines and included in the plots. The plots of G* versus frequency for the three sample preparation methods are shown in Figures 3.4 to 3.6. The figures show the greater repeatability of the hot pour method, although the repeatability of the silicone mould and weighing methods is only marginally lower.

Although the hot pour method showed relatively consistent CoV values for the three testing geometry/temperature regimes, there was a significant increase in the CoV values for the silicone mould and weighing methods (particularly the weighing method) for the 8 mm diameter spindle geometry (see Table 3.3). The reasons for this can be attributed, firstly, to the increased difficulty of accurately weighing out the small quantity of material required for this particular geometry (100.5 mg for the weighing method) and centring the samples in the 8 mm geometry (both methods).

3.3.2.2 Complex Modulus Parameter Study

In addition to assessing the repeatability of the three preparation methods, the values of complex modulus as a function of each sample preparation method were also compared. The average values of G* for the three preparation methods, using different spindle geometries and testing temperatures, are shown in Tables 3.6 and 3.7 and in Figure 3.7. The results show that compared to the hot pour method, the silicone mould and weighing methods give slightly higher and slightly lower values of G* respectively.

Table 3.6: Average values of complex modulus, G*, for SBS PMB (Radial)

DSR Testing Frequency (Hz)	Complex Modulus (Pa)								
	Hot Pour Method			Silicone Mould Method			Weighing (Mass) Method		
	40°C/ 8 mm	40°C/ 25 mm	75°C/ 25 mm	40°C/ 8 mm	40°C/ 25 mm	75°C/ 25 mm	40°C/ 8 mm	40°C/ 25 mm	75°C/ 25 mm
0.1	5,951	5,572	254	7,053	6,126	289	5,021	4,738	241
1.13	34,404	32,271	1,160	44,822	41,963	1,252	28,813	30,769	1,101
10	193,938	181,874	4,706	243,817	205,685	4,989	160,264	172,546	4,419

Table 3.7: Average values of complex modulus, G*, for 50 penetration grade bitumen

DSR Testing Frequency (Hz)	Complex Modulus (Pa)		
	Hot Pour Method	Silicone Mould Method	Weighing (Mass) Method
0.1	10,111	10,332	8,534
1.13	90,645	90,687	75,745
10	546,764	542,308	450,187

Sample prepared and tested @ 40°C with 25 mm diameter spindle and 1 mm gap height.

The hot pour and silicone mould methods are very similar in that both supply excess bitumen to the DSR testing geometry and require subsequent trimming of the bitumen before producing a bulge around the specimen periphery by lowering the upper spindle a further 50 μm. However, whilst the bitumen is above its softening point (predominantly viscous in nature) when it is poured in the hot pour method (typically greater than 100°C), in the case of the silicone mould method the bitumen sample is at ambient temperature when it is mounted in the DSR (below its softening point and therefore more elastic in nature). This results in the generation of internal stresses in the sample when it is squeezed between the plates, which are not dissipated prior to testing. This would explain the slightly higher G* of the binder, particularly evident

for the more elastic SBS PMB. The more comparable results for the penetration grade bitumen (see Table 3.7) suggests that due to its lower softening point and slightly greater viscous behaviour at 40°C, the internal stresses described above may be dissipated in the sample during the temperature equilibrium period prior to testing. The lower G* values for the weighing method are inevitable due, firstly, to the lack of a bitumen bulge around the periphery of the sample and, secondly, to a possible lack of adhesion between the plates and binder, resulting in a slight reduction in the torque required to achieve the same strains as that achieved with the hot pour method.

Whether the hot pour, silicone mould or weighing method is used, it is recommended that the sample is at a temperature either above its softening point temperature or 80°C, whichever is the lower, when the plates are closed to their testing gap. This will generally be the case for the hot pour method, but will require the heating of the silicone mould sample and the weighed sample after they are mounted in the DSR. This step should allow any stresses, generated in the sample during sample preparation, to be dissipated prior to testing.

3.4 Summary

The operational limitations of the DSR were investigated. A large number of tests at different strain levels and temperatures was carried out to define the stress-strain limitations of this machine. Frequency sweep tests were performed in the controlled strain mode, over the entire range of temperatures and strain levels that the DSR was capable of generating. The complex modulus, phase angle, strain and stress were measured under different conditions of temperature, frequency and strain level. The values of complex modulus, phase angle, strain and stress versus frequency were then plotted in the form of isothermal plots. The results showed that the DSR has testing limitations at low and high stress levels due to the minimum and maximum torque levels of the machine.

Three sample preparation methods, the Hot Pour, Silicone Mould and Weighing (Mass) method were compared. The hot pour method was found to be the most repeatable method (lowest CoV values) for all frequencies, temperatures, spindle configurations and bituminous binders, although the repeatability of the silicone

mould and weighing methods was only marginally lower. In addition to assessing the repeatability of the three preparation methods, the values of complex modulus as a function of each sample preparation method were also compared. The results showed that compared to the hot pour method, the silicone mould and weighing methods gave slightly higher and lower values of G* respectively.

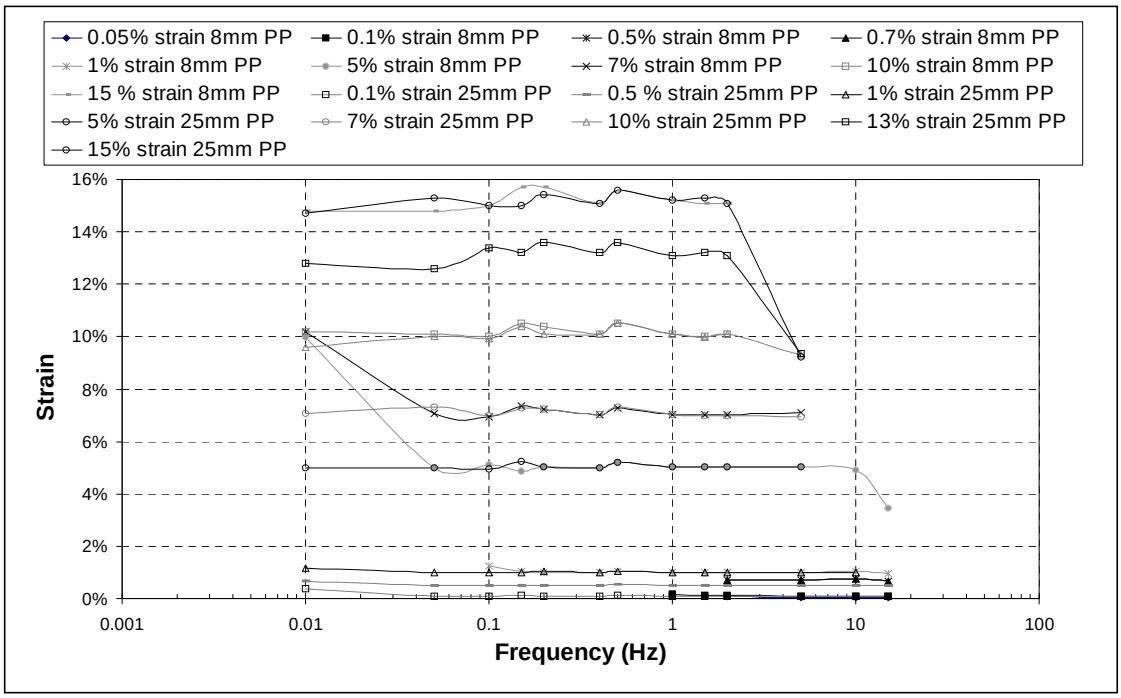

Figure 3.1: Strain versus frequency at 40°C for 50 pen bitumen using 8 and 25 mm parallel plate geometry

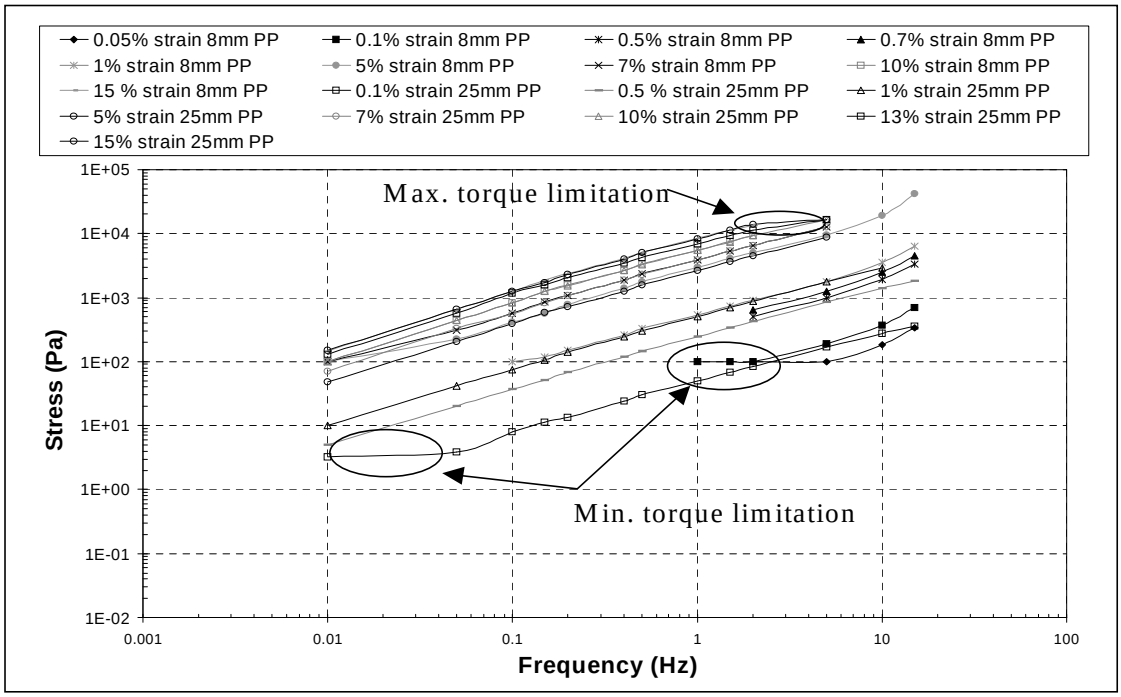

Figure 3.2: Stress versus frequency at 40°C using 8 and 25 mm parallel plate geometry for 50 pen bitumen

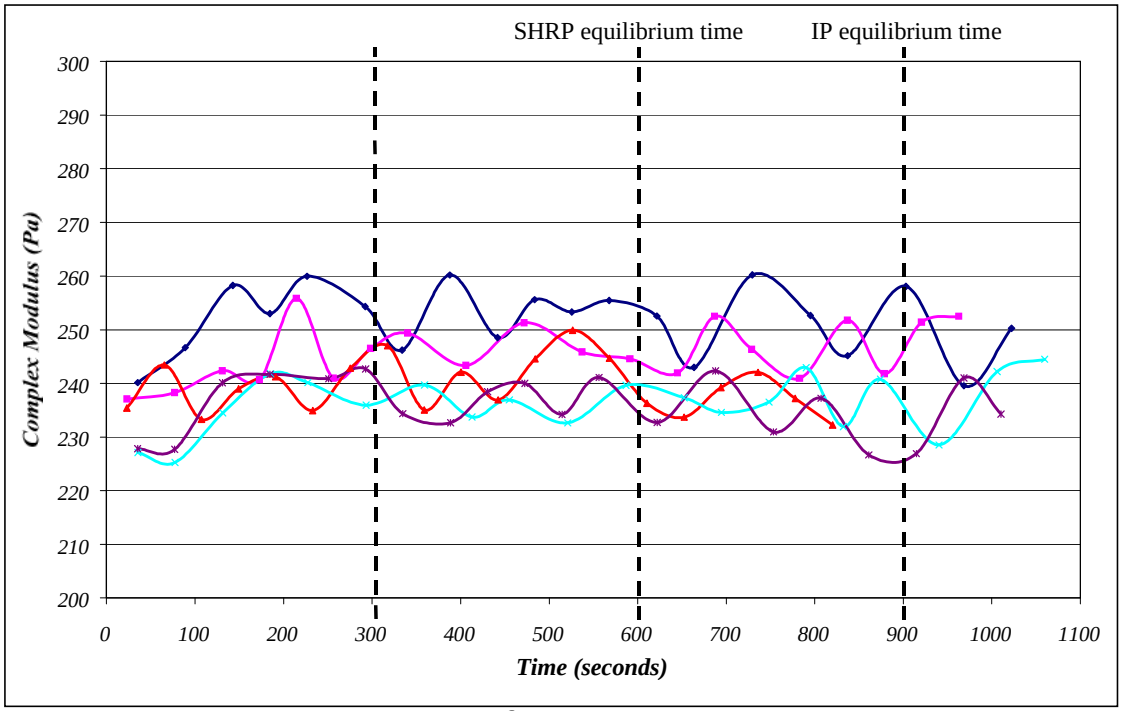

Figure 3.3: Complex modulus profile versus temperature equilibrium time @ 80°C after ramping the temperature from ambient conditions to 80°C

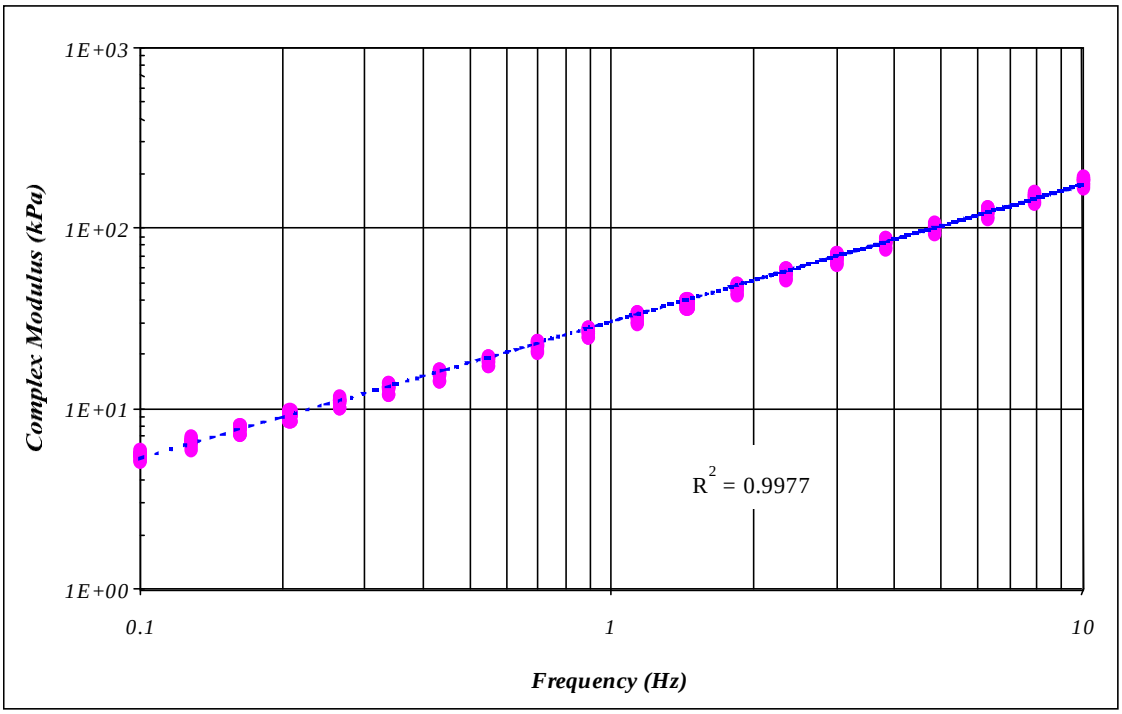

Figure 3.4: Repeatability of complex modulus for SBS PMB (radial) using the hot pour method @ 40°C with 25 mm diameter spindle

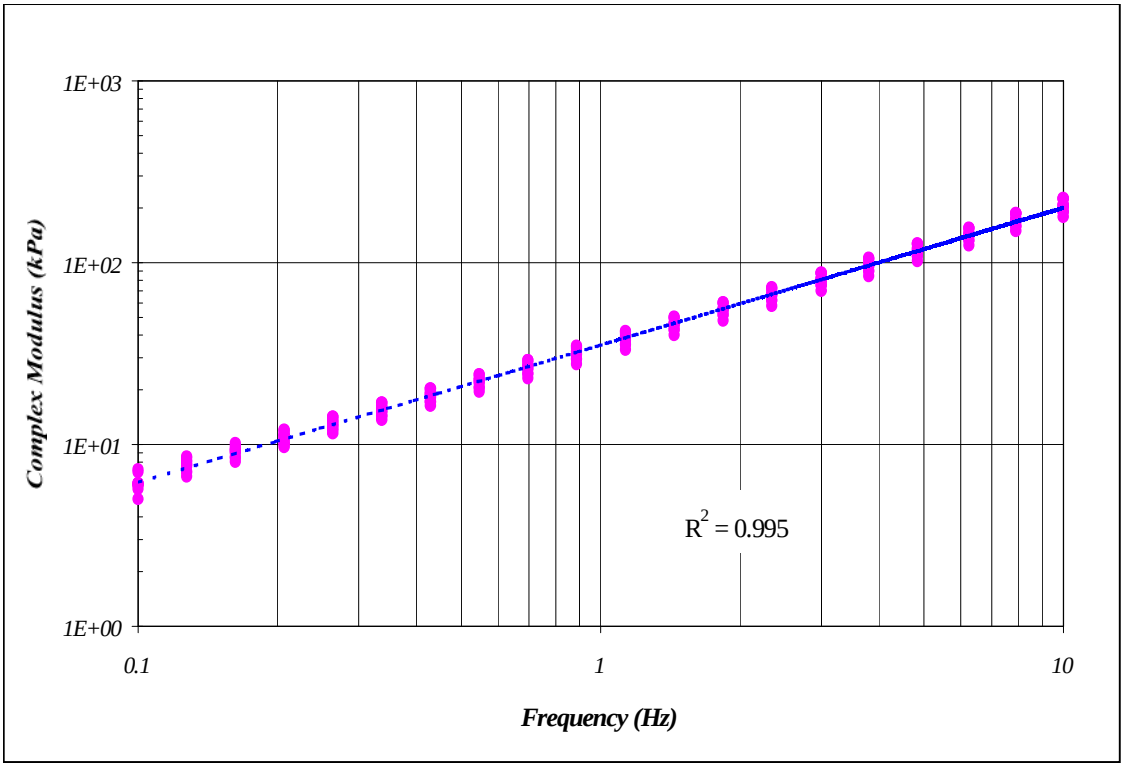

Figure 3.5: Repeatability of complex modulus for SBS PMB (radial) using the silicone mould method @ 40°C with 25 mm diameter spindle

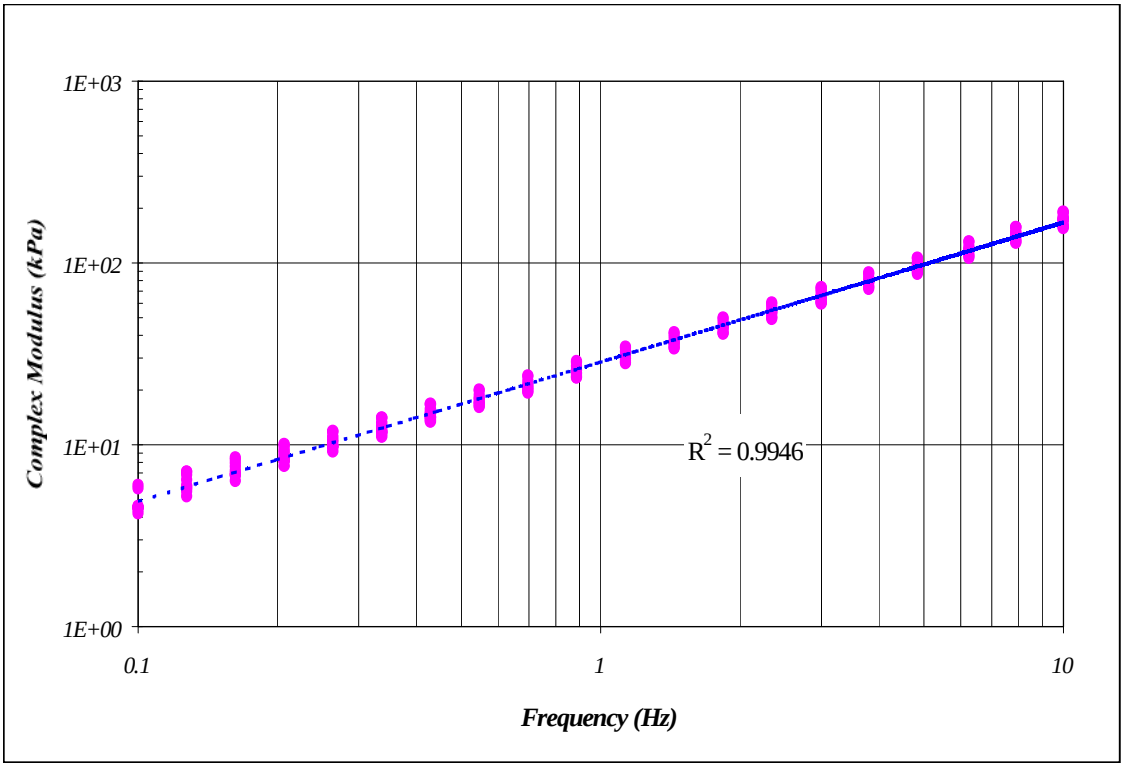

Figure 3.6: Repeatability of complex modulus for SBS PMB (radial) using the weighing method @ 40°C with 25 mm diameter spindle

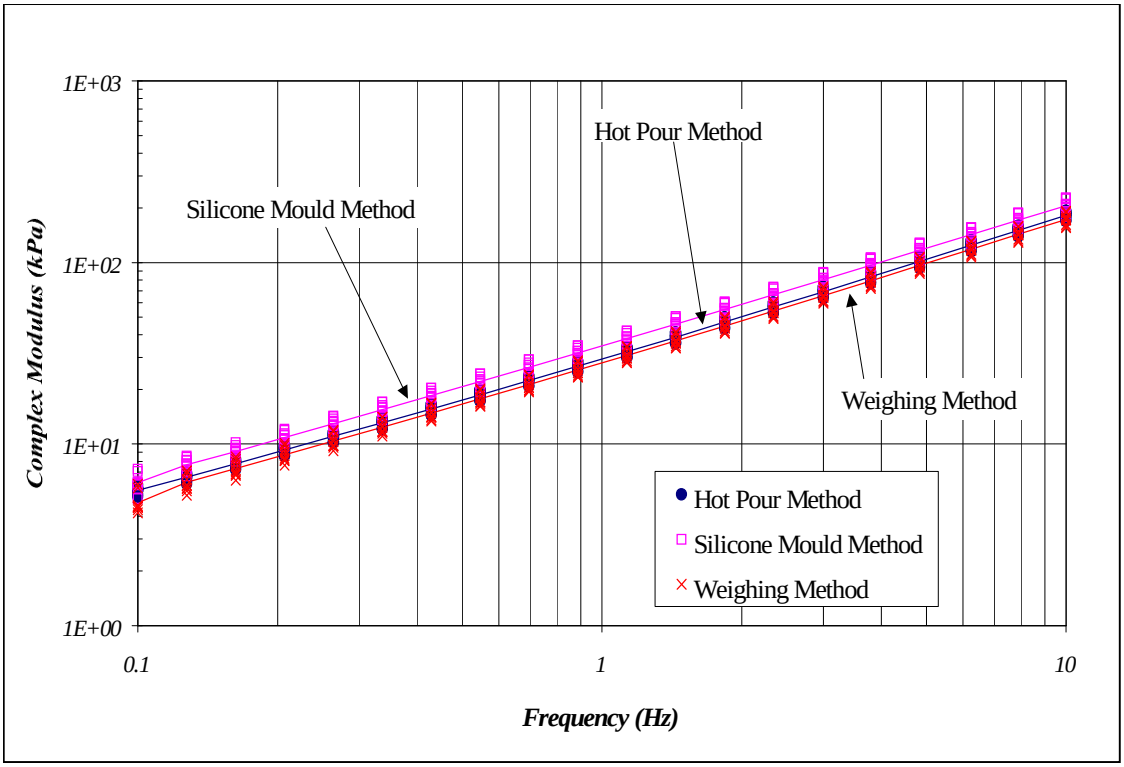

Figure 3.7: Complex modulus for SBS PMB (radial) for the hot pour, silicone mould and weighing methods @ 40°C with 25 mm diameter spindle

Chapter 4

BITUMEN TESTING

4.1 Introduction

Understanding the stress-strain behaviour of any material is necessary to quantify its engineering performance. Materials such as bitumens, which exhibit aspects of both elastic and viscous behaviour, must be characterised with test methods and analytical techniques that account for the time (or rate) of loading and temperature. Dynamic (oscillatory) testing is considered as one of the best bitumen testing techniques as it covers a wide range of loading conditions in a relatively short testing time to give a wide range of properties [22]. In addition, it is the best technique at explaining the unique behaviour of bitumen [23]. Using dynamic shear rheometers (DSRs) it is possible to perform dynamic mechanical analysis (DMA) over a wide range of temperatures and frequencies. Using this type of test equipment, rheological parameters (such as complex modulus and phase angle) can be obtained under different conditions. Although rheometers have long been considered too expensive and unsuitable for use in routine tests, research work has clearly shown that rheological, DMA measurements can be related to pavement performance [18, 88].

When analysing the stress-strain behaviour of bitumen by dynamic testing, two behavioural domains appear: the linear domain and the non-linear domain. It is necessary to take into account both these domains before defining the complete rheological response of a material. Generally bitumen behaviour is linear at strain or stress amplitudes smaller than a certain limit (depending on the material under consideration). Above this limit, bitumen behaviour is non-linear and finding this linear limit is a very important aspect in the rheological investigation of bituminous materials.

This chapter focuses on identifying the linear viscoelastic (LVE) limit of different unmodified and modified bitumens as a function of different loading times and

temperatures. Additionally, upon establishing the LVE limit, the viscoelastic properties of these bitumens in their linear region are evaluated.

4.2 Materials

In the early stage of this research, efforts were made to obtain unmodified and a range of modified bitumens with different levels of modification. Eventually, five different unmodified and modified bituminous binders were selected for this investigation. These bitumens were:

- Conventional 50 penetration grade bitumen (Venezuelan crude source),
- Intermediate polymer content (4%) radial Styrene-Butadiene-Styrene (SBS) PMB,
- High polymer content (7%) linear SBS PMB,
- Intermediate polymer content (4%) Ethylene-Vinyl-Acetate (EVA) PMB, and
- Multi-grade bitumen (35/50).

Conventional test methods such as penetration and softening point were initially carried out to characterise these bituminous binders according to current highway specifications and practices. The results of these tests are shown in Table 4.1.

As oxidative ageing and loss of volatiles occurs during asphalt mixture preparation and since one of the objectives of this research was to study the relationship between the rheological properties of bitumen and asphalt mixtures, it was decided to test all bitumens after subjecting them to short-term ageing. To simulate short-term ageing, all the binders were aged using the RTFOT. In addition, the 50 pen bitumen and radial SBS PMB were studied in both their unaged and aged conditions to compare the results for these two situations.

4.3 Testing Methodology

4.3.1 Instrumentation

Dynamic mechanical tests were performed using a Bohlin DSR with parallel plate geometry in an oscillatory shear mode. At sub-ambient temperatures, due to the high

stiffness of bitumen, high shear stresses are required to achieve a certain strain level. This is generally achieved by using a small diameter rotating plate. Therefore, a 8 mm diameter plate was used to perform tests at temperatures less than 40˚C and tests at temperatures above 40˚C were performed using a 25 mm diameter plate. To maintain a specified constant temperature during tests, the samples were completely immersed in a temperature-controlled testing chamber. A pump-equipped water bath circulated the water around the specimen throughout the test. Operation of the rheometer and temperature control unit, along with data acquisition and analysis were controlled by a computer. The DSR used for this research is shown in Figure 4.1.

The operation of the DSR is based on measuring applied torque and the angular deflection of a sample as described in Chapter Two. In this apparatus, a disk of binder is mounted between two parallel plates. The upper plate is free to rotate around a vertical axis, while the lower plate is fixed. The specimen is subjected to a specified shear stress at a certain frequency through the application of a torque to the upper plate. The response is monitored by measurement of the angular deflection of the sample.

Calibration of the DSR at regular intervals is essential to maintain reasonable repeatability and reproducibility of rheological data. Therefore, prior to conducting any experimental work, the torque measurement transducer, the deflection measurement transducer and the platinum resistance thermometer were calibrated by the DSR manufacturer.

Once all the above mentioned steps were completed, the DSR performance was verified by conducting measurements with a reference fluid oil.

4.3.2 Sample Handling Procedures

The following procedure was used to prepare samples of bitumen. The bitumens were received in containers ranging from 1 kg to 25 kg. The containers were placed in an oven preheated to 140˚C, and the bitumens were heated at this temperature until they became sufficiently fluid to pour. The bitumen was then stirred and batches of approximately 400 g were poured into several half-litre cans. These cans were tightly

sealed and appropriately labelled. To prepare short-term aged bitumen samples, one can of bitumen at a time was placed in a preheated oven until the bitumen became sufficiently soft and after stirring, 35 g of bitumen was poured into special bottles and aged in accordance with the RTFOT procedure. The aged samples were then transferred to sealed 20 ml vials and stored at ambient temperatures for further testing.

4.3.3 Sample Preparation

Sample preparation is one of the most critical aspects of DSR testing particularly for modified bitumens as these bitumens tend to be sticky when warm, especially elastomer modified bitumens, and so cutting and trimming can be very difficult. Additionally a cold sample may not adhere well to the plates of the measuring system. According to the earlier study described in Chapter three which addressed possible errors associated with inaccurate temperature control during DSR testing, the hot pour method was chosen for this study. This was because of its simplicity and speed of sample assembly when compared with the other methods.

4.3.4 Testing Procedures

Two types of dynamic shear tests were performed during this investigation:

- Stress sweep tests, and
- Frequency sweep tests.

In the first stage, stress sweep tests were performed to determine the linear viscoelastic limit for each of the binders. Within the linear region, the viscoelastic parameters, such as complex modulus, are independent of the applied stress amplitude. However, in the non-linear region, the modulus will decrease with increasing stress. In the second stage, the results obtained from the first stage were used as target stresses to perform frequency sweep tests in the linear viscoelastic range of response.

4.3.4.1 Stress Sweep Tests

To establish the linear viscoelastic range for each bitumen, stress sweep tests were performed for all bitumens at the following temperatures and frequencies:

- Temperatures: 10, 20, 30, 40, 60 and 70˚C, and
- Frequencies: 0.1, 1, 5 and 10 Hz.

A 8 mm diameter plate with a gap of 2 mm for temperatures between 10 to 40˚C and a 25 mm diameter plate with 1 mm gap for temperatures 60 and 70˚C were used. All stress sweep tests were carried out on separate samples of bitumen. In this test, hot bitumen was mounted in the rheometer according to the hot pour method of preparation and allowed to equilibrate at the selected test temperature. The stress was then allowed to increase until the measured modulus had decreased to approximately 30 percent of its highest observed value. This ensured that the sweep was carried out well into the non-linear region [20]. In the course of performing the stress sweeps, it was observed that due to gradual variations of the complex modulus, drawing an exact line between the linear and non-linear region was very difficult. Therefore, the linear viscoelastic (LVE) limit was defined in accordance with the SHRP study as the point where the complex modulus has decreased to 95 percent of its initial value [20].

The non-linearity of the five binders was established by analysing the following parameters; stress, strain, complex modulus and phase angle generated during the stress sweep tests. To define the linear and non-linear regions and establish the LVE limit, different methods of presenting the parameters were investigated.

4.3.4.2 Frequency Sweep Tests

Upon completing the stress sweep tests and establishing the target stresses or strains, frequency sweep tests were performed on all the samples at the following test conditions:

- Mode of loading: Controlled stress,
- Temperatures: 10, 20, 30, 40, 60 and 70˚C, and
- Frequencies: from 0.1 to 20 Hz.

All of the frequency sweep tests were conducted at stresses below the linear limit, as determined using the procedure described above. This ensured linear viscoelastic behaviour during the dynamic testing. Parallel plates with diameters of 8 mm and 25 mm were used in the temperature ranges of 10 to 40 and 40 to 70˚C, respectively. The final gap was adjusted to 1 mm for a 25 mm plate and 2 mm for the 8 mm spindle. For the 8 mm diameter plates, the DSR and test specimen were allowed to equilibrate at 40˚C for approximately 10 min before testing. This procedure ensured sufficient bond was developed between the specimen and the confining plates. The test temperature was then progressively lowered in intervals of 10˚C, the test specimen allowed to equilibrate for 10 minutes and then, at each target temperature, subjected to an ascending frequency sweep. Measurements with the 25 mm diameter plate always started at 40˚C. In a similar manner the test temperature was progressively increased in intervals of 10˚C, and frequency sweeps were performed in ascending frequency order at each target temperature up to 70˚C.

The results from the frequency sweep tests in the form of complex modulus and phase angle parameters have been presented as isothermal plots, isochronal plots, black diagrams and master curves for each type of bitumen. Because of the large amount of data generated in these tests, these plots were very useful in presenting and interpreting the results. Master curves allow the rheological data to be presented over a wide range of frequencies and temperatures in one plot. Therefore, to avoid presenting a large number of graphs, the results are mainly presented and analysed as master curves.

4.4 Linear Viscoelastic Limits

4.4.1 Stress-Strain Relationships

Strain amplitude versus stress amplitude was plotted for each stress sweep test. Figures 4.2 and 4.3 show log-log scale plots of the test results for the 50 pen and linear SBS PMB at different testing conditions. It can be seen from these figures that the initial part of the data generated straight lines, indicating linear behaviour, followed by curves bending upwards away from the horizontal axis. This indicates that the bitumens showed larger strains than would be predicted by the linear portion

of the graph at higher stress values. In other words, the bitumens showed non-linear behaviour at higher stresses. Such behaviour was observed for all the binders tested in this investigation with the exception of some low temperature and high frequency (e.g. 10˚C and 10 Hz) tests, where the stiffness of the bitumen was too high for the DSR to generate high enough stress levels to reach the non-linear limit of the bitumen. The DSR used in this investigation was capable of applying a maximum stress level of 0.5 MPa.

As shown in Figures 4.2 and 4.3, two trendlines were plotted in the linear and non-linear regions. These trendlines can be described using a power-law equation as follow:

$$\tau = K\varepsilon^{n} \qquad \textbf{(4.1)}$$

Where, K and n are rheological parameters with n being equal to 1 in the linear region. As shown in these figures, this method allows a transition range between linear and non-linear behaviour to be identified between the linear and non-linear trendlines. However, a unique stress/strain limit could not be established. Therefore, another method was used to define the linear region of the five bitumens.

4.4.2 LVE Limit Calculation

As mentioned previously, a material can be defined as acting in the LVE region if, for a given frequency of loading, the phase angle and the ratio of stress to strain remain constant with changes in the amplitude of the strain or stress. Therefore the effect of stress level, at different temperatures and frequencies, was evaluated by plotting complex modulus and phase angle versus strain or stress level. Typical curves of complex modulus against stress or strain amplitudes were plotted and some of these are shown in Figures 4.4 to 4.7. These plots show that there is a clear distinction between the linear and non-linear regions as the complex modulus results show a very small decrease (almost constant value) with increasing stress level in the linear region, whereas in the non-linear region the complex modulus of the bitumen decreases dramatically with increasing stress level.

The effect of stress or strain levels on the phase angle can be as significant as the effect on the complex modulus in the LVE region. Figures 4.8 and 4.9 show phase angle versus stress and strain for the EVA PMB at 20˚C and 1 Hz. It can be seen from these figures that there is a very small increase (almost constant value) in phase angle with increasing stress or strain levels in the linear region followed by a dramatic increase in phase angle in the non-linear region.

Similar behaviour to that of the complex modulus was observed for the storage modulus (G') and loss modulus (G"). Figures 4.10 and 4.11 show the comparison of stress sweep test results of G*, G' and G" for the 50 pen bitumen at 20˚C and 1 Hz. It can be seen from these figures that within the linear range of response, values of storage modulus and loss modulus are independent of the applied stress amplitudes. In the non-linear range, however, the moduli decrease with increasing stress.

In analysing the stress sweep data, the SHRP method, which was explained earlier, was used to determine the linear region. As shown in Figures 4.4 through 4.7, the linear strain limit was therefore somewhat arbitrarily established as the stress or strain at which the complex modulus decreased to 95 percent of its initial value.

It should be noted that at temperatures below 20˚C and especially at high frequencies, no decrease in complex modulus could be observed over the entire range of the applied stresses. This was due to the high stiffness of the bitumen and the low strain values that could be generated by the rheometer. This meant that at these temperatures and frequencies, even at the highest possible generated stress, the sample was still within its linear region. Therefore, defining the LVE region at low temperatures (e.g 10˚C) for some of the bitumens was not possible. The LVE limits of the bitumens at all conditions of frequency and temperature are presented in Tables 4.2 to 4.8.

The data from these stress sweeps was analysed and the linear stress or strain limits plotted against temperature. These graphs are shown in Figures 4.12 to 4.21. It can be seen from Figures 4.12 to 4.16 that generally the LVE strain limit increases with temperature for all the bitumens. In addition, the radial and linear SBS PMBs show a relative stable LVE strain limit at high temperatures (60˚C and 70˚C).

Figures 4.17 to 4.21 clearly show a decrease in LVE stress limit with temperature, although the LVE stress limits for the 50 pen, EVA PMB and process modified bitumen are relatively stable at high temperatures (60˚C and 70˚C).

4.4.3 LVE Limit versus Complex Modulus

Plotting the LVE limits as a function of the rheological parameters of complex modulus and phase angle was found to be a very useful method for evaluating the linearity behaviour of the five binders. Plots of LVE strain limits as functions of complex modulus are shown in Figures 4.22 and 4.23. It can be seen from these graphs that there is a clear relationship between complex modulus and linear strain limit for different ranges of complex modulus. Above a complex modulus value of approximately 1 MPa, which corresponds to high frequency and low temperature testing conditions, there is a strain dependent LVE criterion between 2% and 6%. Below this 1 MPa threshold, the LVE strain limit increases with decreasing complex modulus.

Figures 4.22 and 4.23 also show that there is a second strain criterion between 50% and 150% for the radial and linear SBS PMBs at very low complex modulus values (below 10 kPa), which corresponds to testing conditions at low frequencies and high temperatures. This can be attributed to the dominance of the SBS polymer matrix at high temperatures and low frequencies.

The LVE stress limits are shown as functions of complex modulus in Figures 4.24 and 4.25. It can be seen from these figures that generally the LVE stress limit increases with increasing complex modulus for bitumens with complex modulus values greater than 10 kPa. This indicates that there is a direct relationship between the LVE stress limits and complex modulus at values greater than 10 kPa, corresponding to testing at temperatures lower than 60˚C. However, as shown in the figures, there is a stress dependent LVE criterion between 1.5 and 7 kPa at low G* values (below 10 kPa) for all the bitumens with the exception of the SBS PMBs. This indicates that the LVE limit of the bitumens, except for the SBS PMBs, is stress dependent rather than strain dependent at high temperatures (≥ 60˚C), where the behaviour of the bitumens is

predominantly viscous in nature. In other words, the deformation behaviour in this region shows linear viscous flow behaviour.

4.4.4 LVE Limit versus Phase Angle

The LVE strain limits as functions of phase angle are shown in Figures 4.26 and 4.27. It can be seen from these figures that there is a strain dependent LVE criterion between 2% and 6% at intermediate to low phase angles (< 55˚). This indicates that the LVE limit of bitumens at lower temperatures and higher frequencies, where bitumen behaviour is more elastic, is strain dependent rather than stress dependent. A second strain dependent criterion can be seen between 50% and 150% for the two SBS PMBs. This second strain dependent region corresponds to testing conditions where the elastomeric nature of the SBS polymer is dominant (high temperatures and/or low frequencies).

Figures 4.28 and 4.29 show the LVE stress limit values, determined from stress sweep tests for the five bitumens at different test temperatures and frequencies, plotted against phase angle. It can be seen from these figures that there may be a stress dependent LVE criterion between 1.5 and 7 kPa at high phase angles (>80˚). This would be consistent with the dominant viscous response of the process modified, plastomeric and conventional binders at high temperatures.

4.4.5 Unaged and Aged Linearity Limits

A comparison of the LVE strain and stress limits for the unaged and RTFOT aged 50 pen bitumen and radial SBS PMB are shown in Figures 4.30 and 4.31. Although DMA has shown slight changes in the rheological properties of the two bitumens before and after RTFOT ageing, the linearity limits and the nature of the linearity behaviour appears to be unchanged. The strain dependent criteria between 2% and 6% at high stiffness values and between 50% and 150% for the radial SBS PMB at low G* values are still evident for both the unaged and aged binders. Likewise the stress dependent criteria between 1.5 and 7 kPa for the 50 pen bitumen can be seen for the unaged and RTFOT aged binders.

4.4.6 Discussion

The results show that there are different LVE criteria for the bitumens studied in this testing programme. These criteria depend on the complex modulus of the bitumens as a function of temperature and frequency. Three criteria can be observed relating to testing at low, intermediate and high temperatures. At low temperatures (<20˚C), where the bitumens exhibit dominant elastic behaviour with minor differences in stiffness between the binders, all the bitumens showed a strain dependent LVE criterion. In other words, the LVE criterion was independent of complex modulus at low temperatures.

At intermediate temperatures (20˚C to 60˚C), the LVE stress and strain limits were functions of complex modulus. The LVE strain limits decreased while the LVE stress limits increased with increasing complex modulus. At high temperatures, where viscous behaviour dominates binder performance, all the bitumens, except for the SBS PMBs, showed a stress dependent LVE criterion. The SBS PMBs showed a strain dependent LVE criterion in this range of temperatures, which can be attributed to the presence of the dominant SBS polymer matrix at high temperatures.

In order to compare and discuss the bitumen linearity results, it was necessary to consider other LVE limit studies of bituminous materials. Cheung [38] found that bitumens exhibit linear viscous behaviour at low stress levels, and power-law creep behaviour at higher stress levels. The bitumen used in his study was a 50 penetration grade bitumen. He conducted constant strain rate tests at high temperatures and constant stress tests at low temperatures to investigate the creep behaviour of pure bitumen. Figure 4.32 shows the steady-state stress/strain-rate relationship at temperatures ranging from –10˚C to 30˚C. Cheung stated that although the behaviour in the upper half of the stress range can be considered to be power-law in nature, it changes gradually to linear behaviour (slope of 1) towards the lower half of the stress range. Moreover, the transition appears to take place at the same value of stress throughout the entire temperature range. Cheung found that the value for the transition stress is approximately 100 kPa (a LVE stress criterion of approximately 100 kPa).

The results from Cheung's study showed that the transition from linear to non-linear behaviour for bitumens, tested under steady state creep conditions, is stress dependent. This agrees with the results obtained in this study for the 50 pen, EVA PMB, and multi-grade bitumens at high temperatures, where the viscous component of the bitumen is dominant.

A series of strain sweep tests using a DSR at different temperatures and a frequency of 10 rad/s were performed during the SHRP study to determine the range of linear behaviour of different bitumens [20]. A plot of the LVE strain limits as a function of complex modulus for more than 40 bitumens at different ageing conditions is shown in Figure 4.33. It can be seen from this graph that there is a clear relationship between complex modulus and linear strain limit. Based on this figure, SHRP stated that strain should be controlled to within ±20 percent of the following equation when using a controlled-strain rheometer to ensure LVE behaviour:

$$\gamma = 12/(G^*)^{0.29} \qquad \textbf{(4.2)}$$

And within ±20 percent of the following equation when using a controlled-stress rheometer:

$$\tau = 0.12/(G^*)^{0.71} \qquad \textbf{(4.3)}$$

These equations were plotted in Figures 4.34 and 4.35 in order to compare the SHRP LVE strain and stress criteria with results from this study. It can be seen from these figures that there is a reasonable agreement between the results of this study and the SHRP work.

4.5 LVE Rheological Characterisation

4.5.1 Complex modulus and Phase Angle Master Curves

The construction of a master curve is an application of the time temperature superposition principle (TTSP), which was described in Chapter Two. Prior to the construction of a master curve, multiple graphs of the absolute value of complex

modulus versus frequency (isothermal plots) at six test temperatures were plotted on a log-log scale. An example of such a graph, which was constructed for the conventional 50 pen bitumen, is shown in Figure 4.36. This figure illustrates the expected increase in complex modulus as the bitumen becomes stiffer and more elastic at higher frequencies and lower temperatures.

Isothermal plots of phase angle were also constructed for all the bitumens. Figure 4.37 shows the isothermal plot of phase angle versus frequency for the linear SBS PMB. As shown in the figure, there is a decrease in phase angle with decreasing frequency at temperatures greater than 20˚C. This is caused by the dominance of the SBS polymer matrix at high temperatures, which causes an increase in the elastic behaviour of PMBs at high temperatures. Similar behaviour was observed for the other bitumens.

After preparing the isothermal plots, the complex modulus master curves were constructed using the principle of superposition. The isothermal curve at 20˚C was selected as the reference temperature and all the other isothermal segments were shifted along the frequency axis to obtain a unique smooth master curve. As an example, Figure 4.38 shows both the shifted and unshifted complex modulus data for the radial SBS PMB.

The amount of shifting required for each isothermal curve to fit the dynamic master curve (horizontal shift factor) was calculated for each binder and plotted against temperature on a semi-log scale as shown in Figure 4.39.

The master curves for phase angle, shifted using the factors derived for complex modulus, were constructed for all the bitumens. Figures 4.40 and 4.41 show the master curves of phase angle for the 50 pen bitumen and linear SBS PMB. It can be seen in Figure 4.41 that the phase angle passes through a maximum plateau region. This kind of behaviour is only observed for the radial and linear SBS PMBs. This is due to the increased dominance of the SBS polymers and increased elastic behaviour of the modified binder as the frequency decreases or temperature increases. This can be attributed to the low viscosity of the bitumen, which allows the elastic network of the polymer to influence the mechanical properties of the modified binder [53].

4.5.2 Storage Modulus, Loss Modulus and Loss Tangent Master Curves

For comparison, different master curves were constructed for the various linear viscoelastic functions, such as the storage modulus, G', the loss modulus, G", and loss tangent, all shifted using shift factors derived for the complex modulus. As mentioned in Chapter Two, G' describes the amount of energy stored and released elastically during each oscillation, and is thus called the storage modulus, while G" describes the energy-dissipation associated with viscous effects, and is thus called the loss modulus. Master curves of storage and loss modulus for all the bitumens are shown in Figures 4.42 to 4.46. The bitumens show a predominantly viscous behaviour at the reference temperature of 20˚C (phase angle > 45˚), although the storage modulus does dominate the loss modulus at stiffness values greater than 10^7 Pa. However, within the low frequency region (corresponding to high temperatures), the rheological behaviour of the SBS PMBs differs from that of the other bitumens. These two bitumens show a second crossover point for G' and G" at low frequencies (stiffness values below approximately 10^3 Pa). In the other words, these bitumens begin to display a dominant elastic behaviour at low frequencies due to the SBS polymer.

The importance of the loss tangent, tan δ, to characterise the behaviour of bitumens has been noted by different researchers [99, 115]. As discussed in the literature review, the loss tangent is proportional to the ratio of the dissipated to stored energy, i.e. the ratio of the viscous to elastic behaviour of the material. The loss tangent master curves for the five bitumens are shown in Figure 4.47. It can be seen that there is a sharp increase in the loss tangent at low frequencies for the straight run bitumen and EVA PMB. This is a consequence of the predominantly viscous behaviour of these binders at low frequencies (corresponding to the highest test temperatures). However, the SBS PMBs show a dramatic decrease in tan δ at low frequencies due to increased elastic behaviour at high temperatures or low frequencies. The process modified, multi-grade bitumen shows only minor changes in loss tangent over the entire frequency range. In other words, the loss tangent for the multi-grade bitumen is less susceptible to variations in frequency or temperature compared to the other bitumens.

Figure 4.47 also shows a plateau region in the loss tangent master curves for the SBS PMBs over the intermediate frequency range (approximately between 0.01 and 1 Hz). This kind of behaviour had been reported for the loss tangent of SBS PMBs [50], storage modulus master curves of SBS PMBs [42], and isochronal loss tangent curves of modified binders [52], and can be attributed to the formation of the polymeric network.

4.5.3 Discussion

A comprehensive analysis using DMA can be carried out by producing master curves of various rheological parameters. The storage and loss modulus can provide insight into the change of balance between the elastic and viscous response of a viscoelastic material such as bitumen. In addition, relationships between the storage and loss modulus can be reflected in the shape of loss tangent.

Three viscoelastic regions can be observed from the master curves of the five bitumens. These three regions are related to high, intermediate and low frequency domains (corresponding to low, intermediate and high temperatures). In the first region, all the binders exhibit dominant elastic behaviour with minor differences between the viscoelastic properties of bitumens. As frequency decreases or temperature increases, the SBS PMBs start to show a difference in viscoelastic behaviour compared to the other binders. This is extremely noticeable in the phase angle master curves where the SBS polymers begin to significantly improve the elasticity of the modified binders at intermediate frequencies. The results also show that there is a plateau in the loss tangent master curves for the SBS PMBs in the intermediate frequency range (between 0.01 and 1 Hz). This signifies the onset of a rubbery plateau that generally results from long-range chain entanglement, which leads to some form of bulk network formation [78]. Therefore, it can be hypothesized that network formation is occurring in the SBS PMBs. At very low frequencies (corresponding to high temperatures), all the bitumens, except for the SBS PMBs, start to lose their elasticity and approach a viscous state. This is seen as a dramatic increase in the loss tangent for these bitumens at low frequencies. However, the polymer plays a dominant role in the properties of the SBS PMBs in this region. Molecular entanglements and hence the formation of a polymeric network result in

the improved elastic behaviour of the SBS PMBs, which causes better resistance to permanent deformation.

4.6 Summary

Dynamic mechanical tests were performed using a Bohlin DSR with parallel plate configuration in an oscillatory shear mode in order to study the linear and non-linear viscoelastic behaviour of five different unmodified and modified bitumens. Stress sweep and frequency sweep tests were performed during this study as part of the dynamic shear testing. Stress sweep tests were used to determine the linear viscoelastic limit while frequency sweep tests in the linear viscoelastic range of response were used to determine the LVE rheological characteristics of the binders.

The non-linearity of the bitumens was demonstrated through measurements of stress, strain, complex modulus and phase angle during stress sweep testing. All the bitumens tested showed non-linear behaviour at high stresses. The effect of stress level, at different temperatures and frequencies, was evaluated by plotting complex modulus and phase angle versus strain or stress. These plots showed that there was a clear distinction between the linear and non-linear regions. In the linear region the complex modulus showed a very gradual decrease with increasing stress level. However, in the non-linear region the complex modulus of bitumen began to decrease dramatically with increasing stress level.

Similar behaviour to that of the complex modulus was observed for the storage modulus (G') and the loss modulus (G"). Within the linear range of response, values of storage and loss modulus were independent of the applied stress amplitudes. However, in the non-linear range the moduli decreased with increasing stress.

In analysing the stress sweep data, the SHRP method was used to determine the linear region. In this method, the linear strain limit is somewhat arbitrarily established as the stress or strain at which the complex modulus decreases to 95 percent of its initial value. The data from these stress sweep tests, i.e. the linear stress or strain limits were plotted against temperature. These graphs showed that the LVE strain limit generally

increases with temperature. In addition, the results for the SBS PMBs showed that the LVE strain limits were relatively stable at high temperatures (60˚C and 70˚C).

The LVE strain limits were plotted as functions of complex modulus for all the bitumens. These plots showed that there was a clear relationship between the complex modulus and the linear strain limit for different ranges of complex modulus. Above a complex modulus of approximately 1 MPa (high frequencies and low temperatures), there is a strain dependent LVE criterion between 2% and 6%. However, below a complex modulus of approximately 1 MPa, the LVE strain limit increases with decreasing complex modulus. The results also indicated that there was a second strain criterion between 50% and 150% for the SBS PMBs at very low complex modulus values (below 10 kPa).

The LVE stress limits were also plotted as functions of complex modulus. These graphs showed that generally the LVE stress limit increases with increasing complex modulus. In other words, the LVE stress limits were higher for bitumens tested at higher temperatures and lower frequencies. However, there was a stress dependent LVE criterion between 1.5 and 7 kPa at low complex modulus values (below 10 kPa) for all the bitumens with the exception of the SBS modified bitumens.

The LVE strain limits as functions of phase angles were also plotted. These plots illustrated that there was a strain dependent LVE criterion between 2% and 6% at intermediate to low phase angles (<55˚). This indicated that the LVE limit for bitumens at low temperatures and high frequencies, where bitumen behaviour is predominantly elastic, was strain dependent rather than stress dependent. There was a second strain criterion between 50% and 150% for the two SBS PMBs. Therefore, the SBS PMBs showed three regions of LVE limit behaviour. At low temperatures and high frequencies, there is a strain dependent LVE criterion, at intermediate temperatures the LVE strain limit changes as a function of complex modulus, and at high temperatures and low frequencies, there is a second strain criterion.

The LVE stress limit observed from the stress sweep tests at different temperatures and frequencies were plotted against phase angle. These plots showed that there was a stress dependent LVE criterion between 1.5 and 7 kPa at high phase angles (>80˚).

Upon completing the stress sweeps and establishing the target stresses or strains, frequency sweeps were performed on all samples. All of the frequency sweep tests were conducted at stresses below the linear limit, as determined using the procedure described above. Prior to the construction of each master curve, multiple graphs of the absolute value of complex modulus versus frequency (isothermal plots) were developed and plotted on log-log scales. Additionally, isothermal plots of phase angle were constructed for all the bitumens. After preparing the isothermal plots, complex modulus master curves were constructed using TTSP with a reference temperature of 20˚C. Phase angles master curves using shift factors derived for complex modulus, were also constructed for all the bitumens. Master curves of the linear viscoelastic functions of storage modulus, G', loss modulus, G" and loss tangent, using shift factors derived for complex modulus, were also produced.

The results showed that, in the low frequency region (high temperatures), the rheological behaviour of the SBS PMBs differed from that of the other bitumens. Both SBS PMBs displayed a predominant elastic behaviour at low frequencies. The loss tangent master curves for the bitumens showed a sharp increase in loss tangent at low frequencies for the straight run bitumen and EVA PMB indicating a dominant viscous behaviour. However, the behaviour of the SBS PMBs displayed the opposite behaviour with tan δ decreasing at low frequencies.

Figure 4.1 Dynamic Shear Rheometer (DSR)

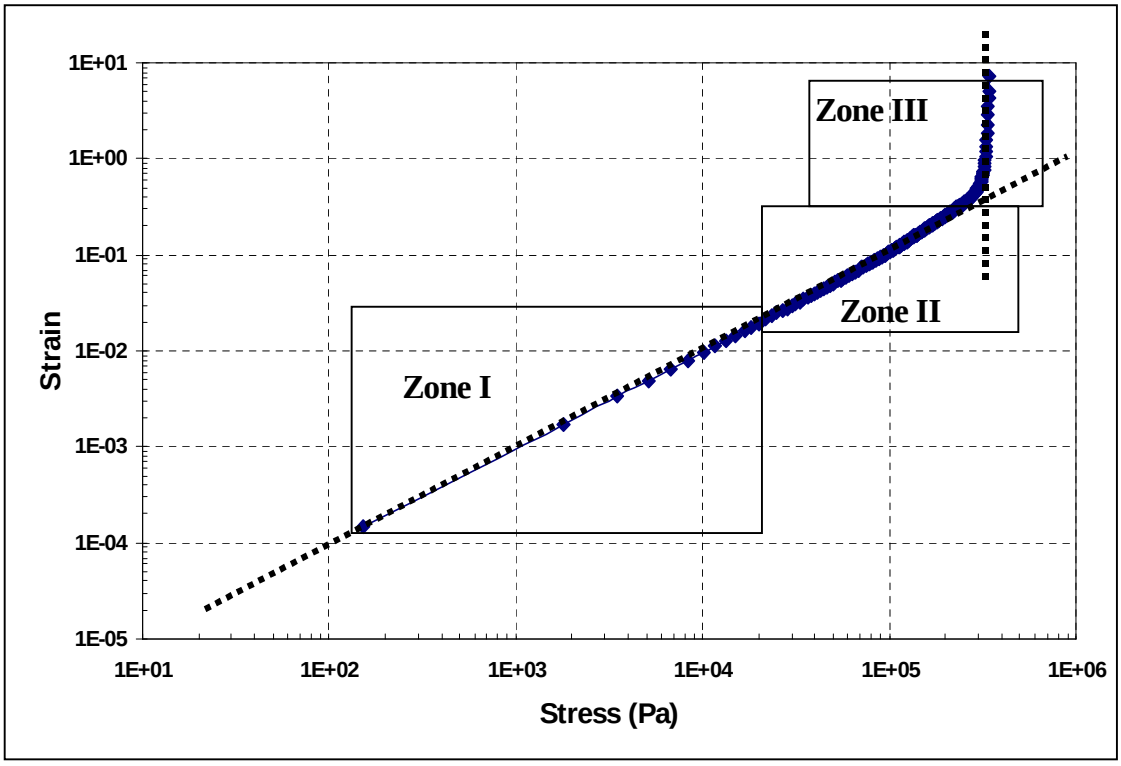

Figure 4.2: Strain versus stress for 50 pen aged bitumen at 20˚C and 0.1 Hz

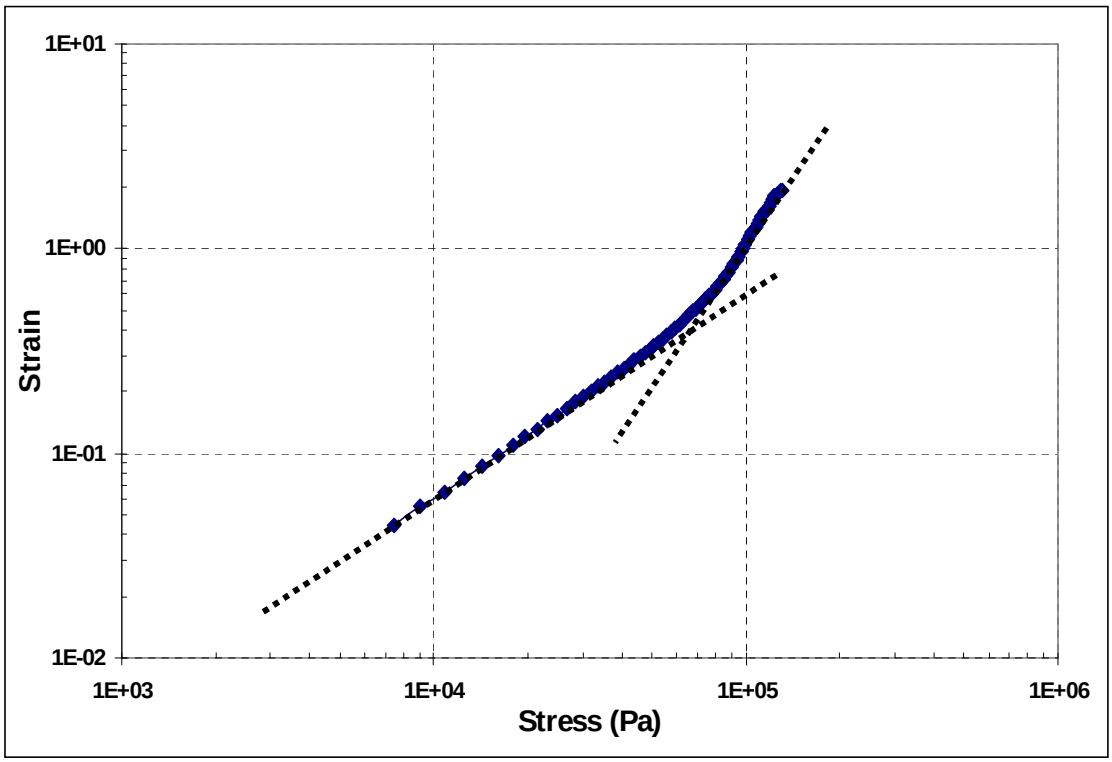

Figure 4.3: Strain versus stress for linear SBS PMB bitumen at 30˚C and 1 Hz

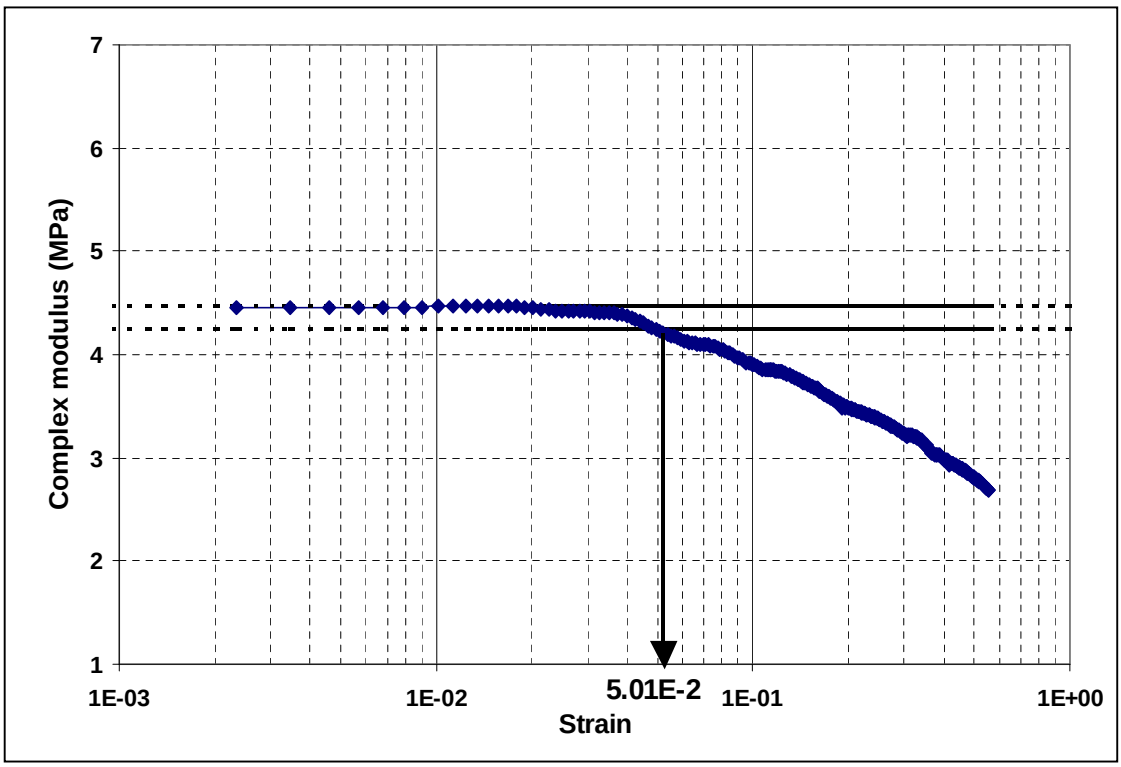

Figure 4.4: Complex modulus versus strain for EVA PMB at 1 Hz and 20˚C

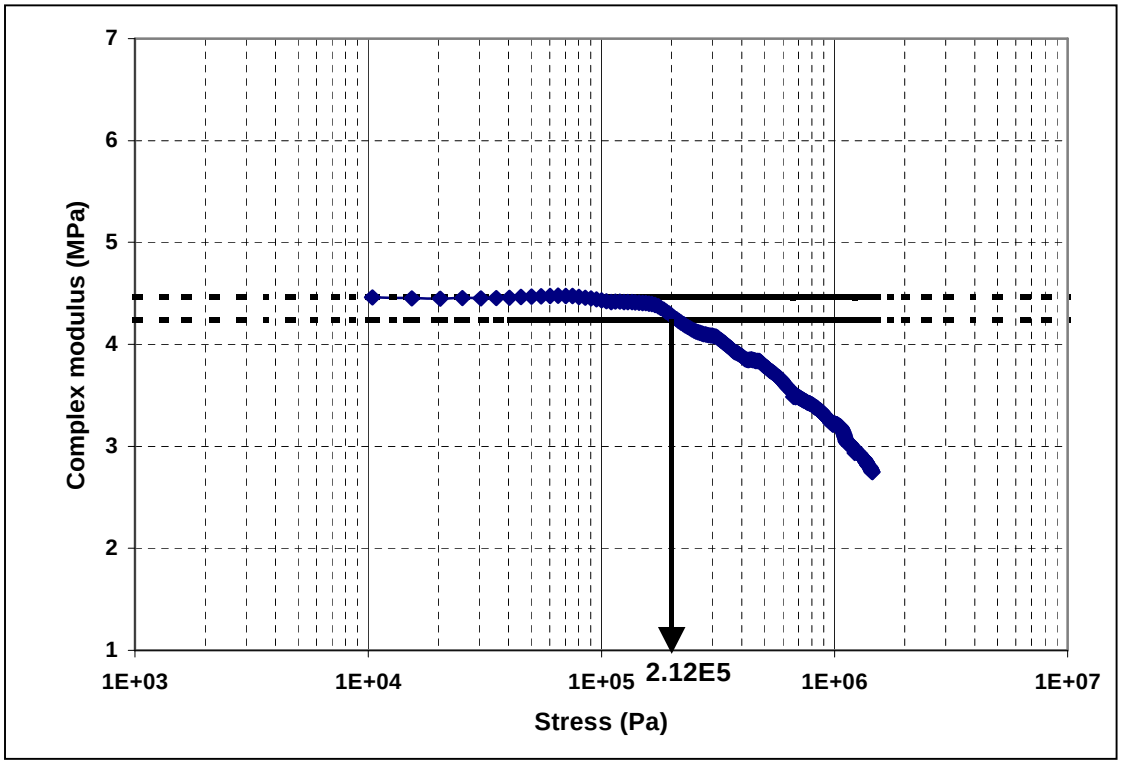

Figure 4.5: Complex modulus versus stress for EVA PMB at 1 Hz and 20˚C

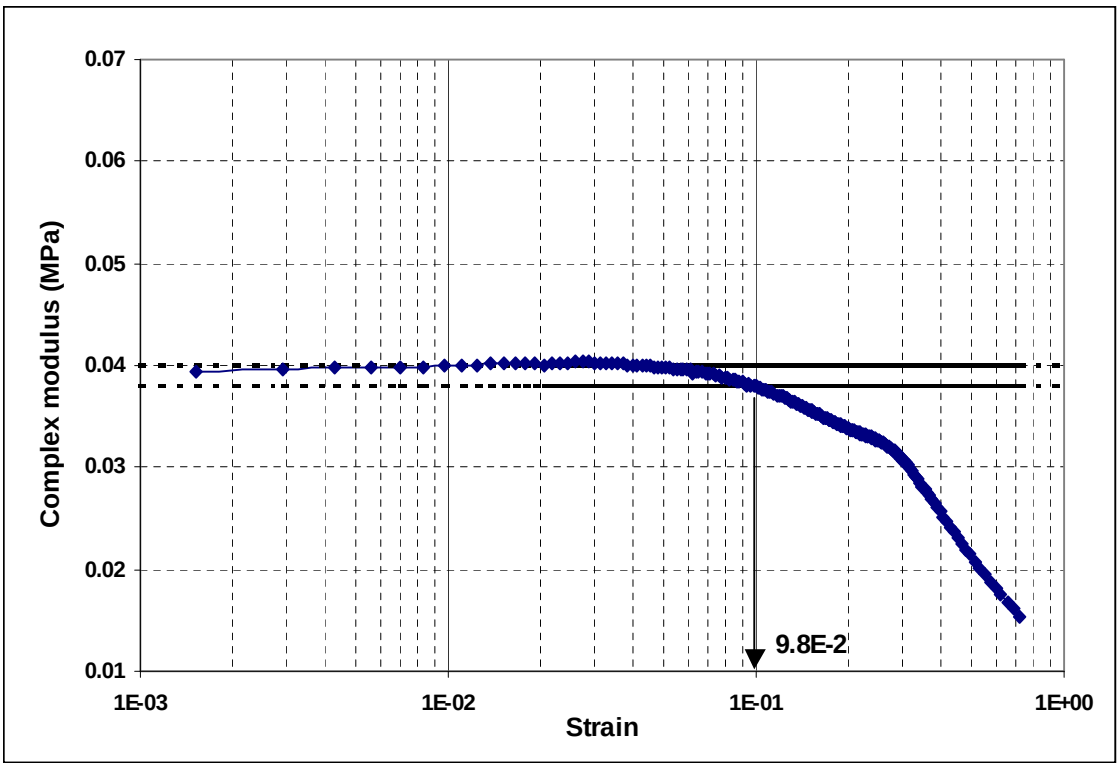

Figure 4.6: Complex modulus versus strain for multigrade (35/50) at 5 Hz and 60˚C

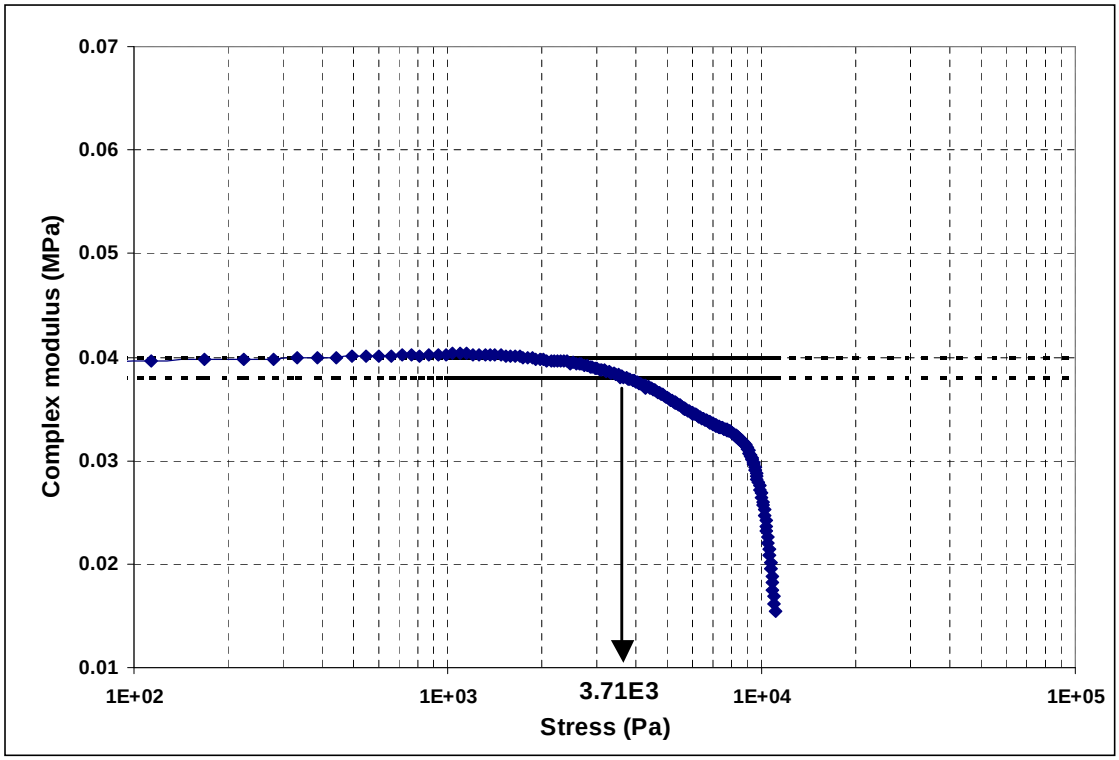

Figure 4.7: Complex modulus versus stress for multigrade (35/50) at 5 Hz and 60˚C

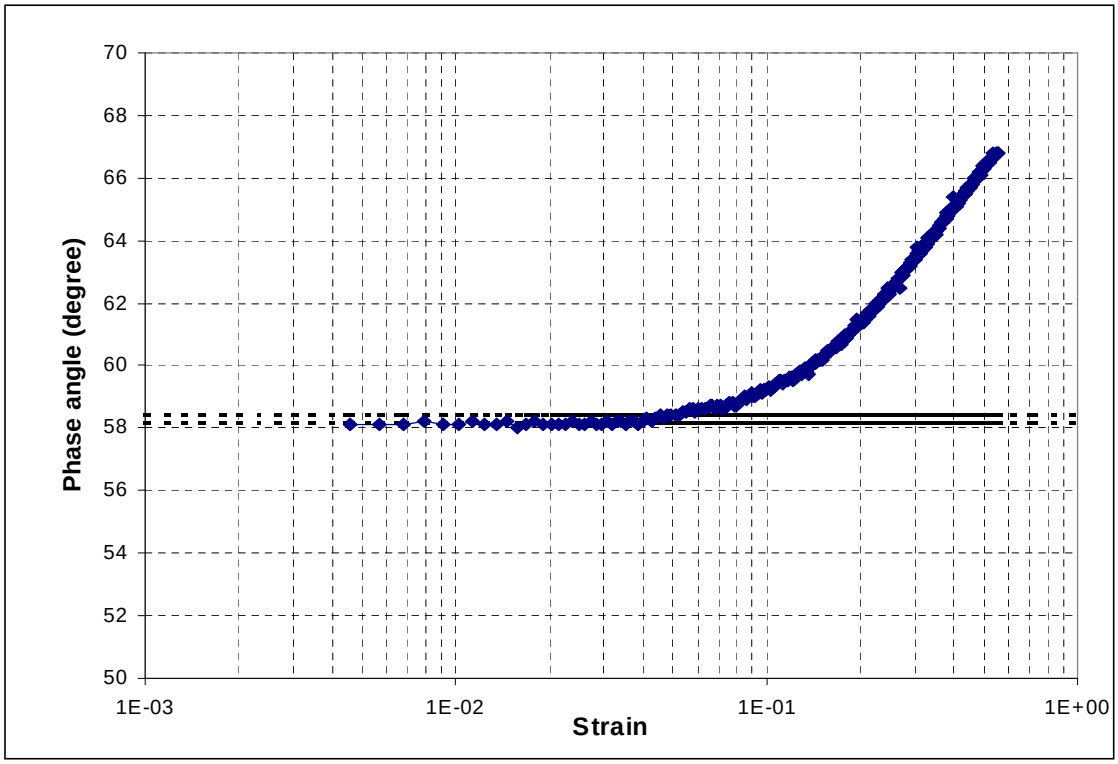

Figure 4.8: Phase angle versus strain for EVA PMB at 20˚C and 1 Hz

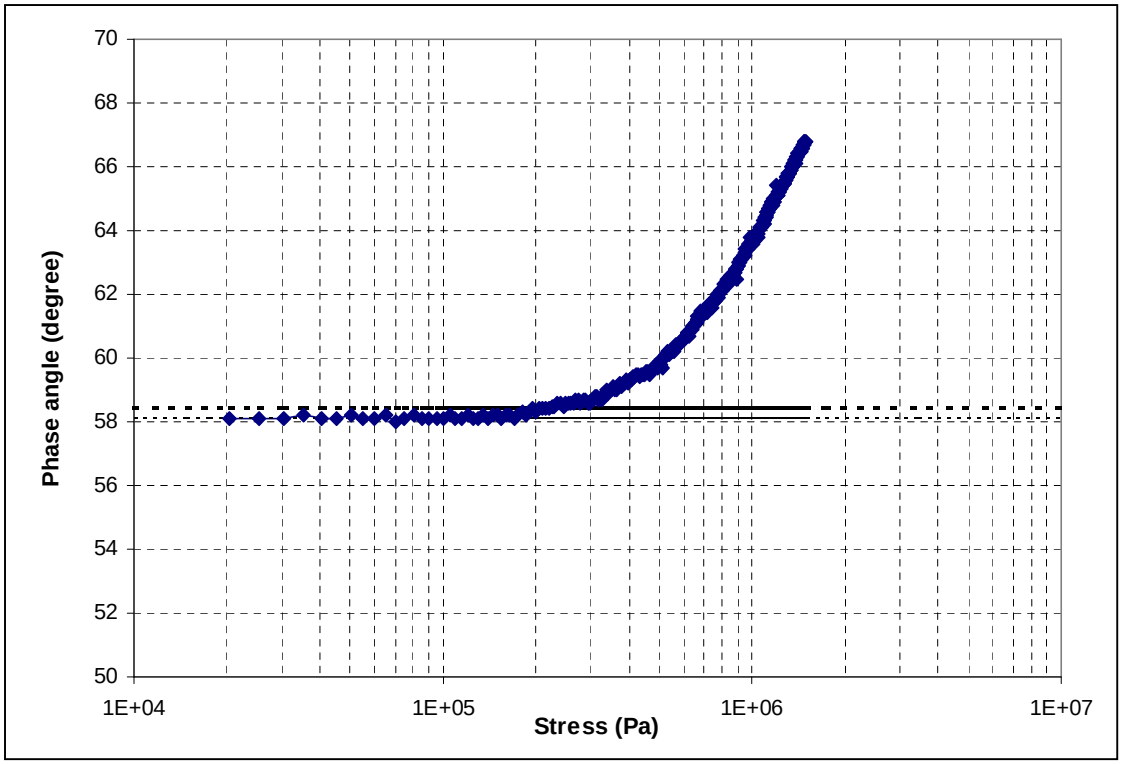

Figure 4.9: Phase angle versus stress for EVA PMB at 20˚C and 1 Hz

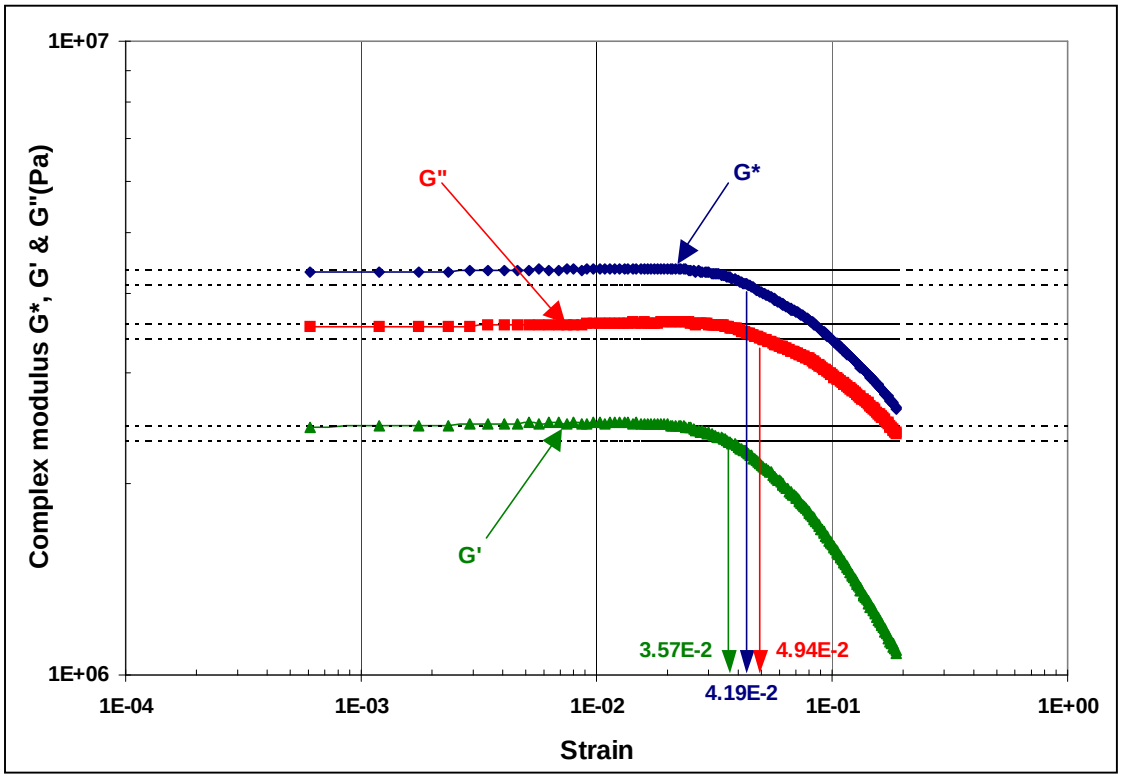

Figure 4.10: G*, G' & G" versus strain for 50 pen aged bitumen at 1 Hz and 20˚C

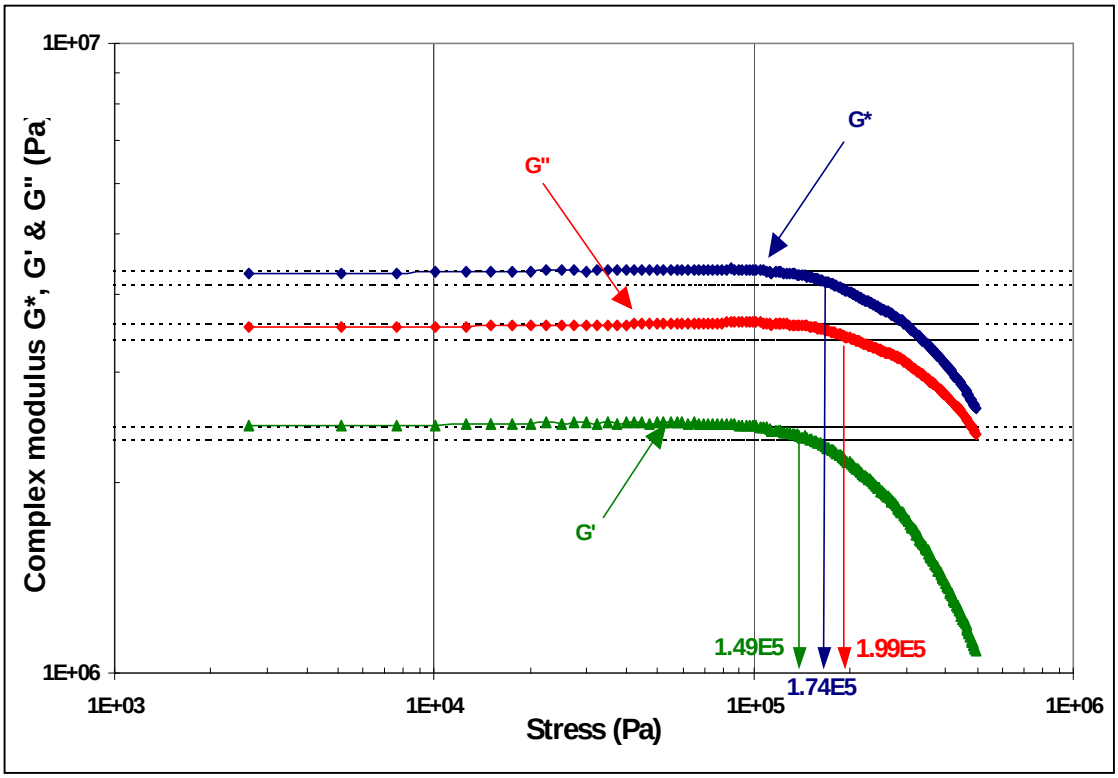

Figure 4.11: G*, G' & G" versus stress for 50 pen aged bitumen at 1 Hz and 20˚C

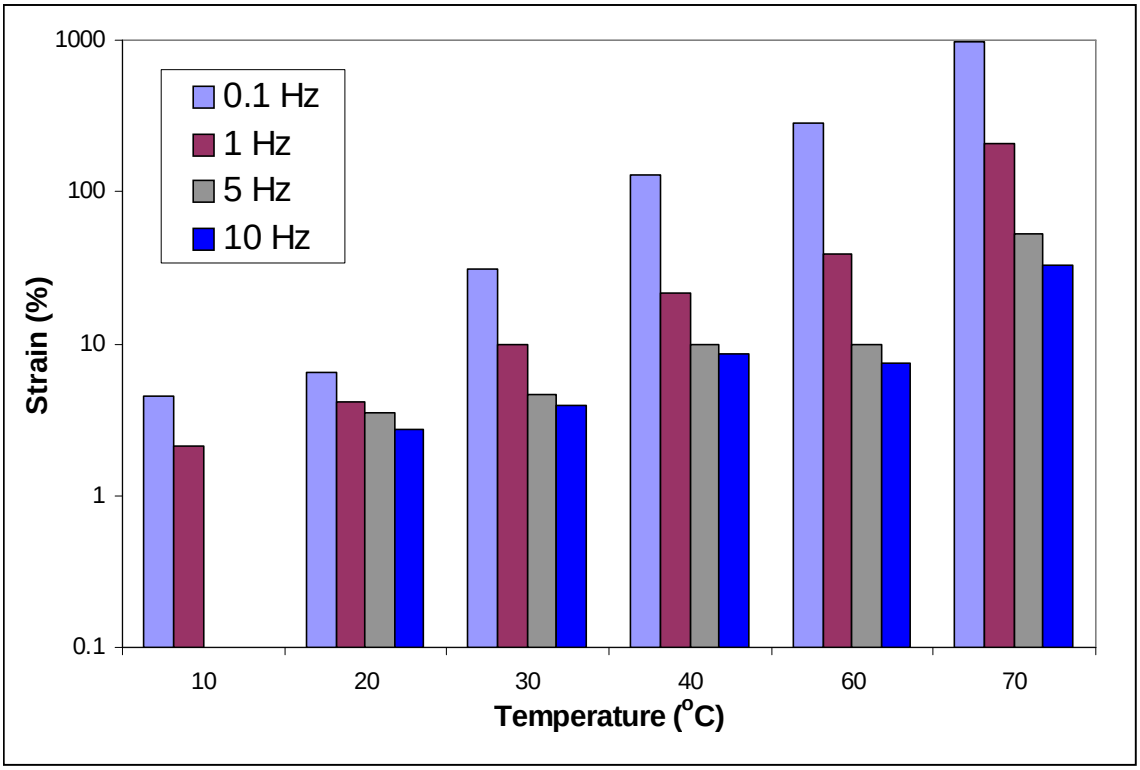

Figure 4.12: Linear limit of strain versus temperature at different frequencies for aged 50 pen bitumen

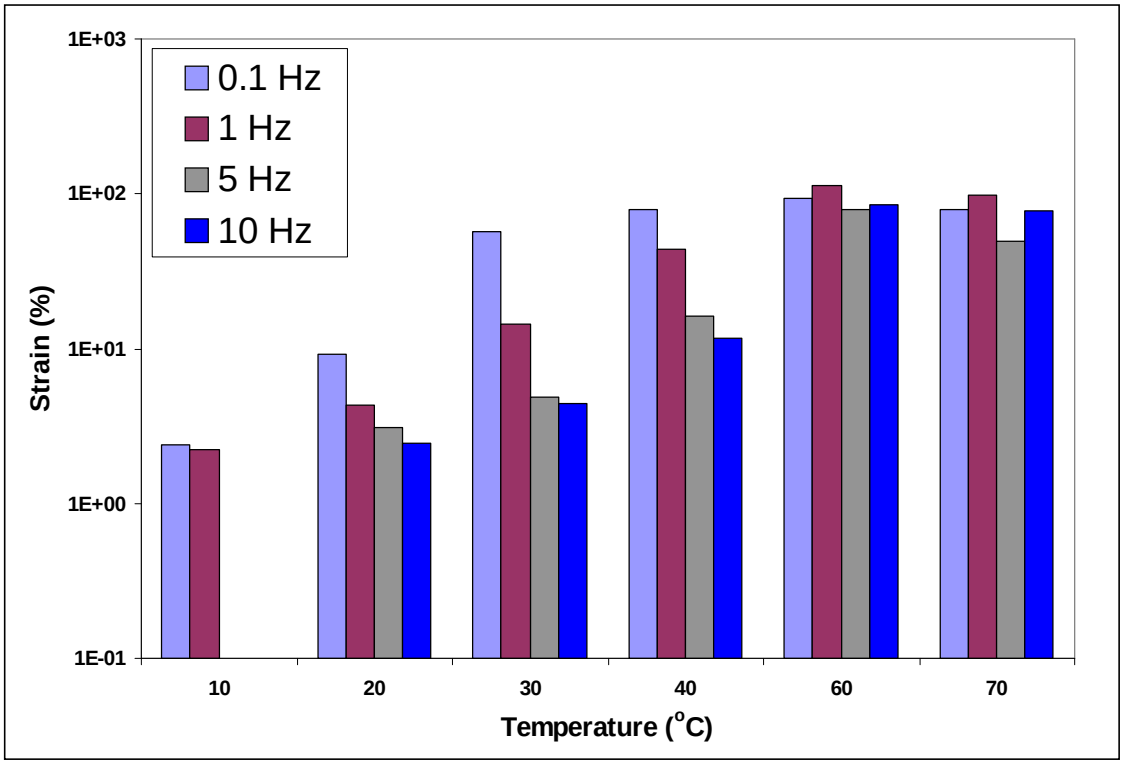

Figure 4.13: Linear limit of strain versus temperature at different frequencies for aged radial SBS PMB

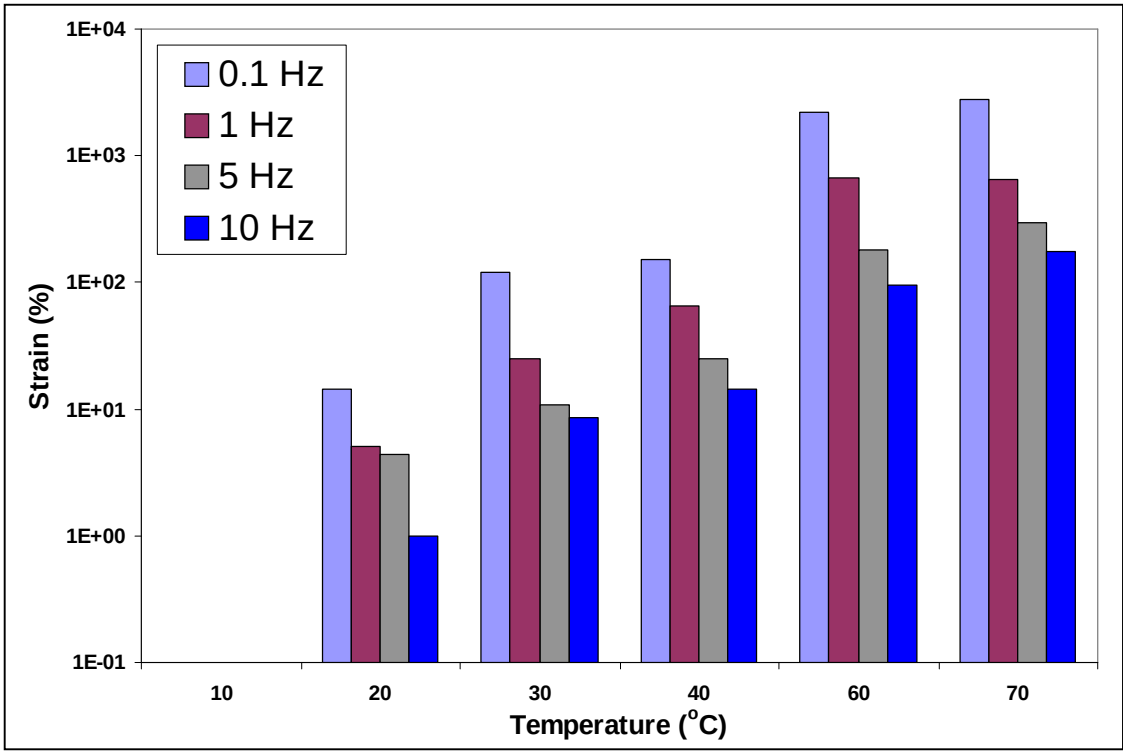

Figure 4.14: Linear limit of strain versus temperature at different frequencies for EVA PMB

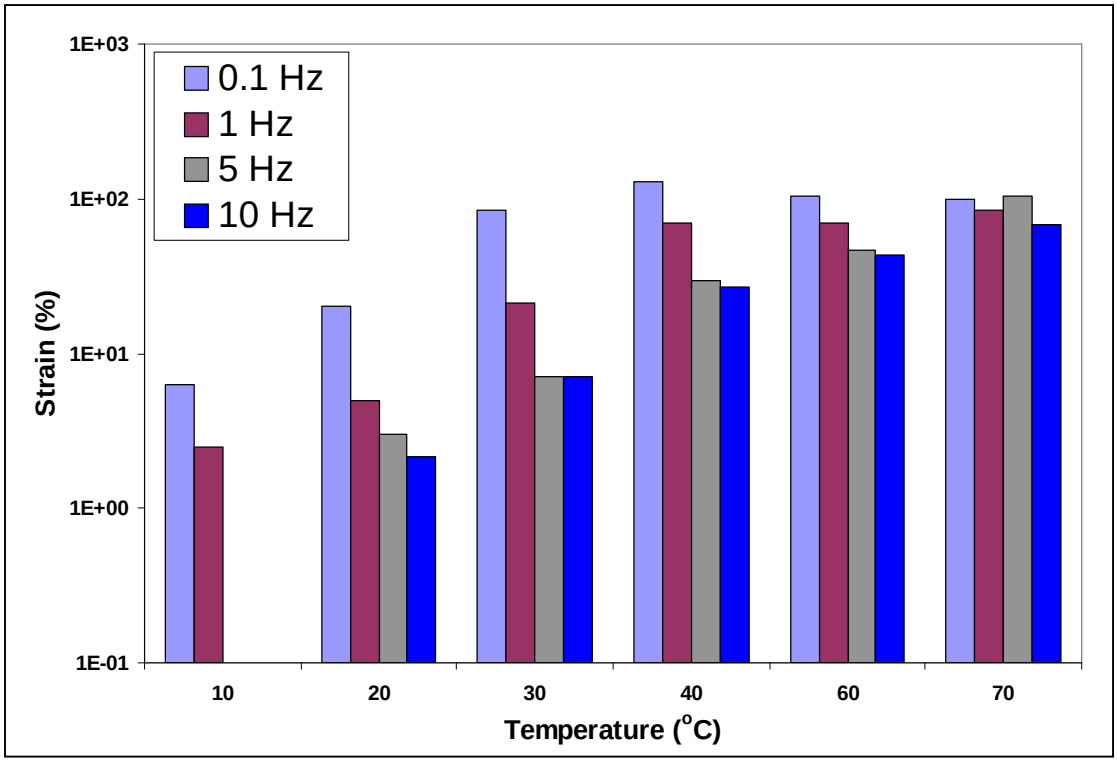

Figure 4.15: Linear limit of strain versus temperature at different frequencies for linear SBS PMB

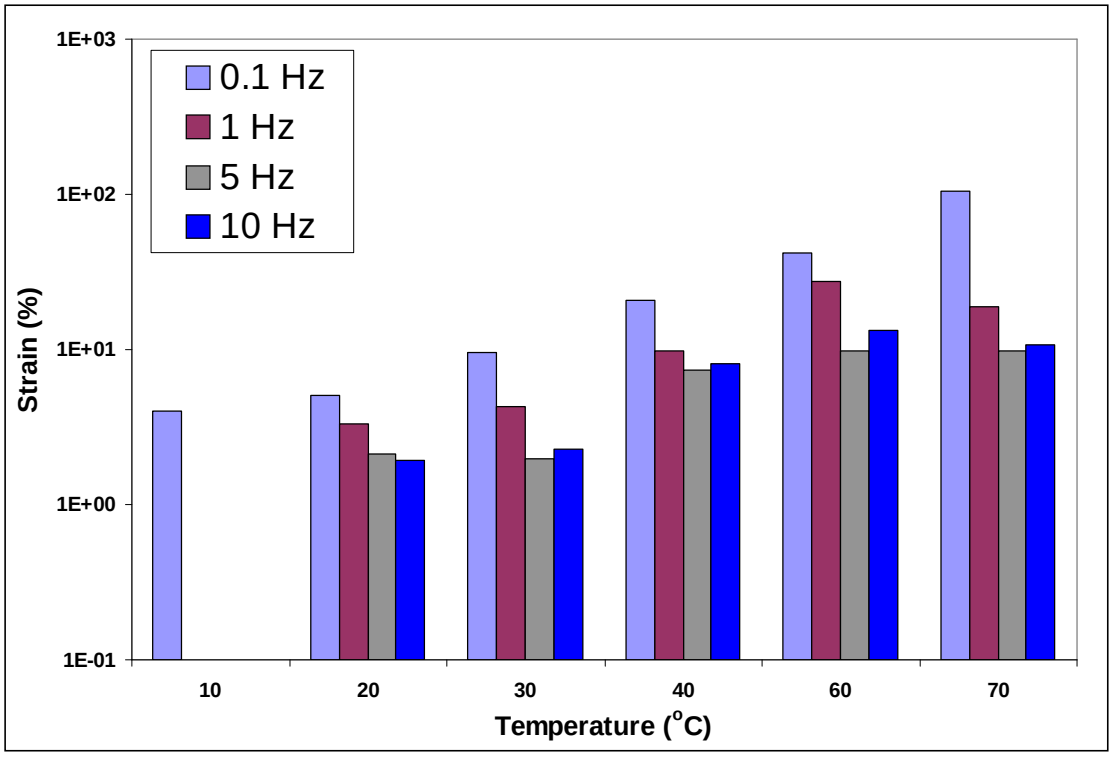

Figure 4.16: Linear limit of strain versus temperature at different frequencies for multigrade (35/50) bitumen

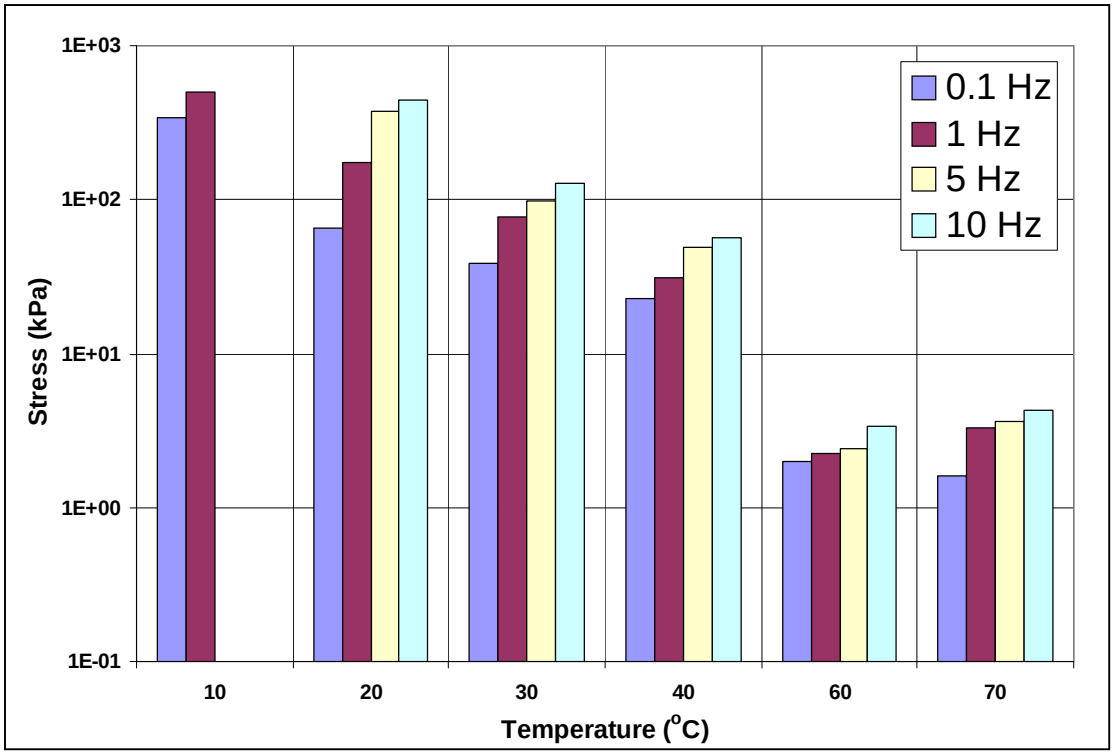

Figure 4.17: Linear limit of stress versus temperature at different frequencies for aged 50 pen bitumen

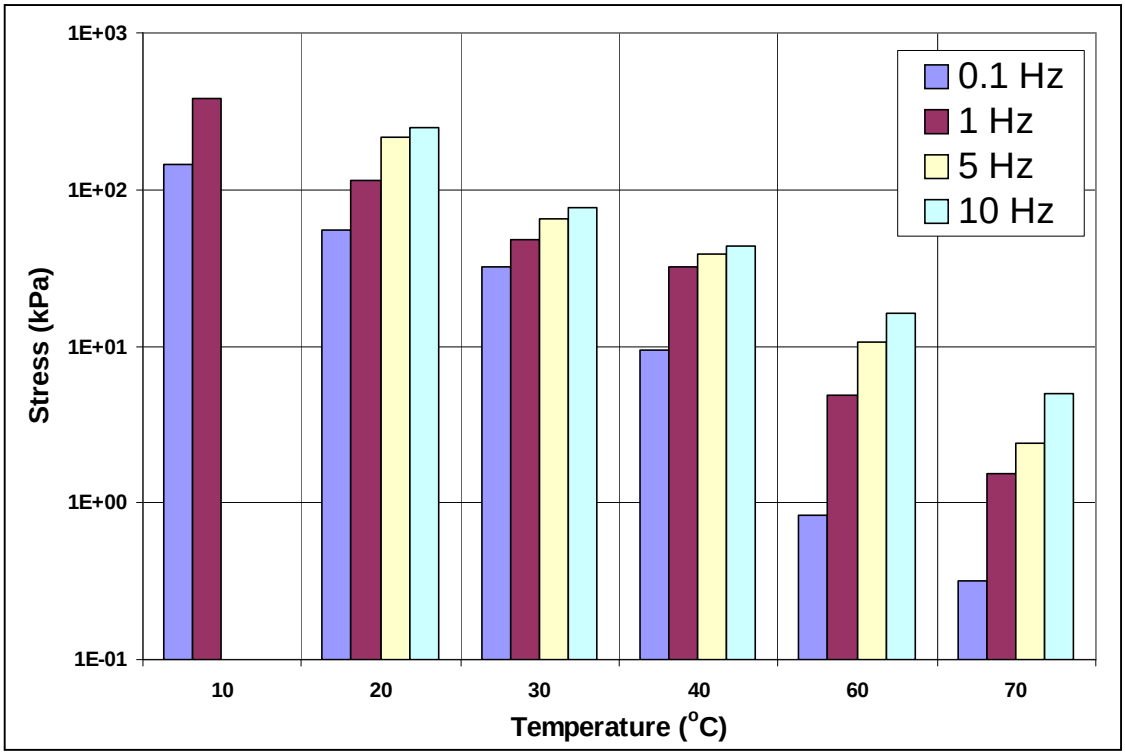

Figure 4.18: Linear limit of stress versus temperature at different frequencies for radial SBS PMB

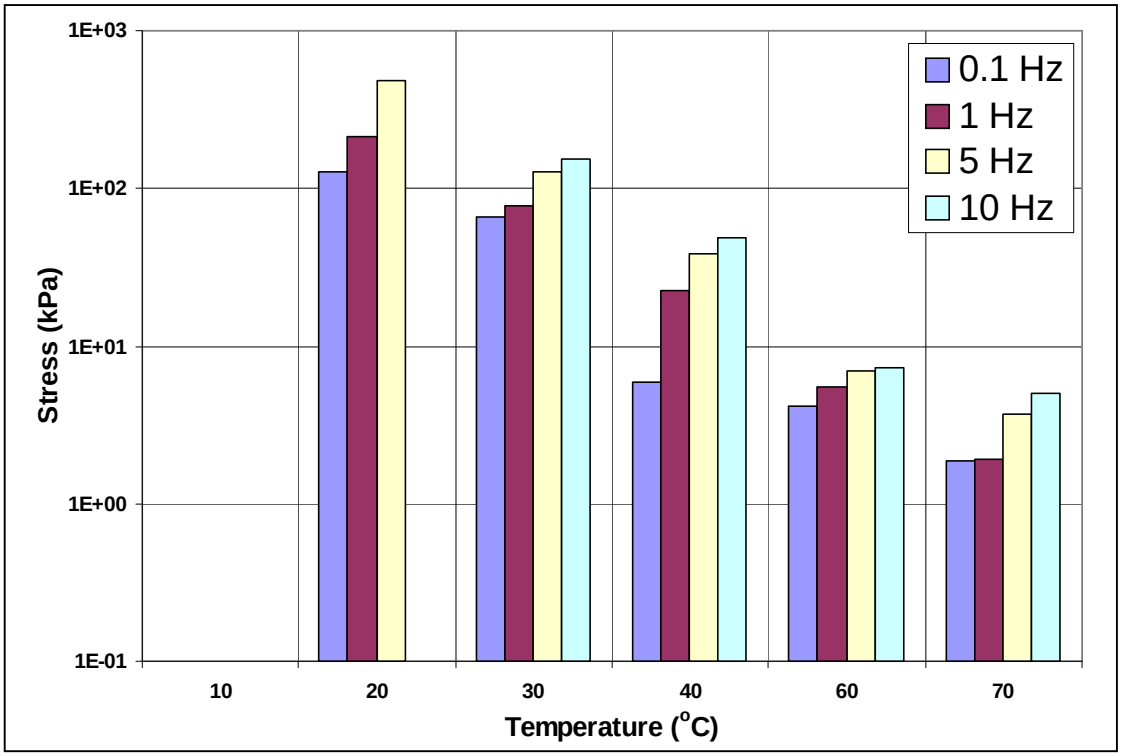

Figure 4.19: Linear limit of stress versus temperature at different frequencies for EVA PMB

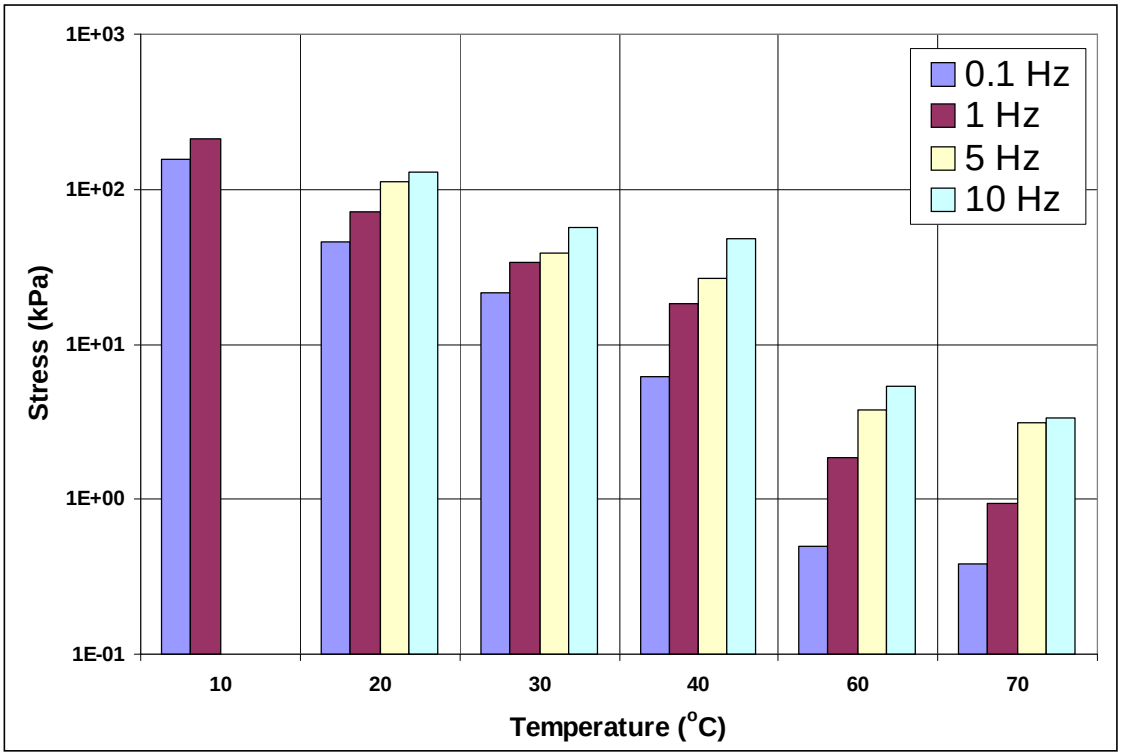

Figure 4.20: Linear limit of stress versus temperature at different frequencies for radial SBS PMB

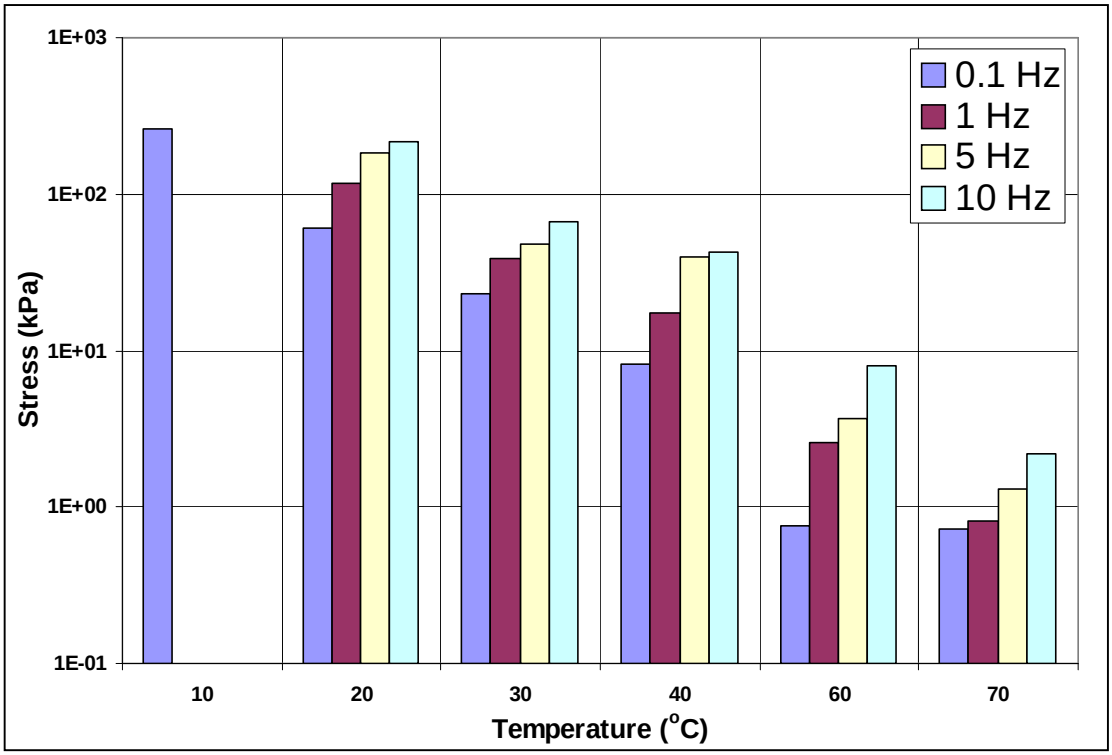

Figure 4.21: Linear limit of stress versus temperature at different frequencies for multigrade (35/50) bitumen

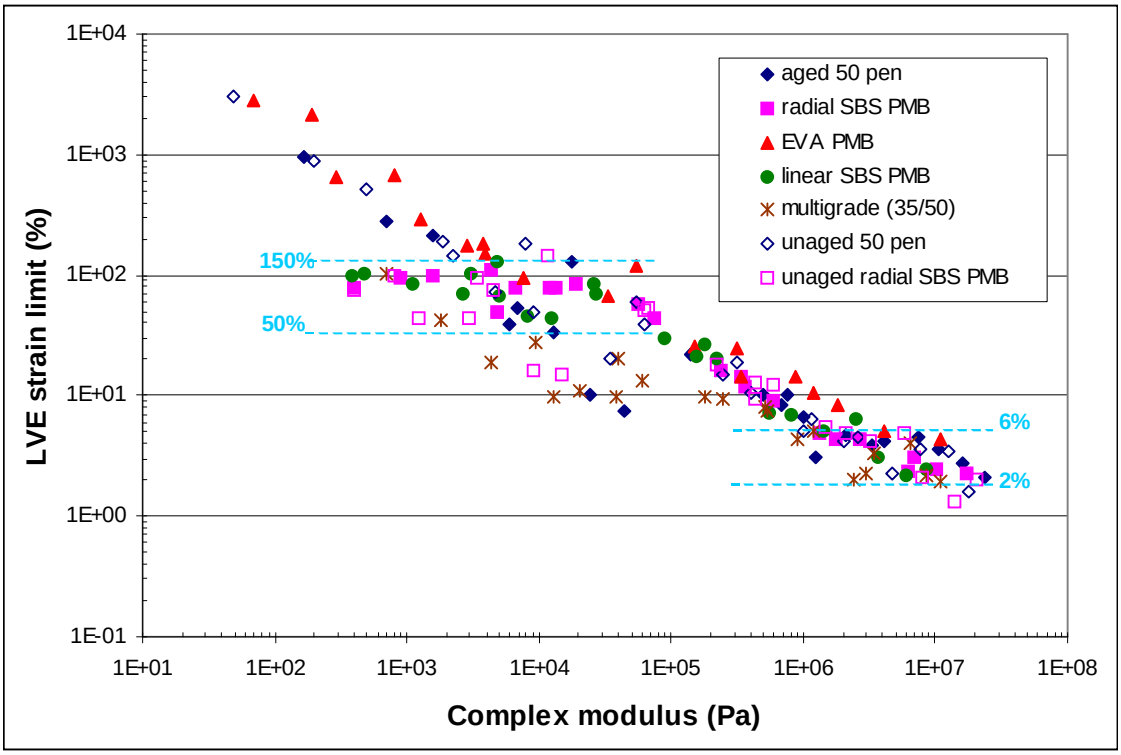

Figure 4.22: Linear viscoelastic strain limits as a function of complex modulus for unaged and RTFOT aged bitumens

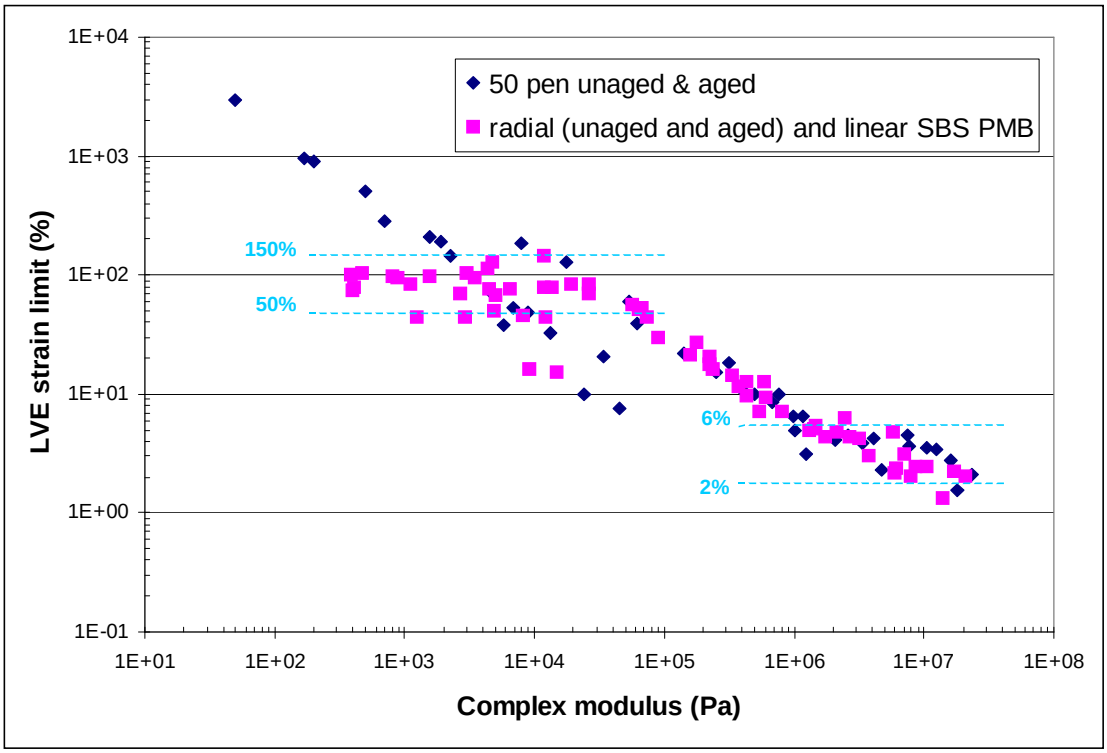

Figure 4.23: Linear viscoelastic strain limits as a function of complex modulus for unaged and aged conventional binders and elastometric modified binders

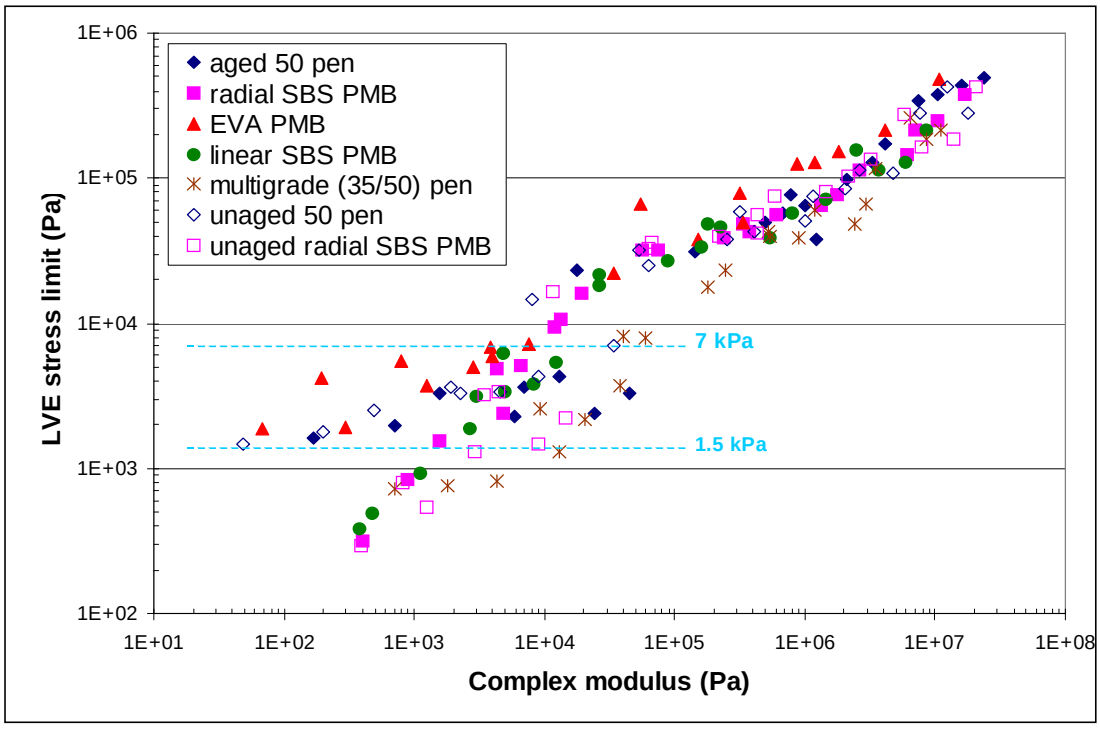

Figure 4.24: Linear viscoelastic stress limits as a function of complex modulus for different bitumens

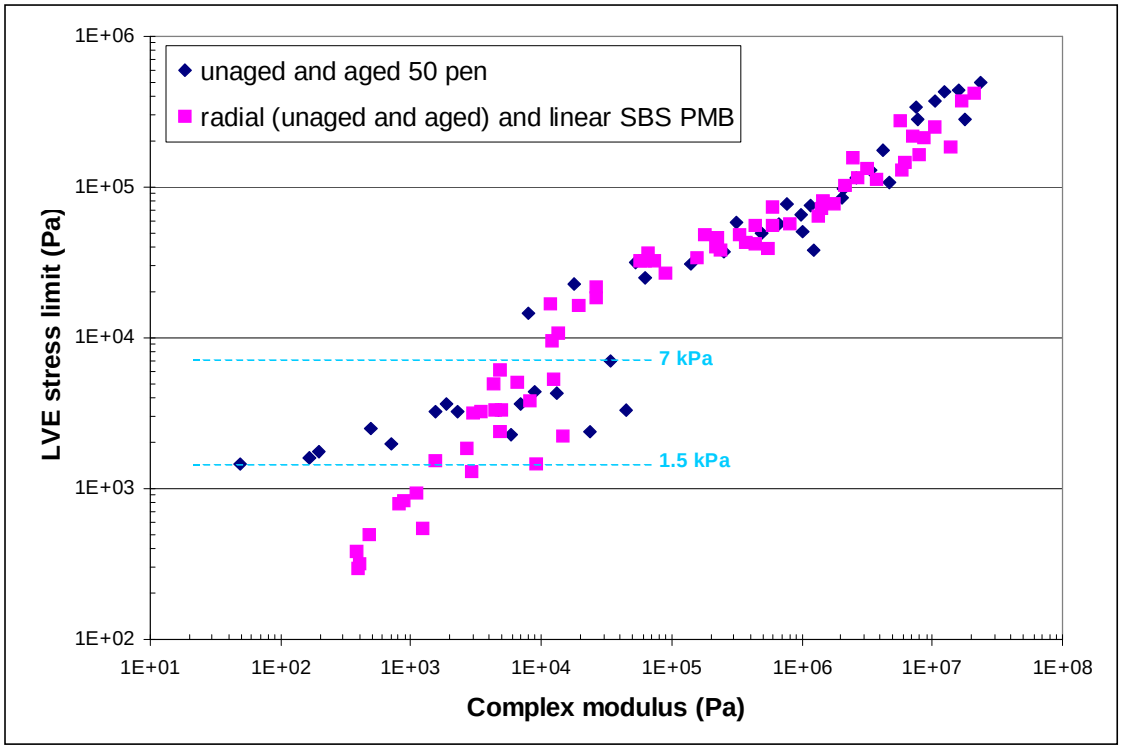

Figure 4.25: Linear viscoelastic stress limits as a function of complex modulus for unaged and aged conventional and elastomeric modified binders

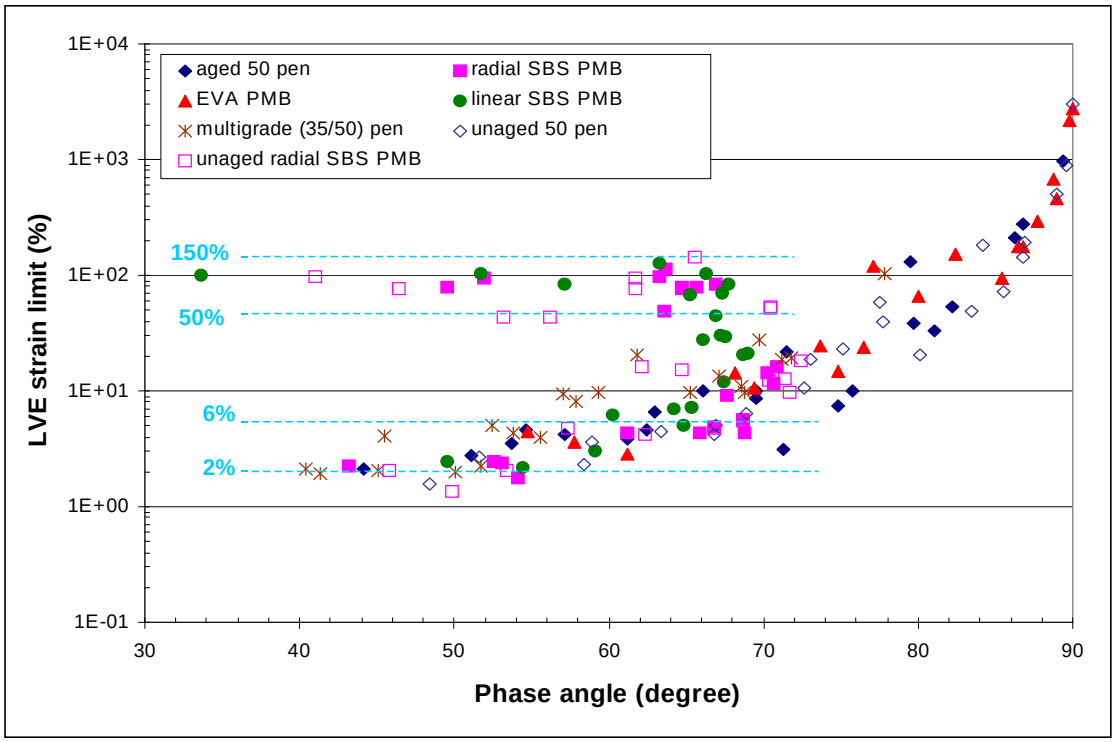

Figure 4.26: Linear viscoelastic strain limits as a function of phase angle for unaged and RTFOT aged bitumens

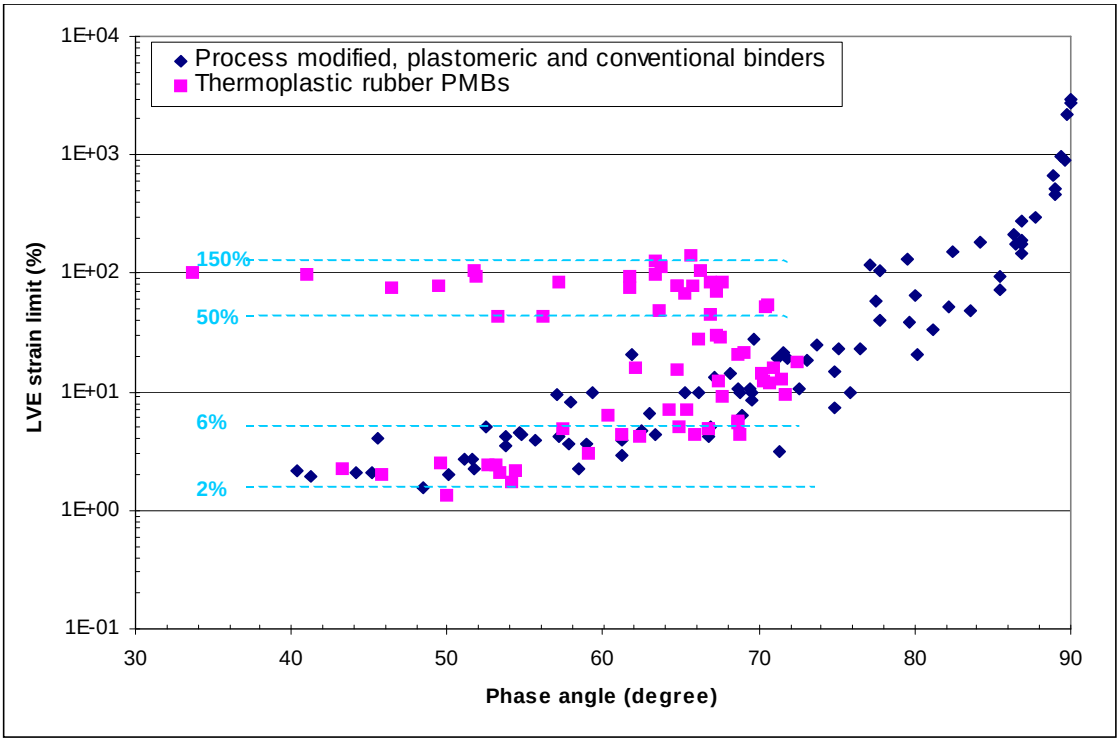

Figure 4.27: Linear viscoelastic strain limits as a function of phase angle for unaged and RTFOT aged conventional, process modified, plastomeric and elastomeric (block co-polymer) modified binders

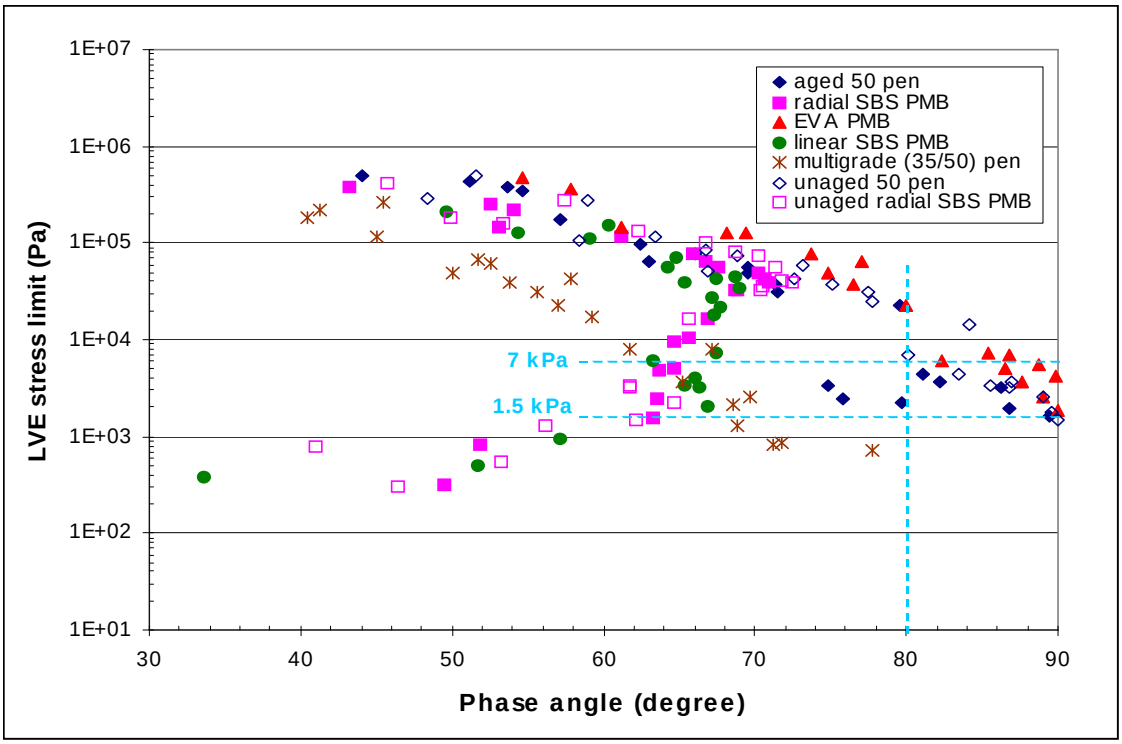

Figure 4.28: Linear viscoelastic stress limits as a function of phase angle for different bitumens

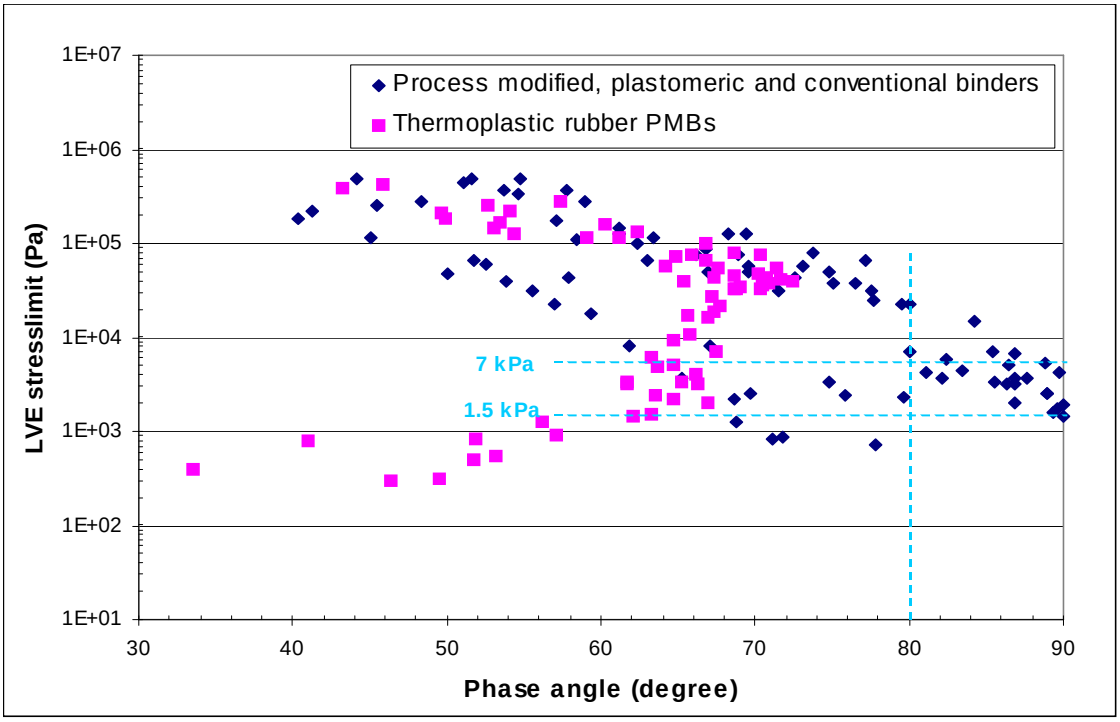

Figure 4.29: Linear viscoelastic stress limit as a function of phase angle for unaged and RTFOT aged conventional, process modified, plastomeric and elastomeric (block co-polymer) modified binders

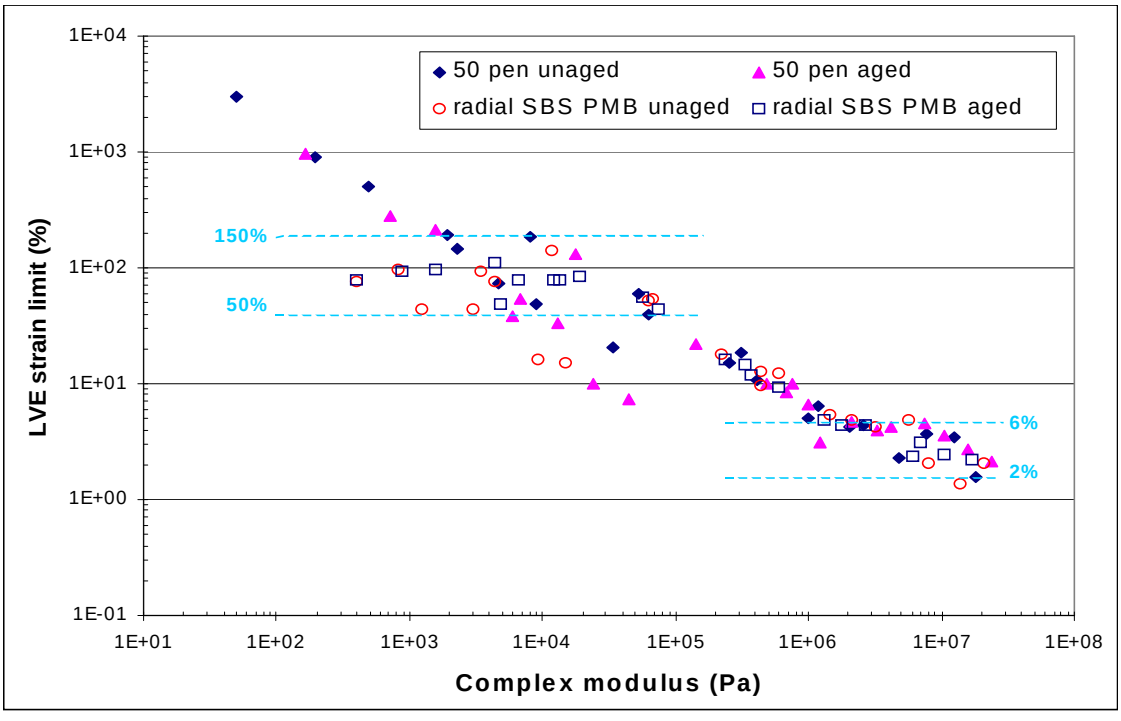

Figure 4.30: Linear viscoelastic strain limits as a function of complex modulus for unaged and RTFOT aged 50 penetration grade bitumen and radial SBS PMB

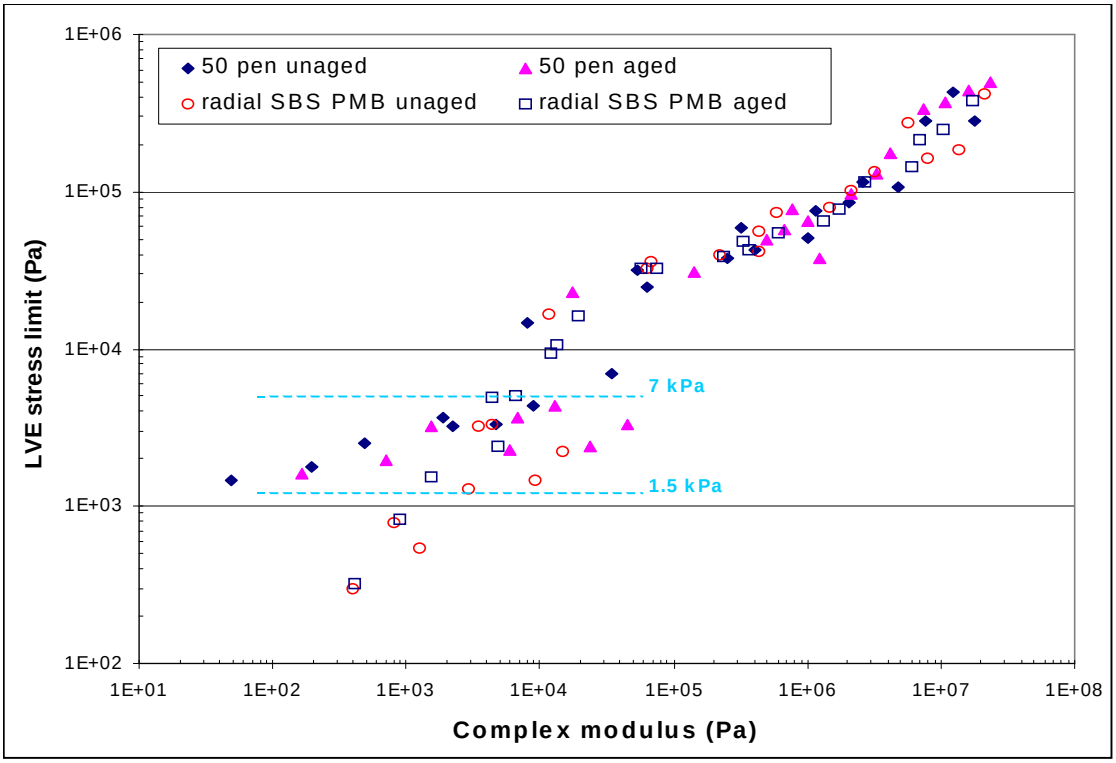

Figure 4.31: Linear viscoelastic stress limits as a function of complex modulus for unaged and RTFOT aged 50 penetration grade bitumen and radial SBS PMB

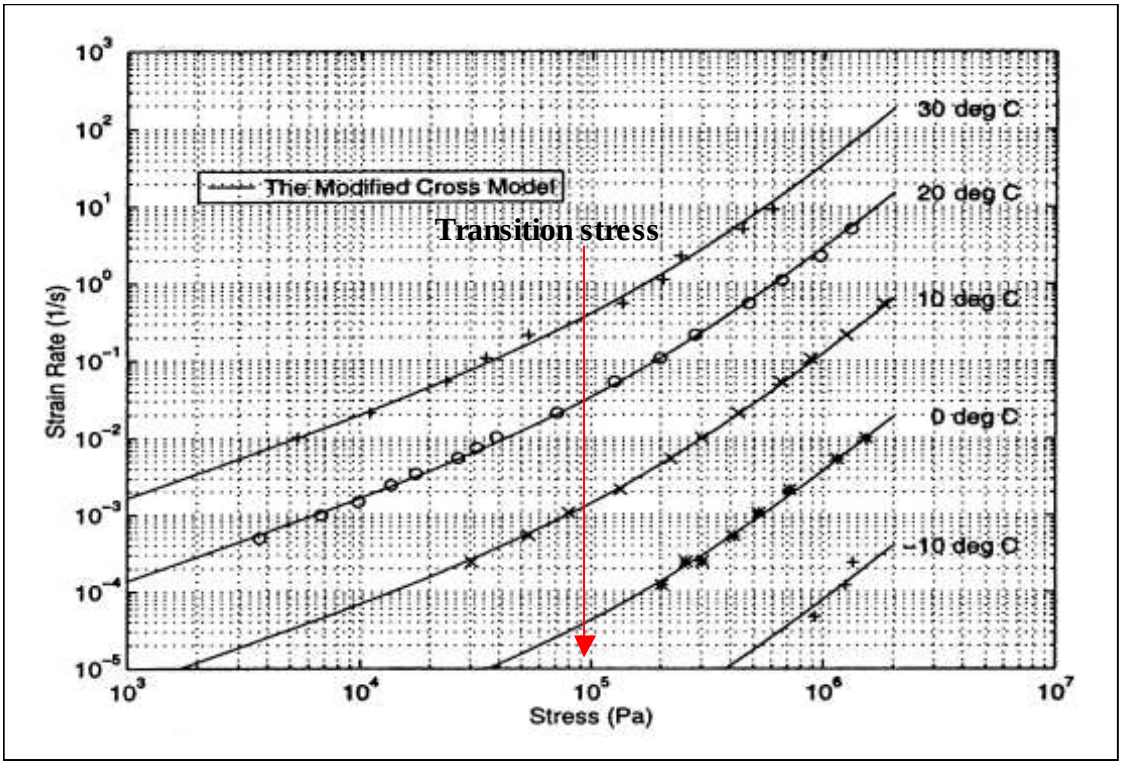

Figure 4.32: Steady-state creep behaviour in tension [39]

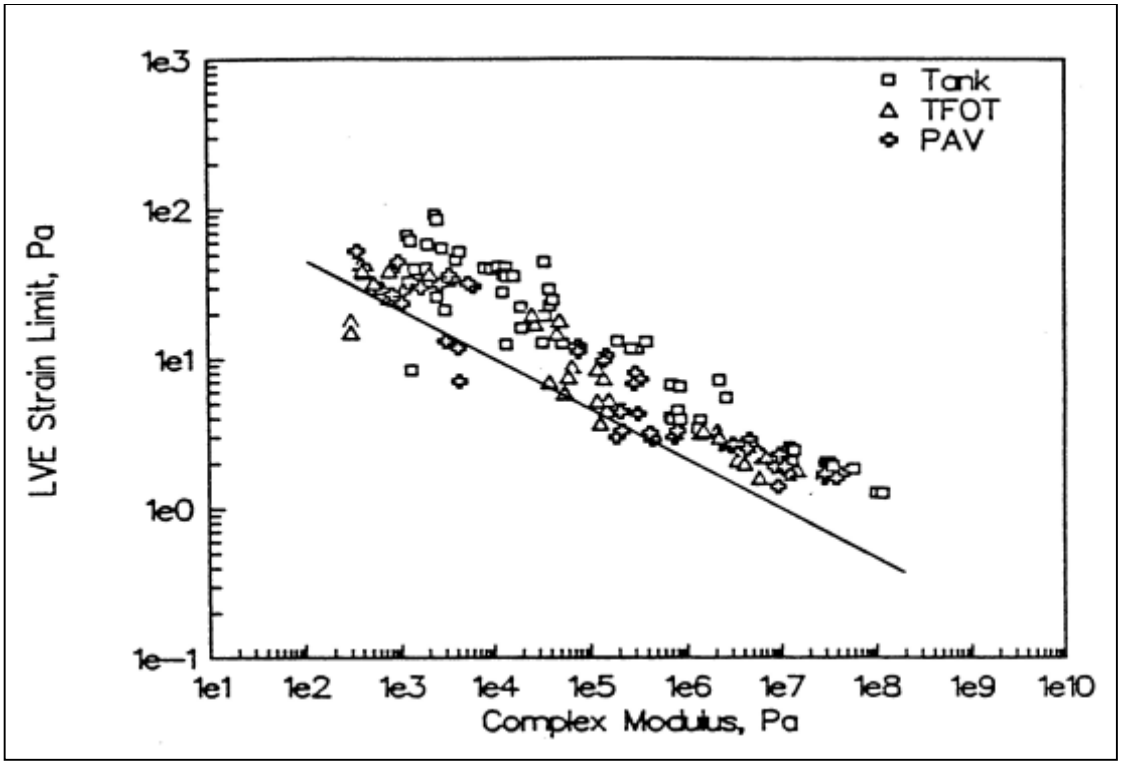

Figure 4.33: Linear viscoelastic strain limit as a function of complex modulus for unaged and aged bitumen from the SHRP study [20]

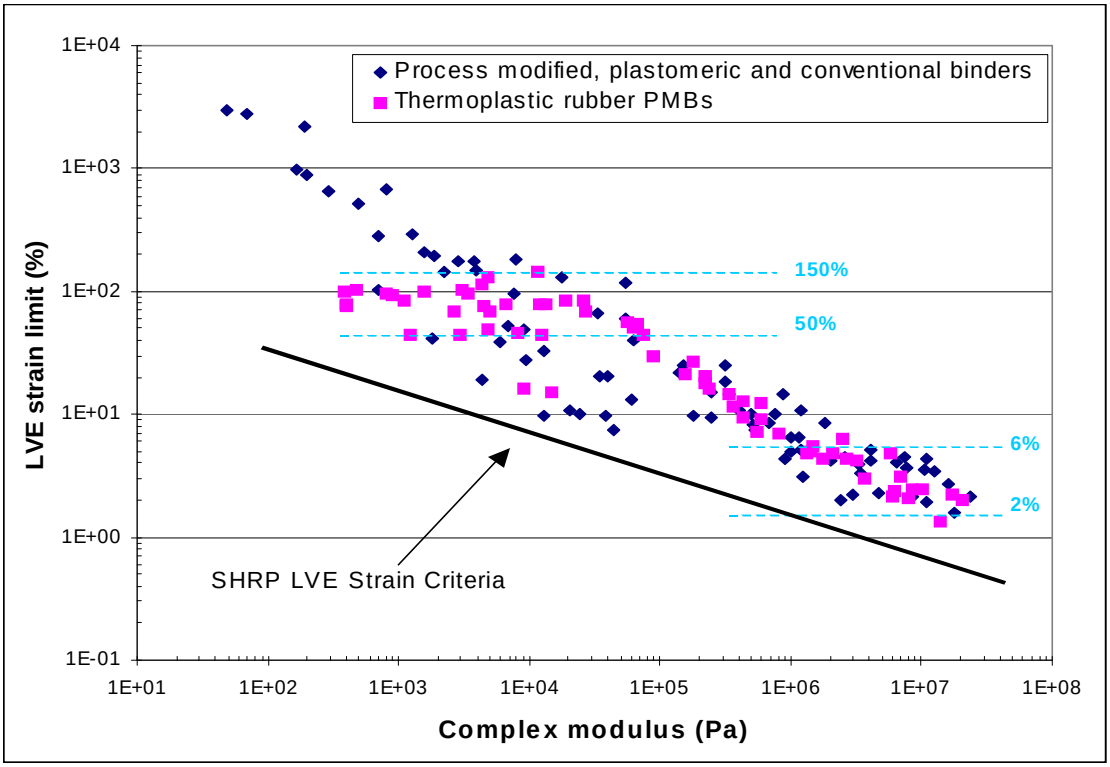

Figure 4.34: Linear viscoelastic strain limits as a function of complex modulus

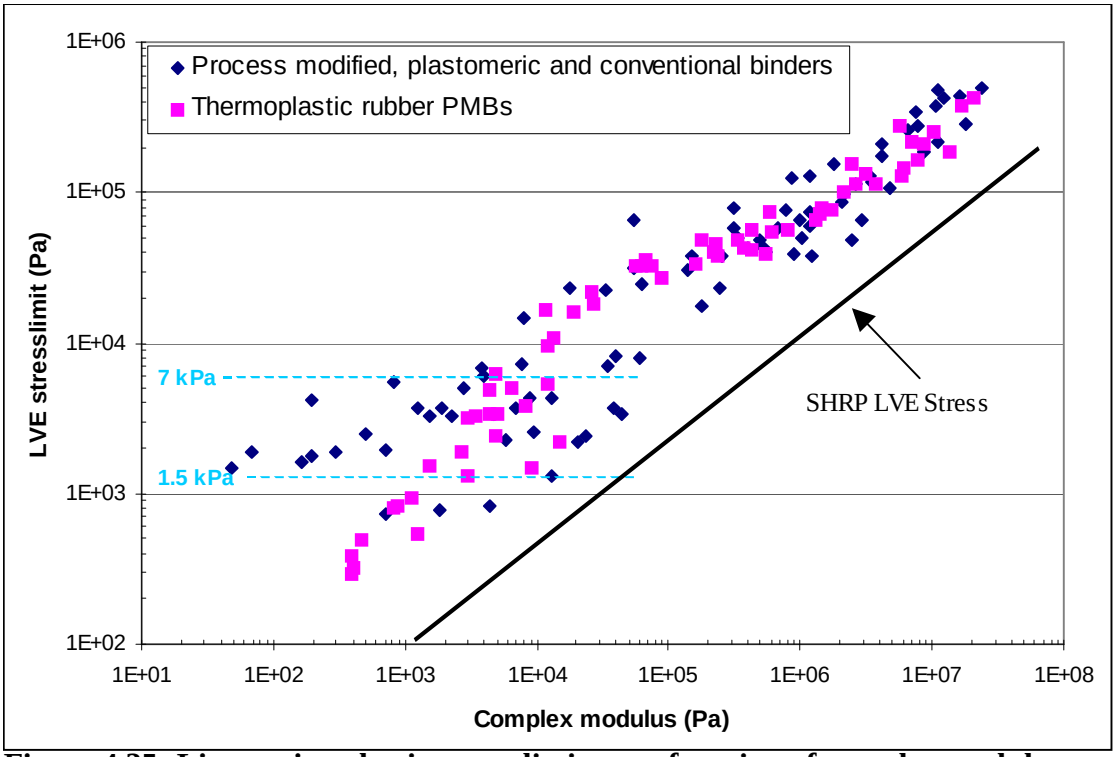

Figure 4.35: Linear viscoelastic stress limits as a function of complex modulus

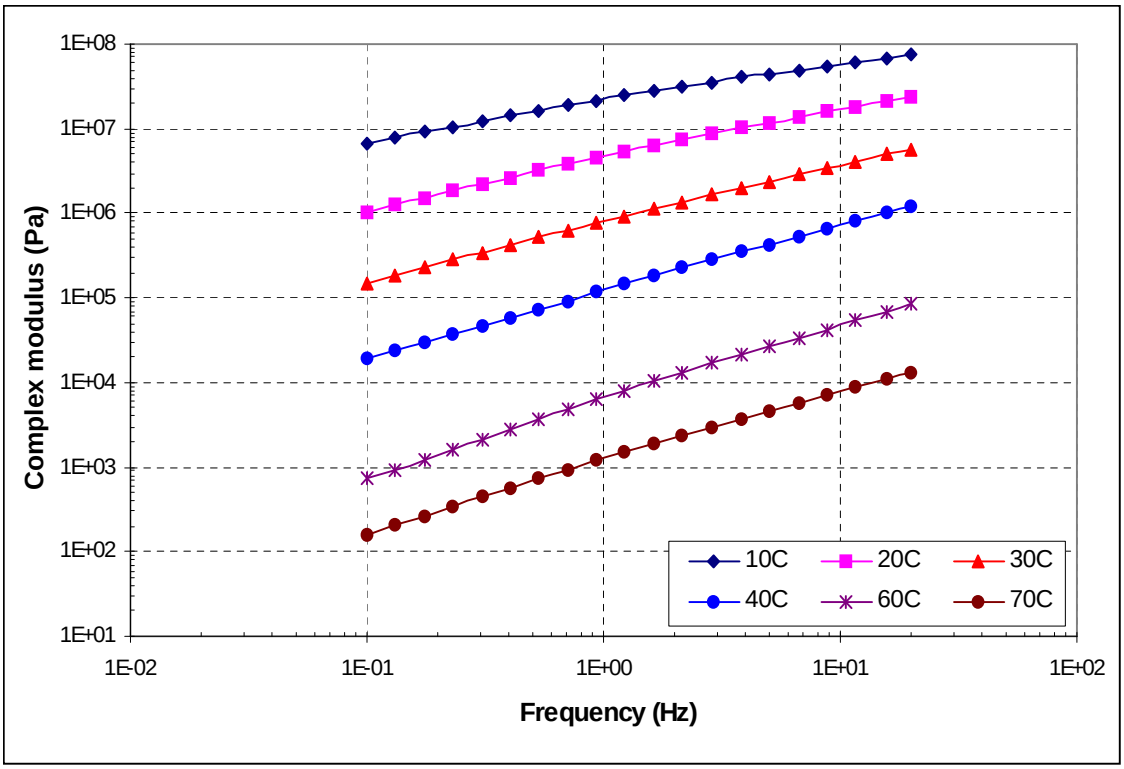

Figure 4.36: Isothermal plot of complex modulus for aged 50 pen bitumen

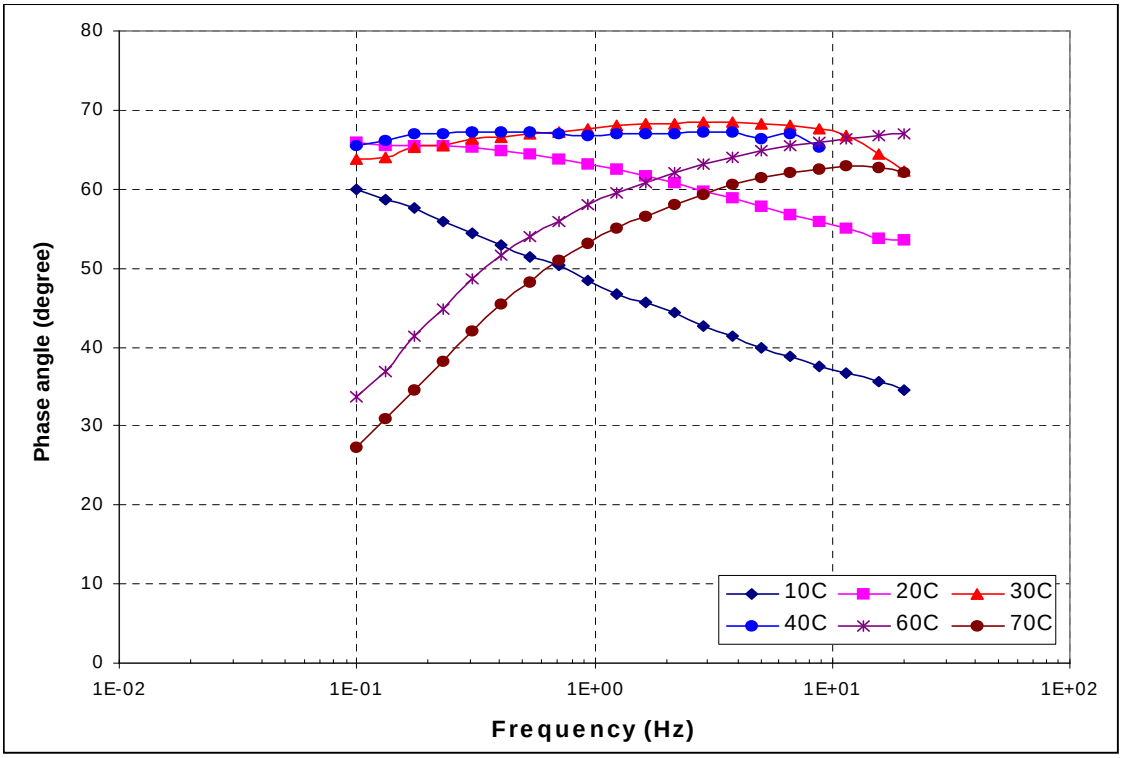

Figure 4.37: Isothermal plot of phase angle for linear SBS PMB

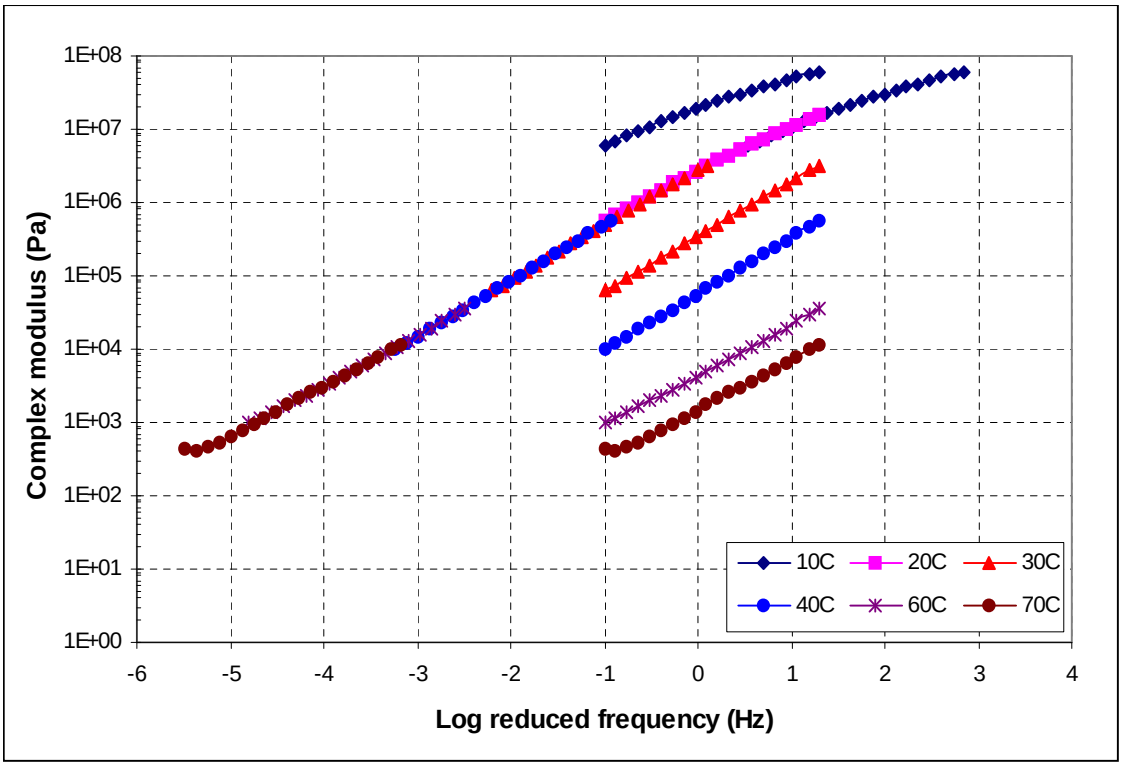

Figure 4.38: Master curve of complex modulus for radial SBS PMB at a reference temperature of 20˚C

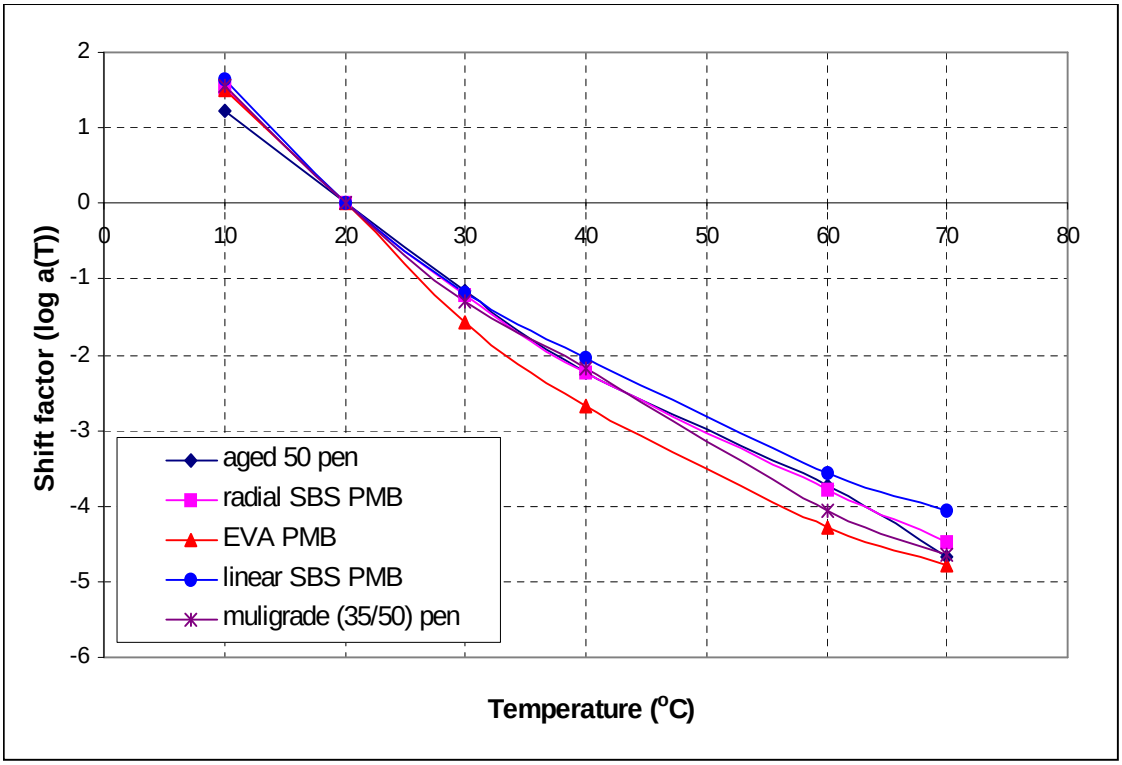

Figure 4.39: Shift factor versus temperature for short term aged bitumens

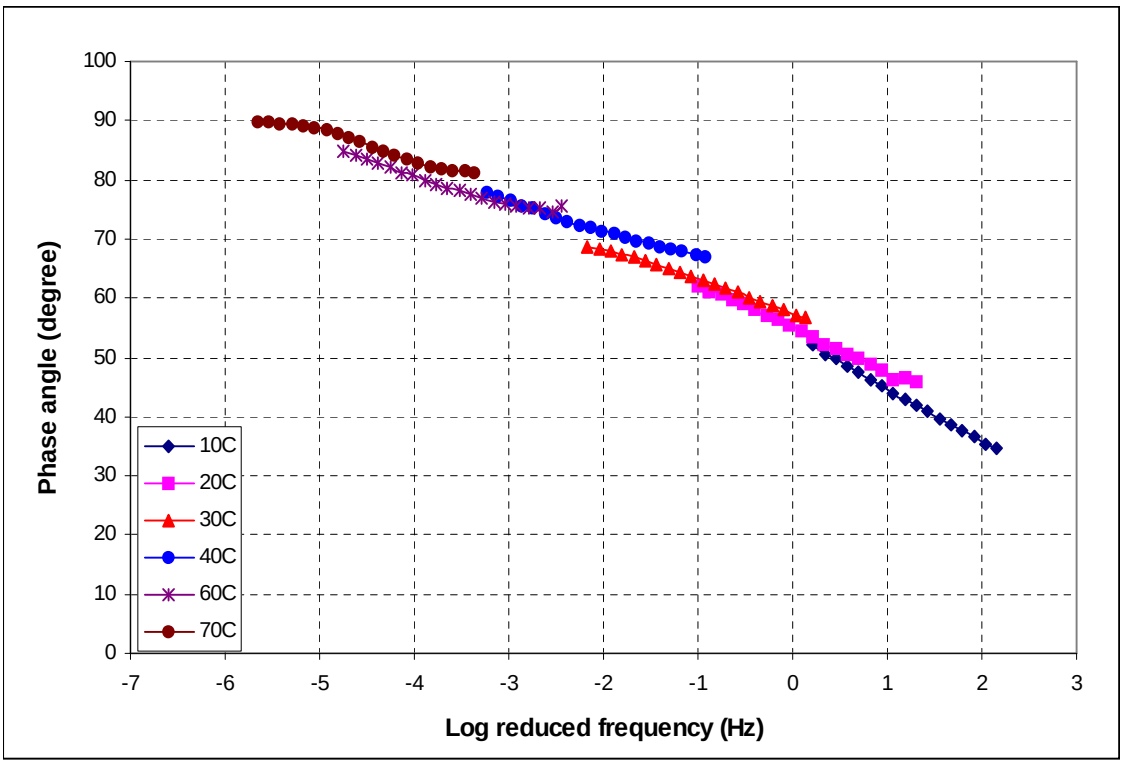

Figure 4.40: Master curve of phase angle for 50 pen aged bitumen at a reference temperature of 20˚C

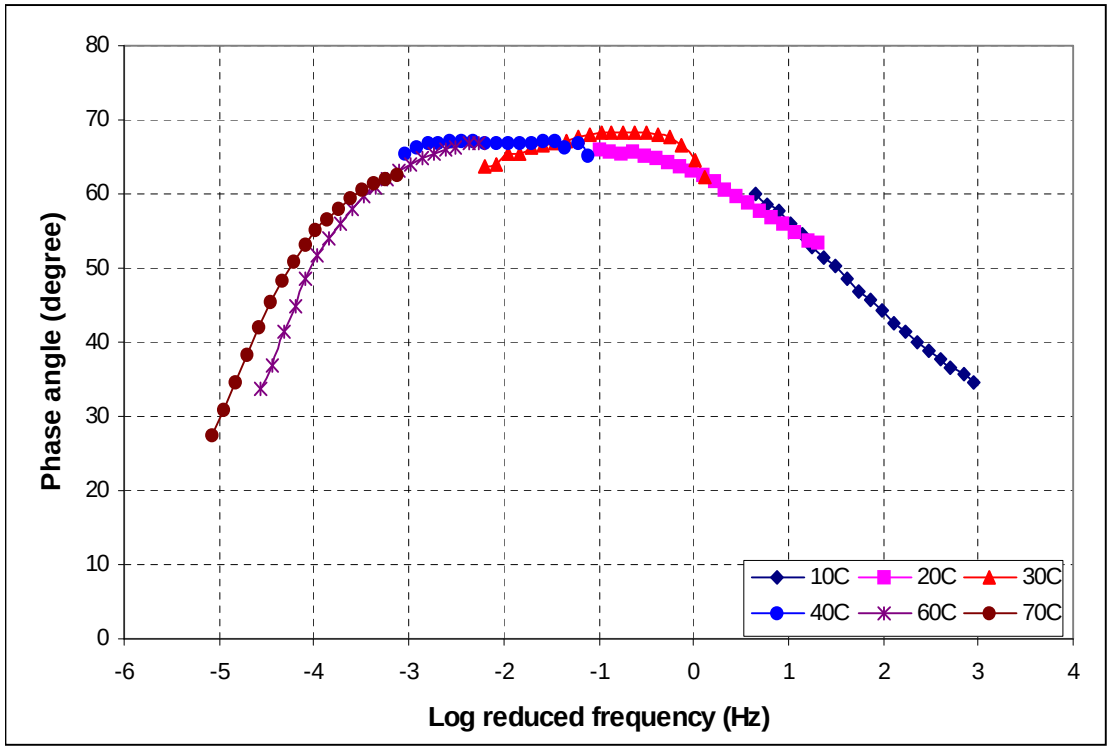

Figure 4.41: Master curve of phase angle for linear SBS PMB at a reference temperature of 20˚C

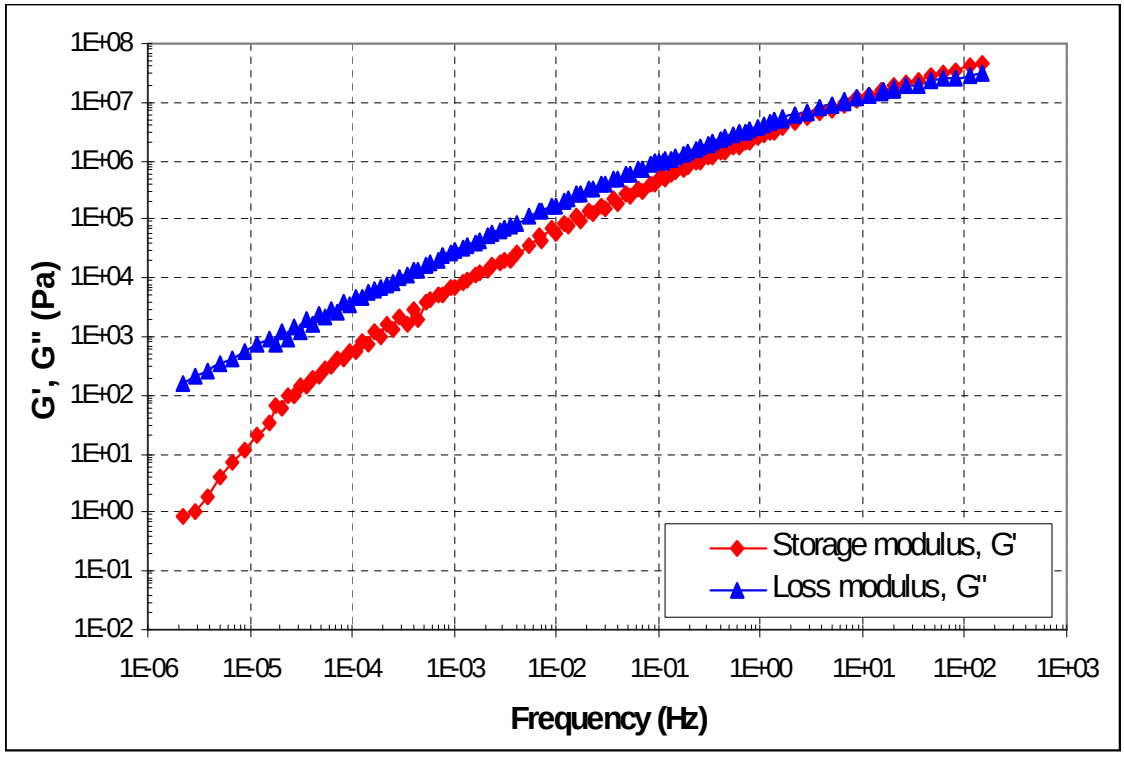

Figure 4.42: Master curves of the storage and loss modulus for 50 pen aged bitumen at a reference temperature of 20˚C

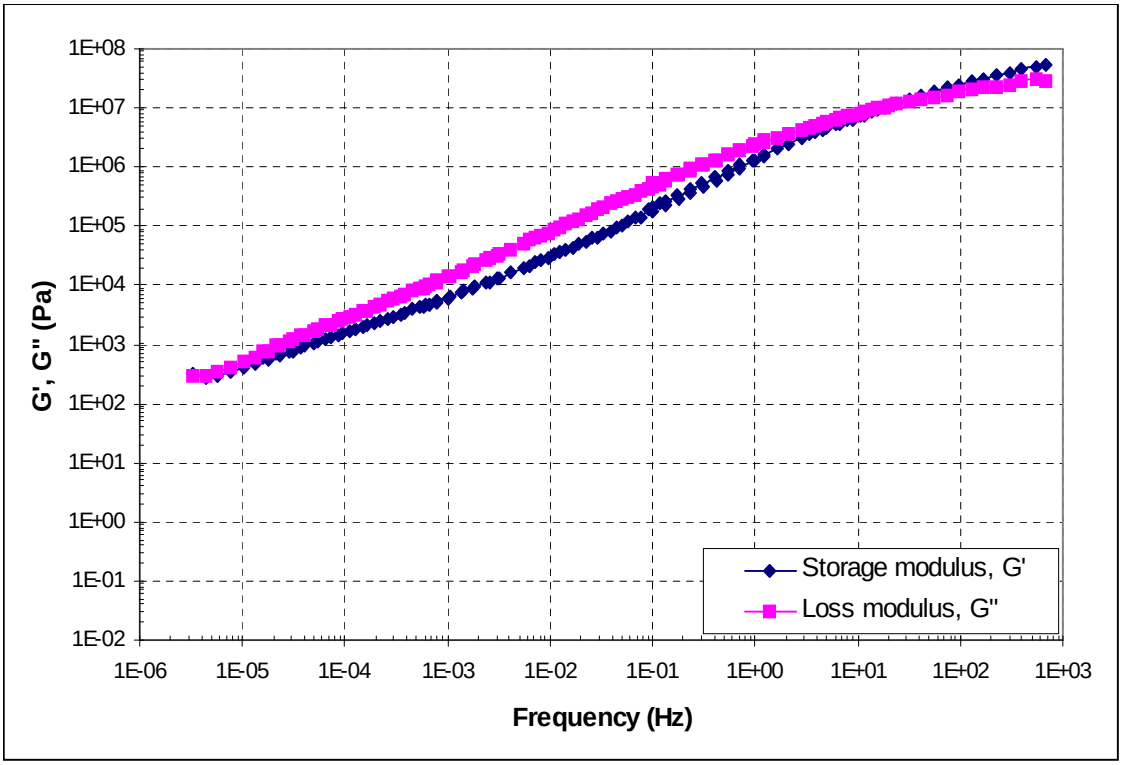

Figure 4.43: Master curves of the storage and loss modulus for radial SBS PMB aged bitumen at a reference temperature of 20˚C

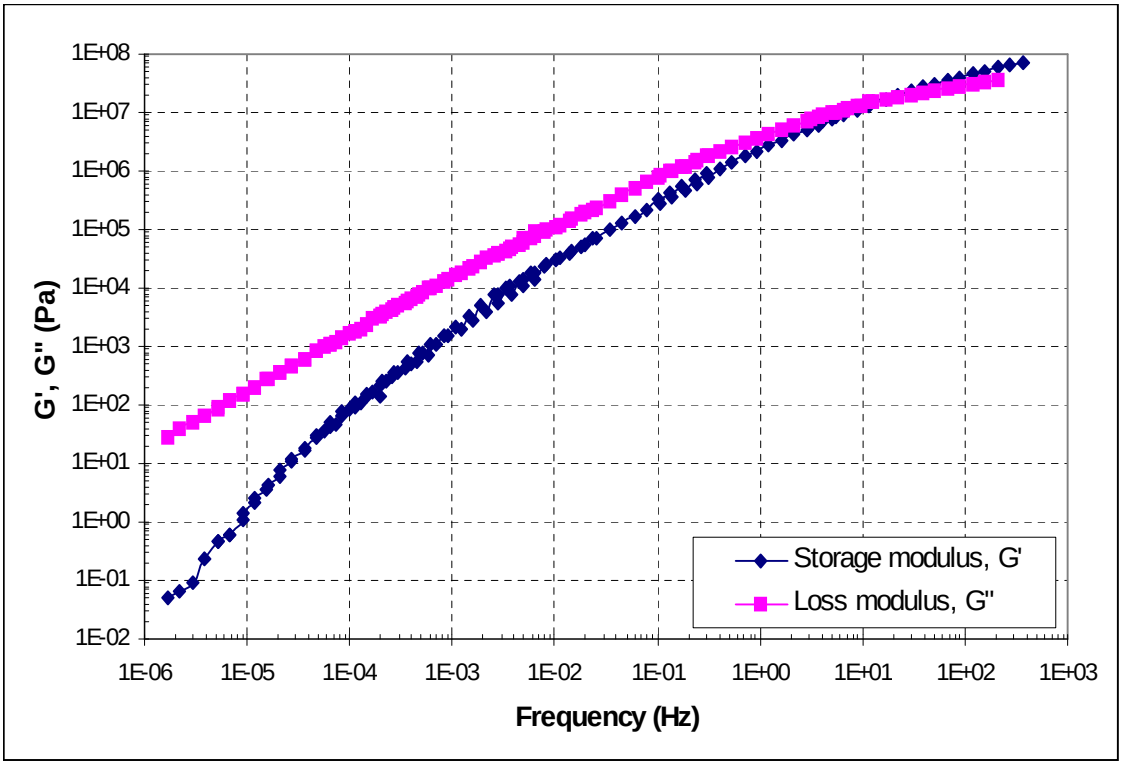

Figure 4.44: Master curves of the storage and loss modulus for EVA PMB aged bitumen at a reference temperature of 20˚C

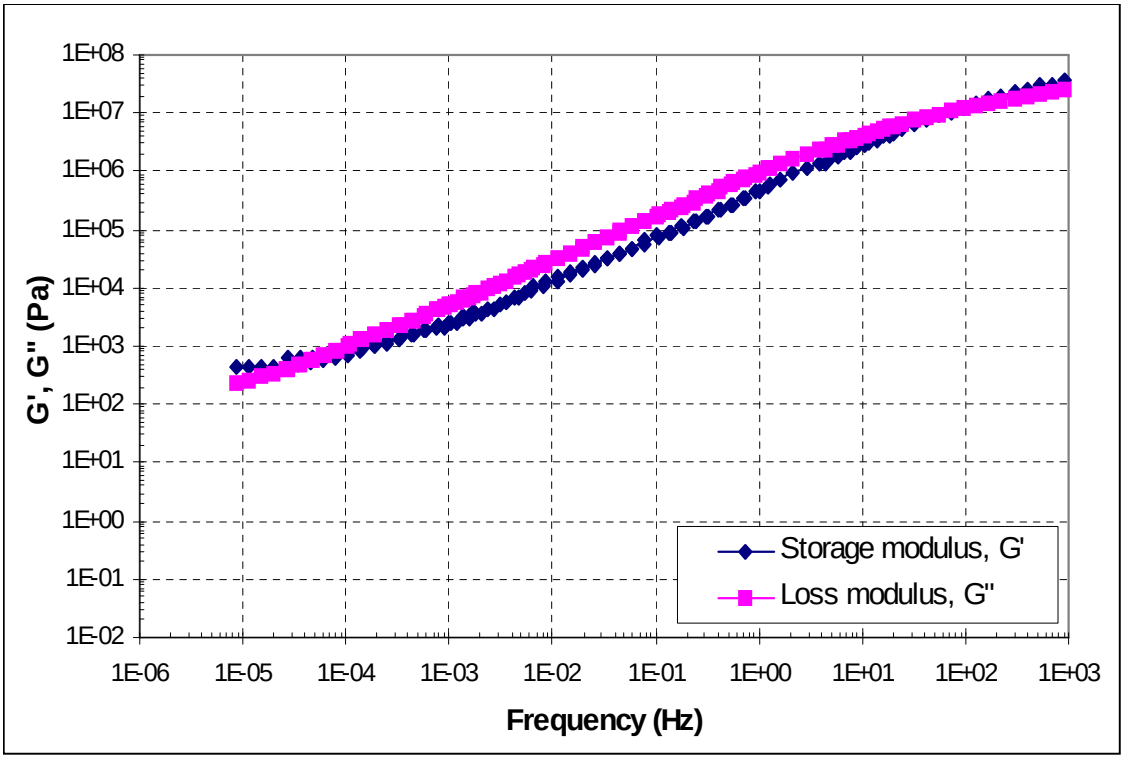

Figure 4.45: Master curves of the storage modulus and loss modulus for radial SBS PMB aged bitumen at a reference temperature of 20˚C

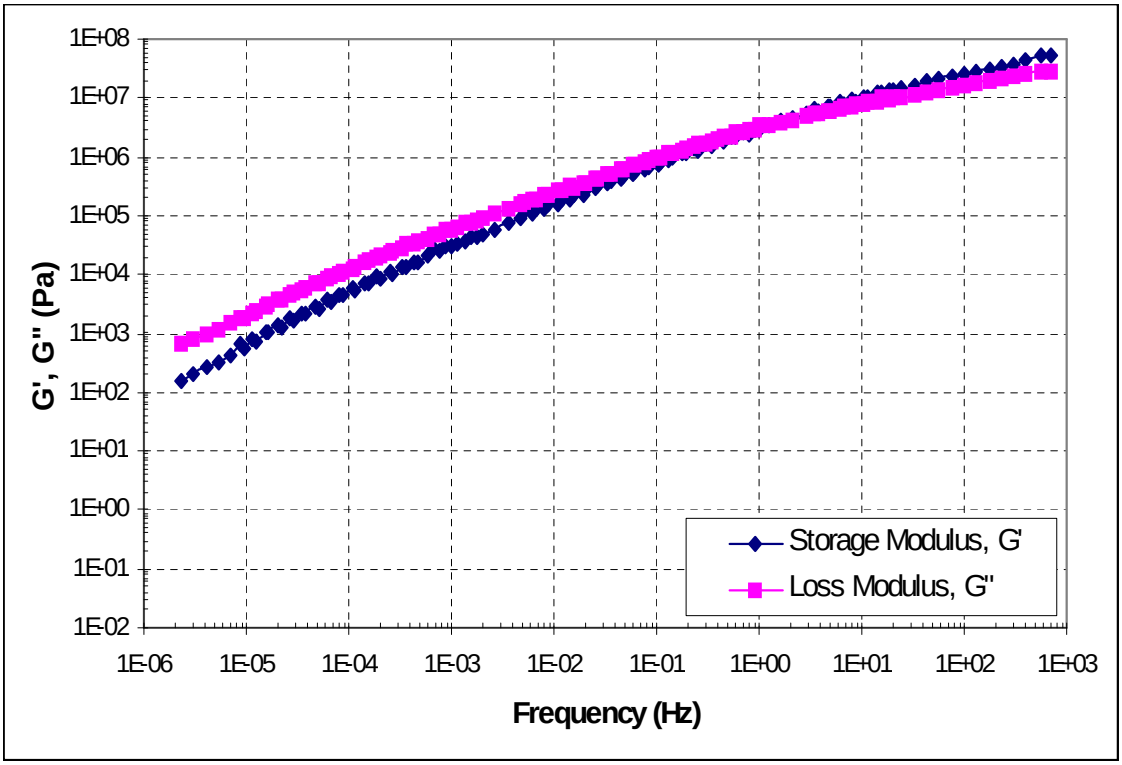

Figure 4.46: Master curves of the storage and loss modulus for aged multigrade (35/50) aged bitumen at a reference temperature of 20˚C

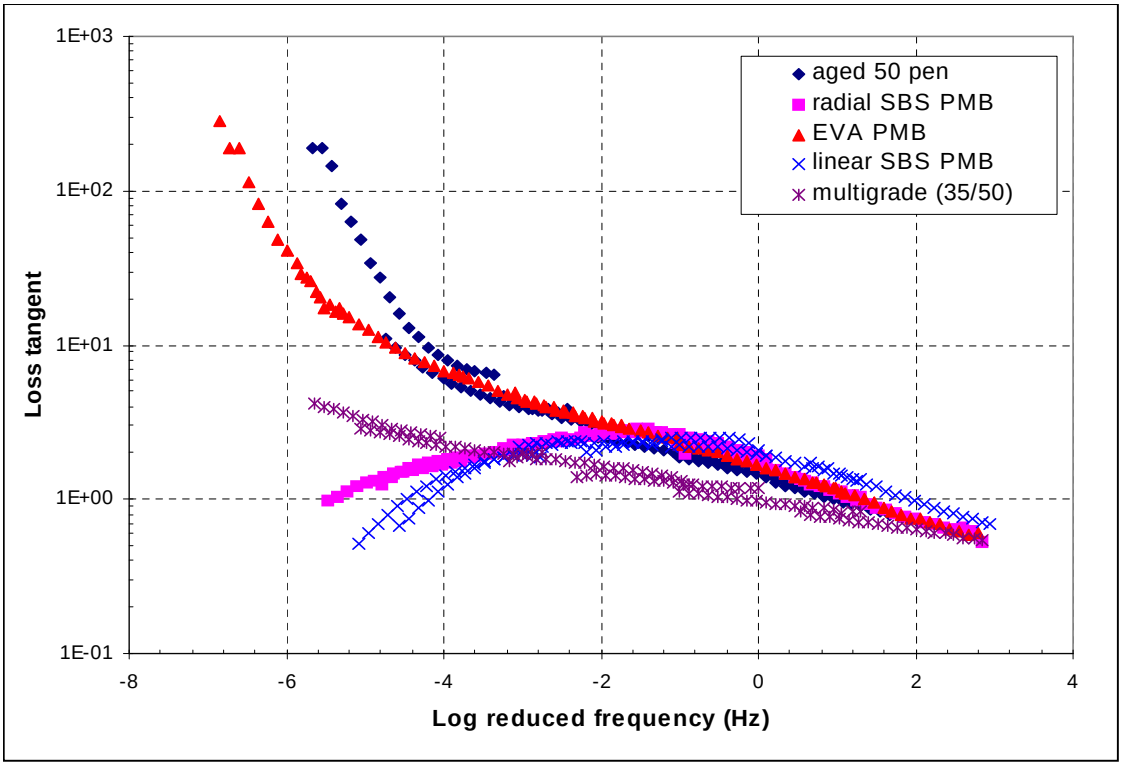

Figure 4.47: Master curve of the loss tangent for five different aged bitumens

Table 4.1: Conventional Properties of Bitumens

Bitumen	Pen.(dmm)	Soft. Pt (˚C)
50 pen control	49	52
Intermediate polymer content radial SBS PMB	61	73
Intermediate polymer content EVA PMB	51	60
High polymer content linear SBS PMB	81	95
Multigrade bitumen 35/50	39	60

Table 4.2: Linearity data for aged 50 pen bitumen

Temperature (°C)	Frequency (Hz)	LVE limit of Strain	LVE limit of Stress (Pa)	LVE limit of Stiffness (Pa)
10	0.1	0.05	3.39E+05	7.45E+06
	1	0.02	4.97E+05	2.34E+07
	5	—	—	—
	10	—	—	—
20	0.1	0.07	6.52E+04	9.97E+05
	1	0.04	1.74E+05	4.15E+06
	5	0.04	3.75E+05	1.06E+07
	10	0.03	4.40E+05	1.61E+07
30	0.1	0.31	3.82E+04	1.24E+05
	1	0.10	7.69E+04	7.69E+05
	5	0.05	9.80E+04	2.10E+06
	10	0.04	1.29E+05	3.32E+06
40	0.1	1.30	2.30E+04	1.77E+04
	1	0.22	3.09E+04	1.42E+05
	5	0.10	4.90E+04	4.90E+05
	10	0.08	5.73E+04	6.75E+05
60	0.1	2.80	1.97E+03	7.04E+02
	1	0.39	2.26E+03	5.87E+03
	5	0.10	2.39E+03	2.39E+04
	10	0.07	3.33E+03	4.47E+04
70	0.1	9.65	1.61E+03	1.67E+02
	1	2.11	3.26E+03	1.55E+03
	5	0.53	3.65E+03	6.89E+03
	10	0.33	4.32E+03	1.31E+04

Table 4.3: Linearity data for aged radial SBS PMB

Temperature (°C)	Frequency (Hz)	LVE limit of Strain	LVE limit of Stress (Pa)	LVE limit of Stiffness (Pa)
10	0.1	2.38E-02	1.46E+05	6.13E+06
	1	2.22E-02	3.77E+05	1.70E+07
	5	—	—	—
	10	—	—	—
20	0.1	9.22E-02	5.53E+04	6.00E+05
	1	4.33E-02	1.15E+05	2.66E+06
	5	3.09E-02	2.17E+05	7.02E+06
	10	2.42E-02	2.51E+05	1.04E+07
30	0.1	5.67E-01	3.23E+04	5.70E+04
	1	1.45E-01	4.83E+04	3.33E+05
	5	4.88E-02	6.47E+04	1.33E+06
	10	4.37E-02	7.66E+04	1.75E+06
40	0.1	7.92E-01	9.48E+03	1.20E+04
	1	4.36E-01	3.22E+04	7.39E+04
	5	1.61E-01	3.84E+04	2.39E+05
	10	1.17E-01	4.32E+04	3.69E+05
60	0.1	9.38E-01	8.32E+02	8.87E+02
	1	1.12E+00	4.90E+03	4.38E+03
	5	7.91E-01	1.07E+04	1.35E+04
	10	8.44E-01	1.62E+04	1.92E+04
70	0.1	7.87E-01	3.19E+02	4.05E+02
	1	9.79E-01	1.53E+03	1.56E+03
	5	4.93E-01	2.40E+03	4.87E+03
	10	7.73E-01	5.05E+03	6.53E+03

Table 4.4: Linearity data for aged EVA PMB

Temperature (°C)	Frequency (Hz)	LVE limit of Strain	LVE limit of Stress (Pa)	LVE limit of Stiffness (Pa)
10	0.1	—	—	—
	1	—	—	—
	5	—	—	—
	10	—	—	—
20	0.1	1.44E-01	1.26E+05	8.75E+05
	1	5.10E-02	2.12E+05	4.16E+06
	5	4.40E-02	4.78E+05	1.09E+07
	10	—	—	—
30	0.1	1.19E+00	6.58E+04	5.53E+04
	1	2.47E-01	7.82E+04	3.17E+05
	5	1.07E-01	1.27E+05	1.19E+06
	10	8.48E-02	1.54E+05	1.82E+06
40	0.1	1.51E+00	5.97E+03	3.95E+03
	1	6.60E-01	2.23E+04	3.38E+04
	5	2.53E-01	3.81E+04	1.51E+05
	10	1.46E-01	4.91E+04	3.36E+05
60	0.1	2.18E+01	4.20E+03	1.93E+02
	1	6.77E+00	5.45E+03	8.05E+02
	5	1.79E+00	6.88E+03	3.84E+03
	10	9.52E-01	7.22E+03	7.58E+03
70	0.1	2.76E+01	1.88E+03	6.81E+01
	1	6.52E+00	1.91E+03	2.93E+02
	5	2.95E+00	3.71E+03	1.26E+03
	10	1.78E+00	5.04E+03	2.83E+03

Table 4.5: Linearity data for aged linear SBS PMB

Temperature (°C)	Frequency (Hz)	LVE limit of Strain	LVE limit of Stress (Pa)	LVE limit of Stiffness (Pa)
10	0.1	6.29E-02	1.56E+05	2.48E+06
	1	2.48E-02	2.13E+05	8.59E+06
	5	—	—	—
	10	—	—	—
20	0.1	2.04E-01	4.58E+04	2.25E+05
	1	5.01E-02	7.16E+04	1.43E+06
	5	3.03E-02	1.13E+05	3.73E+06
	10	2.16E-02	1.28E+05	5.93E+06
30	0.1	8.32E-01	2.17E+04	2.61E+04
	1	2.12E-01	3.36E+04	1.58E+05
	5	7.13E-02	3.88E+04	5.44E+05
	10	7.04E-02	5.68E+04	8.07E+05
40	0.1	1.28E+00	6.15E+03	4.80E+03
	1	6.93E-01	1.84E+04	2.66E+04
	5	2.98E-01	2.67E+04	8.96E+04
	10	2.69E-01	4.80E+04	1.78E+05
60	0.1	1.04E+00	4.95E+02	4.76E+02
	1	6.91E-01	1.86E+03	2.69E+03
	5	4.61E-01	3.80E+03	8.24E+03
	10	4.36E-01	5.36E+03	1.23E+04
70	0.1	9.98E-01	3.86E+02	3.87E+02
	1	8.37E-01	9.30E+02	1.11E+03
	5	1.04E+00	3.14E+03	3.02E+03
	10	6.75E-01	3.35E+03	4.96E+03

Table 4.6: Linearity data for aged multigrade 35/50

Temperature (°C)	Frequency (Hz)	LVE limit of Strain	LVE limit of Stress (Pa)	LVE limit of Stiffness (Pa)
10	0.1	4.02E-02	2.59E+05	6.44E+06
	1	—	—	—
	5	—	—	—
	10	—	—	—
20	0.1	5.08E-02	6.04E+04	1.19E+06
	1	3.35E-02	1.16E+05	3.46E+06
	5	2.14E-02	1.85E+05	8.64E+06
	10	1.95E-02	2.16E+05	1.11E+07
30	0.1	9.46E-02	2.30E+04	2.43E+05
	1	4.28E-02	3.87E+04	9.04E+05
	5	1.99E-02	4.83E+04	2.43E+06
	10	2.25E-02	6.66E+04	2.96E+06
40	0.1	2.05E-01	8.13E+03	3.97E+04
	1	9.70E-02	1.76E+04	1.81E+05
	5	7.34E-02	3.98E+04	5.42E+05
	10	8.17E-02	4.25E+04	5.20E+05
60	0.1	4.20E-01	7.67E+02	1.83E+03
	1	2.75E-01	2.57E+03	9.35E+03
	5	9.80E-02	3.71E+03	3.79E+04
	10	1.33E-01	7.95E+03	5.98E+04
70	0.1	1.04E+00	7.31E+02	7.03E+02
	1	1.90E-01	8.21E+02	4.32E+03
	5	9.85E-02	1.29E+03	1.31E+04
	10	1.08E-01	2.18E+03	2.02E+04

Table 4.7: Linearity data for unaged 50 pen

Temperature (°C)	Frequency (Hz)	LVE limit of Strain	LVE limit of Stress (Pa)	LVE limit of Stiffness (Pa)
10	0.1	2.23E-02	1.08E+05	4.85E+06
	1	1.57E-02	2.83E+05	1.80E+07
	5	—	—	—
	10	—	—	—
20	0.1	5.00E-02	5.06E+04	1.01E+06
	1	4.44E-02	1.15E+05	2.59E+06
	5	3.65E-02	2.80E+05	7.67E+06
	10	3.44E-02	4.28E+05	1.24E+07
30	0.1	5.91E-01	3.17E+04	5.36E+04
	1	1.85E-01	5.85E+04	3.16E+05
	5	6.43E-02	7.53E+04	1.17E+06
	10	4.17E-02	8.55E+04	2.05E+06
40	0.1	1.84E+00	1.46E+04	7.93E+03
	1	3.96E-01	2.48E+04	6.26E+04
	5	1.55E-01	3.75E+04	2.42E+05
	10	1.07E-01	4.32E+04	4.04E+05
60	0.1	8.97E+00	1.77E+03	1.97E+02
	1	1.93E+00	3.65E+03	1.89E+03
	5	4.85E-01	4.35E+03	8.97E+03
	10	2.07E-01	7.03E+03	3.40E+04
70	0.1	3.00E+01	1.47E+03	4.90E+01
	1	5.10E+00	2.52E+03	4.94E+02
	5	1.45E+00	3.27E+03	2.26E+03
	10	7.23E-01	3.35E+03	4.63E+03

Table 4.8: Linearity data for unaged radial SBS PMB

Temperature (°C)	Frequency (Hz)	LVE limit of Strain	LVE limit of Stress (Pa)	LVE limit of Stiffness (Pa)
10	0.1	4.80E-02	2.76E+05	5.75E+06
	1	2.03E-02	4.23E+05	2.08E+07
	5	—	—	—
	10	—	—	—
20	0.1	1.25E-01	7.42E+04	5.94E+05
	1	4.21E-02	1.34E+05	3.18E+06
	5	2.06E-02	1.63E+05	7.91E+06
	10	1.34E-02	1.85E+05	1.38E+07
30	0.1	5.38E-01	3.60E+04	6.69E+04
	1	1.28E-01	5.55E+04	4.34E+05
	5	5.46E-02	8.00E+04	1.47E+06
	10	4.80E-02	1.02E+05	2.13E+06
40	0.1	1.43E+00	1.67E+04	1.17E+04
	1	5.12E-01	3.24E+04	6.33E+04
	5	1.80E-01	3.98E+04	2.21E+05
	10	9.57E-02	4.15E+04	4.34E+05
60	0.1	9.72E-01	7.89E+02	8.12E+02
	1	4.37E-01	1.29E+03	2.95E+03
	5	1.60E-01	1.46E+03	9.13E+03
	10	1.52E-01	2.23E+03	1.47E+04
70	0.1	7.53E-01	2.96E+02	3.93E+02
	1	4.36E-01	5.39E+02	1.24E+03
	5	9.45E-01	3.25E+03	3.44E+03
	10	7.56E-01	3.35E+03	4.43E+03

Chapter 5

ASPHALT MIXTURE TESTING

5.1 Introduction

The response of an asphalt mixture under load depends upon the rate of loading and the temperature of the material. As early as the 1950's, Van der Poel [104] introduced the concept of asphalt mixture stiffness as a function of temperature and time of loading (frequency) and the use of this parameter in pavement design procedures.

As mentioned earlier in Chapter Two, asphalt materials generally display non-linear stress/strain behaviour with a decrease in stiffness modulus with increasing stress/strain amplitude. This non-linear behaviour of asphalt mixtures may be the result of the non-linear behaviour of either the aggregate, bitumen or a combination of these two (asphalt mixture). As non-linear behaviour generally becomes negligible at stress/strain amplitudes less than a certain limit (dependent on the material properties), bituminous materials can be defined as linear when subjected to small stresses/strains.

This chapter investigates the stress and strain behaviour of a range of unmodified, process and polymer modified asphalt mixtures using a purpose built dynamic uniaxial tension-compression, servo-hydraulic testing apparatus. The results of these tests have been used to determine the linearity limits, stress/strain dependence and LVE dynamic mechanical properties of the different asphalt mixtures at various temperatures and frequencies.

5.2 Materials

Five different unmodified and modified bitumens were selected to produce the different asphalt mixtures tested in this research. The physical properties, including the penetration and softening point of these five bitumens were shown in Table 4.1 of Chapter Four.

A Dense Bitumen Macadam (DBM) 10 mm wearing course and a Hot Rolled Asphalt (HRA) 30/10 were selected and manufactured in accordance with BS 4978 Part 1: 1988 [7] and BS 594 Part 1: 1992 [10] respectively. The aggregate gradation of the DBM and HRA mixtures are shown in Table 5.1. The aggregate type selected for these two mixtures was a crushed limestone. The bitumen contents for the DBM and HRA mixtures were 5.5 and 7 percent by weight of mixture respectively. Both mixtures were compacted to achieve 4 percent air voids. Gradation curves and specification limits for the DBM and HRA mixtures are shown in Figures 5.1 and 5.2.

Table 5.1: Aggregate gradation

Sieve Size (mm)	Percent Passing by Mass (DBM)	Percent Passing by Mass (HRA)
14	100	100
10	95.4	98.5
6.3	66.6	75.1
3.35	35.9	68.4
2.36	-	66
1.18	22.1	61.6
0.6	-	58.4
0.075	5.4	9.5

In addition to the two asphalt mixtures, tests were also performed on a HRA mortar. As the HRA mortar has a higher percentage of bitumen compared to the HRA mixture, the performance of the mortar can be considered to be between that of the asphalt mixtures and the binders in Chapter 4. The HRA mortar was designed by removing the coarse aggregates to give the approximate volumetric proportions presented in Table 5.2 together with the volumetric composition of the two asphalt mixtures.

Table 5.2: Volumetric composition of 10 mm DBM, HRA (30/10) and HRA mortar

Asphalt Mixture Type	DBM (10 mm)	HRA (30/10)	HRA mortar
Coarse Aggregate (10mm & 6mm)	50 %	24 %	-
Fine Aggregate	32 %	11 %	-
Sand	-	38 %	54 %
Filler	1 %	7 %	17 %
Bitumen	13 %	16 %	21 %
Air Void Content	4 %	4 %	8 %
VMA	17%	20%	29%

In order to study the effects of different bitumen types on asphalt mixture behaviour, asphalt mixtures were produced using different unmodified and modified bitumens. In total, five DBM, two HRA and two HRA mortar mixtures were manufactured and tested in this study. Table 5.3 shows the different mixtures, classified according to both mixture and bitumen type, that were included in the testing programme.

Table 5.3: Different type of mixtures incorporated in the testing programme

Bitumen	Mixture		
	DBM	HRA	HRA Mortar
Conventional 50 pen	√	√	√
Radial SBS PMB	√	√	√
EVA PMB	√	-	-
Linear SBS PMB	√	-	-
Multigrade (35/50)	√	-	-

5.3 Direct Tension-Compression Test Apparatus

5.3.1 Test Configuration

The essential details of the test apparatus are shown in Figure 5.3. In this configuration, dynamic loads were applied to the top of the cylindrical asphalt specimen. The bottom loading platen was fixed to the steel frame and the top loading platen attached to the load cell and loading rig. It can be seen in Figure 5.3 that the

load applied to the specimen was monitored by a load cell while the vertical deformations of each specimen were measured by two linear variable differential transformers (LVDTs) attached to the outer wall of the cylindrical specimens 180˚ apart. As the system operates as a computer controlled servo-hydraulic closed-loop feedback system, it was important to have a fast and accurate data acquisition system and the capability of tension-compression testing without eccentricity in the loading alignment. In order to accurately control the test temperature, the entire test assembly was located in a temperature controlled room.

5.3.2 Tension Coupling Assembly

To enable tensile forces (stresses) to be applied during the tension-compression tests, each sample needed to be glued to top and bottom steel end plates. Several sinusoidal tension-compression tests were initially conducted at frequencies of 1, 5 and 10 Hz with the testing configuration shown in Figure 5.4. However, the accuracy of the sinusoidal stress and strain waves was not considered satisfactory to model the rheological characteristics of the asphalt mixtures.

To improve the accuracy of the sinusoidal waveform, it was necessary to adjust the proportional and differential feedback gains of the servo-hydraulic system and to ensure precise axial alignment of the applied loads and the sample. The tension coupling arrangement shown in Figure 5.4 was therefore changed to that shown in Figure 5.5 so that it was possible to accurately adjust the axis of the specimen in line with the axis of the loading actuator.

The stress and strain data for each test was then modelled to generate sinusoidal stress and strain waves as shown in Figure 5.6. The peak stress and strain values were then determined and used to calculate $|E^*|$ and δ.

5.3.3 Load and Displacement Calibration

Before commencing the asphalt mixture testing programme, a number of items of equipment had to be calibrated in order to provide quantitative results. In addition, a

number of checks and tests were carried out before and during the testing programme to ensure that no incorrect or biased results were obtained.

The load cell was calibrated by placing a proving ring under the load cell and applying 1 kN load increments while monitoring the output through the data acquisition system. The load versus output voltage calibration curve is plotted in Figure 5.7. Loads were calculated from measured voltage by simply using the calibration equation.

The LVDTs were calibrated against a micrometer fixed into a calibration frame. Increments of 20 μm were used and the calibration equations are given in Figures 5.8 and 5.9. The displacements were therefore simply calculated by inputting the voltage output of the LVDTs into these equations.

5.3.4 Data Measurement Sensitivity

As the tests were conducted at low strains, a low noise to signal ratio on the strain measurement signal was required. Two LVDTs were used for this measurement, mounted centrally, 180˚ apart on the cylindrical specimen. An oscilloscope was used to check the noise and sensitivity of each LVDT and associated signal conditioning amplifier.

The noise level for LVDT A, defined in terms of the standard deviation of the normal distribution of LVDT readings, was found to be 0.169 μm (Figure 5.10). LVDT B was found to have a similar noise level of 0.143 μm. A similar method was used to determine the noise level associated with the load cell, which was found to be 8.913 N.

The measurement of phase difference between stress and strain should not be affected by the response of the load cell amplifiers and the LVDT signal conditioning. In order to confirm this, a series of dynamic tests at different frequencies was carried out on purely elastic material. An aluminum cylinder was initially tested but was found to be too stiff to generate sufficient strains. Consequently tests were conducted using a steel spring and the phase difference was checked using modelled load and displacement

sinusoidal waves as shown in Figure 5.11. The phase difference was calculated as 0.07°, which was considered to be effectively zero, thereby providing the confidence needed to measure phase angles between 0° and 90°.

5.3.5 Stiffness and Phase Angle Calculation Procedures

As described above, the two sinusoidal waveform traces of load and deflection were recorded in units of volts by the data acquisition system. Load and deformation measurements were collected for the last five cycles of the first thirty recorded cycles. A minimum of 50 data points were collected for each cycle. Load and deflection were then calculated from the voltages by using the calibration equations established in section 5.3.3. Sinusoidal curves of strain and stress were then fitted to the experimental data using a Matlab programme (see Figure 5.12) and these sinusoidal curves used to calculate phase angle and complex modulus using the following equations:

$$\phi = \frac{t_i}{t_p} \times (360°) \qquad \textbf{(5.1)}$$

Where: ϕ = phase angle

t_i = time lag between the peak sinusoidal stress and strain, and

t_p = time for a complete stress cycle.

$$\left|E^*\right| = \left[\frac{stress\ amplitude}{strain\ amplitude}\right] \qquad \textbf{(5.2)}$$

It should be noted that the average deformation measured by the two LVDTs was used in the calculations and final values of complex modulus and phase angle considered as the average of three tests on the same specimen.

5.4 Testing Methodology

5.4.1 Sample Preparation

For consistency the following procedure was used for mixing and compacting all the asphalt mixtures.

The required aggregate for each batch was prepared in accordance with the pre-determined grading and then heated in a thermostatically controlled oven for approximately four hours. Heating temperatures were varied between 160 and 180˚C depending on bitumen type (normally 160˚C for 50 pen bitumen and 180˚C for polymer modified bitumens). The bitumen was heated at the required temperature for approximately two hours and the moulds for approximately one hour.

The hot aggregate was then placed in a sun-and-planet type mixture (Figure 5.13). This mixer controls the temperature by a heated oil jacket that surrounds the mixing pan. The required amount of bitumen was then added to the aggregate and mixed for approximately 6 minutes at 160˚C. The fully coated mixture was then placed in a preheated mould ready for compaction. The moulds used in this investigation were designed for manufacturing slabs with dimensions, 404 mm in length, 280 mm wide and 100 mm high.

The rolling wheel compaction method was used to compact the slabs. This compaction technique is ideal for comparing laboratory and field data because the laboratory specimens can be cored in the same manner used to obtain field cores. In addition, both NCHRP AAMAS [107] and SHRP A-003 [98] studies have concluded that the rolling wheel compaction method is one of the best methods for simulating field compaction. The rolling wheel compactor used in this study is shown in Figure 5.14.

The compacted slabs of asphalt mixture were allowed to cool to room temperature after which they were stripped from their moulds. Specimens 82 mm in diameter were then cored from the 100 mm thick slabs and the edges trimmed to produce cylindrical specimens 220 mm in length. Four cores were taken from each slab generated and as

the direction of coring was horizontal, the direction of the axial stresses during the dynamic tests could be considered to simulate horizontal stresses occurring in a pavement. Figure 5.15 shows a compacted and cored slab.

5.4.2 Volumetric Proportions

After the specimens were trimmed they were allowed to dry at room temperature. To measure air voids, the specimens were sealed using aluminium sealing film and weighed in air and water. The bulk compacted density was then calculated according to the following formula:

$$\rho = \frac{M_{au} \times 1000}{\left[M_{ac} - M_{wc} - \left(\frac{M_{ac} - M_{au}}{G_f} \right) \right]} \quad \textbf{(5.3)}$$

Where: ρ = Bulk compacted density (kg/m^3)

M_{au} = Mass in air uncoated (g)

M_{ac} = Mass in air coated (g)

M_{wc} = Mass in water coated (g)

G_f = Specific gravity of aluminium sealing film (1650 g/cm^3)

The air voids content of the samples were calculated using the bulk compacted density and the maximum theoretical density (ρ_{max}) using the following formula:

$$V_v = \left(1 - \frac{\rho}{\rho_{max}} \right) \times 100 \quad \textbf{(5.4)}$$

The theoretical maximum density of a bituminous mixture can be considered as the density corresponding to zero air voids content. This density is a function of the binder and aggregate contents and their specific gravities and is calculated from the following formula:

$$\rho_{max} = \frac{M_B - M_A}{\left(\frac{M_B}{G_b}\right) - \left(\frac{M_A}{G_a}\right)} \gamma_w \qquad \textbf{(5.5)}$$

Where: M_B = Binder content (percent by mass of total mixture)

M_A = Aggregate content (percent by mass of total mixture)

G_b = Specific gravity of bitumen (generally assumed 1.03 g/cm^3)

G_a = Specific gravity of combined aggregates

γ_w = Unit weight of water (1000 kg/m^3)

The specific gravity of the combined aggregates is calculated using the following formula:

$$G_a = \frac{100}{\left(\frac{X}{G_x}\right) + \left(\frac{Y}{G_y}\right) + \cdots} \qquad \textbf{(5.6)}$$

Where X, Y, etc are the percentages of each aggregate fraction having specific gravities G_x, G_y, etc.

Table 5.4 presents the mean, maximum, minimum and standard deviation of the air voids content for the DBM, HRA and HRA mortar mixtures. To avoid the effect of variations in air voids content on test results, only specimens with air voids within ± 0.5 percent of the target air voids were used in the testing programme.

Table 5.4: Air voids content

Mixtures	No. of Samples	Air Voids Content (%)			
		Mean	Minimum	Maximum	Standard Deviation (%)
DBM	40	4.56	3.92	4.95	0.13
HRA	16	4.35	3.74	4.86	0.12
HRA mortar	16	9.21	7.5	10.65	0.59

5.4.3 Testing Programme

As the test specimens were subjected to direct tension-compression testing, it was necessary to bond the specimens to end plates using epoxy resin. To maintain the end plates in parallel, a jig shown in Figure 5.16 was used to align and fix the end plates. The resin was allowed to harden for a minimum of 24 hours prior to testing. Four 'pips' were glued onto the two opposite diametric sides of each specimen to measure axial deformation over an effective gauge length of 100 mm within the central portion of the specimen. The end plates were subsequently bolted to the loading platens of the testing apparatus. A series of uniaxial tension-compression dynamic tests were then performed in the servo-hydraulic testing apparatus.

The test procedure consisted of conditioning the test specimens in a temperature controlled room for at least eight hours at the required testing temperature. At the end of this period, the specimens were subjected to sinusoidal loads (stresses) over a range of amplitudes and frequencies, and the resulting axial displacements (strains) were measured in order to calculate complex modulus and phase angle.

The testing programme consisted of two main parts. The aim of the first part was to investigate the LVE limits of the asphalt mixtures using stress sweep tests under the following test conditions:

- Mode of loading: controlled stress
- Temperatures: 10, 20, 30 and 40ºC
- Frequencies: 0.1, 1, 5 and 10 Hz

During the stress sweep tests, the specimens were subjected to progressively larger loads with a short rest period of five minutes between each loading phase.

As mentioned in Chapter Two, within the linear viscoelastic region, the ratio of stress to strain is a function of time and temperature and not stress magnitude [47]. However, in the non-linear region, stiffness will decrease with increasing stress or strain level. However, in the course of performing the stress sweeps, it was observed that due to gradual variations of the complex modulus, defining an exact dividing line

between the linear and non-linear region was very difficult. Therefore, in a manner similar to that used with the bituminous binders, the LVE limit was defined in accordance with the SHRP study as the point where the complex modulus decreased to 95 percent of its initial value [20].

After completing the stress sweeps and establishing the target stresses or strains, frequency sweeps were performed on all the samples under the following test conditions:

- Mode of loading: controlled-stress
- Temperatures: 10, 20, 30 and 40°C
- Frequencies: 0.1, 1, 2, 3, 5, 7, 10, 15 and 20 Hz.

All the frequency sweep tests were conducted at stresses below the linear limit to ensured linear viscoelastic (LVE) behaviour during the dynamic tests.

5.5 Linear Viscoelastic Limits

5.5.1 Linear Limits of Stress and Strain

Plots of stress amplitude versus strain amplitude were produced for each stress sweep test. Examples of these graphs are shown in Figures 5.17 to 5.19. In all cases it can be seen that the relationship was initially a straight line (indicating linear behaviour) followed by a curve bending towards the strain axis (curved portion indicating non-linear behaviour).

As shown in Figures 5.17 to 5.19, it was difficult to define the LVE limits of the asphalt mixtures using this form of data presentation. Therefore other methods of presenting the results were used to determine the LVE limits. As mentioned previously, the linear and non-linear domain of a material can be obtained by plotting complex modulus versus strain or stress. In this form, the non-linearity is observed as a decrease in complex modulus after an initial constant value. The linear region can be defined by identifying the point beyond which the measured value of complex modulus decreases to 95 percent of its initial value [85]. Therefore, the results of the

stress sweep tests were plotted as complex modulus versus stress or strain for each mixture at different temperatures and frequencies and the LVE limits calculated according to the SHRP method. Figures 5.20 and 5.21 show two of the graphs produced for the DBM mixture with 50 pen bitumen at 0.1 Hz and 10˚C. It can be seen from these graphs that there is clearly a decrease in complex modulus at higher stresses or strains (non-linear behaviour) and a relatively stable region at low stresses or strains (linear behaviour). Results of LVE stress, strain and complex modulus limits for all the mixtures are presented in Tables 5.5 to 5.13.

After determining the linear region for the asphalt mixtures, the LVE limits of stress and strain were plotted as functions of frequency and temperature. As an example, Figures 5.22 to 5.27 show a selection of these graphs. It can be seen from these figures that the LVE stress limit decreases with increasing temperature or decreasing frequency. In other words, asphalt mixtures show lower LVE stress limits at higher temperatures or lower frequencies. However, Figures 5.23, 5.25 and 5.27 show that the LVE strain limits are relatively stable for all the asphalt mixtures, indicating a strain dependent LVE criterion.

In order to compare the LVE stress limits of the asphalt mixtures incorporating different bitumens, three-dimensional plots of LVE stress limit versus temperature and mixture type were plotted for the DBM, HRA and HRA mortar mixtures. Some of these plots are presented in Figures 5.28 to 5.31. As shown in these figures, all the DBM mixtures show similar LVE stress limits at the same temperature except for the linear SBS PMB mixture, which shows slightly lower LVE stress limits. The same results can be seen for the HRA and HRA mortar mixtures.

The LVE strain limits of all the DBM, HRA and HRA mortar mixture are shown in Figures 5.32, 5.33 and 5.34 respectively. It can be seen from Figures 5.32 and 5.33 that the LVE strain limits for all the DBM and HRA asphalt mixtures, at different temperatures and frequencies, are between 20 and 100 microstrain. As shown in Figure 5.34, the LVE strain limits of the HRA mortars are slightly higher being between 50 and 150 microstrain.

5.5.2 LVE Limits versus Complex Modulus and Phase Angle

Plotting LVE strain and stress limits as a function of rheological parameters such as complex modulus and phase angle was found to be a very useful method for evaluating the results. Figures 5.35 to 5.37 show the LVE strain limits as a function of complex modulus for the DBM, HRA and HRA mortar mixtures. It can be seen from these figures that the LVE strain limits are between 20 and 100 microstrain for all the DBM and HRA mixtures and between 50 and 150 microstrain for all the HRA mortars over the entire complex modulus range.

The LVE stress limits are shown as functions of complex modulus for the DBM, HRA and HRA mortar mixtures in Figures 5.38 to 5.40. It can be seen from these figures that there is a general increase in the LVE stress limit with an increase in complex modulus for all the mixtures. This represents a direct relationship between the LVE stress limits and complex modulus at all testing conditions for all the mixtures.

Figures 5.41 to 5.46 present the LVE strain and stress limits as a function of phase angle. An interesting observation that can be made from these figures is the hyperbolic shape of the LVE stress limit versus phase angle function. This is due to the increased interaction and dominating effect of the aggregate structure at high temperatures (low binder stiffness) resulting in increased elastic response (low phase angles) at both low and high frequencies.

5.5.3 Discussion

The test results show that non-linearity occurs in all asphalt mixtures at various temperatures and frequencies. The direct consequence of this non-linearity is the reduction in asphalt mixture stiffness with increasing stress/strain. Since pavement design methods rely on predicted or measured values of stiffness modulus for the various pavement layers, the significance of non-linear behaviour of pavement materials cannot be ignored. However, any changes in stiffness modulus due to non-linear effects must be compared with changes in stiffness due to other factors, particularly temperature. Examination of the stiffness modulus values determined in

this investigation indicates that for a change in temperature of 10ºC there is a change in asphalt mixture stiffness by a factor of two to three. Hence it can be argued that the non-linear effect is of little significance when compared with temperature induced stiffness changes. However, significant reduction in stiffness can occur at high stress levels and no doubt should be considered by designers.

The non-linear behaviour and LVE limits of asphalt mixtures have been investigated by various researchers. Pell [83] showed non-linear behaviour to be dependent on strain amplitude, especially at high temperatures for dynamic torsional stiffness tests. Sayegh [93] found marked non-linearity behaviour for specimens tested above 20 microstrain. He also found non-linearity to be accentuated at higher temperatures. Subsequently, he concluded that asphalt mixtures are linear for strains less than 40 microstrain. Gardner and Skok [51], using pure compression repeated loading tests, reported that the studied materials could be considered linearly viscoelastic under small stresses and strains. Pell and Taylor [84] conducted a series of cantilever bending tests on asphalt mixtures and found a marked stress dependence of stiffness modulus, with the degree of dependence increasing with temperature. Taylor [100] conducted a series of tests to measure the stiffness of asphalt mixtures under dynamic loading by using a rotating-bending fatigue machine. He stated that non-linear effects were detected in some asphalt mixtures at nominal strain levels of between 50 and 200 microstrain. This means that linear behaviour will have occurred locally at strain values somewhat below these values.

All the studies mentioned above identified non-linearity behaviour in asphalt mixtures and the existence of a strain dependent LVE criteria for asphalt mixtures, which is in agreement with the results obtained from this investigation. However, this investigation showed that the same strain dependent LVE criteria was evident for both unmodified as well as modified asphalt mixtures. In addition, increasing the binder content (HRA mortar) resulted in an increase in the value of the strain dependent LVE criteria.

5.6 LVE Rheological Characterisation

Various researchers have studied the LVE rheological characteristics of asphalt mixtures [28, 49, 53]. Goodrich used dynamic torsional tests on rectangular asphalt mixture specimens to investigate the effects of binder and aggregate on asphalt mixture rheology. Figure 5.47 presents the rheological properties of a range of asphalt mixtures with different binders and summarizes the main conclusions from the research undertaken by Goodrich [53]. It can be seen in Figure 5.47 that the rheology of an asphalt mixture at low temperatures is largely dependent on binder rheology, while at high temperatures the mixture rheology is predominately influenced by the aggregate. In between these two extremes, at temperature between 10 and 50˚C, asphalt mixture rheology is influenced by both the binder and the aggregate.

In order to study the linear rheological characteristics of the asphalt mixtures incorporated in this study, a number of frequency sweep tests were conducted on all the asphalt mixtures at temperatures between 10 and 40°C and frequencies between 0.1 and 20 Hz in the linear region. The objective of these tests was to investigate the time and temperature dependent rheological properties of the asphalt mixtures. The results have been presented in the form of isothermal plots, isochronal plots and master curves for each mixture type. Because of the large number of graphs, only a few are presented in this chapter.

5.6.1 Isochronal Plots

Figures 5.48 and 5.49 show the isochronal plots of complex modulus and phase angle for the HRA mixture with 50 pen bitumen. In these figures the temperature and time dependent nature of the asphalt mixture is clearly evident (increased complex modulus and reduced phase angles at lower temperatures and higher loading frequencies). This is due to viscoelastic materials behaving more elastically at higher loading frequencies and lower temperatures, resulting in higher complex modulus values and lower phase angles. It can also be seen in Figure 5.49 that there is not a continuous increase in phase angle with increasing temperature, but rather an increase up to a peak phase angle followed by a subsequent decrease. This behaviour highlights the increased dominance of the aggregate skeleton at high temperatures

resulting in lower phase angles and increased elastic response compared to higher phase angles and increased viscous response found for bituminous binders. These results are identical to those described by Goodrich [53].

The rheological properties of the different asphalt mixtures have been compared in the form of isochronal plots at 1 Hz in Figures 5.50 to 5.55. It can be seen in Figures 5.50 and 5.51 that the rheological properties of the five DBM mixtures are all very similar, particularly the conventional 50 pen bitumen, radial SBS PMB and EVA PMB mixtures. The linear SBS PMB, due to its softer base bitumen, showed the lowest complex modulus values and highest phase angles at low temperatures but, due to its high polymer content, demonstrated comparable complex modulus and phase angle values at 30 and 40˚C. The DBM mixture with multigrade 35/50 showed the highest E* values at temperatures greater than 20˚C with consistently high elastic behaviour over the entire temperature range.

The complex modulus results for the DBM, HRA and HRA mortars mixtures with 50 pen bitumen and radial SBS PMB can be seen in Figures 5.52 and 5.53. The E* values for the DBM and HRA mixtures are very similar and both considerably greater than those measured for the HRA mortars. This is not surprising as the volumetric proportions for the DBM and HRA mixtures are similar with the HRA mortars having higher bitumen and air void volumetric proportions (see Table 5.2). The isochronal plots of phase angle for the different asphalt mixtures (Figures 5.54 and 5.55) are again similar, although the HRA mortar demonstrated greater elastic response (lower phase angles) at high temperatures compared to the larger aggregate sized DBM and HRA mixtures. This may be caused by the smaller aggregate sizes in the HRA mortar producing a more effective aggregate interlock at low strains and therefore a greater elastic response compared to that achieved for the conventional asphalt mixtures.

5.6.2 Master Curves

Complex modulus and phase angle master curves were constructed at a reference temperature of 20˚C. A comparison of complex modulus master curves for all the DBM asphalt mixtures is presented in Figure 5.56. The figure shows that the DBM mixture with linear SBS PMB has the lowest complex modulus values at high

frequencies and low temperatures due to the softer base binder used to produce the high polymer content linear SBS PMB. The DBM mixture with EVA PMB had the largest change in complex modulus as a function of loading frequency having the highest complex modulus values of all the mixtures at high frequencies and lowest values at low frequencies. The multigrade 35/50 DBM mixture showed the lowest susceptibility to loading frequency by maintaining high complex modulus values, relative to the other DBM mixtures, over the entire frequency range.

Figure 5.57 shows the shift factor versus temperature relationship used to produce the master curves at 20˚C for the 50 pen bitumen and 50 pen DBM, HRA, HRA mortar mixtures. It can be seen from the figure that the shift factor versus temperature relationship is very similar for the three asphalt mixtures and the pure bitumen.

The complex modulus master curves for the DBM, HRA and HRA mortar mixtures are compared in Figures 5.58 and 5.59. The results clearly show that the complex modulus values for the HRA mortar are approximately 50% less than those found for the DBM and HRA mixtures. This is due to the lower aggregate volume and higher air voids content of the mortar compared to the DBM and HRA asphalt mixtures (see Table 5.2).

Figure 5.60 presents a comparison of the phase angle master curves for the five DBM mixtures. It can be seen in the figure that all the mixtures tend to converge towards the same phase angle versus loading frequency relationship at high frequencies (low temperatures). This can be attributed to the high elastic response of both bituminous binders and asphalt mixtures at low temperatures and high frequencies irrespective of binder type. Over the central frequency region, the phase angle master curves of the five DBM mixtures differ considerably. This central frequency region corresponds to the region identified by Goodrich [53] where the rheological properties of asphalt mixtures are a function of both aggregate and binder properties. It is within this central region that the unique rheological properties of the conventional, process and polymer modified bitumens have the greatest influence on the rheological properties of the asphalt mixtures. Finally, although the testing was limited to a maximum temperature of 40°C, there is an indication that at low frequencies (high temperatures)

the master curves of the different mixtures start to converge to a second unique phase angle versus frequency relationship as the viscoelastic response of the mixtures become dominated by the aggregate structure.

Figures 5.61 and 5.62 show the phase angle master curves for the DBM, HRA and HRA mortar mixtures produced with 50 pen bitumen and radial SBS PMB. It can be seen from these figures that the master curves for the two standard mixtures and the mortar are all relatively similar. However, what is noticeable is that at low frequencies (high temperatures), where the effect of aggregate structure and properties on mixture rheology becomes increasingly more significant, the HRA mortars have lower phase angles than the DBM and HRA mixtures. This could be the result of greater interlock between the aggregate particles in the HRA mortar compared to that achieved in the other asphalt mixtures due to the smaller sized aggregates of the HRA mortar.

Comparisons of the phase angle master curves for the 50 pen bitumen and radial SBS PMB together with the DBM and HRA mixtures incorporating these binders are shown in Figures 5.63 and 5.64. It can be seen in the figures that the effect of the aggregate skeleton results in a reduction in phase angle and increased elastic response for the mixtures compared to the pure binders. This is particularly noticeable at low frequencies where there is a considerable difference between the increasing viscous response of the conventional binder and the increasing elastic response of the asphalt mixtures. Although the rheological behaviour of the SBS PMB shows a similar decrease in phase angle at low frequencies due to the dominating effect of the SBS polymer, this is still not as significant as the effect of the aggregate skeleton.

5.6.3 Discussion

The LVE rheological characteristics of the five DBM, two HRA and two HRA mortar mixtures have shown that although the mixtures differed from each other in terms of their gradings, any substantial variations in their rheological properties could be attributed mainly to a combination of volumetrics and binder type. Admittedly aggregate grading does have an effect on asphalt mixture rheological behaviour. However, the test results indicate that where the volumetric proportions are almost identical, the rheological properties in terms of both complex modulus and phase

angle tend to be similar. The greater binder and air voids content of the HRA mortar meant that the complex modulus values were lower than those obtained for the DBM and HRA mixtures, although the differences in phase angle were not as marked. In terms of binder type, there were differences in complex modulus and phase angle for the asphalt mixtures incorporating these binders, particularly at intermediate temperatures and loading frequencies where the binder's unique rheological properties are evident and to a certain extent at low temperatures where the stiffness of the base bitumen is important.

5.7 Summary

The chapter describes the development of a hydraulic tension-compression testing apparatus that has been used to determine the linearity limits of a range of asphalt mixtures in terms of stress and strain. The materials incorporated in the study consisted of unmodified, process modified and polymer modified dense bitumen macadam (DBM) 10 mm wearing course, hot rolled asphalt (HRA) 30/10 and HRA mortar mixtures. Cylindrical specimens of these asphalt mixtures were produced and subjected to sinusoidal loading conditions at temperatures between 10 and 40°C, firstly under stress sweep conditions and then under frequency sweep conditions, both within and outside the linear region of behaviour of the material. The resultant axial strains were measured and used to calculate the rheological parameters of complex modulus and phase angle. The linear region of each mixture was obtained by plotting complex modulus versus strain or stress from the stress sweep tests and found to be strain dependent rather than stress dependent. The strain linear limit was found to be between 20 and 100 microstrain for all the DBM and HRA mixtures and between 50 and 150 microstrain for all the HRA mortars over a range of complex modulus values measured at various temperatures and frequencies.

Once the linear region for the different asphalt mixtures had been determined, dynamic tests were conducted at temperatures between 10 and 40°C and frequencies between 0.1 and 20 Hz within the linear viscoelastic region. The results were presented as isothermal plots, isochronal plots and master curves. In general, the linear SBS PMB modified mixture showed the lowest complex modulus values at high frequencies and low temperatures. This could be attributed to the softer base

binders used to produce these PMBs, especially the high polymer content linear SBS PMB. The EVA PMB mixture showed the greatest susceptibility to temperature and frequency changes, while the multigrade 35/50 mixture showed the lowest susceptibility. Overall the five DBM and two HRA mixtures all showed very similar rheological characteristics over the temperature and frequency range used in this study. With regard to the two HRA mortars, due to their higher binder and air void volumetric proportions, their stiffness values tended to be approximately half that of the DBM and HRA mixtures.

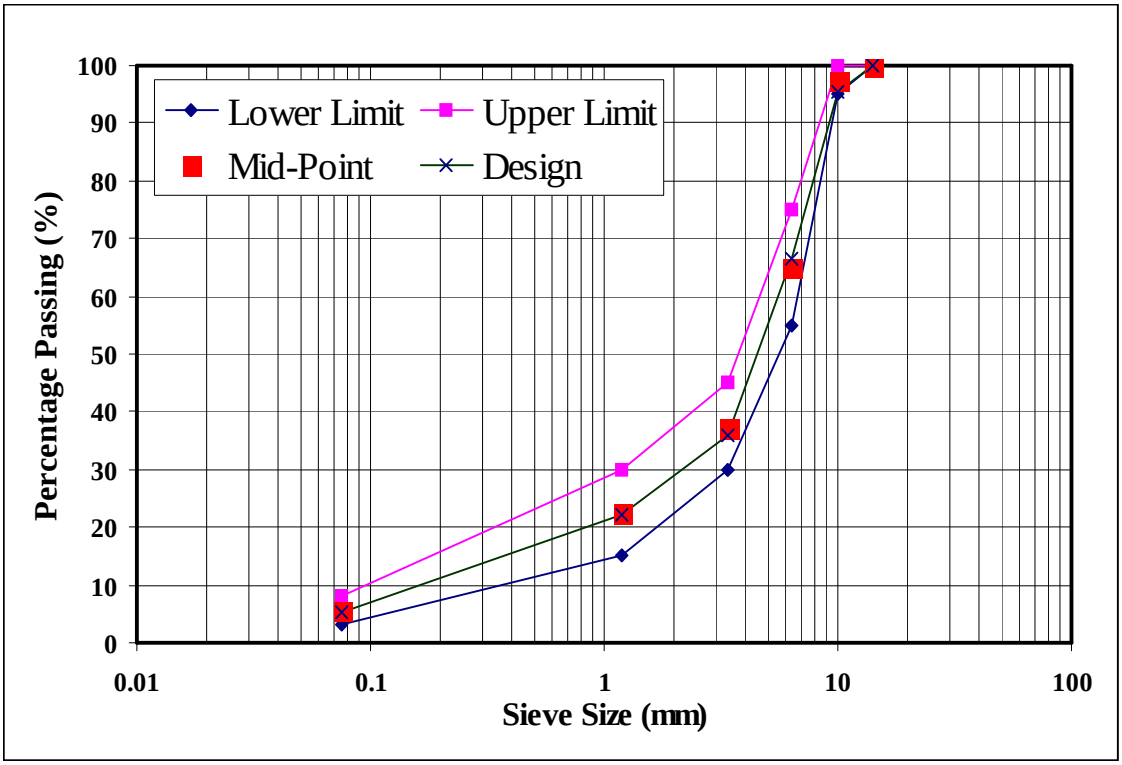

Figure 5.1: Design grading for 10 mm DBM

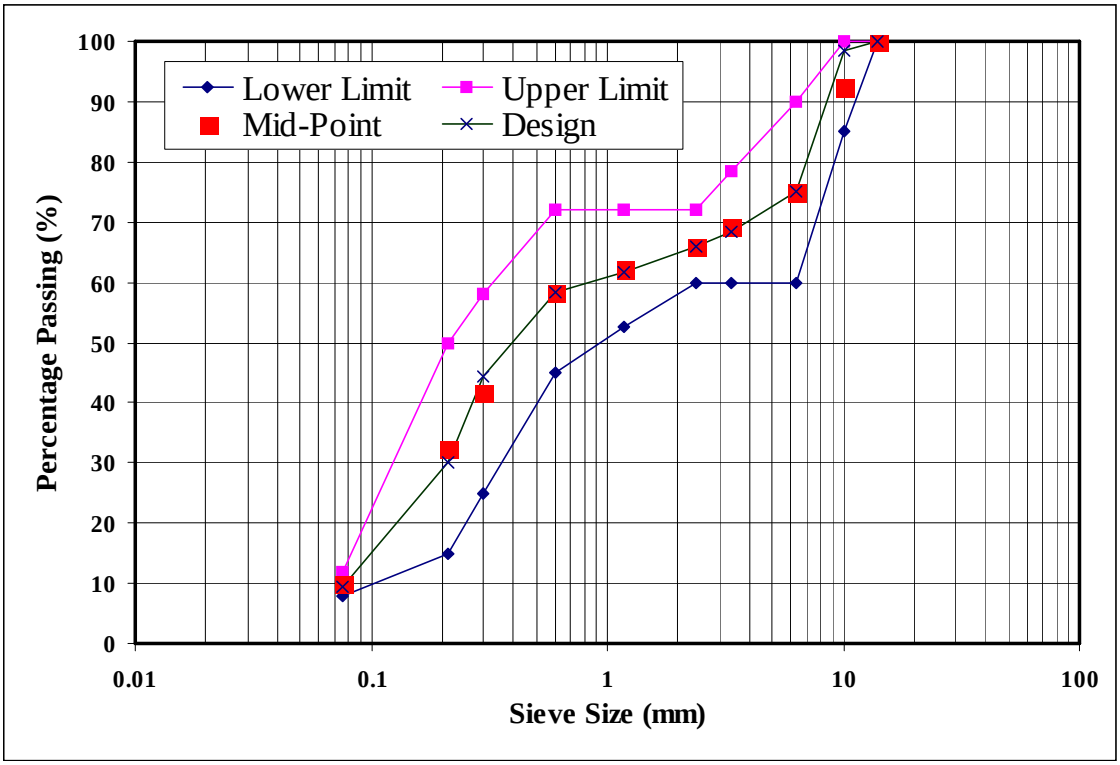

Figure 5.2: Design grading for HRA 30/10

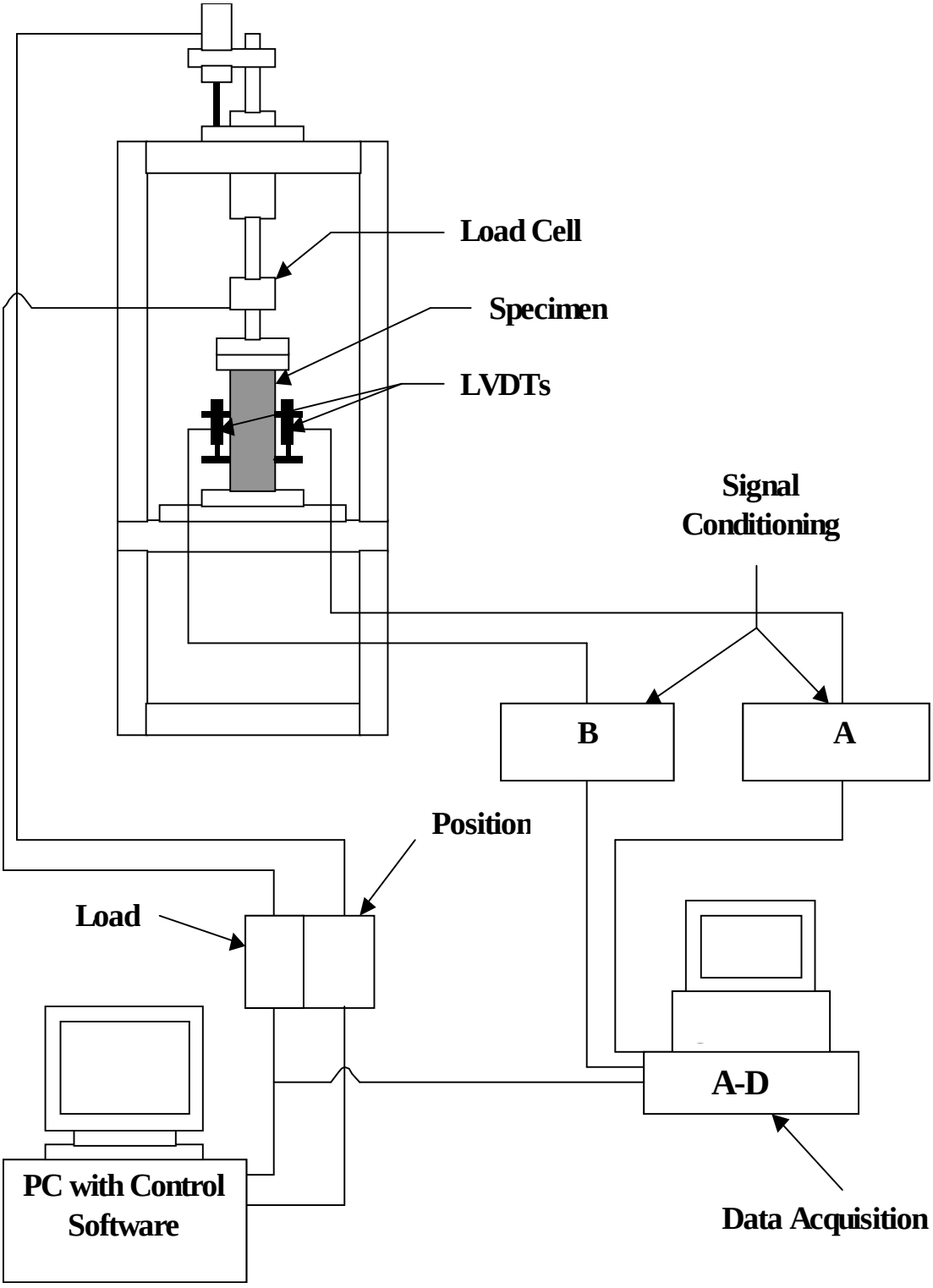

Figure 5.3: Hydraulic testing equipment for dynamic tension compression testing

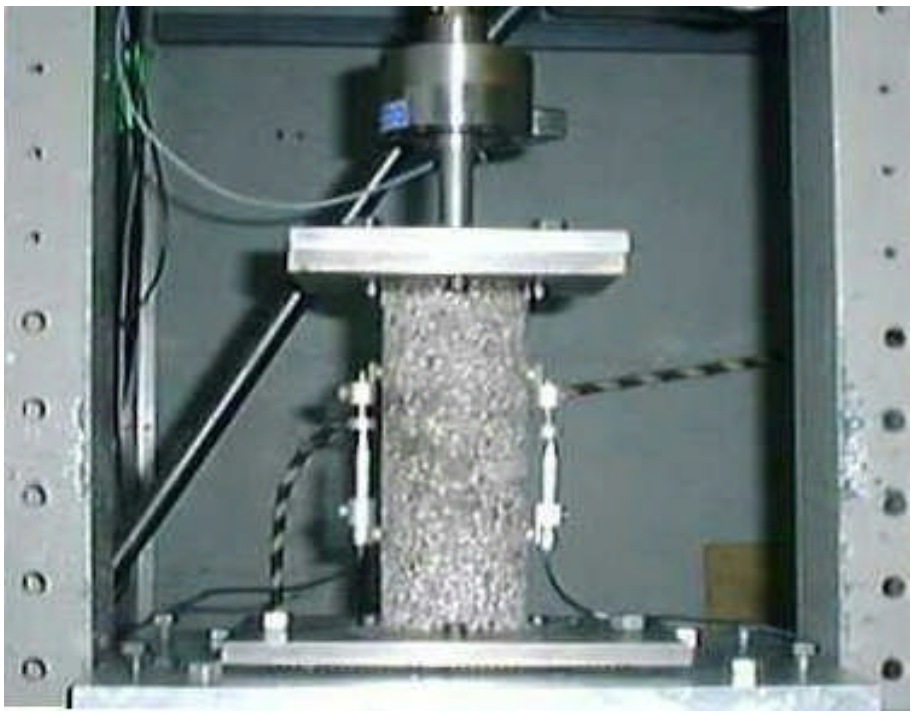

Figure 5.4: Initial arrangement for tension-compression testing

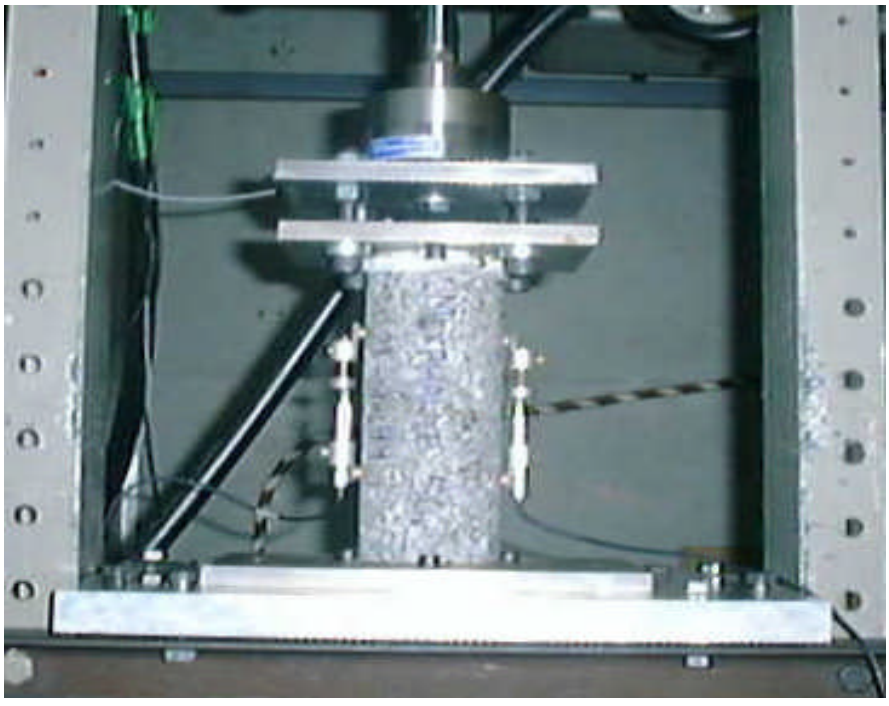

Figure 5.5: Final arrangement for tension-compression testing

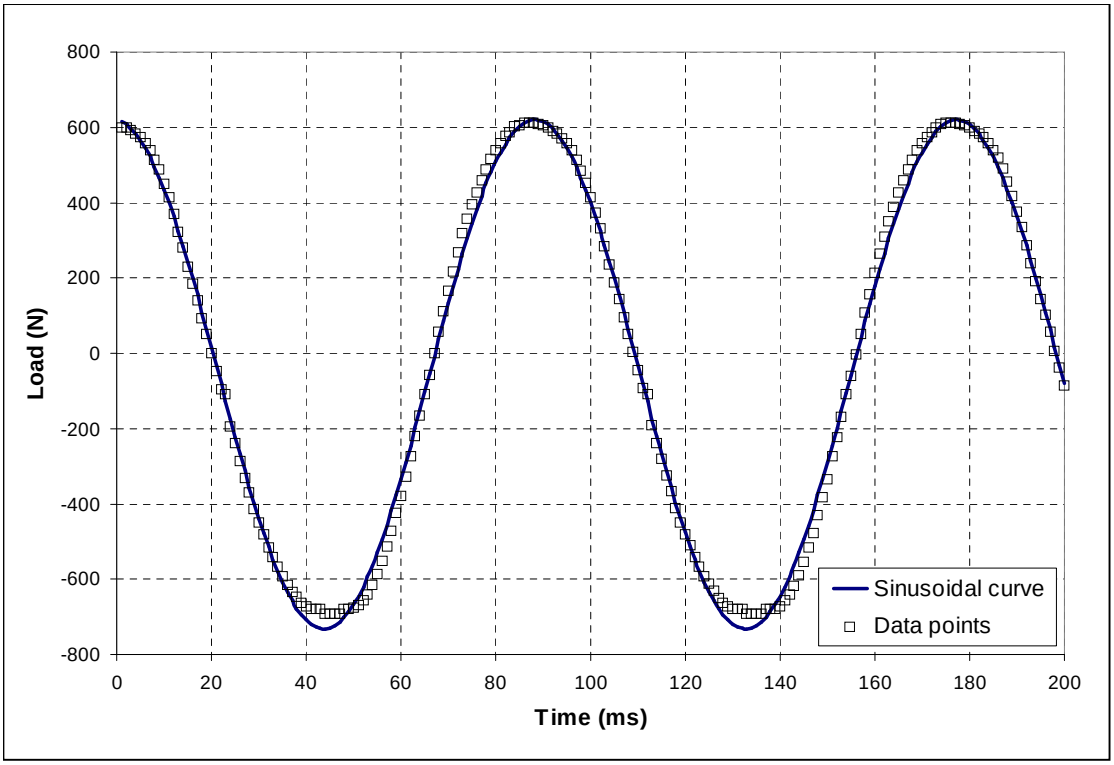

Figure 5.6: Data points and fitted sinusoidal curve at 10 Hz

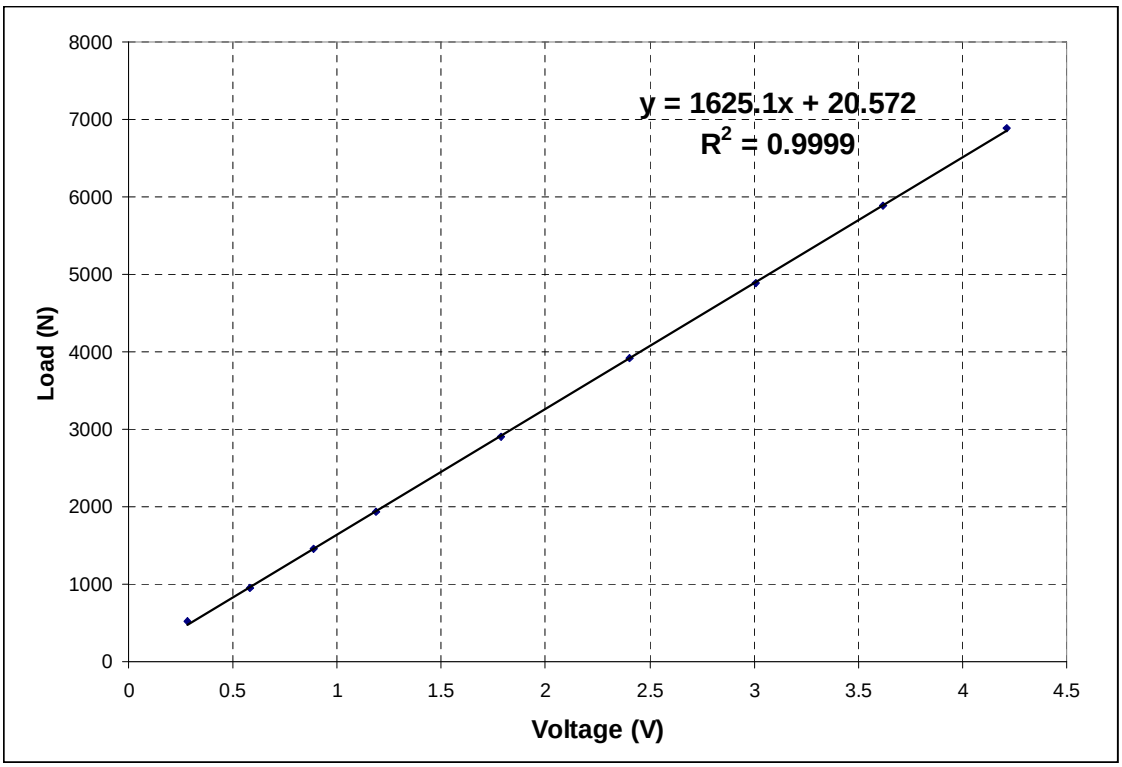

Figure 5.7: Calibration for load cell

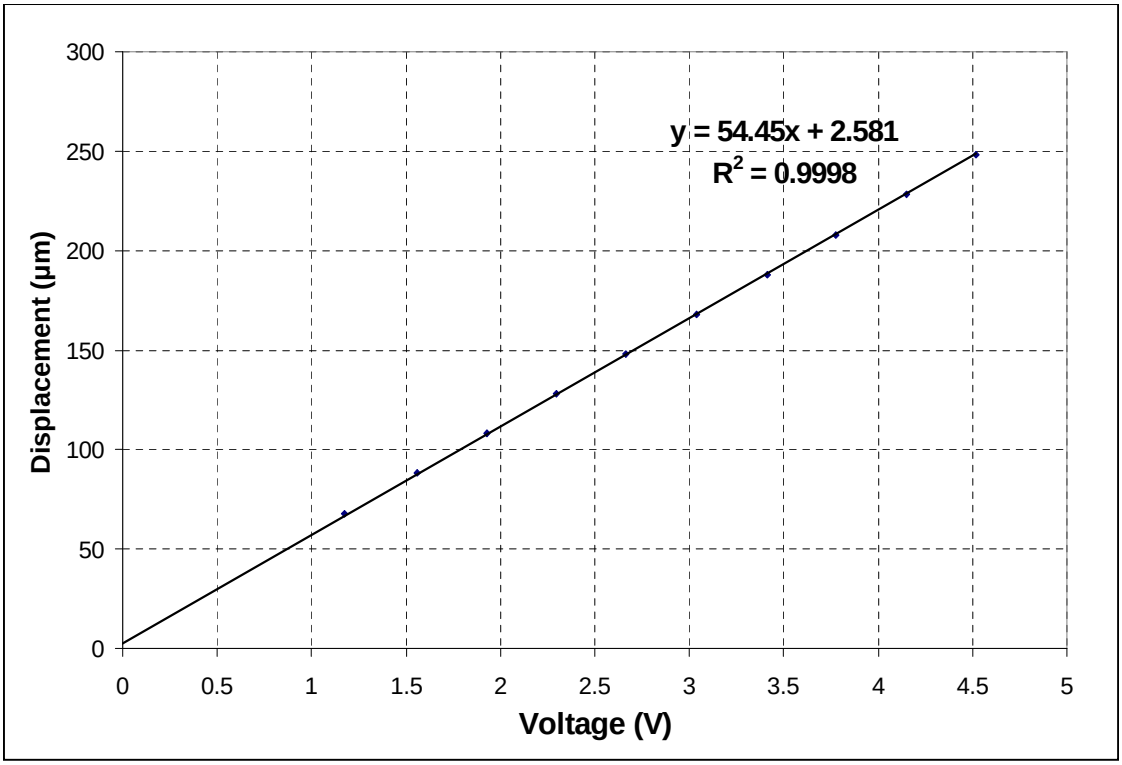

Figure 5.8: Calibration for LVDT A

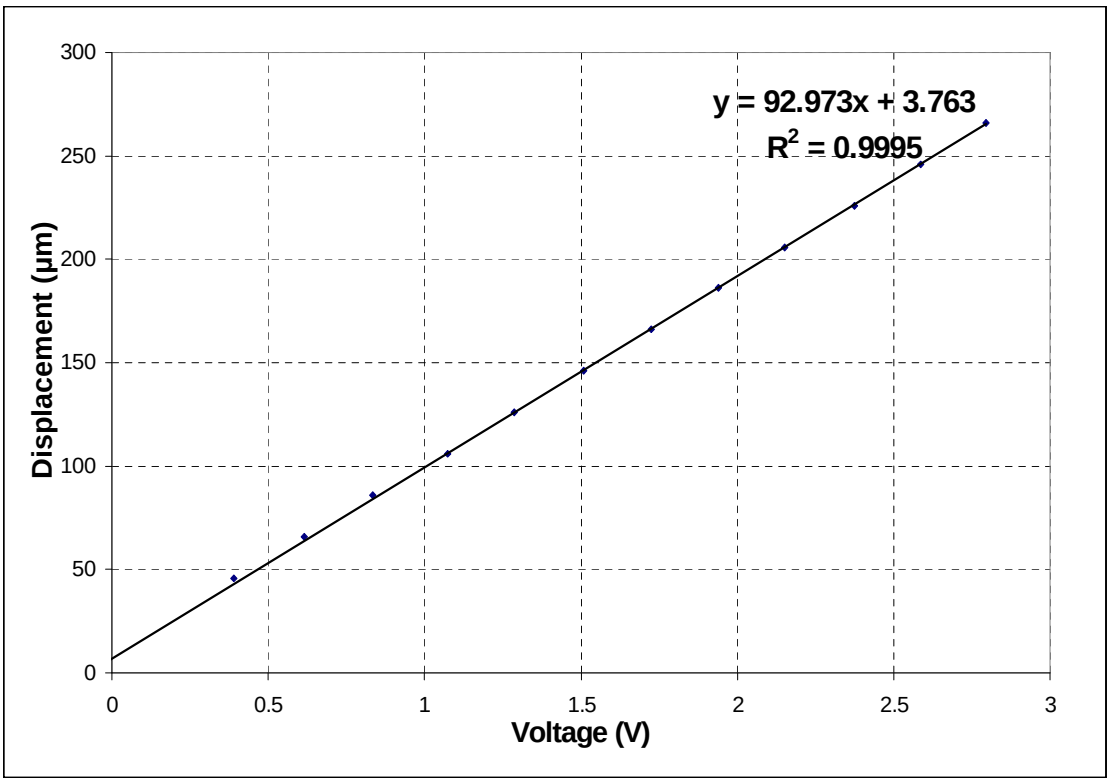

Figure 5.9: Calibration for LVDT B

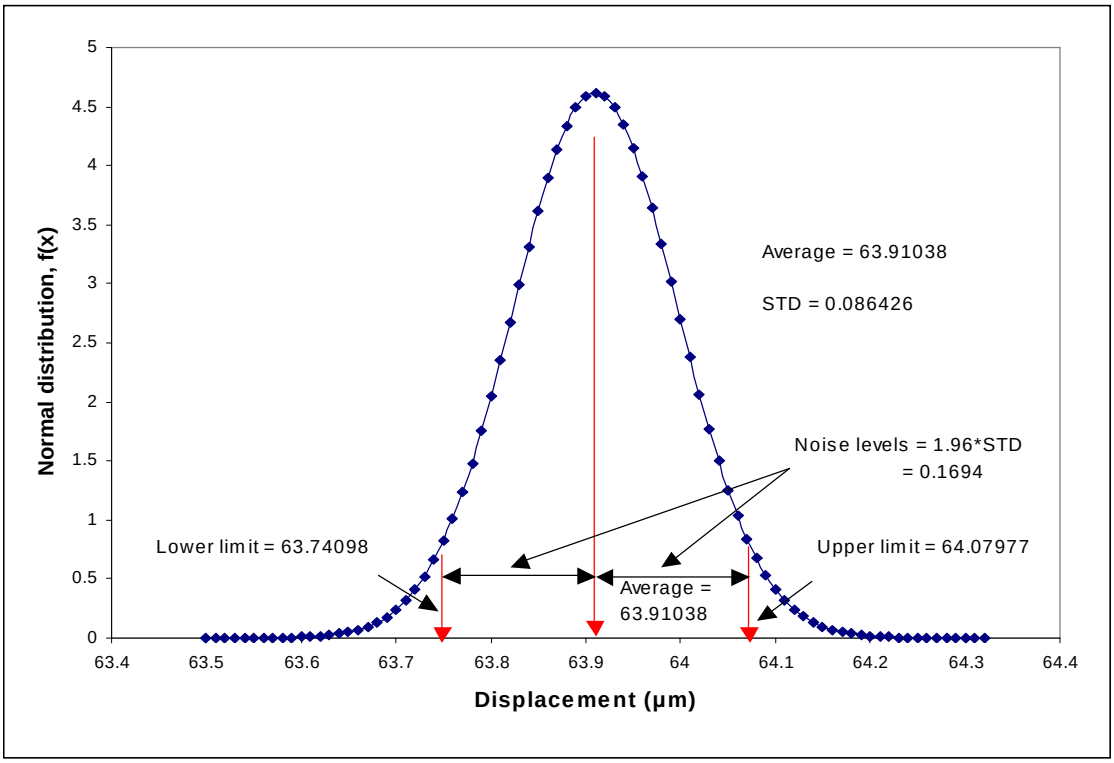

Figure 5.10: Normal distribution of noise for LVDT A

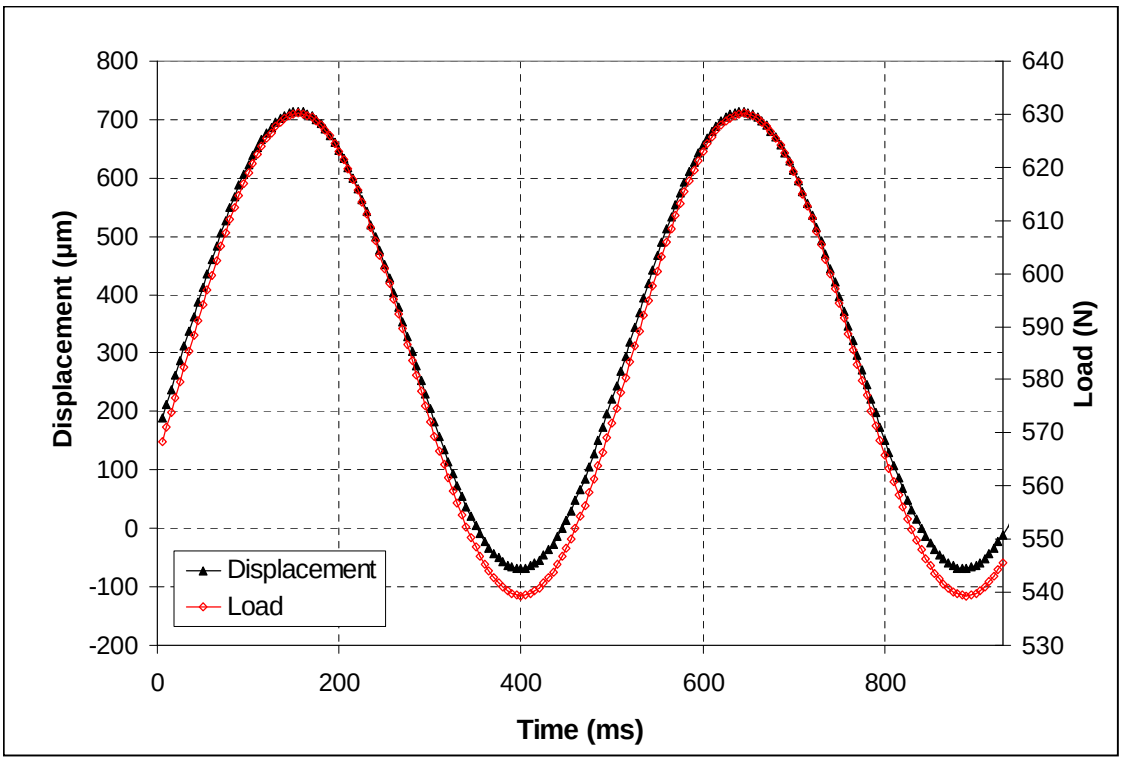

Figure 5.11: Load and displacement curves for elastic spring

```
clear

% Open control file and read in number of files to be processed
control=input('Enter control file name: ','s');
freq=input('Enter test frequency / Hz: ');
fid=fopen(control);
nfiles=fscanf(fid,'%5d',1);

for i=1:nfiles,
disp(['Run number ' num2str(i) ' out of ' num2str(nfiles)])

% read in file name from control file, load data and store in
% array called 'data'
fname = fscanf(fid,'%s',1);
eval(['load ' fname])
len=length(fname);
eval(['data=' fname(1:len-4) ';']);

% transfer data to separate arrays for time, stress and strain"

time=data(:,1);
stress=((data(:,4).*1625.1+20.572).*4)./(pi.*82e-3.*82e-3);
strain1=((data(:,3).*54.45+2.581)./100e-3);
strain2=((data(:,2).*92.973+3.763)./100e-3);

% select the last 5 cycles to analyse
tcuta=0;
tcutb=50000;
j=find(tcuta<time & time<tcutb);
time=time(j);
stress=stress(j);
strain1=strain1(j);
strain2=strain2(j);

% fit a sine wave to the stress of the form:
% stress=A*sin((w*t) - phi) + B
opts=foptions;
opts(1)=0;opts(3)=1e-1;opts(14)=4000;
varinit=[(max(stress)-min(stress))/2 freq 1 (max(stress)+min(stress))/2 0];
var1=fmins('sin_stress',varinit,opts,[],time,stress);
freq=var1(2);
fstress=(var1(1).*sin((2*pi*freq.*time)/1000-var1(3)))+var1(4);
if var1(1)<0,
   var1(3)=unwrap(var1(3))+pi;
end
plot(time,stress./1e6,'+',time,fstress./1e6)
grid on
xlabel('Time / Secs')
ylabel('Stress / MPa')
shg;pause

% fit a sine wave to the strain1 of the form
% stress=A*sin((w*t) - phi) + B
opts(1)=0;opts(3)=1e-3;opts(14)=2000;
varinit=[(max(strain1)-min(strain1))/2 1 (max(strain1)+min(strain1))/2];
var2=fmins('sin_strain',varinit,opts,[],time,strain1,freq);
fstrain1=(var2(1).*sin((2*pi*freq.*time)/1000-var2(2)))+var2(3);
if var2(1)<0,
   var2(2)=unwrap(var2(2))+pi;
end
plot(time,strain1,'+',time,fstrain1)
xlabel('Time / Secs')
ylabel('Strain1 / Microstrain')
grid on
shg;pause

% fit a sine wave to the strain1 of the form
% stress=A*sin((w*t) - phi) + B
```

```
opts(1)=0;opts(3)=1e-3;opts(14)=2000;
varinit=[(max(strain2)-min(strain2))/2 1 (max(strain2)+min(strain2))/2];
var3=fmins('sin_strain',varinit,opts,[],time,strain2,freq);
fstrain2=(var3(1).*sin((2*pi*freq.*time)/1000-var3(2)))+var3(3);
if var3(1)<0,
   var3(2)=unwrap(var3(2))+pi;
end
plot(time,strain2,'+',time,fstrain2)
xlabel('Time / Secs')
ylabel('Strain2 / Microstrain')
grid on
shg;pause


% calculate the complex modulus, the phase angle and the stress and
% strain amplitudes
Estar(i)=abs(2*var1(1)/(var2(1)+var3(1)));
phase1(i)=abs(abs(unwrap(var1(3)))-abs(unwrap(var2(2))))*180/pi;
phase2(i)=abs(abs(unwrap(var1(3)))-abs(unwrap(var3(2))))*180/pi;
phase(i)=(phase1(i)+phase2(i))/2;
eps1(i)=2*abs(var2(1));
eps1_mean(i)=var2(3);
sig(i)=2*abs(var1(1));
sig_mean(i)=var1(3);
eps2(i)=2*abs(var3(1));
eps2_mean(i)=var3(3);
eps(i)=(eps1(i)+eps2(i))/2;
Load(i)=((mean(max(stress)-min(stress)))*((pi*82e-3*82e-3)/4))*.5;
Stress(i)=mean(max(fstress)-min(fstress))/1000;
end

% close control file
fclose(fid);

%print of results
z=[Estar;phase;eps;Load;Stress];
fid=fopen('test7.txt','w');
fprintf(fid, Estar     phase     eps    load    stress\n');
fprintf(fid,'%6.2f %6.2f %6.2f %6.2f %6.2f\n',z);
fclose(fid)

% plot out Estar and phase versus strain
plot(eps,Estar,eps,Estar,'+')
xlabel('Strain Amplitude / Microstrain')
ylabel('Complex Modulus / GPa')
grid on
shg;pause

plot(eps,phase,eps,phase,'+')
xlabel('Strain Amplitude / Microstrain')
ylabel('Phase Angle / Degrees')
grid on
shg
```

Figure 5.12: Typical Matlab program used to calculate complex modulus and phase angle

Figure 5.13: Sun-and-planet type mixture

Figure 5.14: The rolling wheel compactor

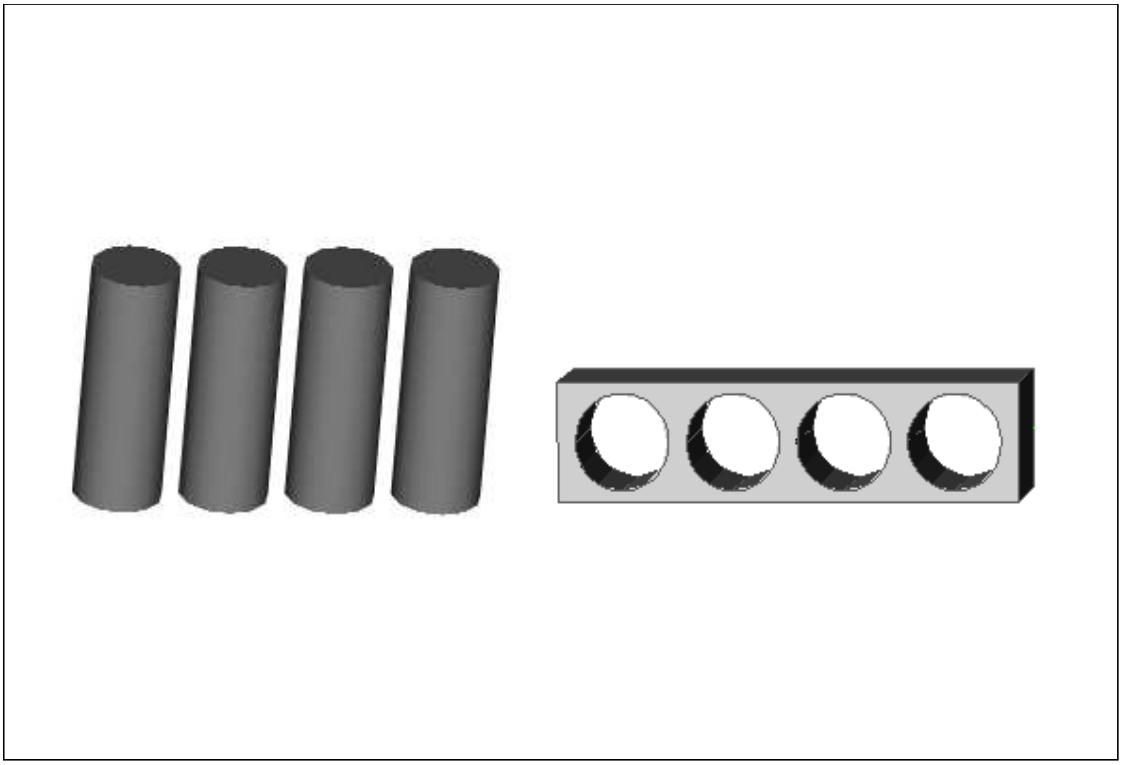

Figure 5.15: A slab after coring and specimen preparation

Figure 5.16: The jig used for fixing end plates

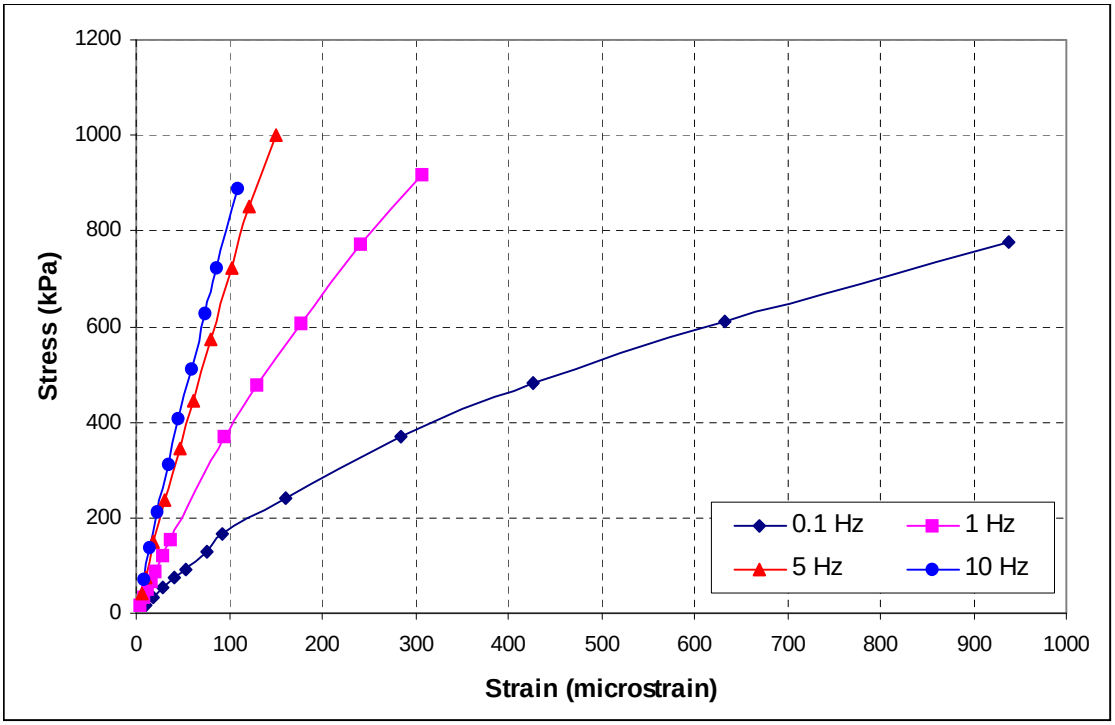

Figure 5.17: Stress versus strain for DBM mixture with 50 pen bitumen at 20˚C

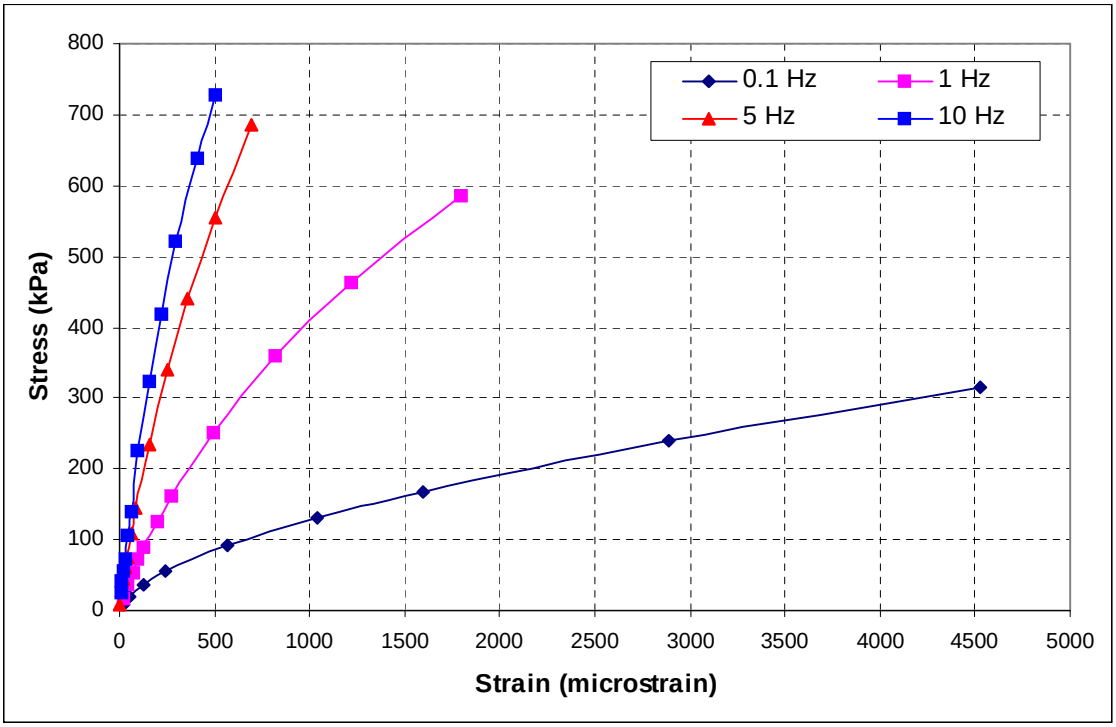

Figure 5.18: Stress versus strain for HRA mixture with radial SBS PMB at 30˚C

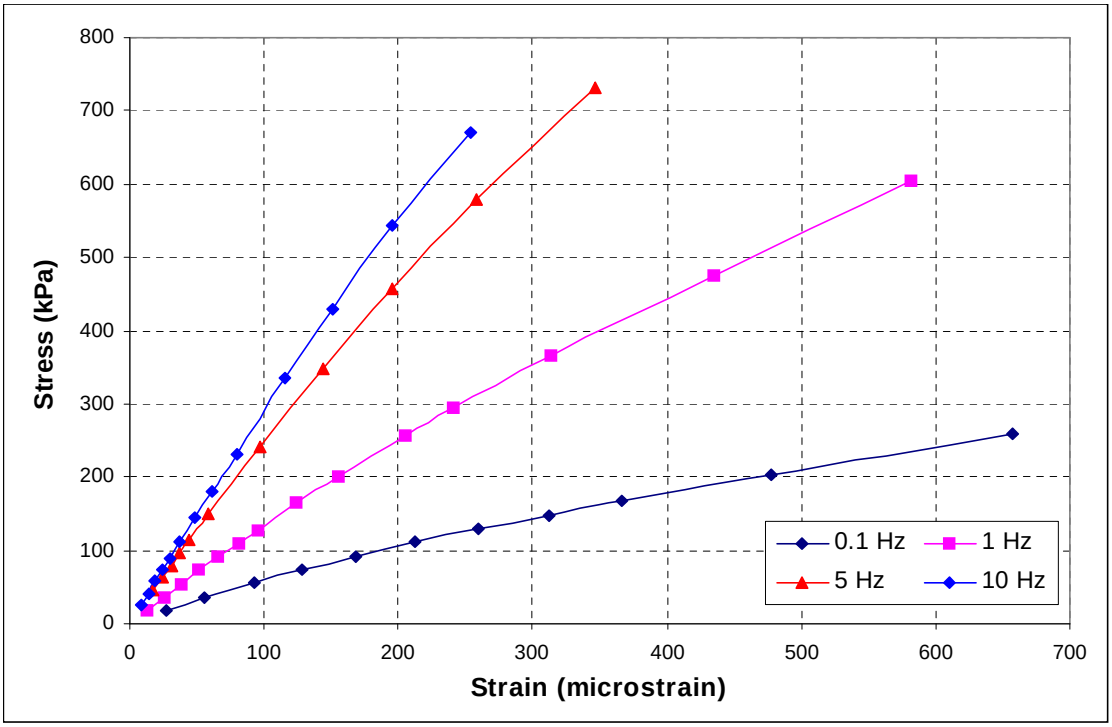

Figure 5.19: Stress versus strain for HRA mortar with 50 pen bitumen at 20˚C

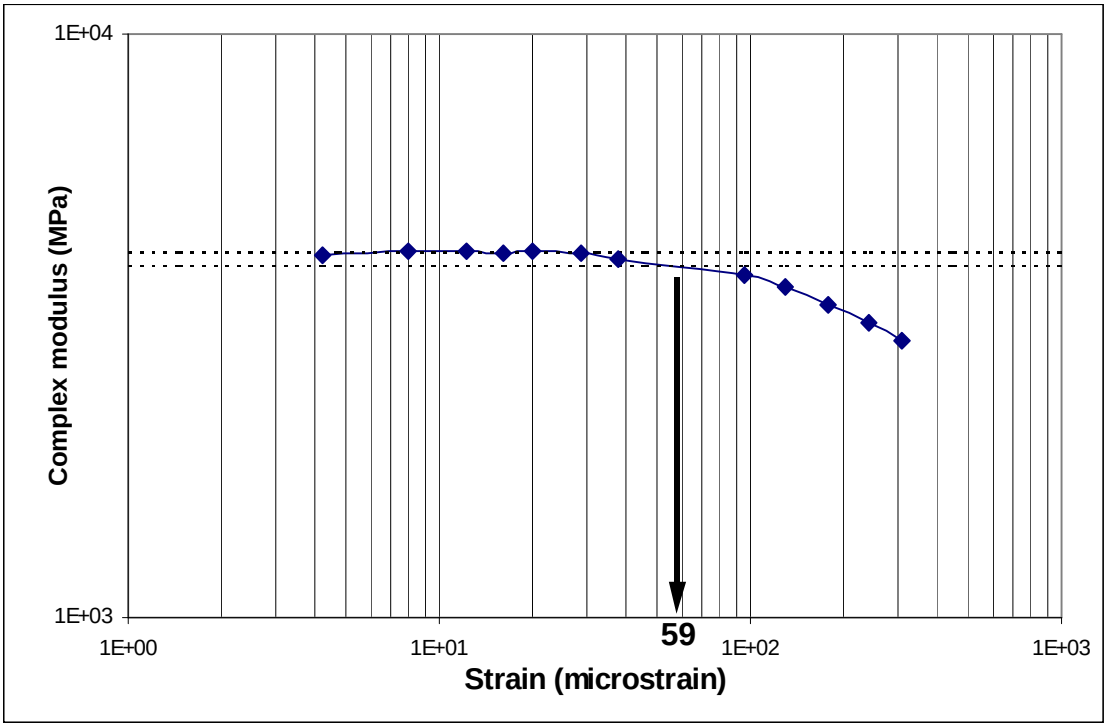

Figure 5.20: Complex modulus versus strain for DBM mixture with 50 pen bitumen at 1 Hz and 20C

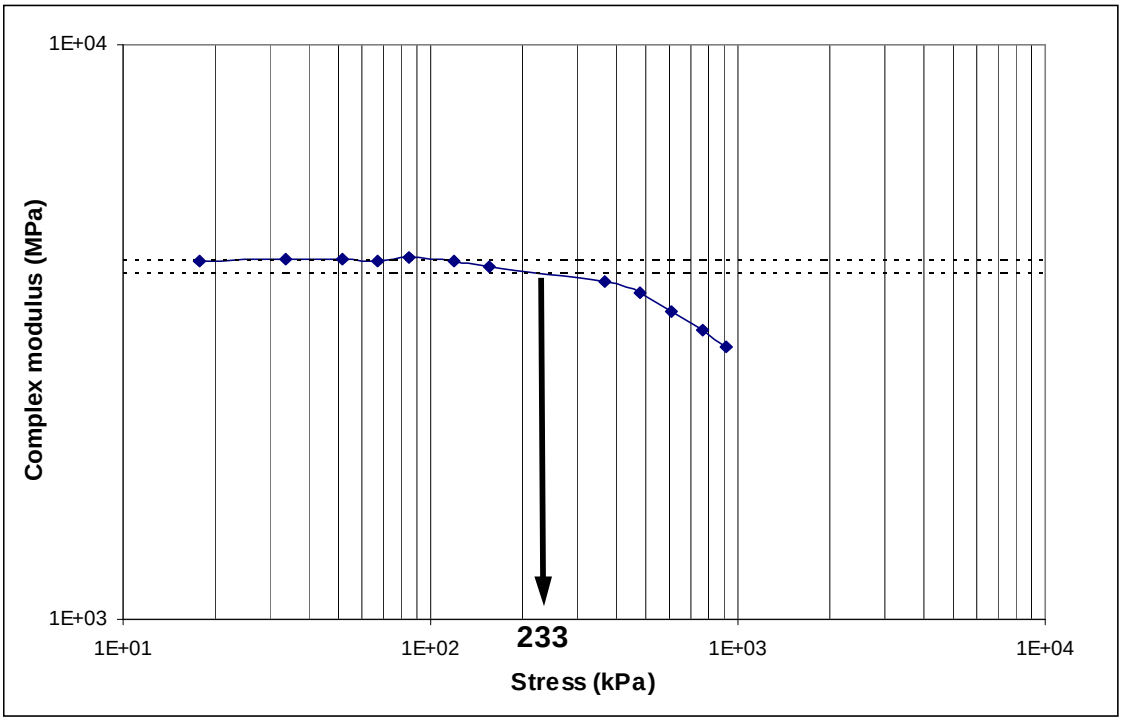

Figure 5.21: Complex modulus versus stress for DBM mixture with 50 pen bitumen at 1 Hz and 20C

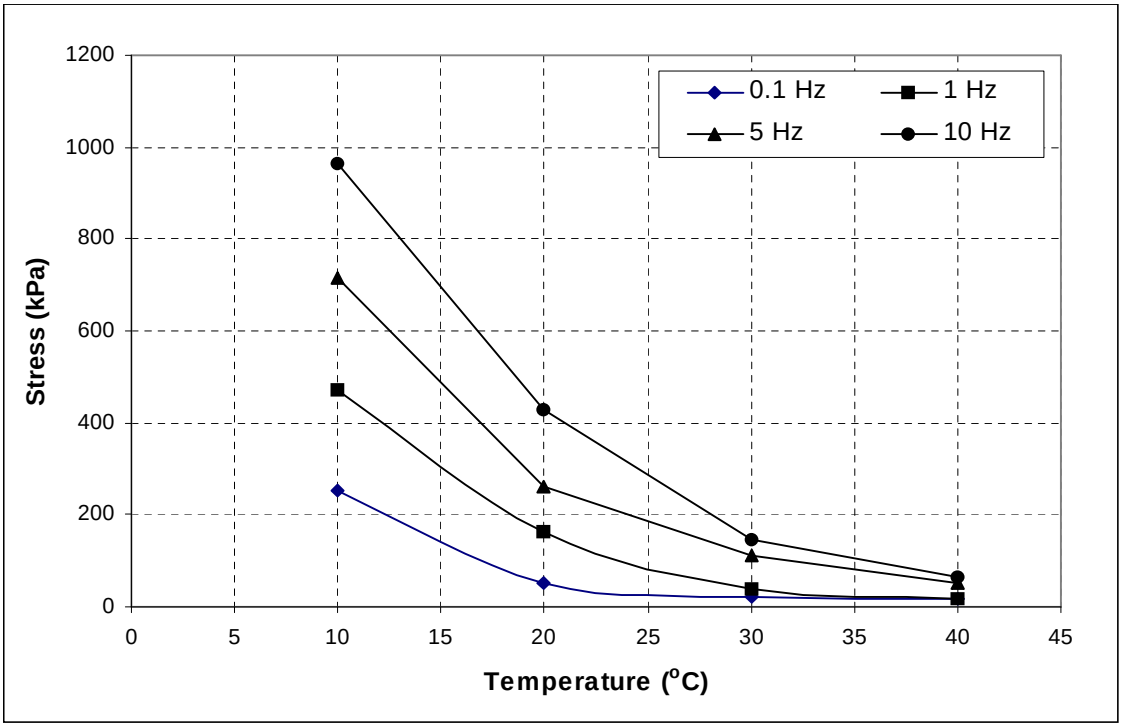

Figure 5.22: Linear limit of stress versus temperature at different frequencies for DBM mixture with radial SBS PMB

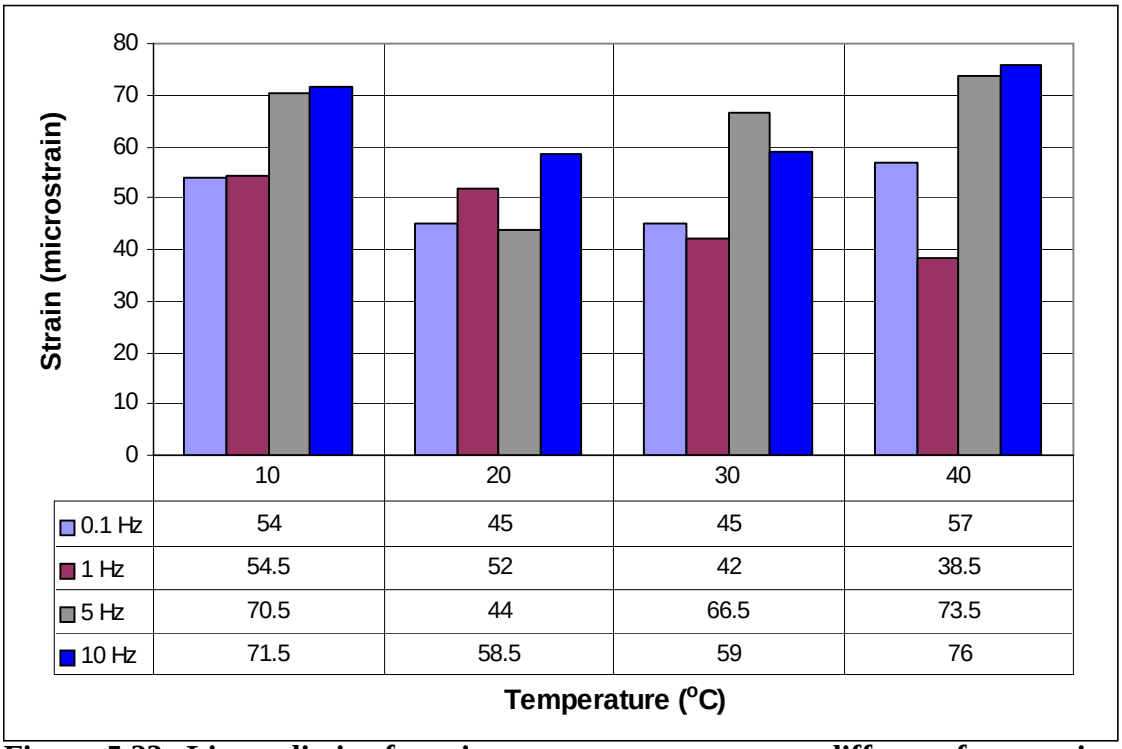

	10	20	30	40
0.1 Hz	54	45	45	57
1 Hz	54.5	52	42	38.5
5 Hz	70.5	44	66.5	73.5
10 Hz	71.5	58.5	59	76

Figure 5.23: Linear limit of strain versus temperature at different frequencies for DBM mixture with radial SBS PMB

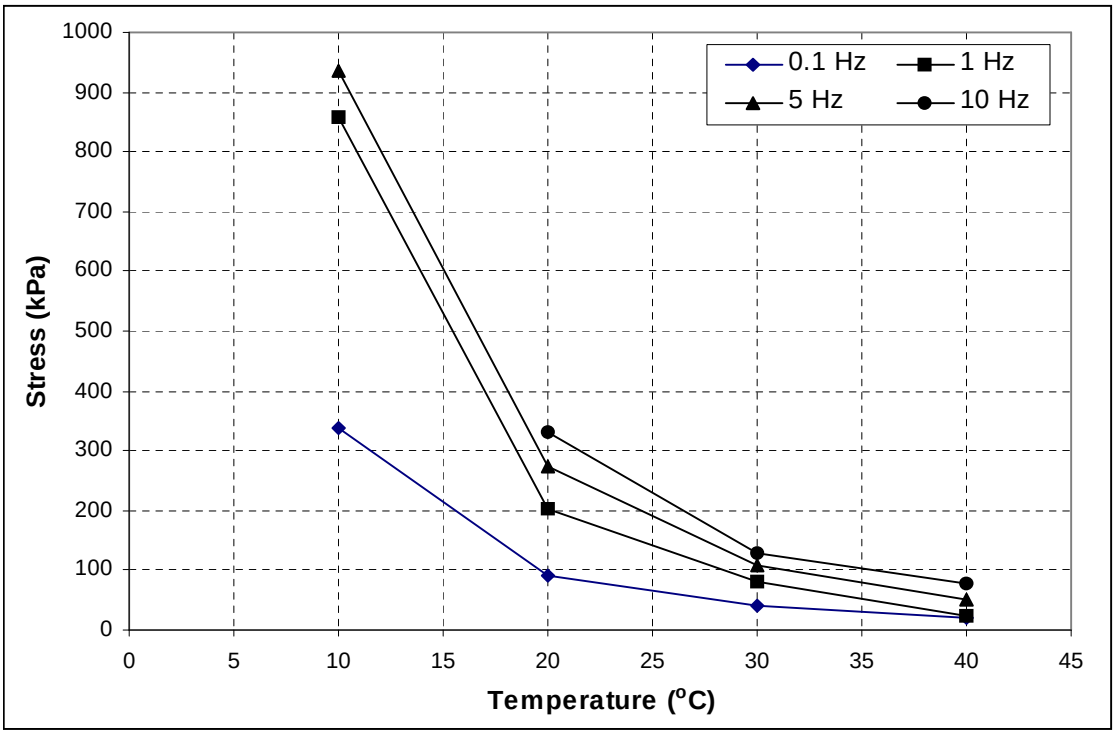

Figure 5.24: Linear limit of stress versus temperature at different frequencies for HRA mixture with 50 pen bitumen

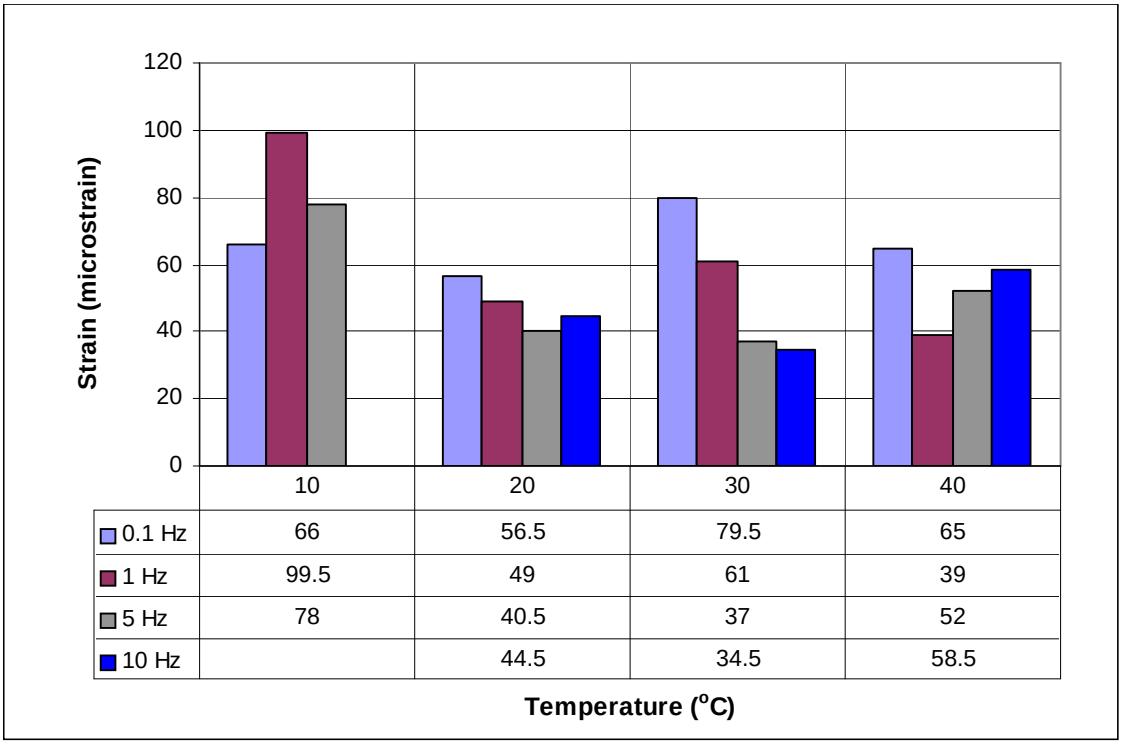

	10	20	30	40
0.1 Hz	66	56.5	79.5	65
1 Hz	99.5	49	61	39
5 Hz	78	40.5	37	52
10 Hz		44.5	34.5	58.5

Figure 5.25: Linear limit of strain versus temperature at different frequencies for HRA mixture with 50 pen bitumen

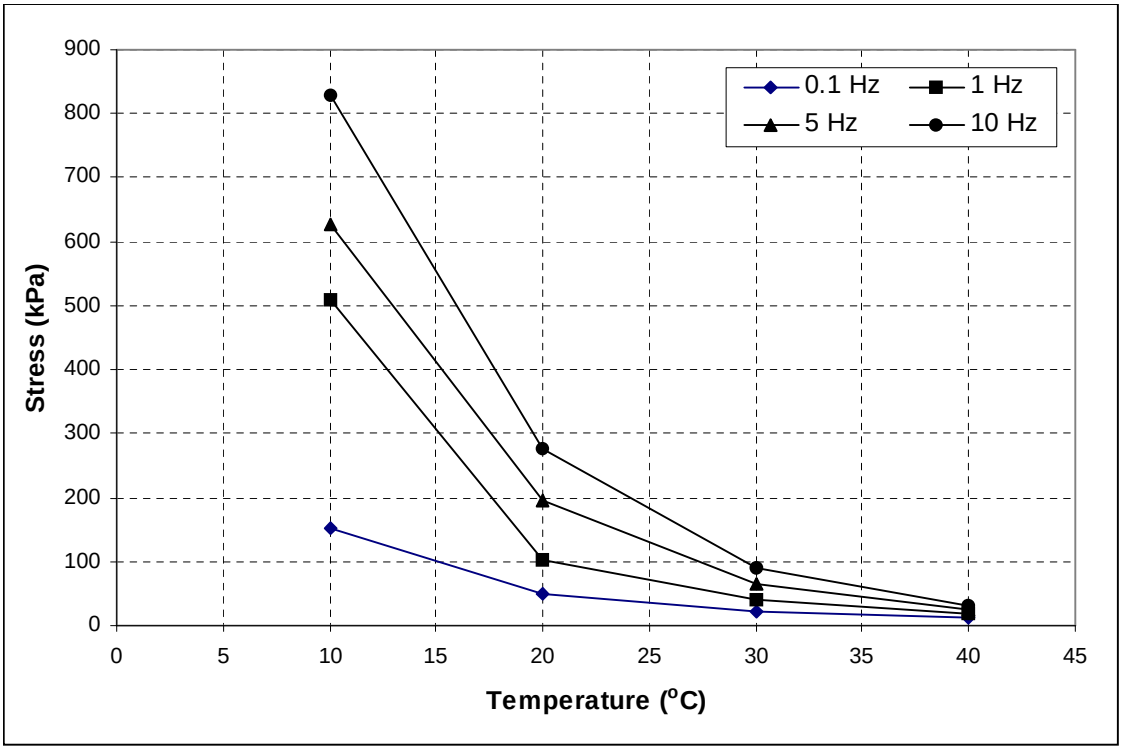

Figure 5.26: Linear limit of stress versus temperature at different frequencies for HRA mortar mixture with 50 pen bitumen

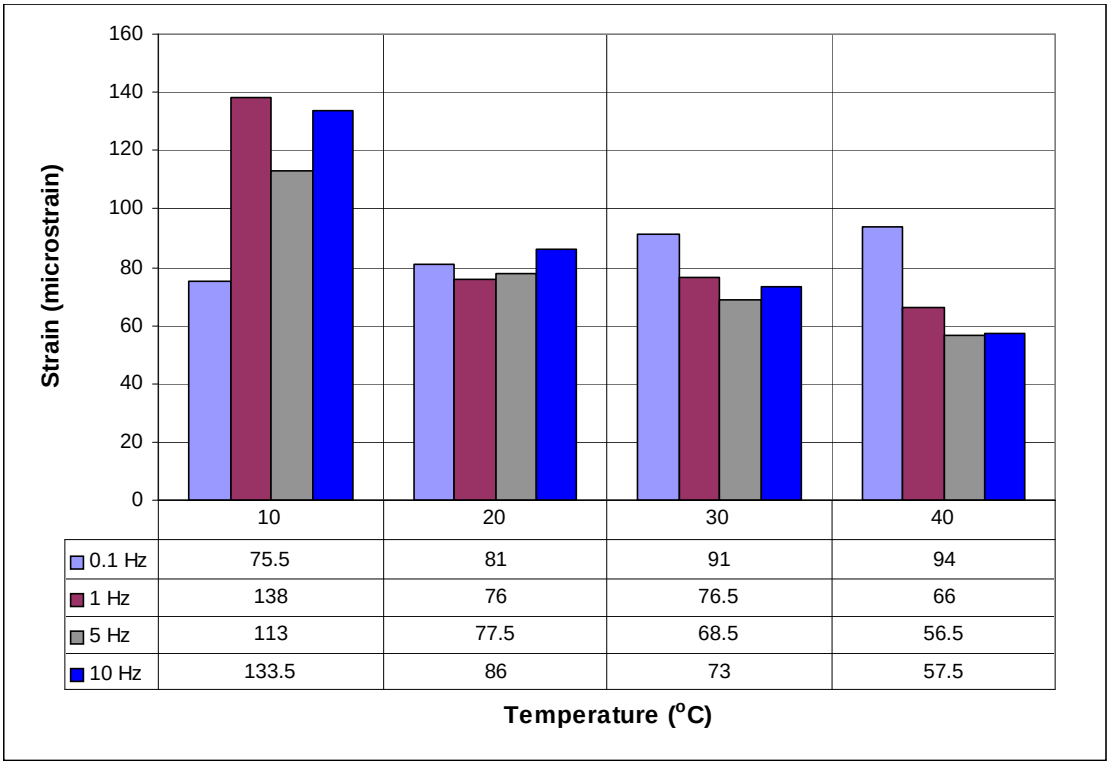

	10	20	30	40
0.1 Hz	75.5	81	91	94
1 Hz	138	76	76.5	66
5 Hz	113	77.5	68.5	56.5
10 Hz	133.5	86	73	57.5

Figure 5.27: Linear limit of strain versus temperature at different frequencies for HRA mortar mixture with 50 pen bitumen

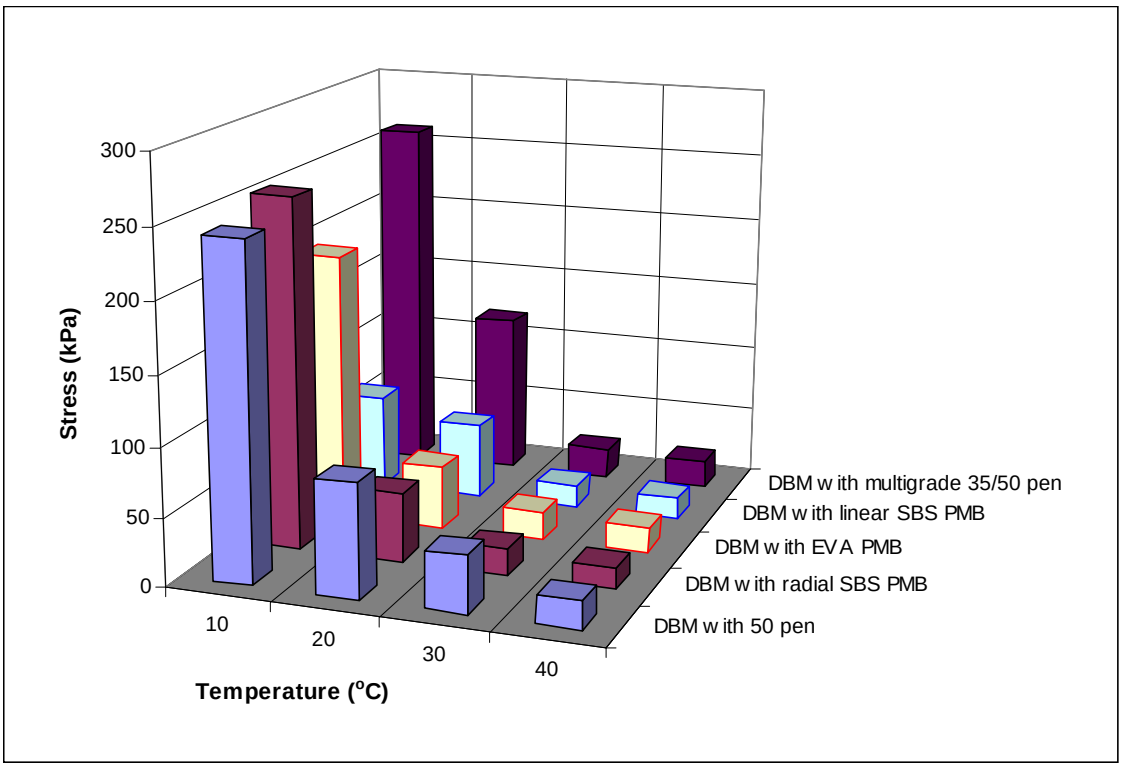

Figure 5.28: Linear limit of stress versus temperature at 0.1 Hz for DBM mixture produced with different binders

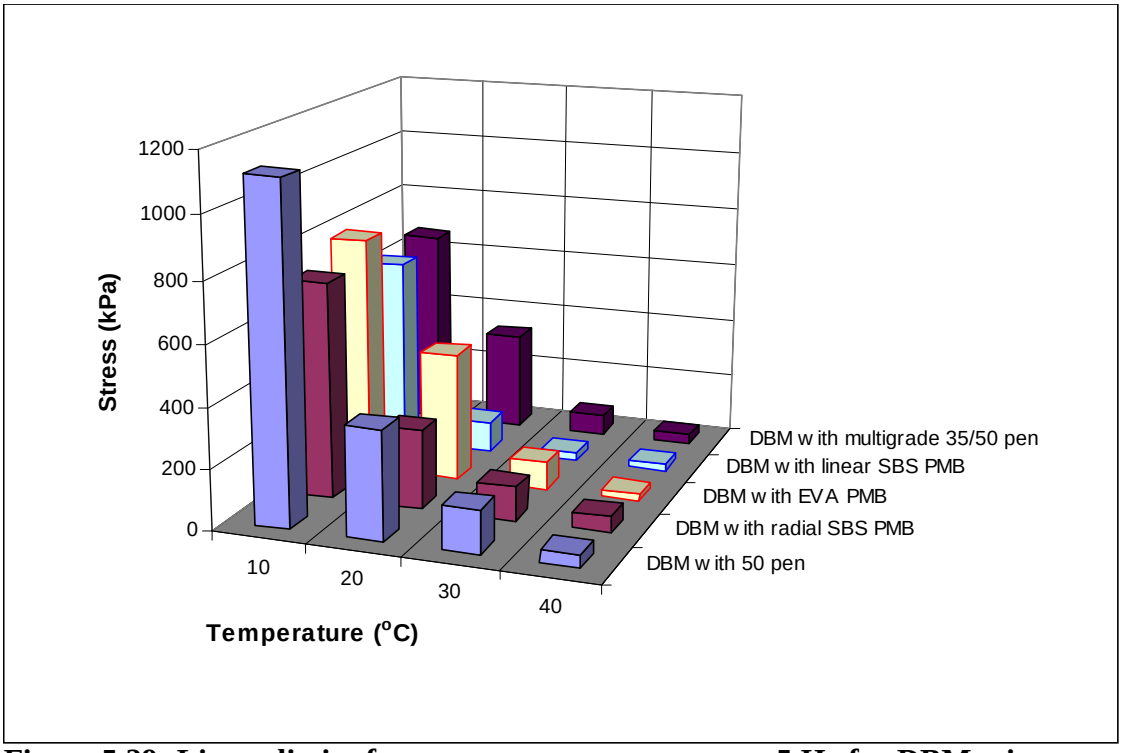

Figure 5.29: Linear limit of stress versus temperature at 5 Hz for DBM mixture with five different bitumens

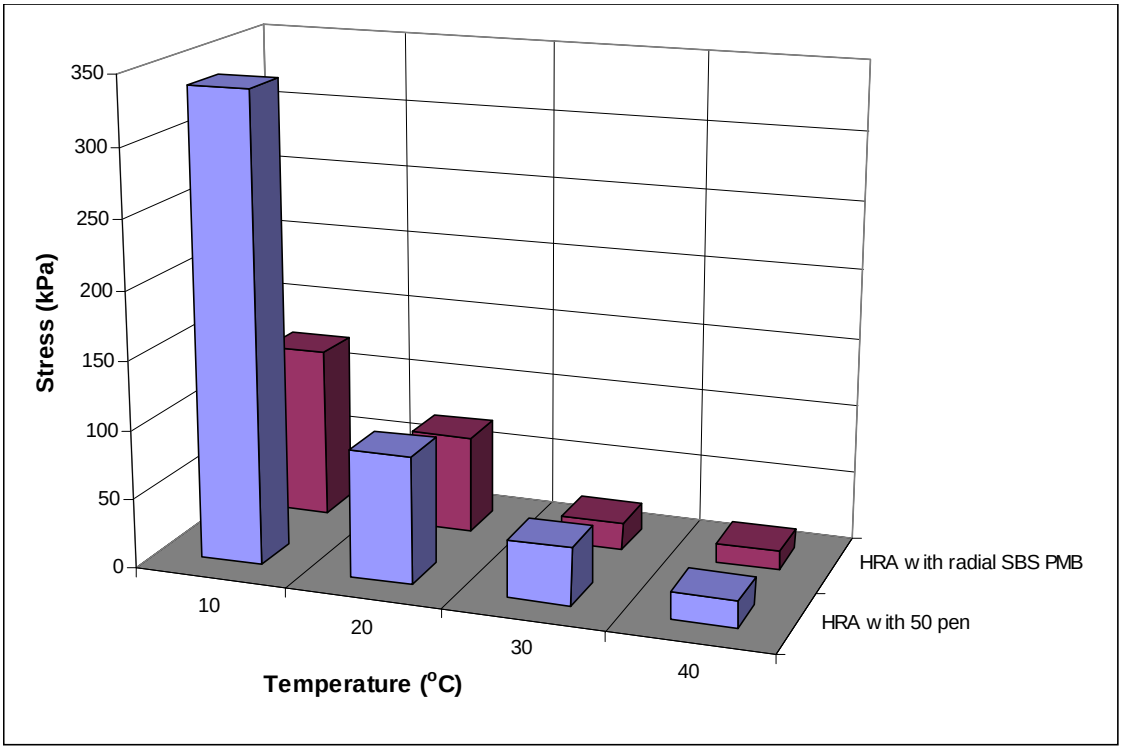

Figure 5.30: Linear limit of stress versus temperature at 0.1 Hz for HRA mixture with two different bitumens

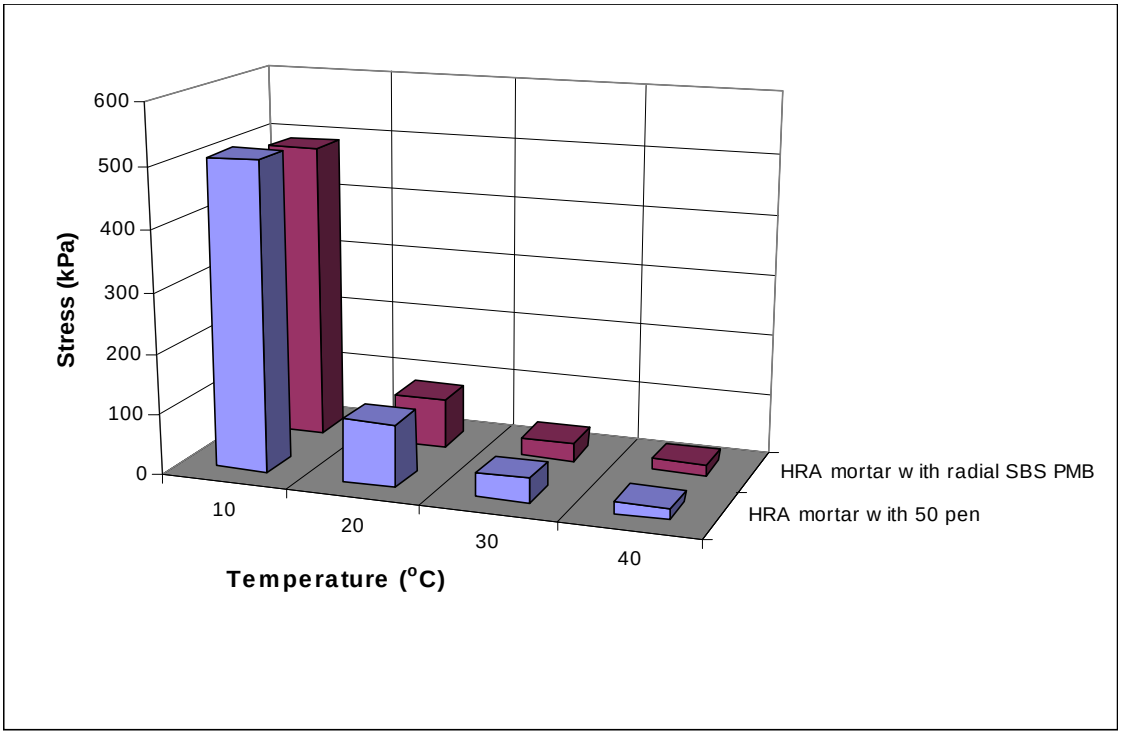

Figure 5.31: Linear limit of stress versus temperature at 1 Hz for HRA mortar mixture with two different bitumens

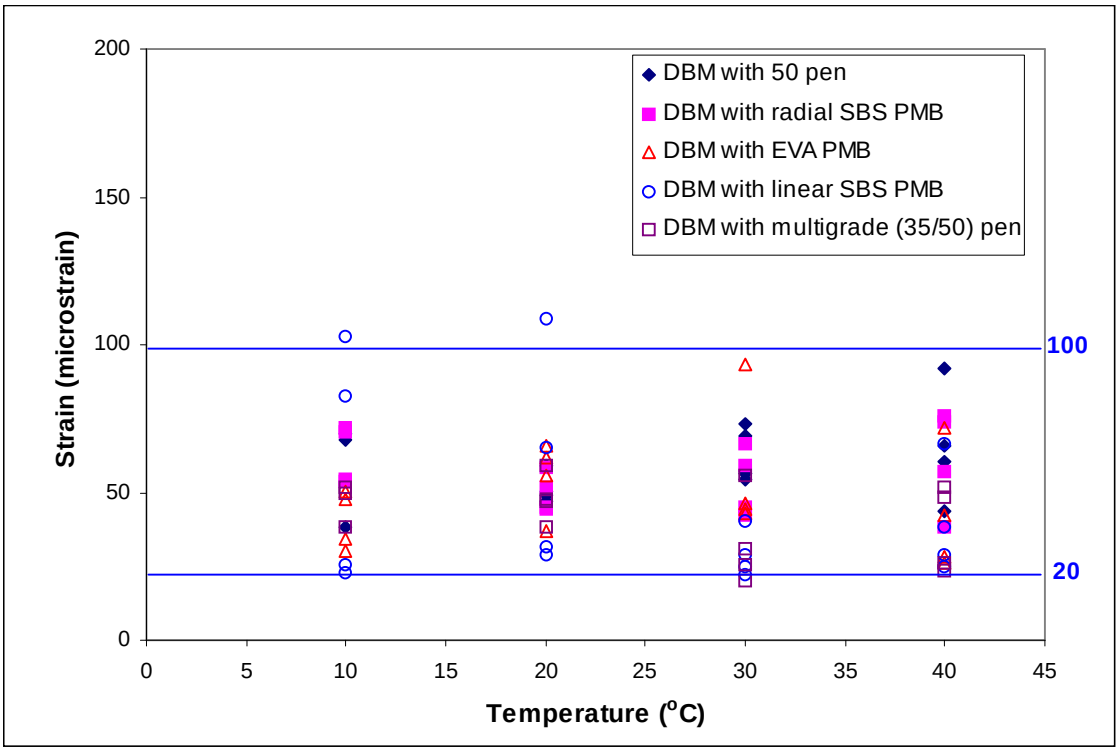

Figure 5.32: Linear limit of strain versus temperature at different frequencies and temperatures for DBM mixture with five different bitumens

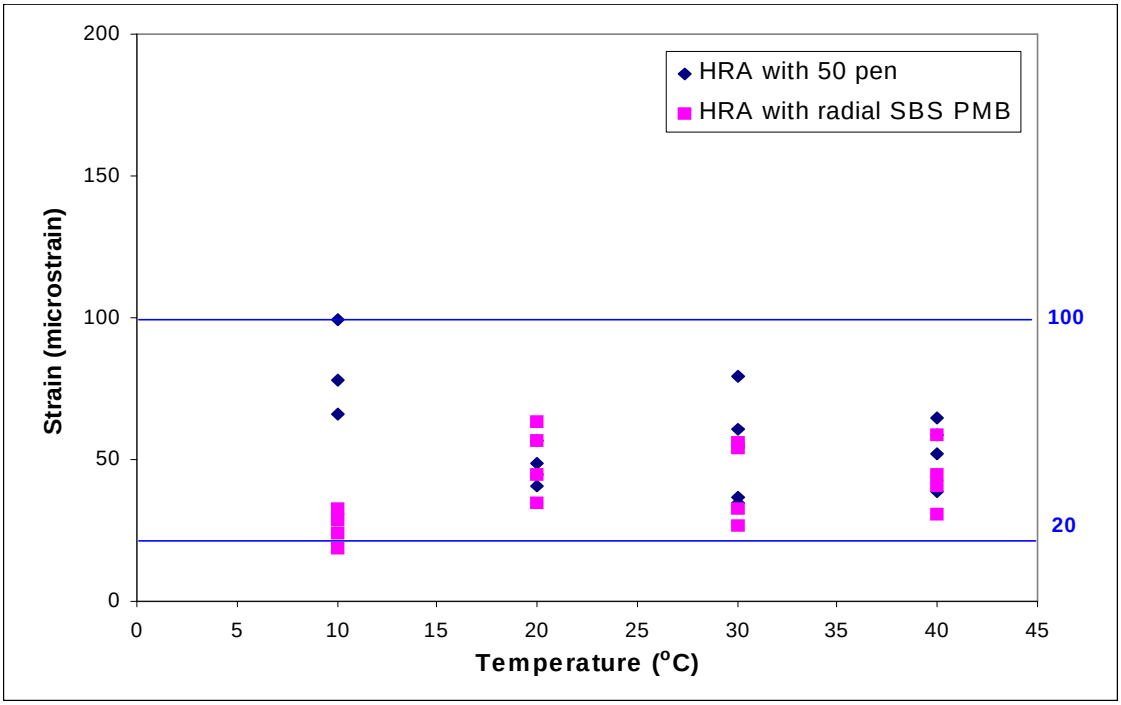

Figure 5.33: Linear limit of strain versus temperature at different frequencies and temperatures for HRA mixture with two different bitumens

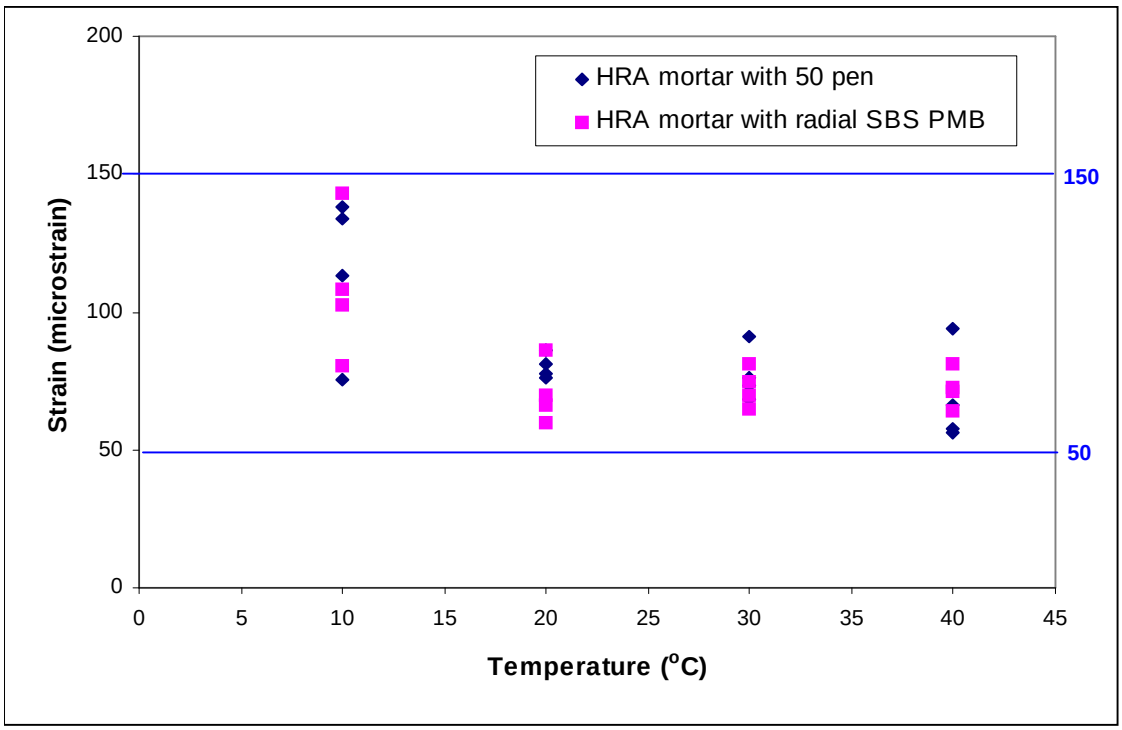

Figure 5.34: Linear limit of strain versus temperature at different frequencies and temperatures for HRA mortar mixture with two different bitumens

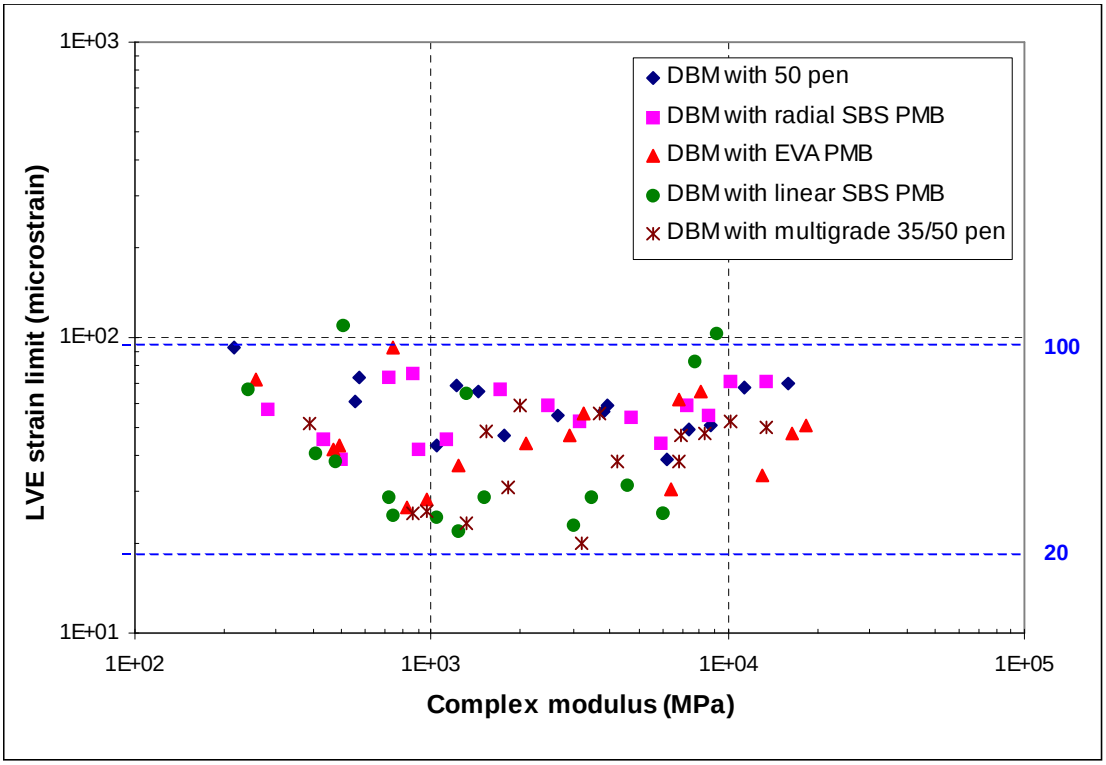

Figure 5.35: Linear viscoelastic range for different DBM mixtures

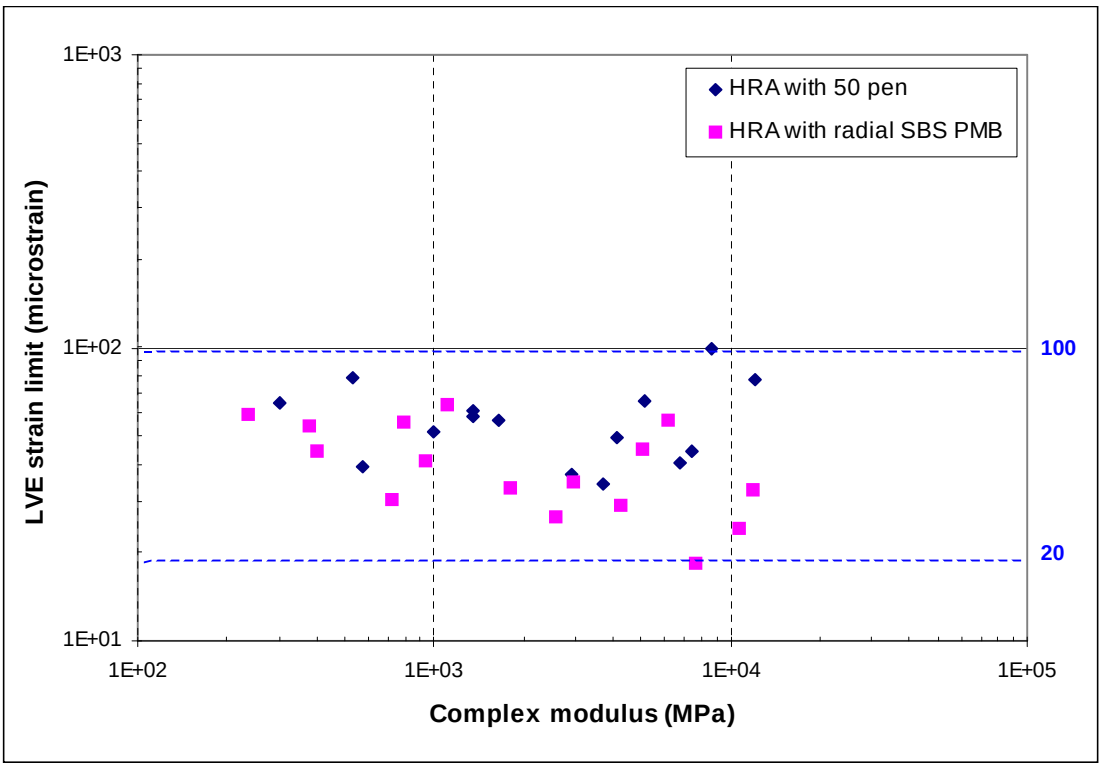

Figure 5.36: Linear viscoelastic range for different HRA mixtures

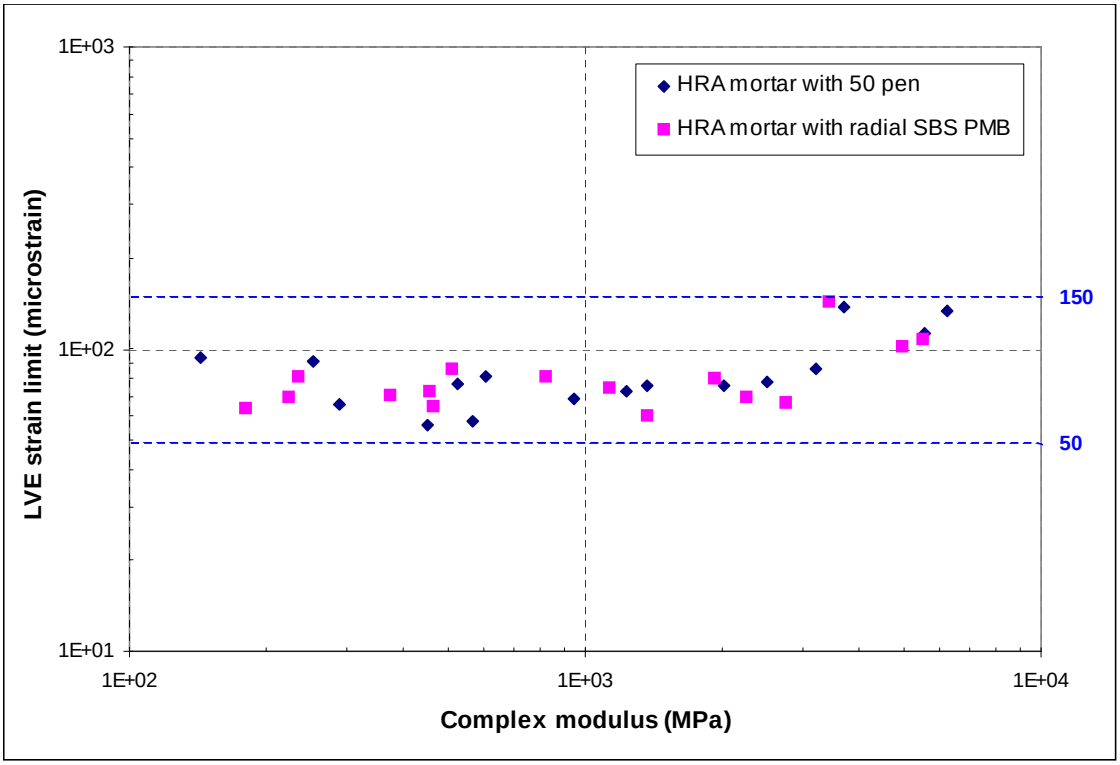

Figure 5.37: Linear viscoelastic range for different HRA mortar mixtures

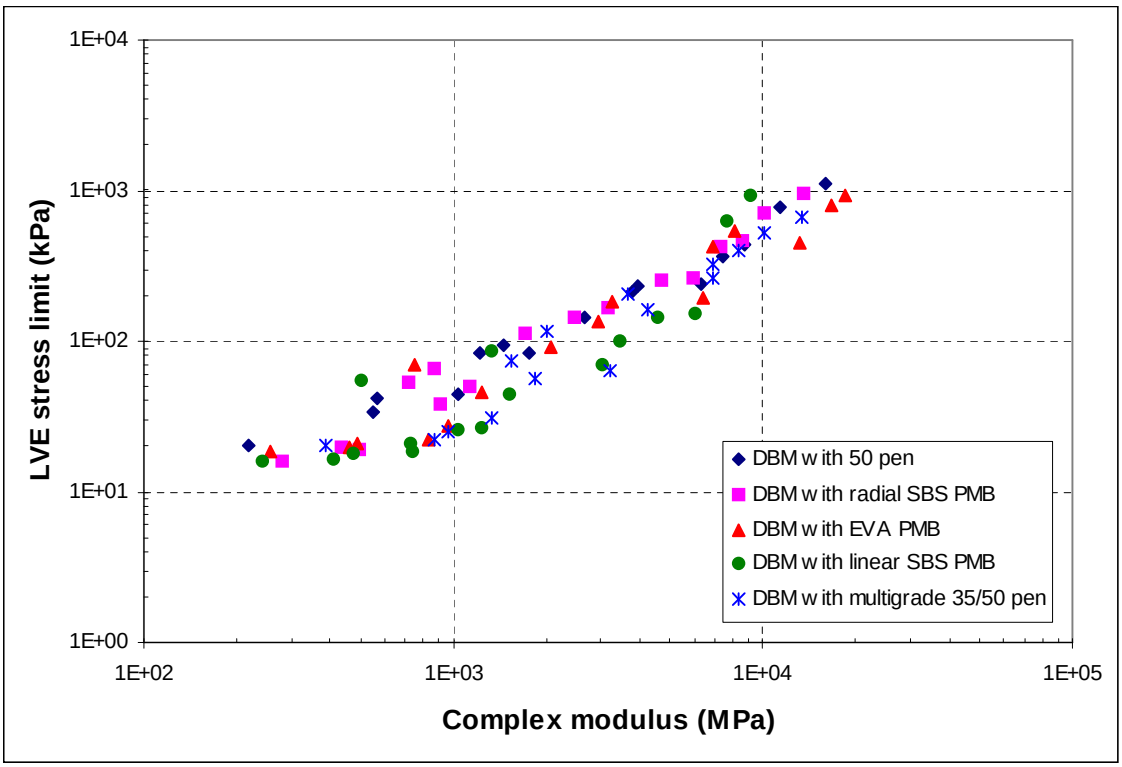

Figure 5.38: LVE stress limits for different DBM mixtures

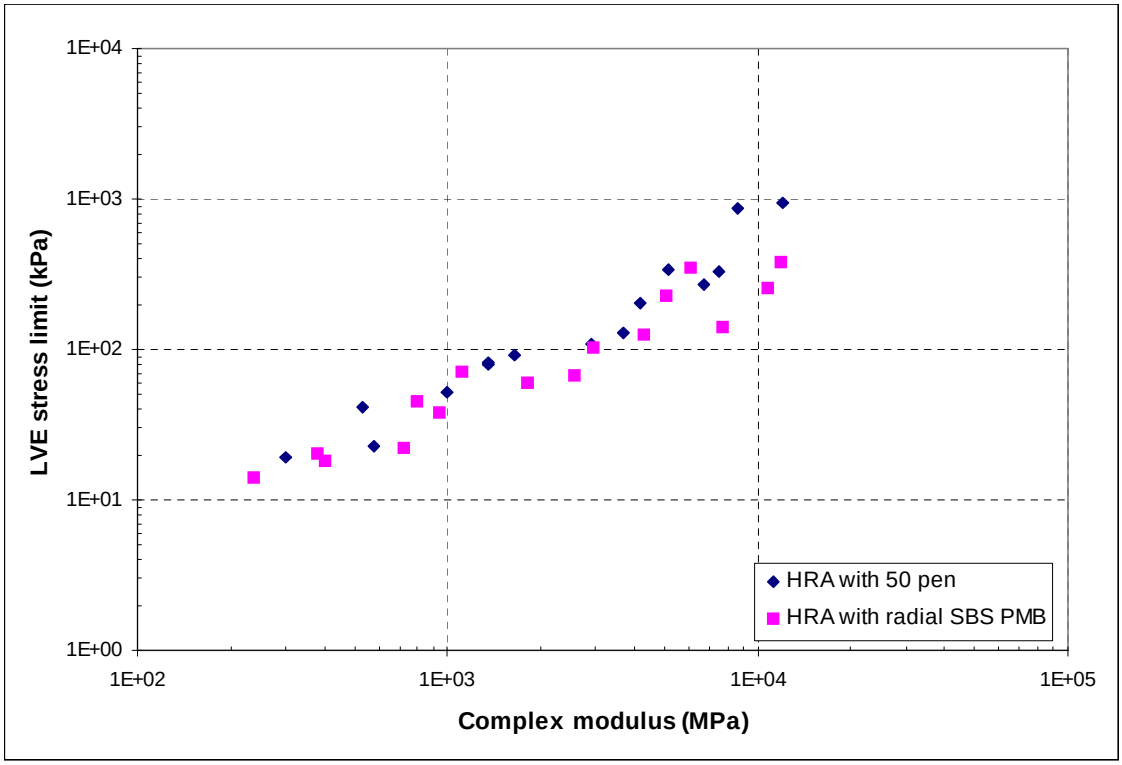

Figure 5.39: LVE stress limits for different HRA mixtures

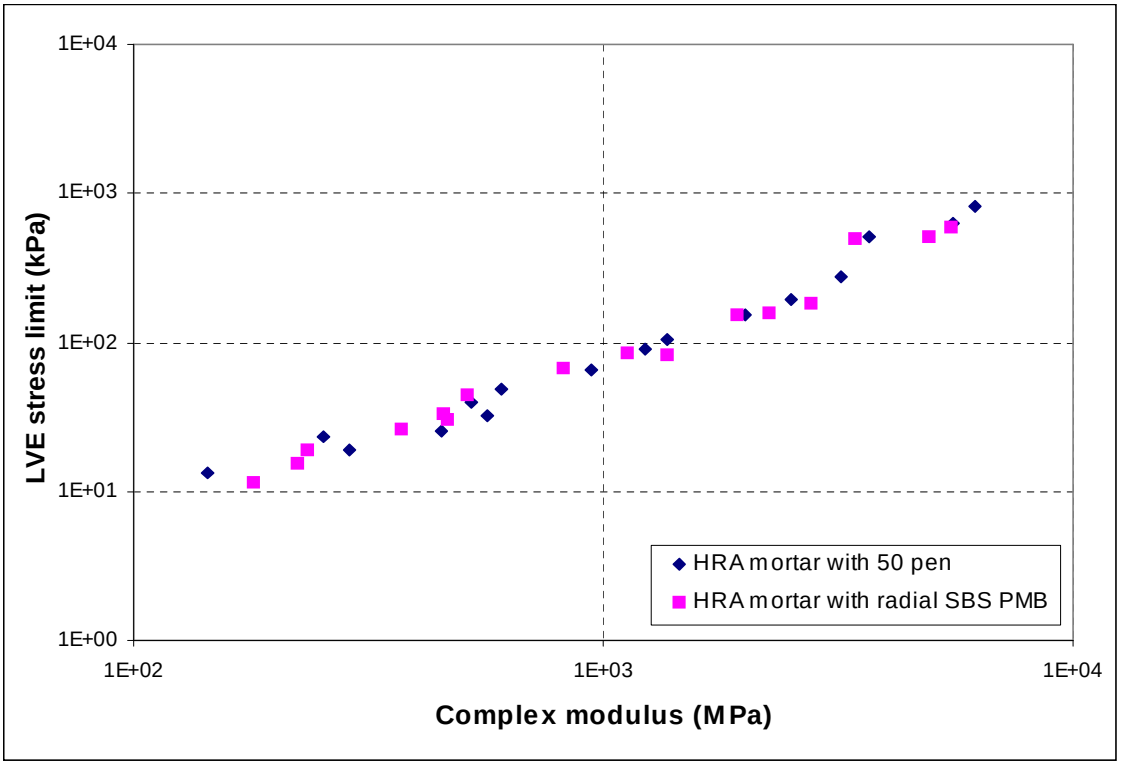

Figure 5.40: LVE stress limits for different HRA mortar mixtures

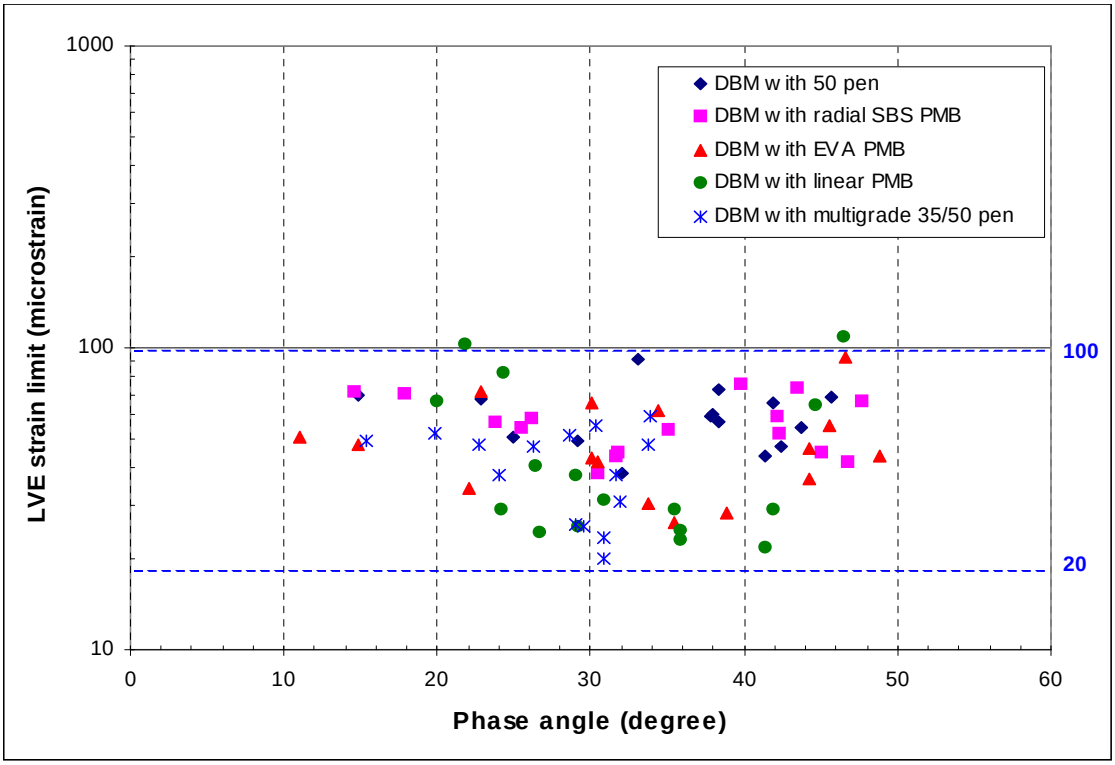

Figure 5.41: LVE strain limits for different DBM mixtures

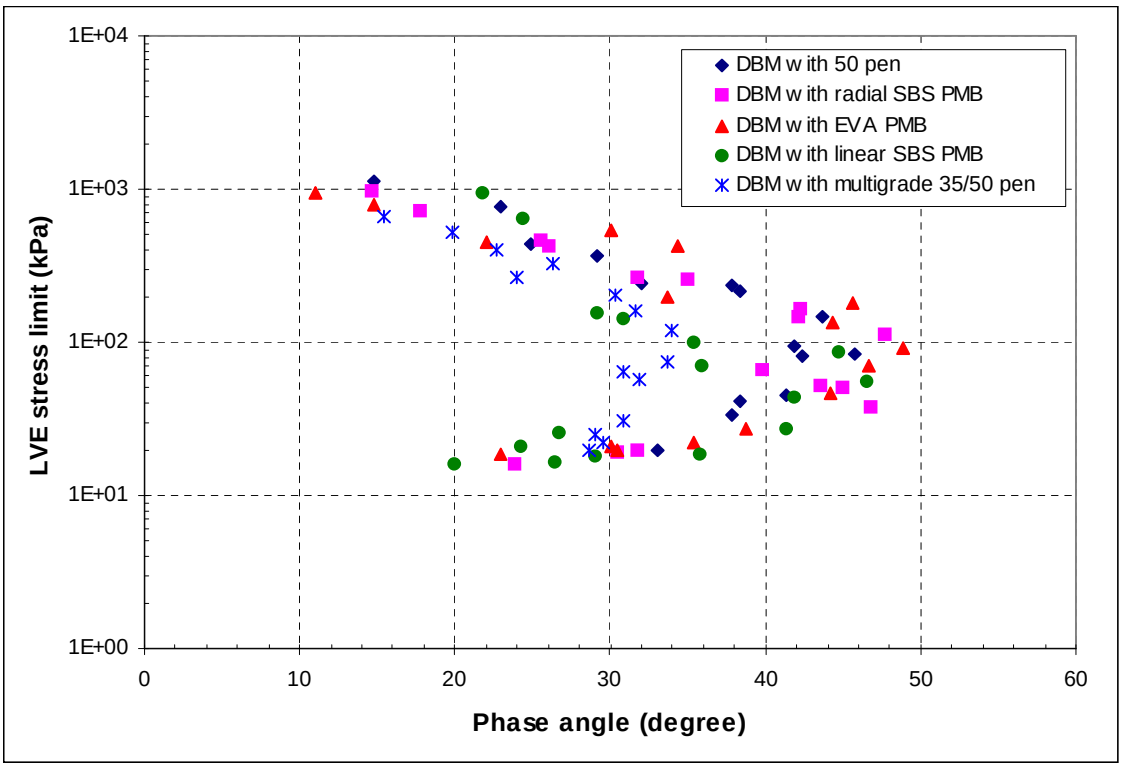

Figure 5.42: LVE stress limits for different DBM mixtures

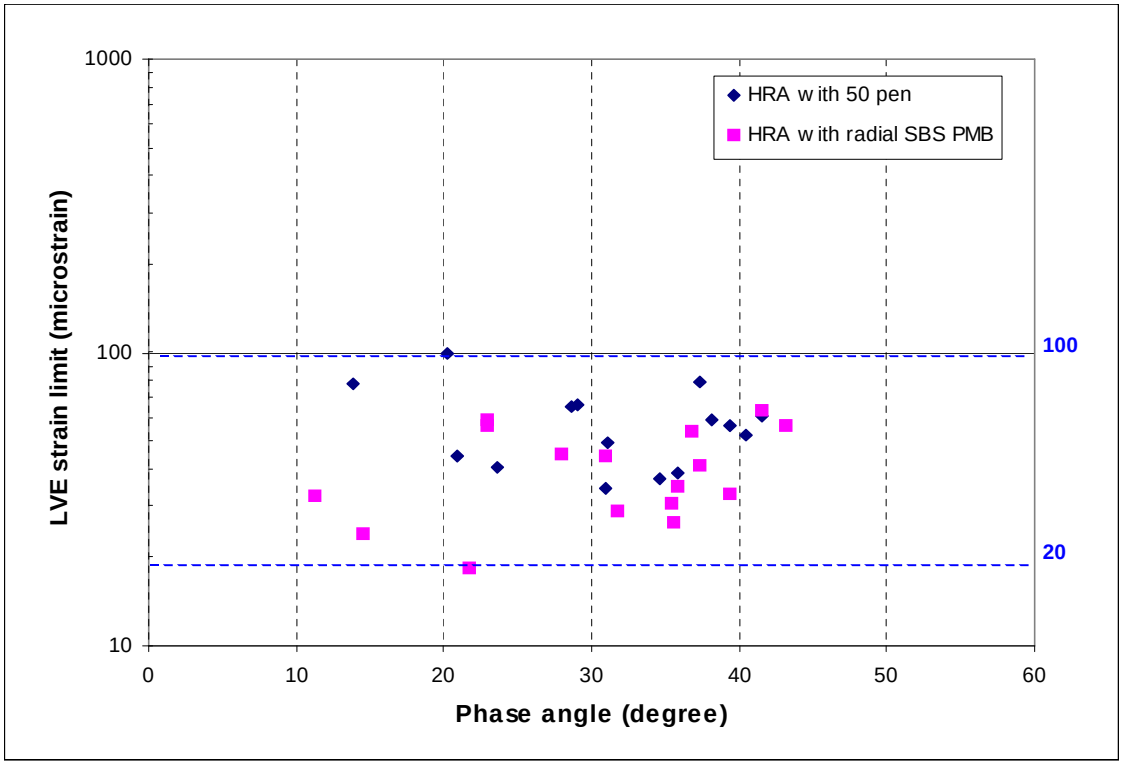

Figure 5.43: LVE strain limits for different HRA mixtures

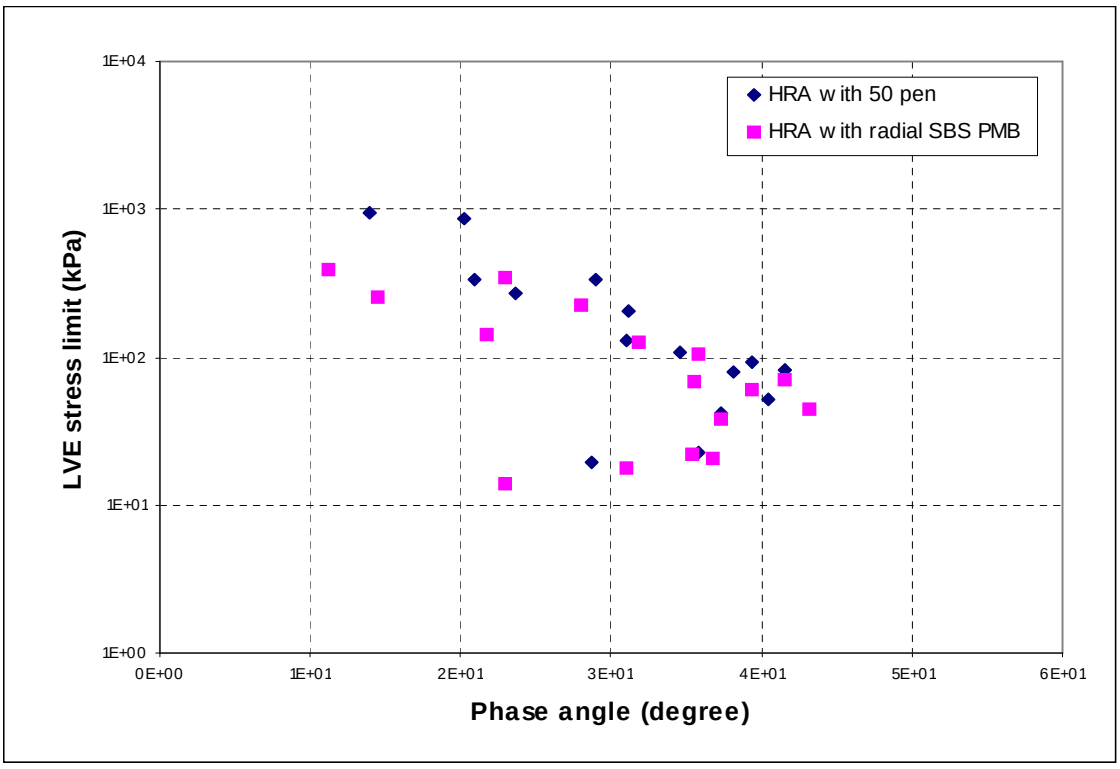

Figure 5.44: LVE stress limits for different HRA mixtures

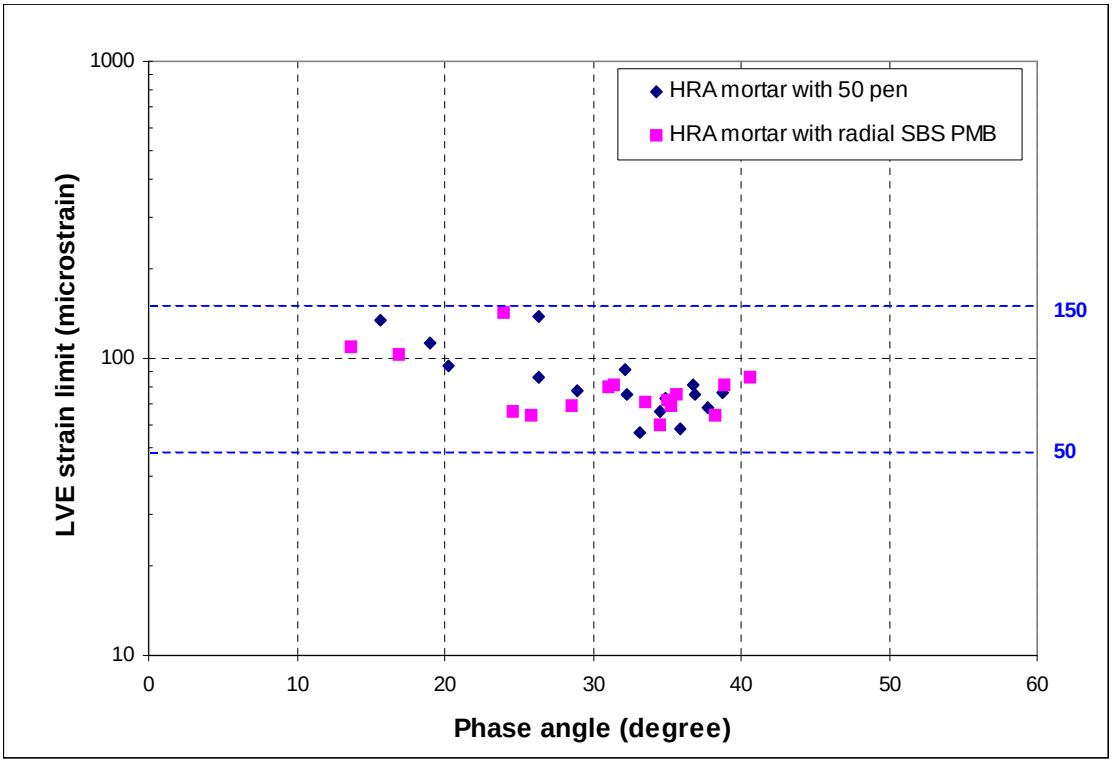

Figure 5.45: LVE strain limits for different HRA mortar mixtures

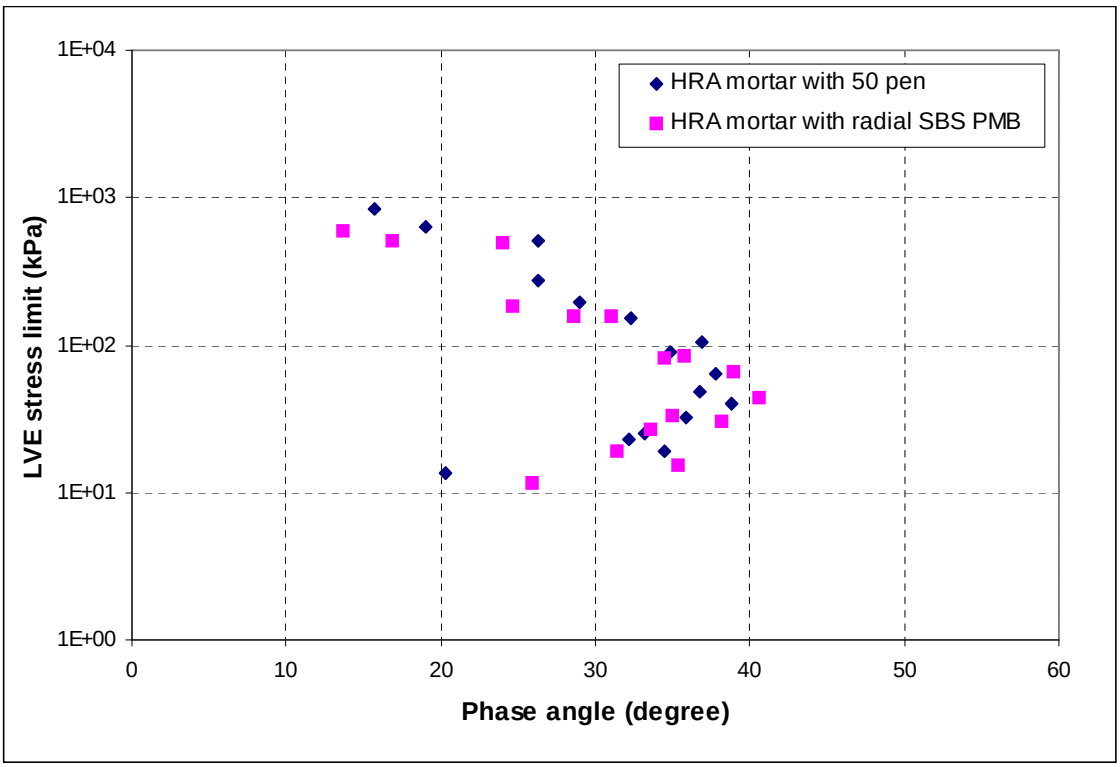

Figure 5.46: LVE stress limits for different HRA mortar mixtures

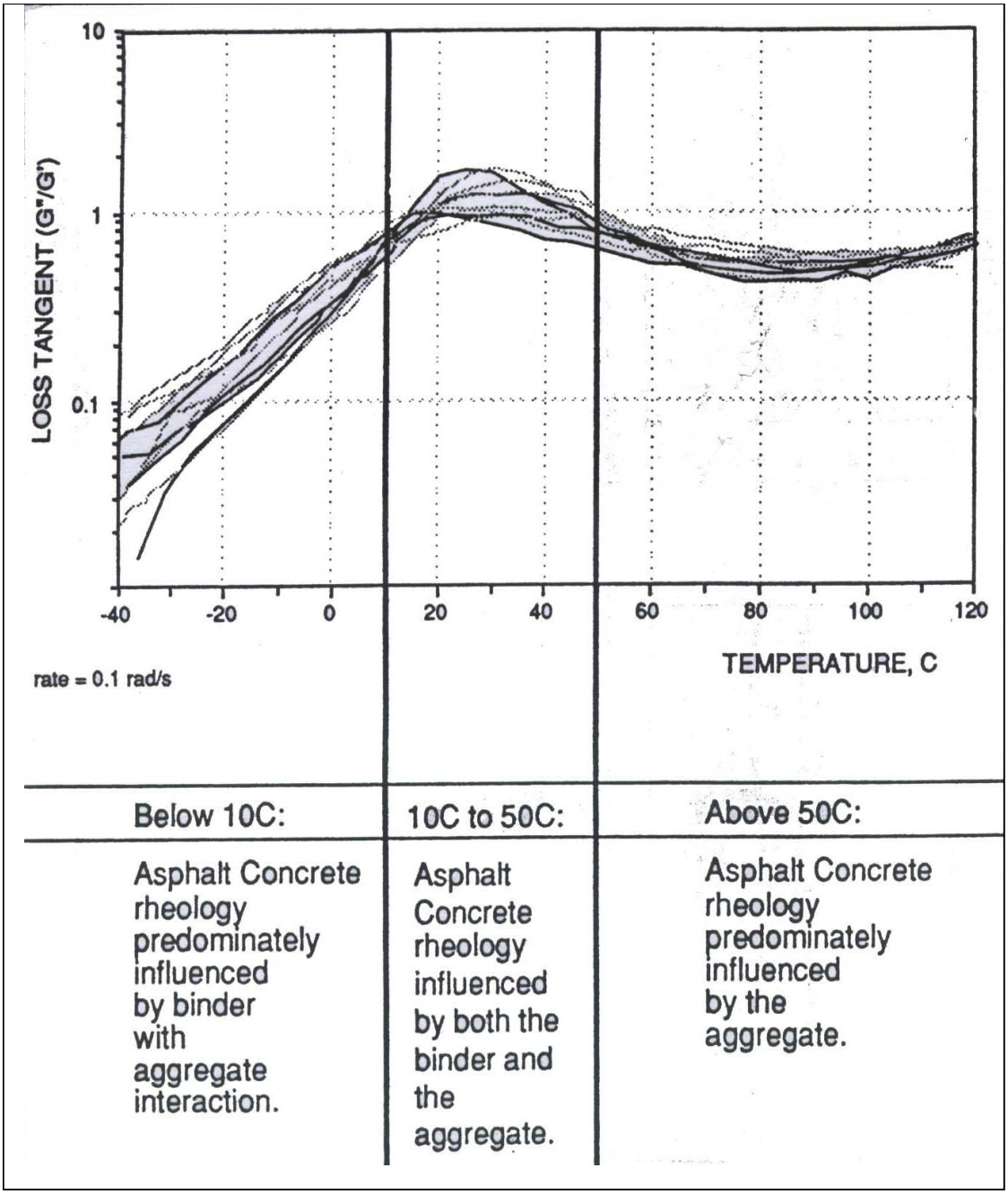

Figure 5.47: Loss tangent versus temperature for different asphalt mixtures [53]

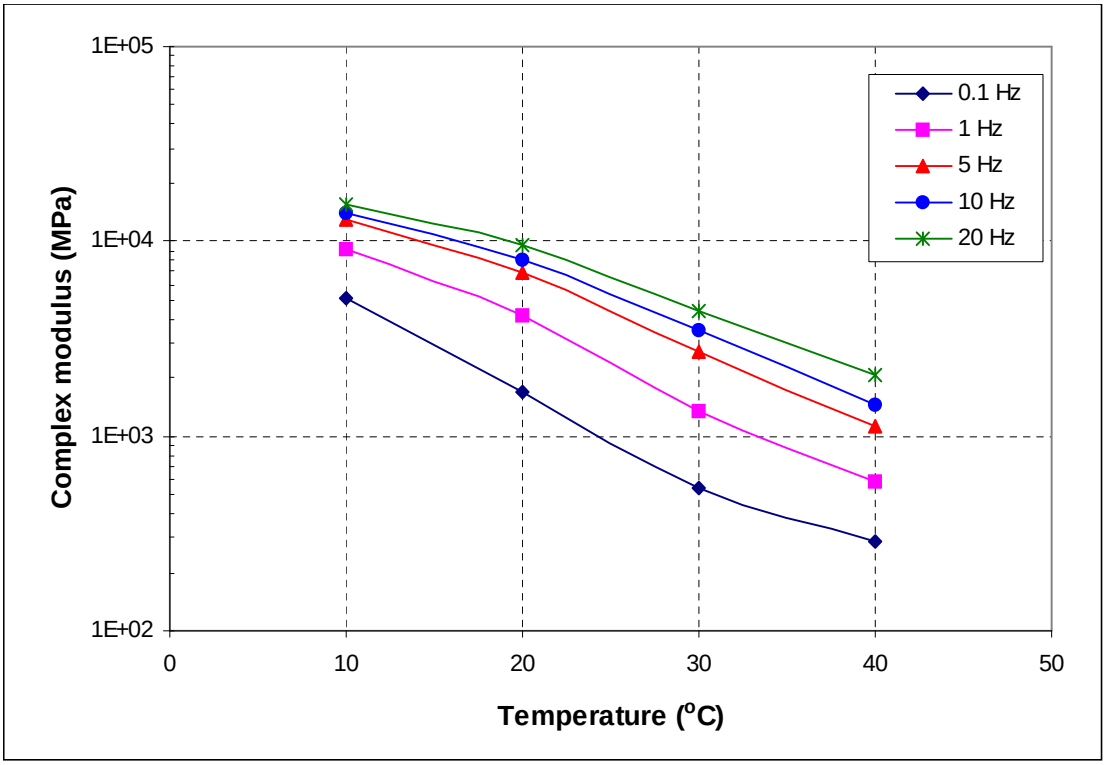

Figure 5.48: Isochronal plot of complex modulus for HRA mixture with 50 pen bitumen

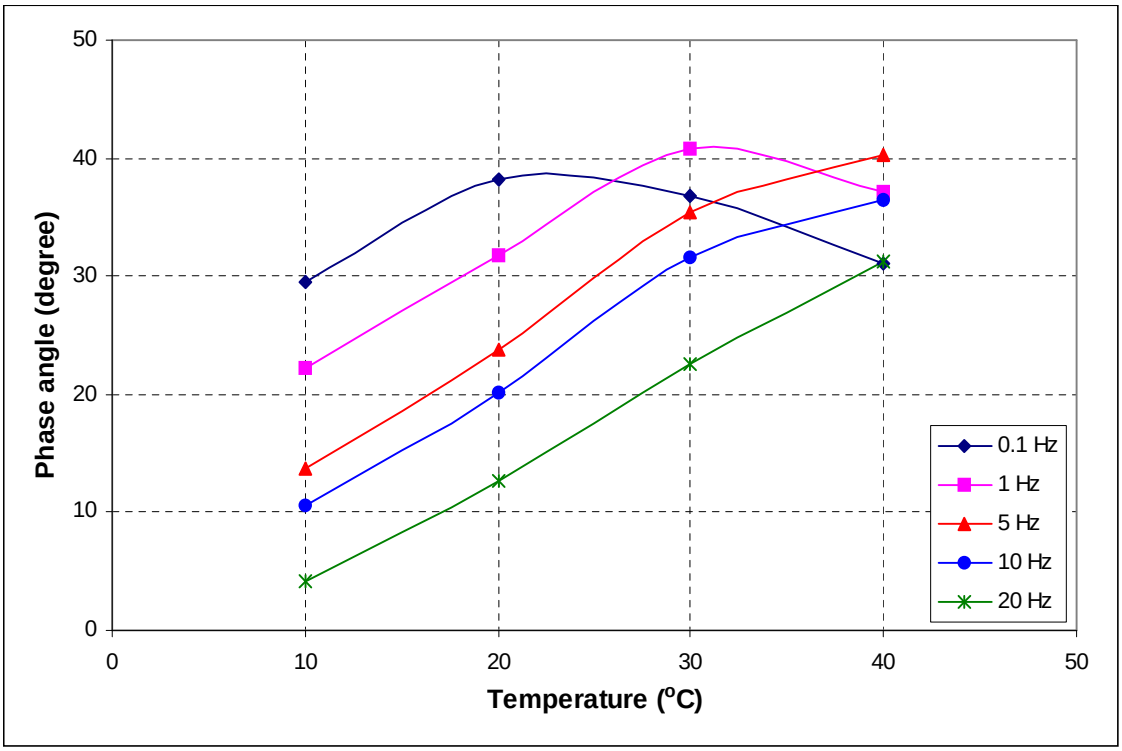

Figure 5.49: Isochronal plot of phase angle for HRA mixture with 50 pen bitumen

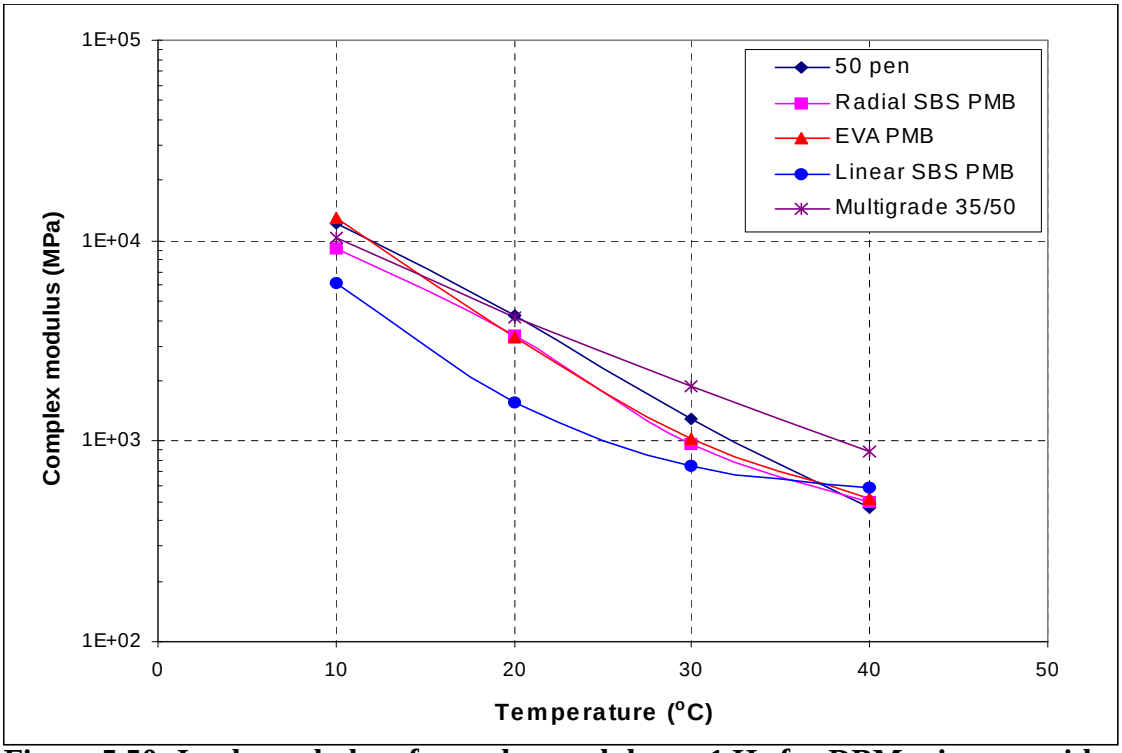

Figure 5.50: Isochronal plot of complex modulus at 1 Hz for DBM mixtures with different bitumens

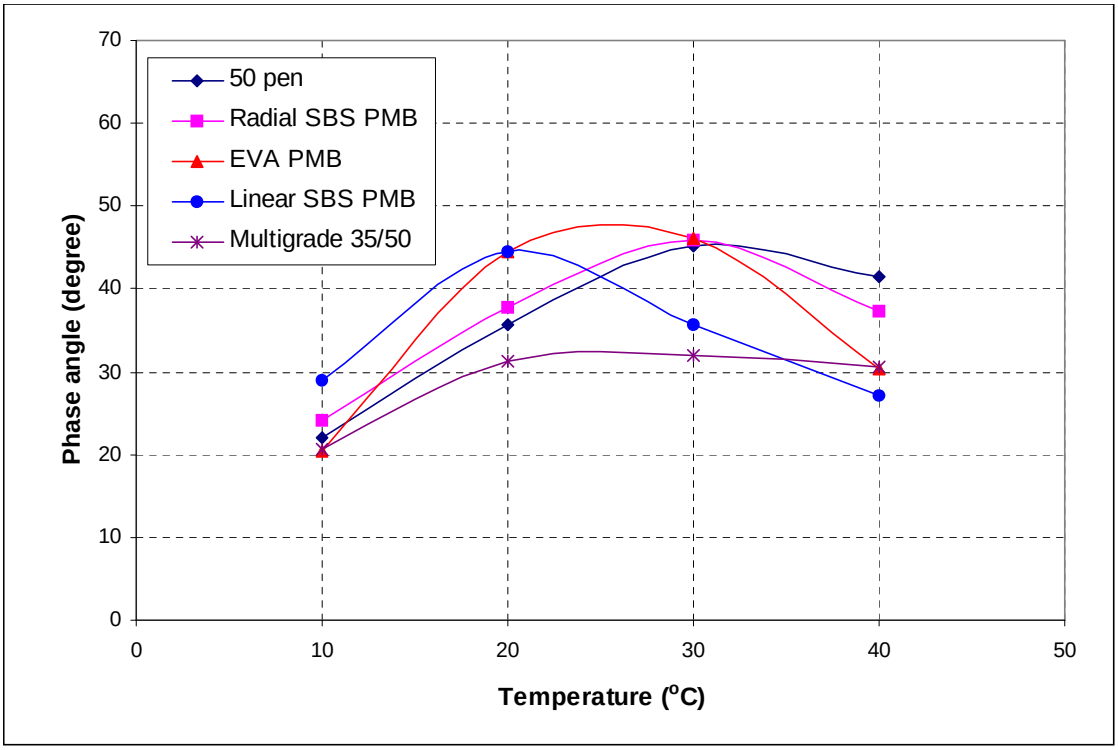

Figure 5.51: Isochronal plot of phase angle at 1 Hz for DBM mixtures with different bitumens

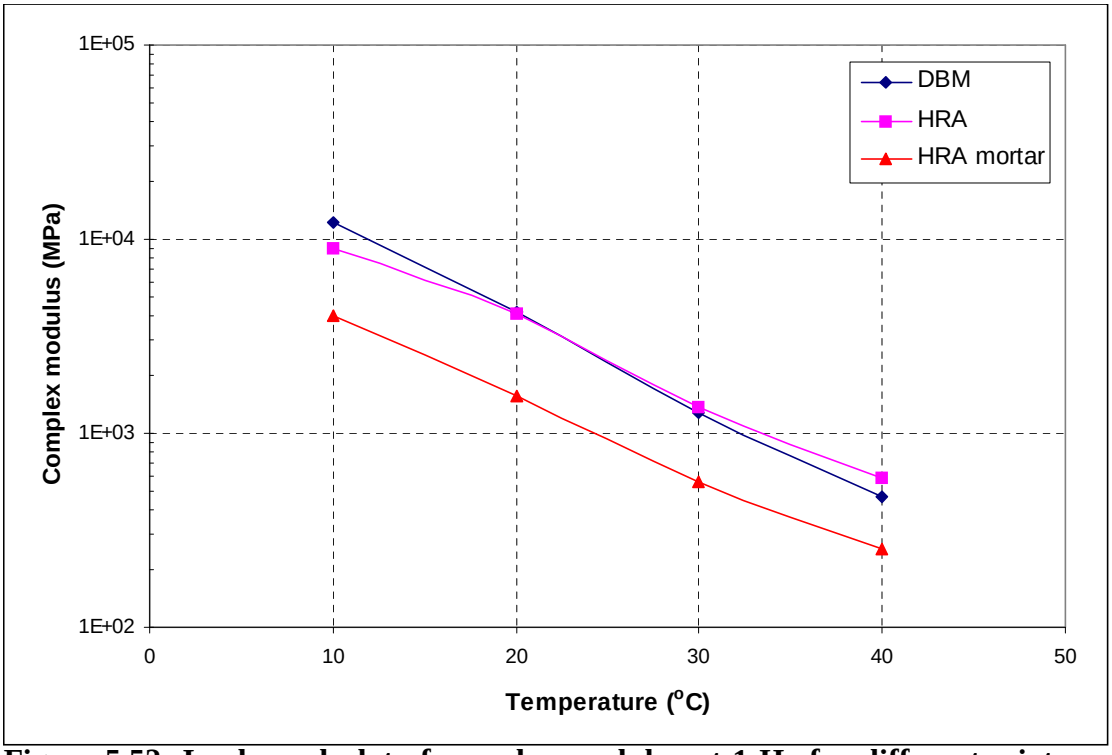

Figure 5.52: Isochronal plot of complex modulus at 1 Hz for different mixtures with 50 pen bitumen

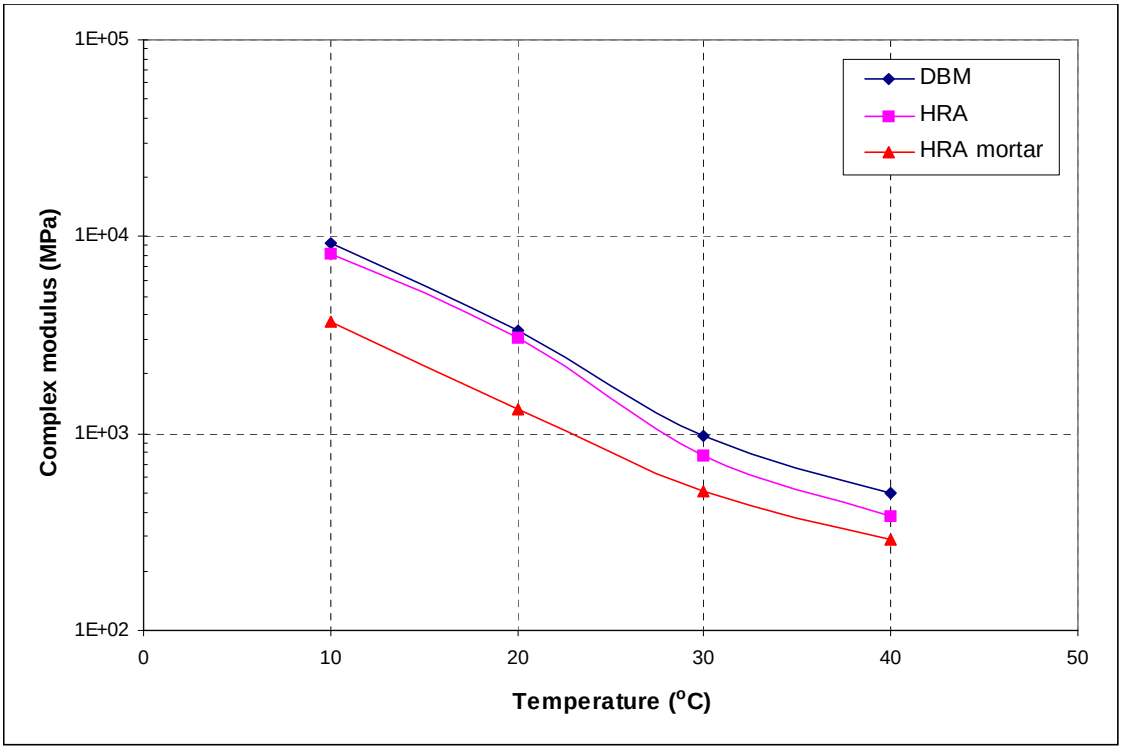

Figure 5.53: Isochronal plot of complex modulus at 1 Hz for different mixtures with radial SBS PMB

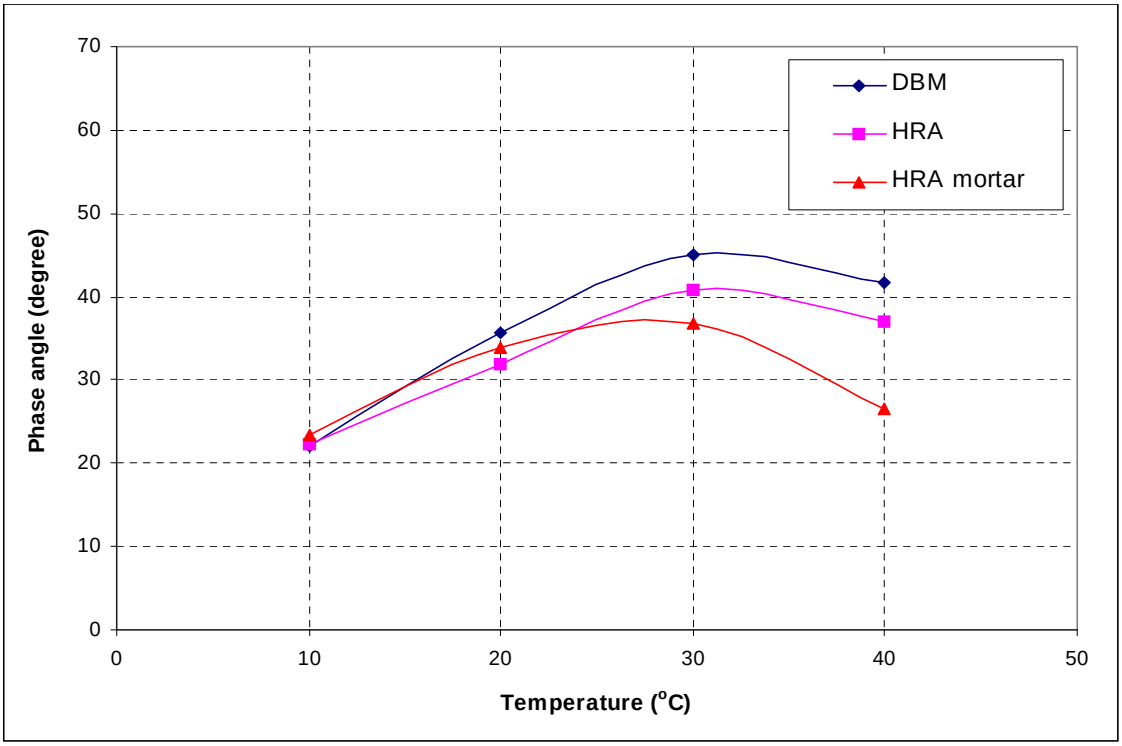

Figure 5.54: Isochronal plot of phase angle at 1 Hz for different mixtures with 50 pen bitumens

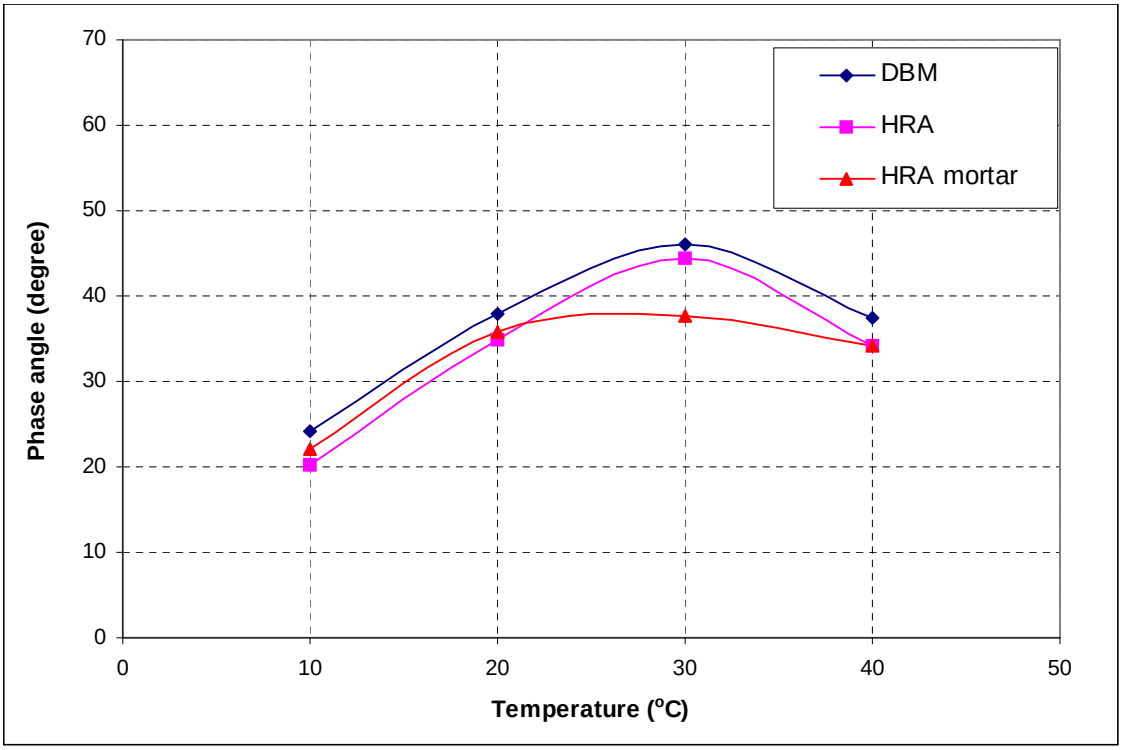

Figure 5.55: Isochronal plot of phase angle at 1 Hz for different mixtures with radial SBS PMB bitumens

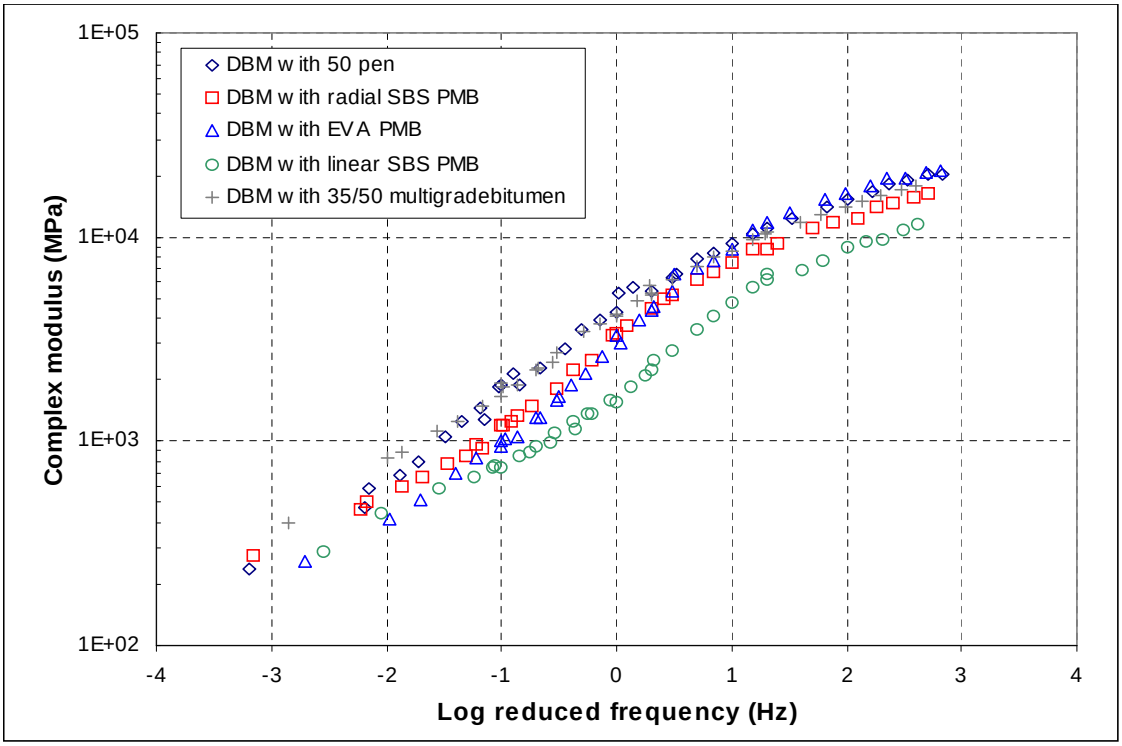

Figure 5.56: Master curves of complex modulus for DBM mixtures with different binders at a reference temperature 20˚C

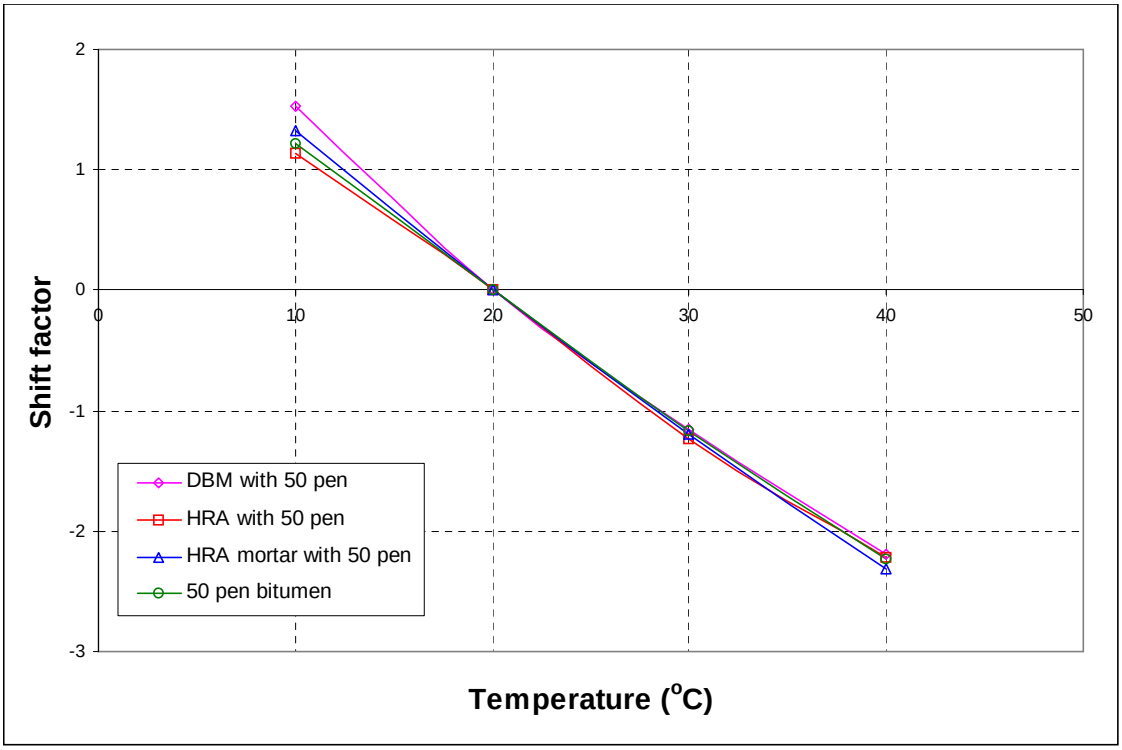

Figure 5.57: Shift factor versus temperature for pure 50 pen bitumen and mixtures with 50 pen bitumen

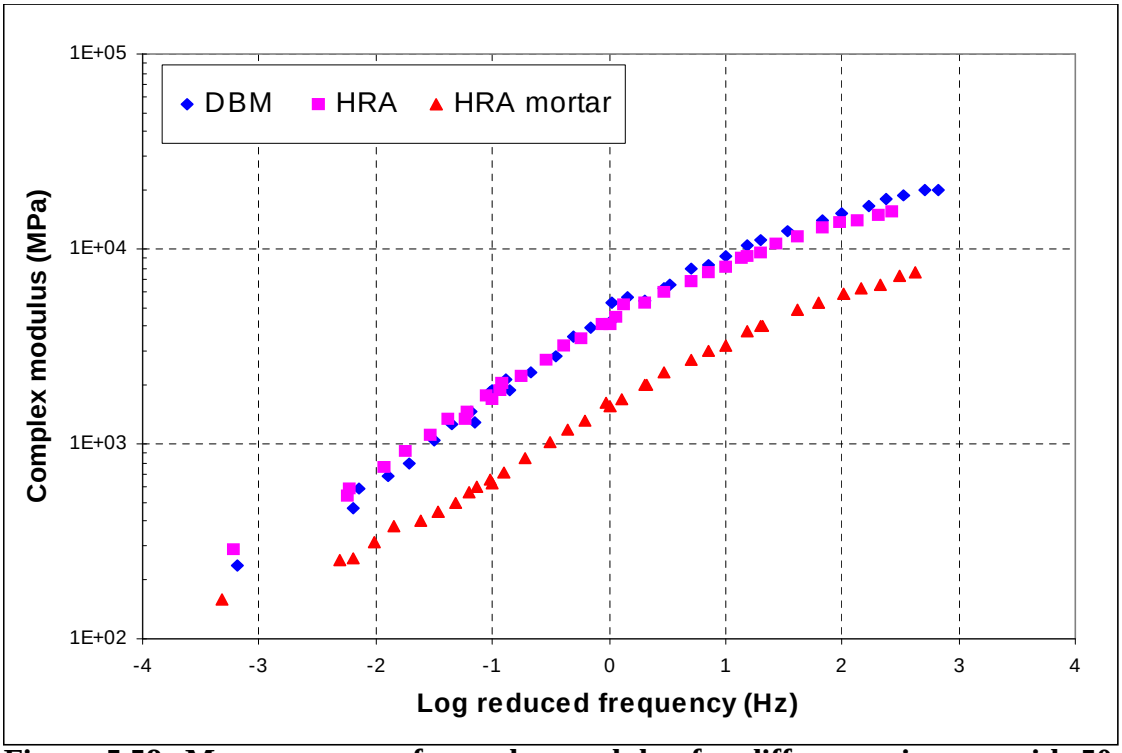

Figure 5.58: Master curves of complex modulus for different mixtures with 50 pen bitumens

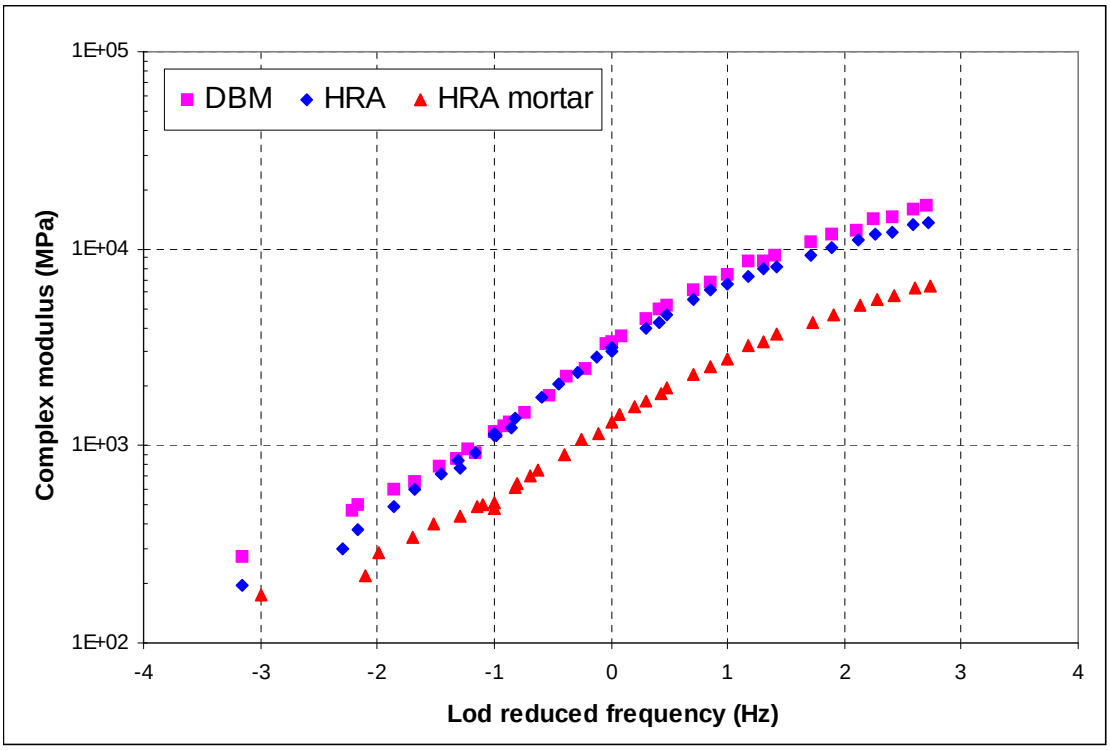

Figure 5.59: Master curves of complex modulus for different mixtures with radial SBS PMB

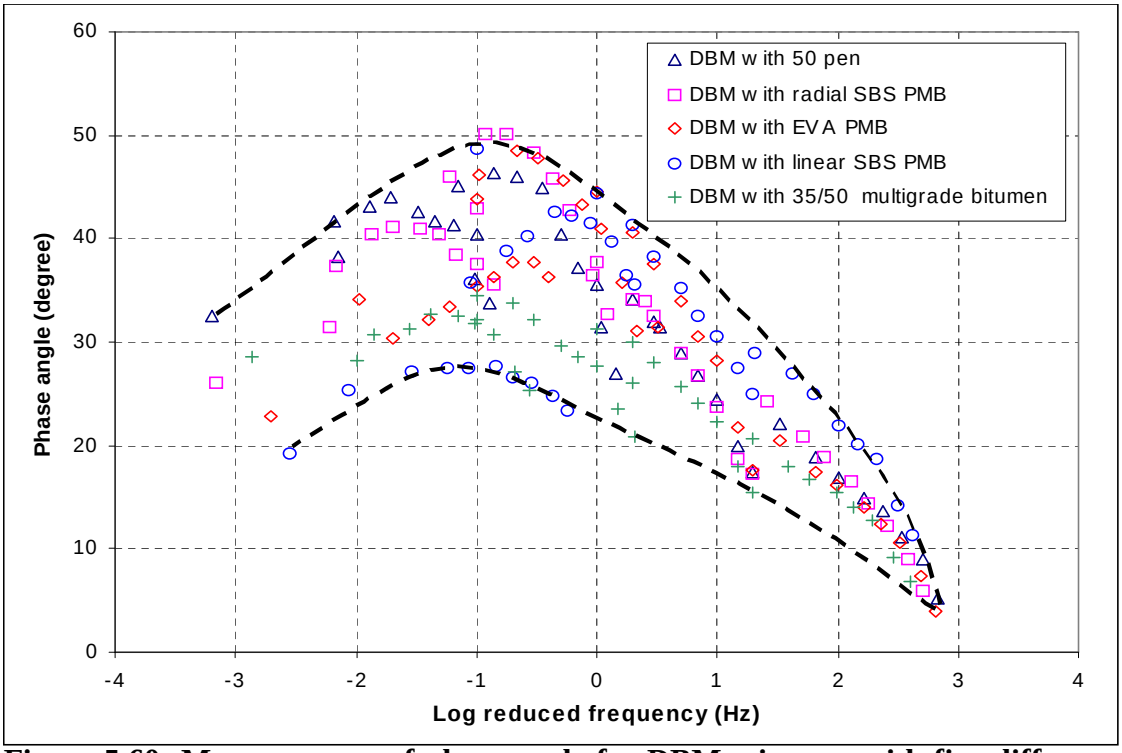

Figure 5.60: Master curves of phase angle for DBM mixtures with five different bitumens at a reference temperature of 20˚C

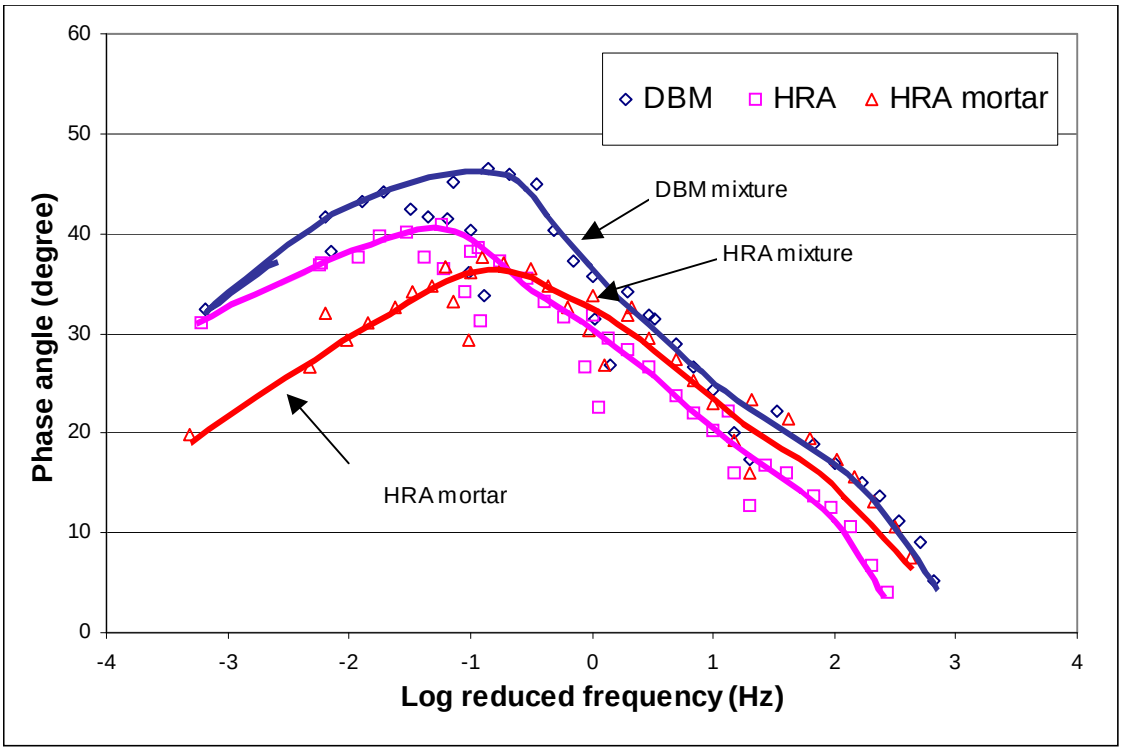

Figure 5.61: Master curves of phase angle for different mixtures with 50 pen bitumen

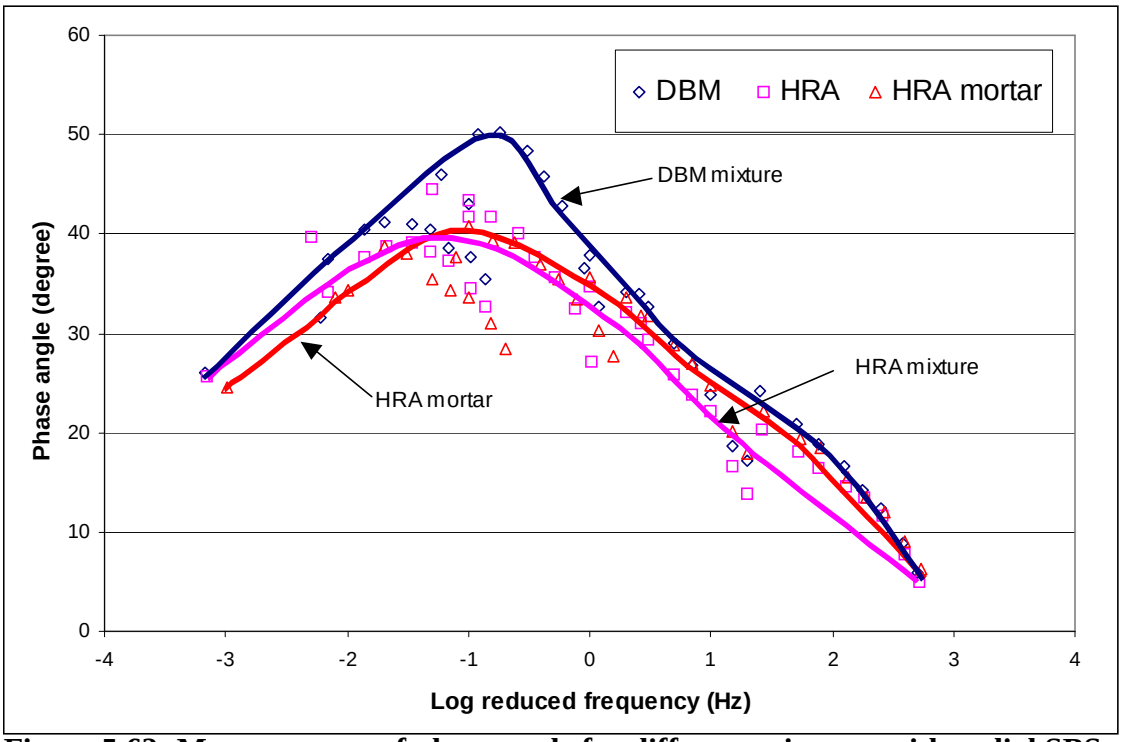

Figure 5.62: Master curves of phase angle for different mixtures with radial SBS PMB

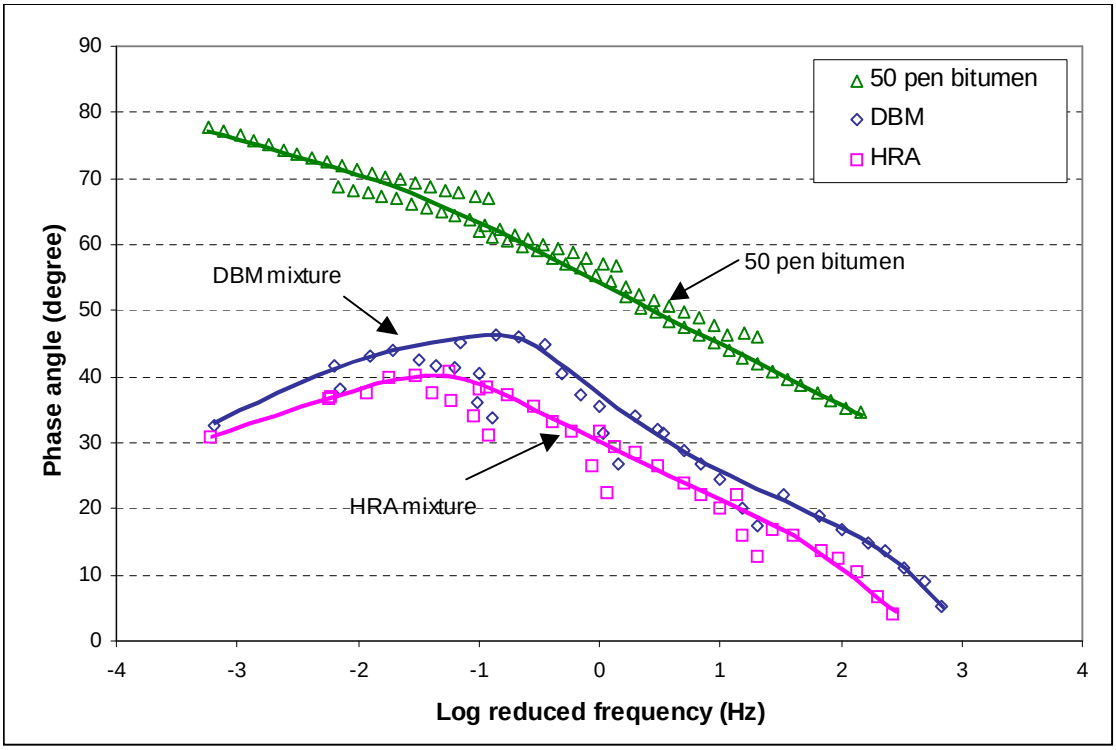

Figure 5.63: Master curves of phase angle for pure 50 pen bitumen and mixtures with 50 pen bitumen

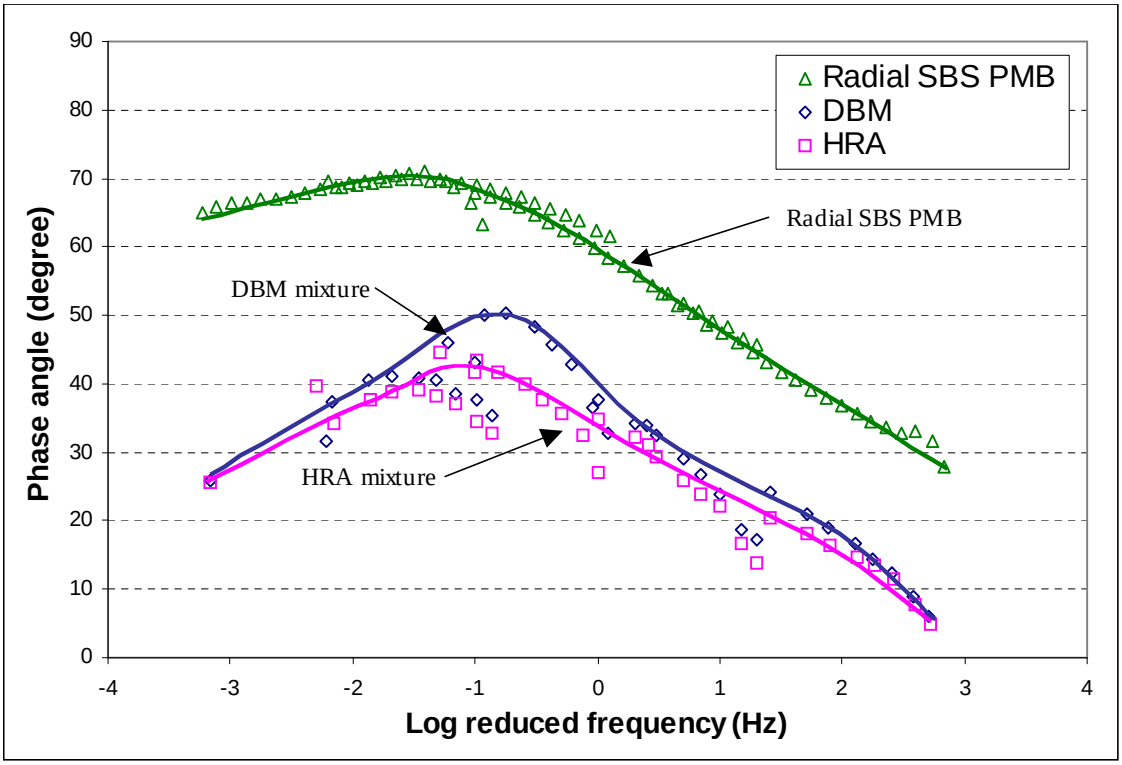

Figure 5.64 Master curves of phase angle for pure radial SBS PMB and mixtures with radial SBS PMB

Table 5.5: DBM mixture with 50 pen bitumen

Temperature (°C)	Frequency (Hz)	LVE limit of strain (με)	LVE limit of Stress (kPa)	LVE limit of Stiffness (MPa)
10	0.1	38.5	2.42E+02	6.27E+03
	1	67.5	7.71E+02	1.14E+04
	5	70.0	1.11E+03	1.59E+04
	10	—	—	—
20	0.1	47.0	8.25E+01	1.76E+03
	1	59.0	2.33E+02	3.95E+03
	5	49.0	3.62E+02	7.39E+03
	10	50.5	4.41E+02	8.72E+03
30	0.1	73.0	4.15E+01	5.68E+02
	1	69.0	8.40E+01	1.22E+03
	5	54.5	1.46E+02	2.67E+03
	10	56.5	2.14E+02	3.79E+03
40	0.1	92.0	2.00E+01	2.17E+02
	1	60.5	3.35E+01	5.54E+02
	5	43.5	4.50E+01	1.03E+03
	10	65.5	9.50E+01	1.45E+03

Table 5.6: DBM mixture with radial SBS PMB

Temperature (°C)	Frequency (Hz)	LVE limit of strain (με)	LVE limit of Stress (kPa)	LVE limit of Stiffness (MPa)
10	0.1	54	2.55E+02	4.72E+03
	1	54.5	4.71E+02	8.63E+03
	5	70.5	7.17E+02	1.02E+04
	10	71.5	9.64E+02	1.35E+04
20	0.1	45	5.05E+01	1.12E+03
	1	52	1.65E+02	3.17E+03
	5	44	2.63E+02	5.98E+03
	10	58.5	4.28E+02	7.32E+03
30	0.1	45	1.95E+01	4.33E+02
	1	42	3.80E+01	9.05E+02
	5	66.5	1.13E+02	1.70E+03
	10	59	1.46E+02	2.47E+03
40	0.1	57	1.60E+01	2.81E+02
	1	38.5	1.90E+01	4.94E+02
	5	73.5	5.25E+01	7.14E+02
	10	76	6.55E+01	8.62E+02

Table 5.7: DBM mixture with EVA PMB

Temperature (°C)	Frequency (Hz)	LVE limit of strain (με)	LVE limit of Stress (kPa)	LVE limit of Stiffness (MPa)
10	0.1	30.5	1.96E+02	6.43E+03
	1	34	4.48E+02	1.32E+04
	5	47.5	7.87E+02	1.66E+04
	10	50.5	9.30E+02	1.84E+04
20	0.1	37	4.60E+01	1.24E+03
	1	55.5	1.82E+02	3.28E+03
	5	62	4.27E+02	6.88E+03
	10	66	5.32E+02	8.06E+03
30	0.1	43	2.10E+01	4.88E+02
	1	93	6.95E+01	7.47E+02
	5	44	9.15E+01	2.08E+03
	10	46.5	1.36E+02	2.92E+03
40	0.1	72	1.85E+01	2.57E+02
	1	42	1.95E+01	4.64E+02
	5	26.5	2.20E+01	8.30E+02
	10	28.5	2.75E+01	9.65E+02

Table 5.8: DBM mixture with linear SBS PMB

Temperature (°C)	Frequency (Hz)	LVE limit of strain (με)	LVE limit of Stress (kPa)	LVE limit of Stiffness (MPa)
10	0.1	23	6.95E+01	3.02E+03
	1	25.5	1.54E+02	6.02E+03
	5	82.5	6.34E+02	7.68E+03
	10	103	9.41E+02	9.14E+03
20	0.1	109	5.50E+01	5.05E+02
	1	65	8.60E+01	1.32E+03
	5	29	1.01E+02	3.47E+03
	10	31.5	1.44E+02	4.57E+03
30	0.1	40.5	1.65E+01	4.07E+02
	1	25	1.85E+01	7.40E+02
	5	22	2.70E+01	1.23E+03
	10	29	4.40E+01	1.52E+03
40	0.1	66.5	1.60E+01	2.41E+02
	1	38	1.80E+01	4.74E+02
	5	29	2.10E+01	7.24E+02
	10	24.5	2.55E+01	1.04E+03

Table 5.9: DBM mixture with multigrade 35/50 bitumen

Temperature (°C)	Frequency (Hz)	LVE limit of strain (με)	LVE limit of Stress (kPa)	LVE limit of Stiffness (MPa)
10	0.1	38	2.62E+02	6.88E+03
	1	52	5.27E+02	1.01E+04
	5	49.5	6.65E+02	1.34E+04
	10	—	—	—
20	0.1	59	1.18E+02	2.00E+03
	1	38	1.61E+02	4.22E+03
	5	47	3.25E+02	6.91E+03
	10	47.5	3.97E+02	8.36E+03
30	0.1	25.5	2.20E+01	8.63E+02
	1	31	5.65E+01	1.82E+03
	5	20	6.45E+01	3.23E+03
	10	55.5	2.04E+02	3.68E+03
40	0.1	51.5	2.00E+01	3.88E+02
	1	26	2.50E+01	9.62E+02
	5	23.5	3.10E+01	1.32E+03
	10	48	7.40E+01	1.54E+03

Table 5.10: HRA mixture with 50 pen bitumen

Temperature (°C)	Frequency (Hz)	LVE limit of strain (με)	LVE limit of Stress (kPa)	LVE limit of Stiffness (MPa)
10	0.1	66	3.39E+02	5.14E+03
	1	99.5	8.58E+02	8.62E+03
	5	78	9.36E+02	1.20E+04
	10	—	—	—
20	0.1	56.5	9.25E+01	1.64E+03
	1	49	2.04E+02	4.16E+03
	5	40.5	2.74E+02	6.75E+03
	10	44.5	3.32E+02	7.45E+03
30	0.1	79.5	4.20E+01	5.28E+02
	1	61	8.20E+01	1.34E+03
	5	37	1.08E+02	2.91E+03
	10	34.5	1.28E+02	3.71E+03
40	0.1	65	1.95E+01	3.00E+02
	1	39	2.25E+01	5.77E+02
	5	52	5.15E+01	9.90E+02
	10	58.5	7.90E+01	1.35E+03

Table 5.11: HRA mixture with radial SBS PMB

Temperature (°C)	Frequency (Hz)	LVE limit of strain (με)	LVE limit of Stress (kPa)	LVE limit of Stiffness (MPa)
10	0.1	29	1.24E+02	4.28E+03
	1	18.5	1.42E+02	7.68E+03
	5	24	2.58E+02	1.07E+04
	10	32.5	3.86E+02	1.19E+04
20	0.1	63.5	7.05E+01	1.11E+03
	1	35	1.04E+02	2.96E+03
	5	45	2.28E+02	5.06E+03
	10	56.5	3.46E+02	6.12E+03
30	0.1	54	2.05E+01	3.80E+02
	1	56	4.45E+01	7.95E+02
	5	33	6.00E+01	1.82E+03
	10	26.5	6.80E+01	2.57E+03
40	0.1	59	1.40E+01	2.37E+02
	1	44.5	1.80E+01	4.04E+02
	5	30.5	2.20E+01	7.21E+02
	10	41	3.85E+01	9.39E+02

Table 5.12: HRA mortar with 50 pen bitumen

Temperature (°C)	Frequency (Hz)	LVE limit of strain (με)	LVE limit of Stress (kPa)	LVE limit of Stiffness (MPa)
10	0.1	75.5	1.52E+02	2.01E+03
	1	138	5.09E+02	3.68E+03
	5	113	6.27E+02	5.55E+03
	10	133.5	8.28E+02	6.20E+03
20	0.1	81	4.90E+01	6.05E+02
	1	76	1.04E+02	1.36E+03
	5	77.5	1.95E+02	2.51E+03
	10	86	2.76E+02	3.21E+03
30	0.1	91	2.30E+01	2.53E+02
	1	76.5	4.00E+01	5.23E+02
	5	68.5	6.45E+01	9.42E+02
	10	73	8.95E+01	1.23E+03
40	0.1	94	1.35E+01	1.44E+02
	1	66	1.90E+01	2.88E+02
	5	56.5	2.55E+01	4.51E+02
	10	57.5	3.25E+01	5.65E+02

Table 5.13: HRA mortar with radial SBS PMB

Temperature (°C)	Frequency (Hz)	LVE limit of strain (με)	LVE limit of Stress (kPa)	LVE limit of Stiffness (MPa)
10	0.1	80.5	1.55E+02	1.92E+03
	1	143	4.91E+02	3.43E+03
	5	102.5	5.06E+02	4.94E+03
	10	108.5	5.97E+02	5.50E+03
20	0.1	86	4.40E+01	5.12E+02
	1	60	8.20E+01	1.37E+03
	5	69.5	1.58E+02	2.27E+03
	10	66.5	1.84E+02	2.77E+03
30	0.1	69.5	1.55E+01	2.23E+02
	1	64.5	3.00E+01	4.65E+02
	5	81	6.65E+01	8.21E+02
	10	75	8.45E+01	1.13E+03
40	0.1	64	1.15E+01	1.80E+02
	1	81	1.90E+01	2.35E+02
	5	71	2.65E+01	3.73E+02
	10	72.5	3.30E+01	4.55E+02

Chapter 6

RELATIONSHIP BETWEEN BITUMEN AND ASPHALT MIXTURE RHEOLOGY

6.1 Introduction

In general, the stiffness of an asphalt mixture is primarily controlled through the rheological properties (stiffness) of the binder. Even though other factors such as voids in the mineral aggregate (VMA), bitumen content, aggregate gradation and aggregate properties have an effect on mixture stiffness, the binder stiffness is usually the dominating factor.

As discussed in Chapter Two, the minimum value of binder stiffness for elastic behaviour is 5 MPa [30]. Above this value, the mixture stiffness only depends on binder stiffness and volumetric proportions. However, when the stiffness of the bitumen is less than 5 MPa, in addition to binder stiffness and the volume of aggregate and bitumen, parameters related to the properties of the aggregate, such as the aggregate grading, shape, texture and degree of interlock, and the method and degree of compaction, become significant as the binder influence decreases [110] (Figure 6.1). Temperature is also an important factor, which affects the relationship between binder and mixture stiffness. Goodrich [53] conducted a fundamental study on the relationship between asphalt mixture and binder rheology and concluded that asphalt mixture rheology is influence by the binder at low temperatures, by both the binder and the aggregate at intermediate temperatures and by the aggregate at high temperatures.

The objective of this chapter is to illustrate the relationship between binder and mixture stiffness, measured in the linear viscoelastic region, for different unmodified and modified binders and asphalt mixtures and discuss the factors that influence this relationship.

6.2 Experimental Methods and Materials

The results of the binder and mixture tests, presented in Chapters Four and Five, were used to study the relationship between binder and mixture stiffness. As it is necessary to study both the binders and asphalt mixtures in the same domain to establish correlations between bitumen and asphalt mixture rheology, the tests were performed in the linear region. Also as oxidative ageing and loss of volatiles occur during asphalt mixture production, it was decided to test all bitumens after subjecting them to short term ageing conditions (RTFOT). The rheological properties of five unmodified and modified bitumens and five DBM, two HRA and two HRA mortar mixtures were determined under the following test conditions:

- Temperatures 10, 20, 30 and 40ºC
- Frequencies 0.1 to 20 Hz

The method used in this investigation was similar to a system developed during the SHRP program [90] to relate binder and mixture stiffnesses at low temperatures. In this method, the log of complex modulus of a mixture was plotted against the log of complex modulus of the corresponding binder, at the frequencies and temperatures mentioned above. A best-fit straight line, described by a power model on a log-log plot was used to form a relationship between the measured binder and mixture stiffnesses.

6.3 Linear Viscoelastic Rheological Relationship between Binders and Asphalt Mixtures

6.3.1 Complex Modulus

The purpose of this section is to illustrate the relationship, which exists between bitumen and asphalt mixture stiffness, and to discuss the factors, which influence this relationship. Figures 6.2 to 6.10 present the plots of asphalt mixture complex modulus versus bitumen complex modulus for all the DBM, HRA and HRA mortar mixtures. It can be seen from these graphs that in general the bitumen to mixture complex modulus relationship is independent of temperature. In other words, for a given bitumen stiffness, there is a unique corresponding mixture stiffness. It can be seen

from Figures 6.2 to 6.10 that the best-fit straight line can be expressed in the form of a first order polynomial (straight line in log-log scale).

Although a straight line relationship can be assigned to the EVA PMB and linear SBS PMB binders (Figures 6.4 and 6.5), Figures 6.11 and 6.12 show that the binder to mixture stiffness relationship exhibits temperature dependence. In other words, for a given binder stiffness, there is not a unique corresponding mixture stiffness value. This may be due to an interaction between the filler or aggregate skeleton of the asphalt mixture and these two polymer modified binders, which causes the mixtures to have greater resistance to deformation (increased stiffness) with increasing temperature. However, more research needs to be done to investigate the effect of polymer modified binders on the temperature dependency of asphalt mixtures. This increased stiffness at high temperatures for the DBM mixtures with EVA PMB and linear SBS PMB compared to the other DBM mixtures can also be seen in Figures 6.13 and 6.14.

The binder to mixture stiffness relationship for the DBM, HRA and HRA mortar mixtures with 50 pen bitumen are compared in Figure 6.15. The results clearly show that the complex modulus values for the HRA mortar are approximately 50% less than those found for the DBM and HRA mixtures. This is due to the lower aggregate volume, higher binder volume and higher air voids content of the mortar compared to the DBM and HRA asphalt mixtures. It can also be seen from this figure that the HRA mixture shows slightly lower stiffness at high binder stiffnesses (corresponding to low temperatures) and slightly higher stiffness at low binder stiffnesses (corresponding to high temperatures) than the DBM mixture. Figure 6.16 presents a comparison of the binder to mixture stiffness relationship for the two HRA mixtures with 50 pen bitumen and radial SBS PMB. It can be seen in the figure that both mixtures show a very similar binder to mixture stiffness relationship. The binder to mixture stiffness relationship for the HRA mortar with 50 pen bitumen and radial SBS PMB are also compared in Figure 6.17. It can be seen from this figure that both mixtures show a similar binder to mixture stiffness relationship at high binder stiffnesses (corresponding to low temperatures) but higher stiffnesses can be observed at low binder stiffnesses (corresponding to high temperatures) for the HRA mortar with radial SBS PMB compared to the 50 pen bitumen. This can be attributed to the high

elastic response of the SBS PMB at high temperatures coupled with the high filler content of the HRA mortar causing the interaction between the PMB and fine aggregate particles to improved the deformation resistance of the mortar.

6.3.2 Phase angle

The plot of asphalt mixture versus bitumen phase angle for all the DBM, HRA and HRA mortar mixtures are shown in Figures 6.18 to 6.26 respectively. It can be seen in the figures that the effect of the aggregate skeleton results in a reduction in phase angle and increased elastic response for the mixtures compared to the pure binders. This is particularly noticeable at low frequencies where there is a considerable difference between the increasing viscous response of the conventional binder and the increasing elastic response of the asphalt mixtures.

Figures 6.27 and 6.28 present a comparison of the binder to mixture phase angle relationship for the DBM, HRA and HRA mortar mixtures with 50 pen bitumen and radial SBS PMB. It can be seen in the figures that there is a very similar binder to mixture phase angle relationship at low binder phase angles (corresponding to low temperatures) for all the binder-mixture combinations. The binder to mixture phase angle relationship for all the DBM mixtures is also shown in Figure 6.29. Two conclusions can be drawn from this figure. Firstly, similar phase angle relationships exist between asphalt mixtures and bitumens at low bitumen phase angles ($\leq 45^{o}$). This can be attributed to dependency of asphalt mixture properties at low temperatures on bitumen properties and the volumetric proportions of the asphalt mixture. However, there are variations in the asphalt mixture-bitumen phase angle relationships between the different mixtures at high bitumen phase angles ($> 45^{o}$). This suggests that other parameters, such as aggregate grading, shape, texture and degree of interlock, and the method and degree of compaction, become as significant as the binder and the volumetric properties of the asphalt mixture. Secondly, asphalt mixture phase angles start to decrease at bitumen phase angle values between 55 and 70^{o}. This corresponds to the increased influence of the aggregate skeleton on asphalt mixture properties at high temperatures and low frequencies resulting in increasing elastic behaviour of the asphalt mixtures.

6.4 Binder and Asphalt Mixture Master Curves

Complex modulus master curves for the binders and asphalt mixtures have been determined at a reference temperature of 20ºC. Figures 6.30 to 6.32 show the master curves of the 50 pen bitumen and radial SBS PMB and their corresponding DBM, HRA and HRA mortar mixtures. These graphs show that the relationship between the rheological behaviour of the asphalt mixture and the bitumen can be divided into three regions. At high frequencies (corresponding to low temperatures) all the binders and asphalt mixtures begin to approach an asymptotic behaviour corresponding to the glassy limiting stiffness modulus of the bitumen. As frequency decreases (corresponding to increasing temperature) both the bitumen and asphalt mixture stiffness decreases. As the frequency decreases further (corresponding to high temperatures $\geq$ 40ºC), it can be seen that as the complex modulus of the bitumens continues to decrease, the complex modulus of the asphalt mixtures approaches a limit. This behaviour indicates the influence of aggregate interlock on the rheological properties of the asphalt mixtures. These results are in agreement with the work undertaken by Goodrich [53] and SHRP [61].

A comparison between shift factors for the DBM, HRA and HRA mortar mixtures and bitumens is presented in Figure 6.33. It can be seen from the figure that there is a direct relationship between the binder and asphalt mixture shift factors.

6.5 Non-linear Viscoelastic Rheological Relationship between Binders and Asphalt Mixtures

Figure 6.34 shows the relationship between a 50 pen bitumen and a DBM asphalt mixture produced with the 50 pen bitumen at various binder strain levels and within the linear viscoelastic response region of the mixture (20 microstrain). It can be seen in the figure that at low strain levels (within the linear region) the binder-mixture stiffness relationship coincides. However, at higher binder strain levels (10% - 50%) the non-linear behaviour of the binder can be seen as different binder-mixture relationships. This indicates that the relationship between bitumen and asphalt mixture complex modulus is highly dependent on strain level within the non-linear region. In order to show the effects of the non-linearity of an asphalt mixture on the binder-

mixture relationship the complex modulus values of the DBM mixture with 50 pen bitumen at a strain level of 0.01 percent (100 microstrain) versus complex modulus of the 50 pen bitumen at different strain levels is plotted in Figure 6.35. It can be seen from this figure that the relationship between asphalt mixture and bitumen complex modulus even at 3 percent strain level, which is within the linear region of bitumen, is different than Figure 6.34. The reason for this is that although bitumen is in its linear region, the asphalt mixture at 0.01 percent strain is in its non-linear region.

6.6 Summary

The results of the binder and mixture tests, presented in Chapters Four and Five, were used to study the relationship between binder and mixture stiffness. The rheological properties of five unmodified and modified bitumens, five DBM, two HRA and two HRA mortar mixtures determined under the different temperatures and frequencies were used in the study. The method used in this investigation was similar to a system developed during the SHRP program to relate binder and mixture stiffnesses at low temperatures. In this method, the log of complex modulus of a mixture was plotted against the log of complex modulus of the corresponding binder, at various frequencies and temperatures. A best-fit straight line, described by a power model on a log-log plot was used to form a relationship between the measured binder and mixture stiffnesses. These plots showed that in general the bitumen to mixture complex modulus relationship is independent of temperature. However, although a straight line could be established for the EVA PMB and linear SBS PMB binders, the results showed that the binder to mixture stiffness relationship exhibits temperature dependence for mixtures produced with these two binders.

The HRA mortar produced with the 50 pen bitumen and the radial SBS PMB showed similar binder to mixture stiffness relationships at high binder stiffness values (corresponding to low temperatures) but the HRA mortar with the radial SBS PMB produced higher stiffnesses at low binder stiffnesses (corresponding to high temperatures). The study of the relationship between bitumen and asphalt mixture phase angle showed that there was very similar binder to mixture phase angle relationships at low binder phase angles (corresponding to low temperatures).

The study of bitumen and asphalt mixture master curves showed that the relationship between the rheological behaviour of the asphalt mixtures and bitumens can be divided into three regions. At high frequencies (corresponding to low temperatures) all the binders and asphalt mixtures begin to approach an asymptotic behaviour corresponding to the glassy limiting stiffness modulus of the bitumen. As frequency decreases (corresponding to increasing temperature) both the bitumen and asphalt mixture stiffness decreases. As the frequency decreases further (corresponding to high temperatures $\geq 40^{o}C$), it can be seen from these figures that as the complex modulus of the bitumens continue to decrease, the complex modulus of the asphalt mixtures approach a plateau. In addition the results showed a direct relationship between the binder and asphalt mixture shift factors. Finally, the study of the relationship between bitumen and asphalt mixture complex modulus in the non-linear region showed that this relationship is a function of the non-linear behaviour of either the bitumen and/or the asphalt mixture.

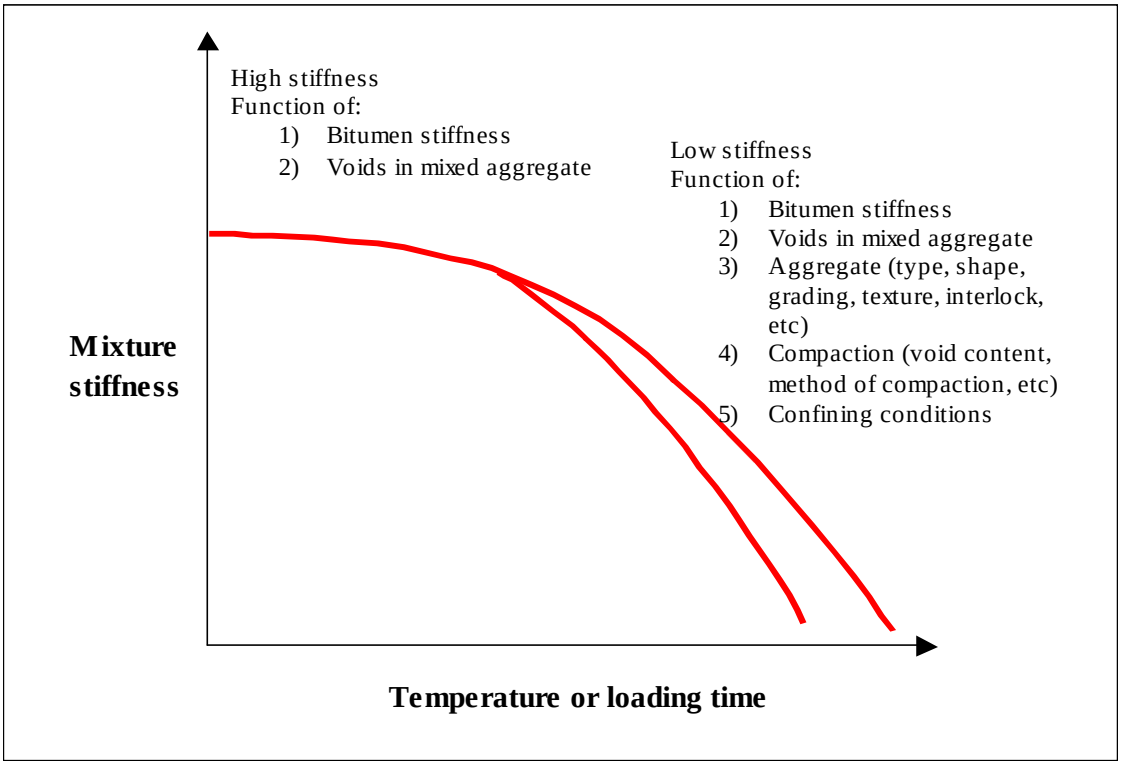

Figure 6.1: Asphalt mixture stiffness as a function of temperature or loading time [110]

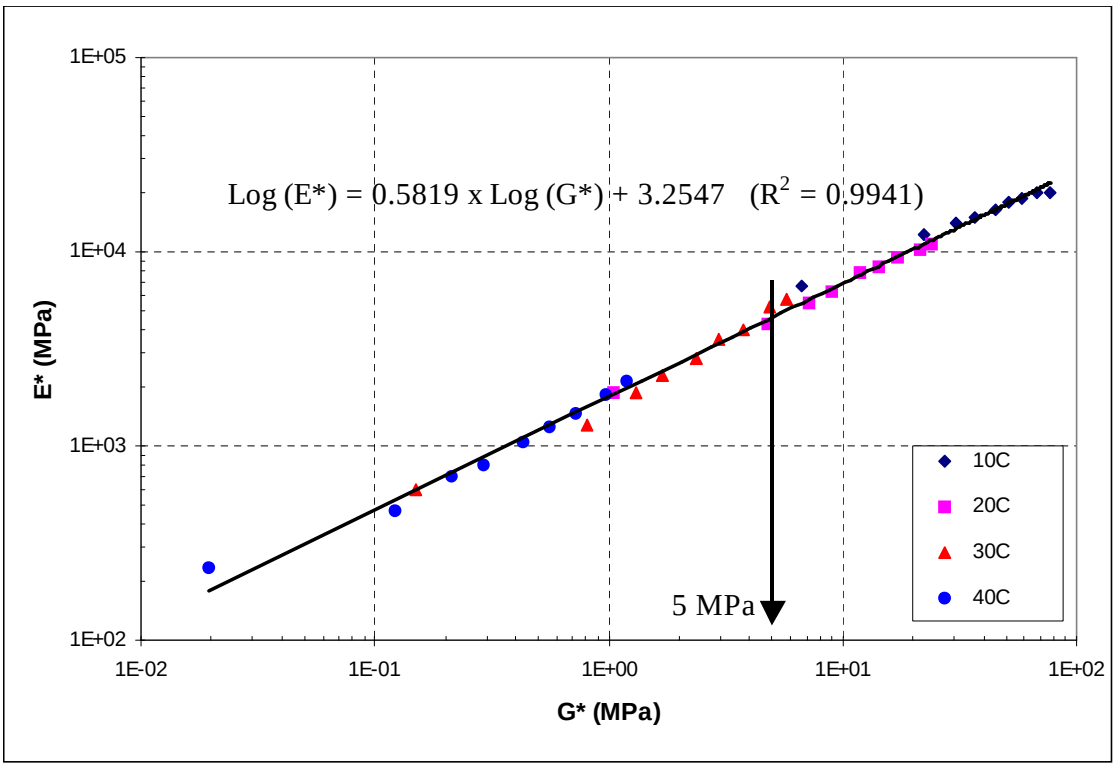

Figure 6.2: Relationship between bitumen-mixture complex modulus for DBM mixture with 50 pen bitumen

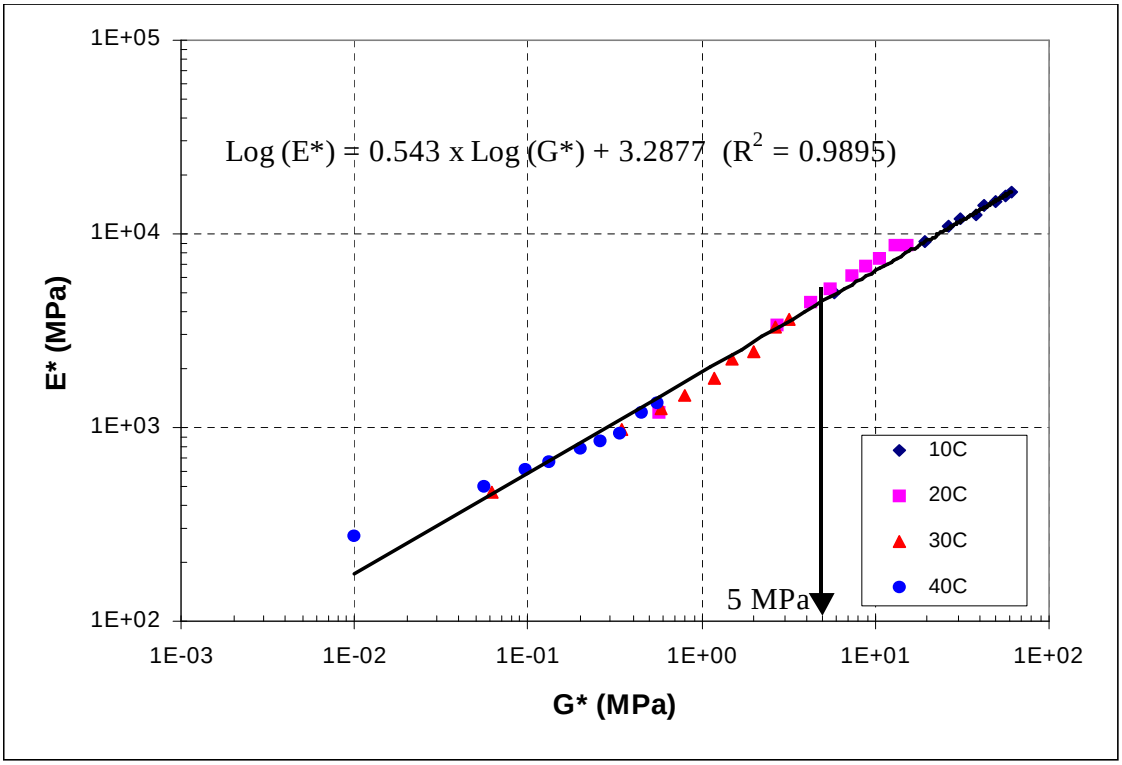

Figure 6.3: Relationship between bitumen-mixture complex modulus for DBM mixture with radial SBS PMB bitumen

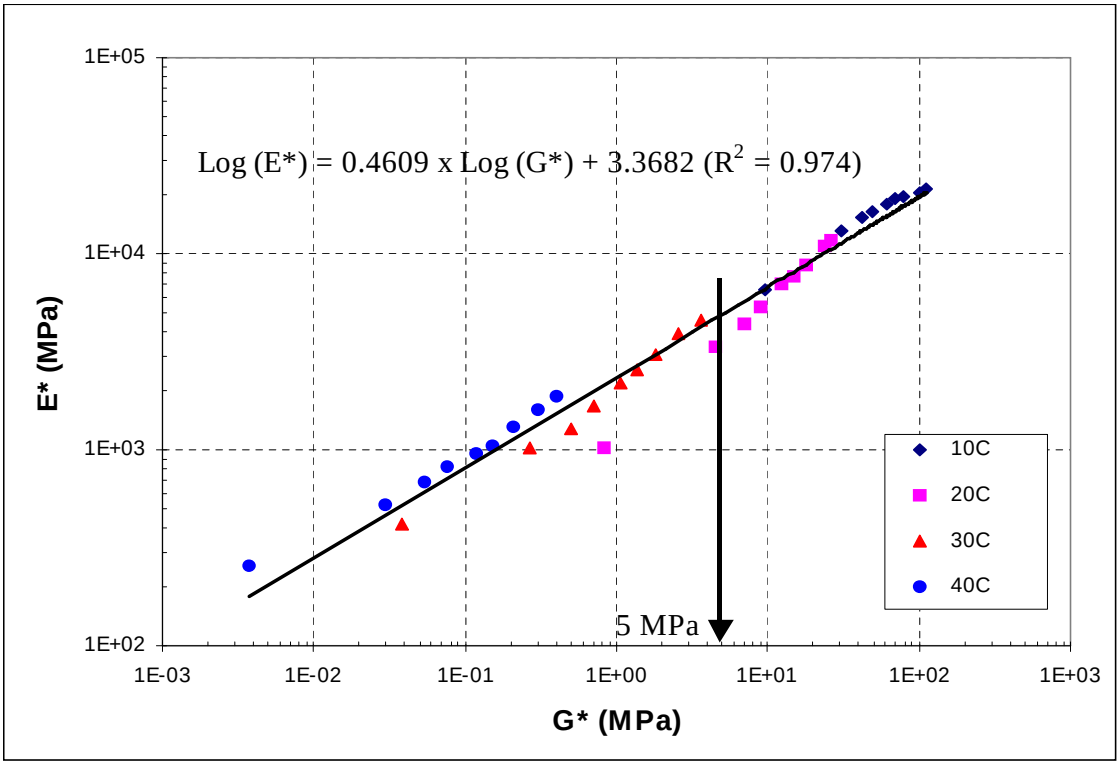

Figure 6.4: Relationship between bitumen-mixture complex modulus for DBM mixture with EVA PMB

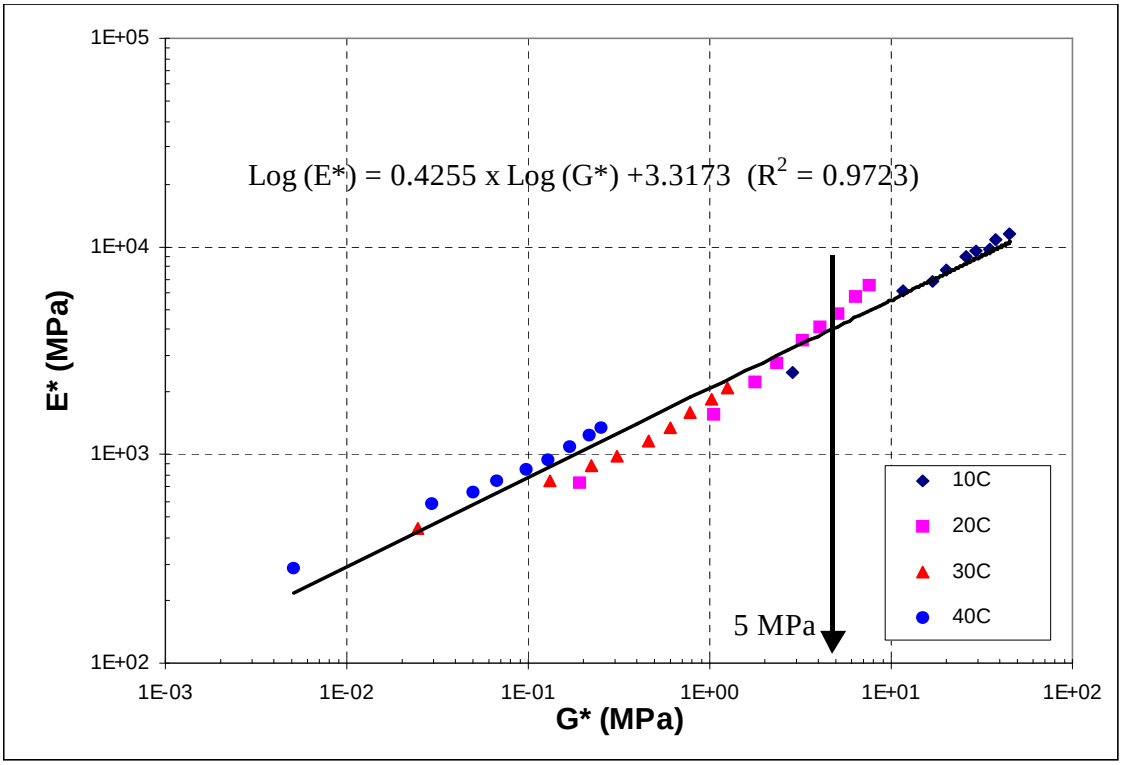

Figure 6.5: Relationship between bitumen-mixture complex modulus for DBM mixture with linear SBS PMB

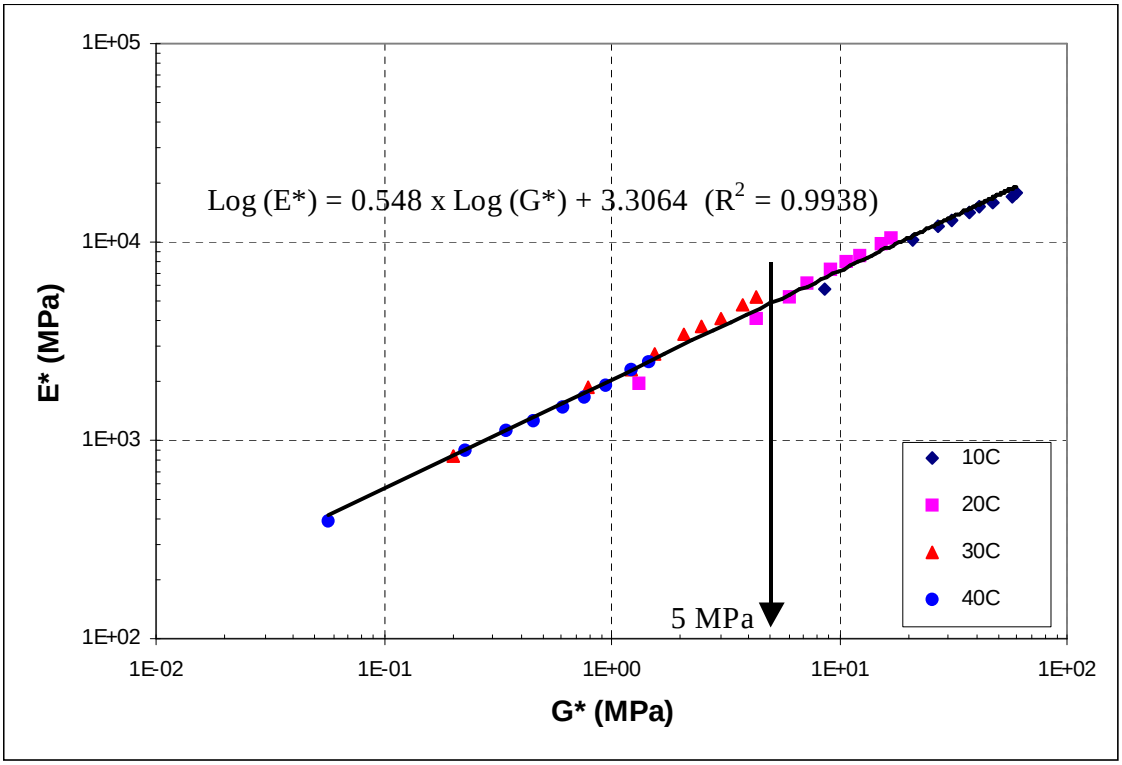

Figure 6.6: Relationship between bitumen-mixture complex modulus for DBM mixture with multigrade 35/50 bitumen

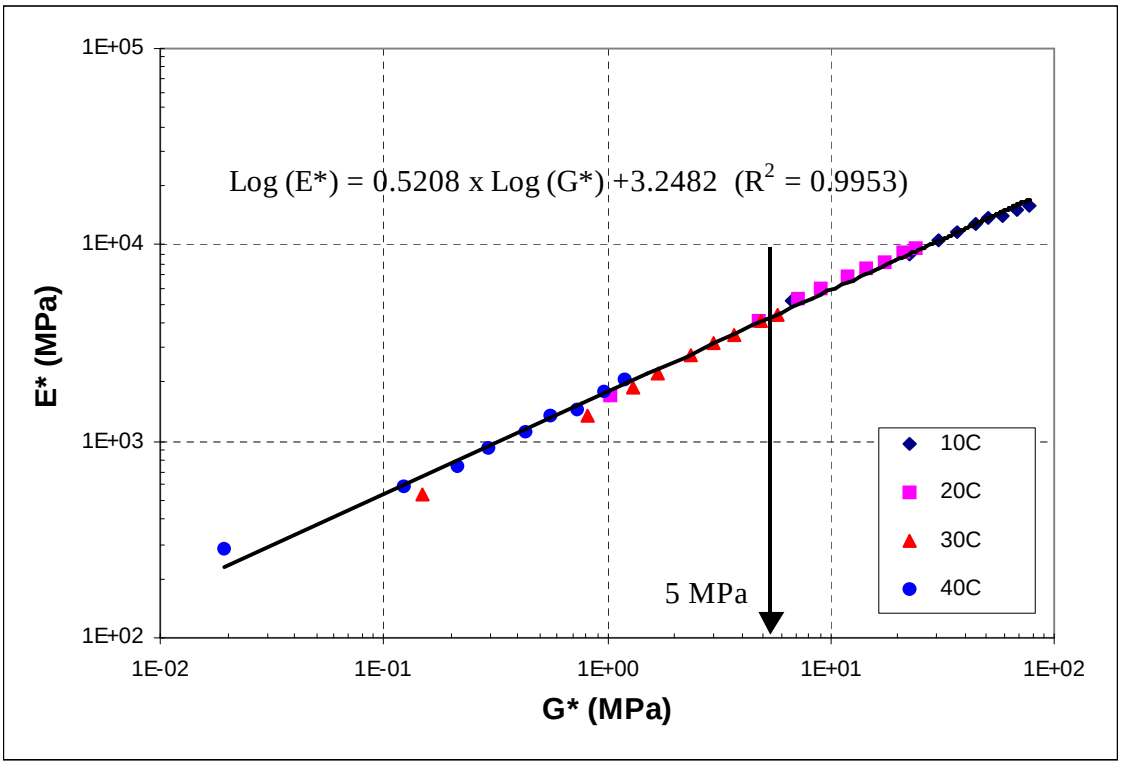

Figure 6.7: Relationship between bitumen-mixture complex modulus for HRA mixture with 50 pen bitumen

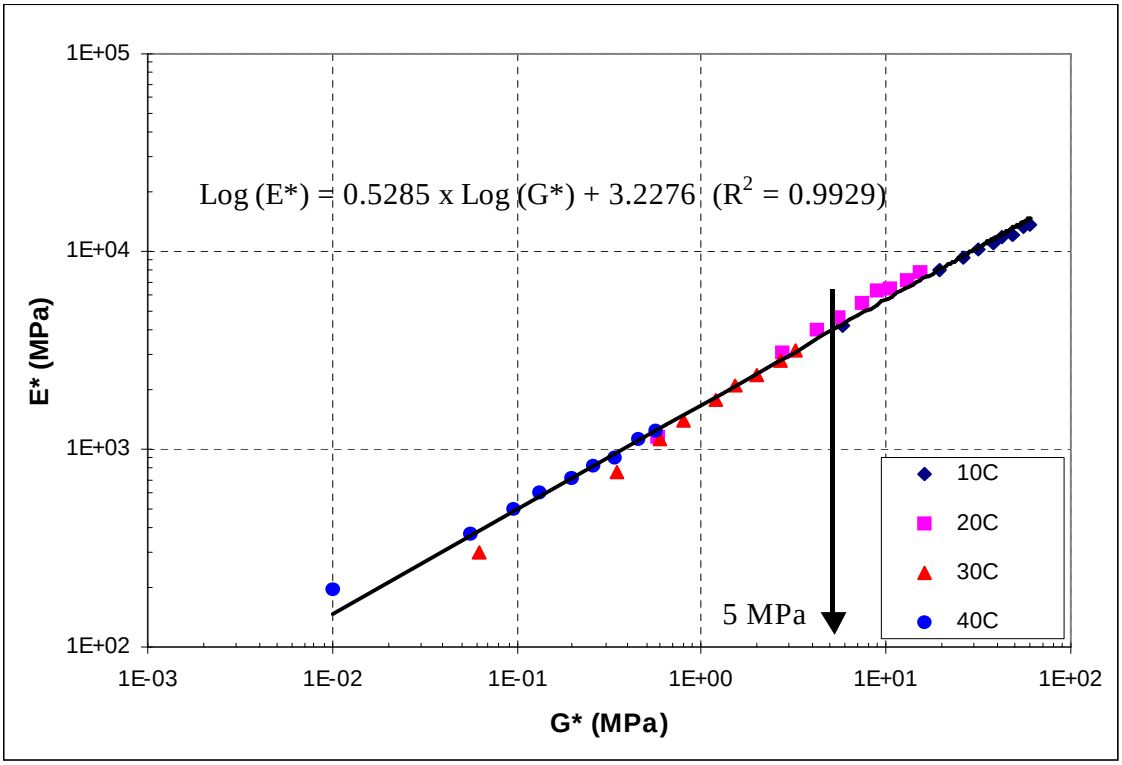

Figure 6.8: Relationship between bitumen-mixture complex modulus for HRA mixture with radial SBS PMB bitumen

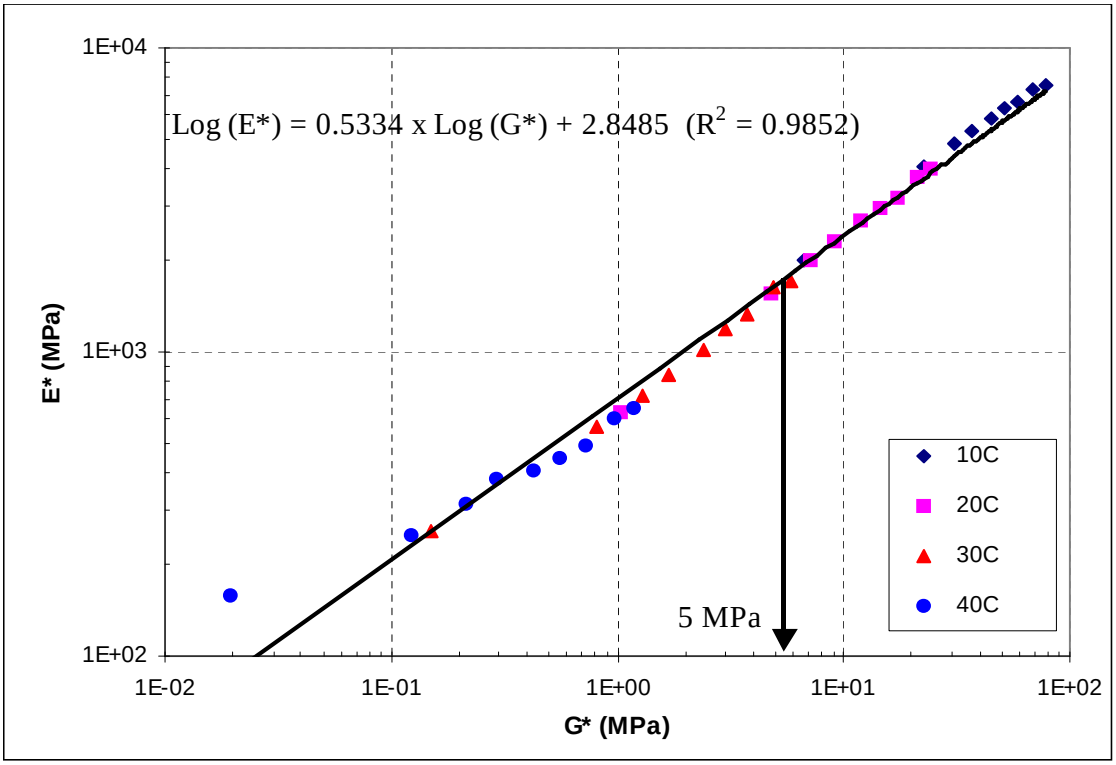

Figure 6.9: Relationship between bitumen-mixture complex modulus for HRA mortar mixture with 50 pen bitumen

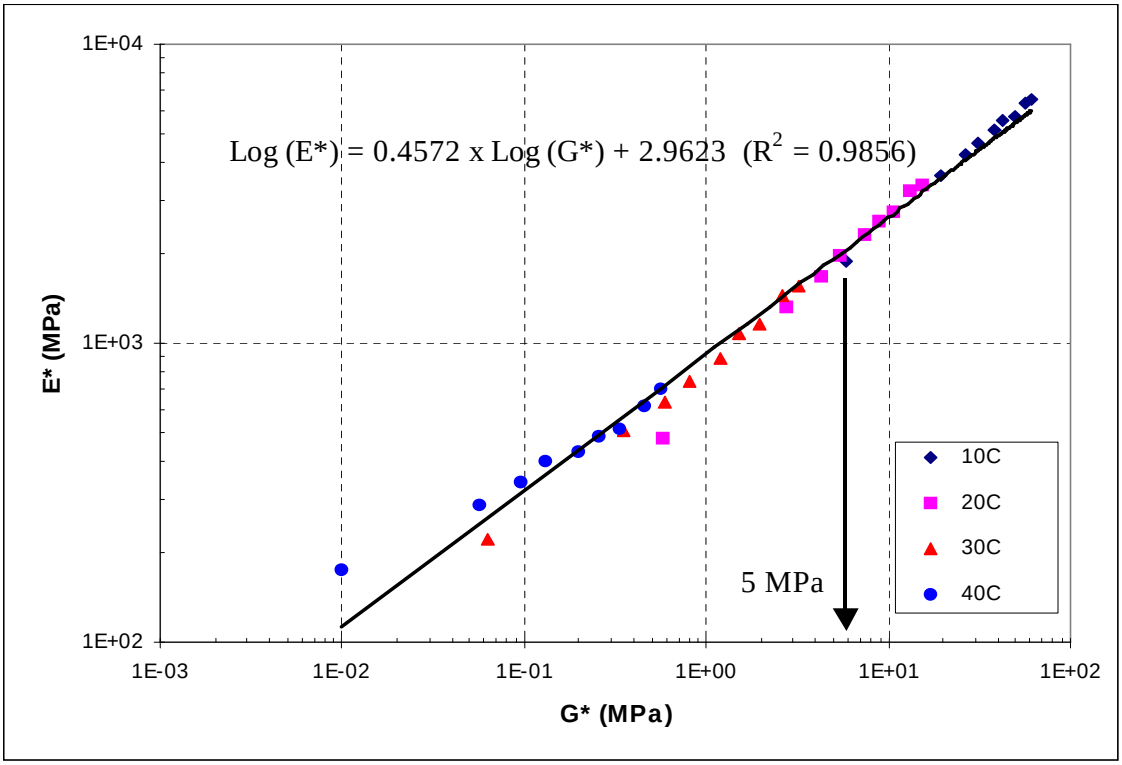

Figure 6.10: Relationship between bitumen-mixture complex modulus for HRA mortar mixture with radial SBS PMB bitumen

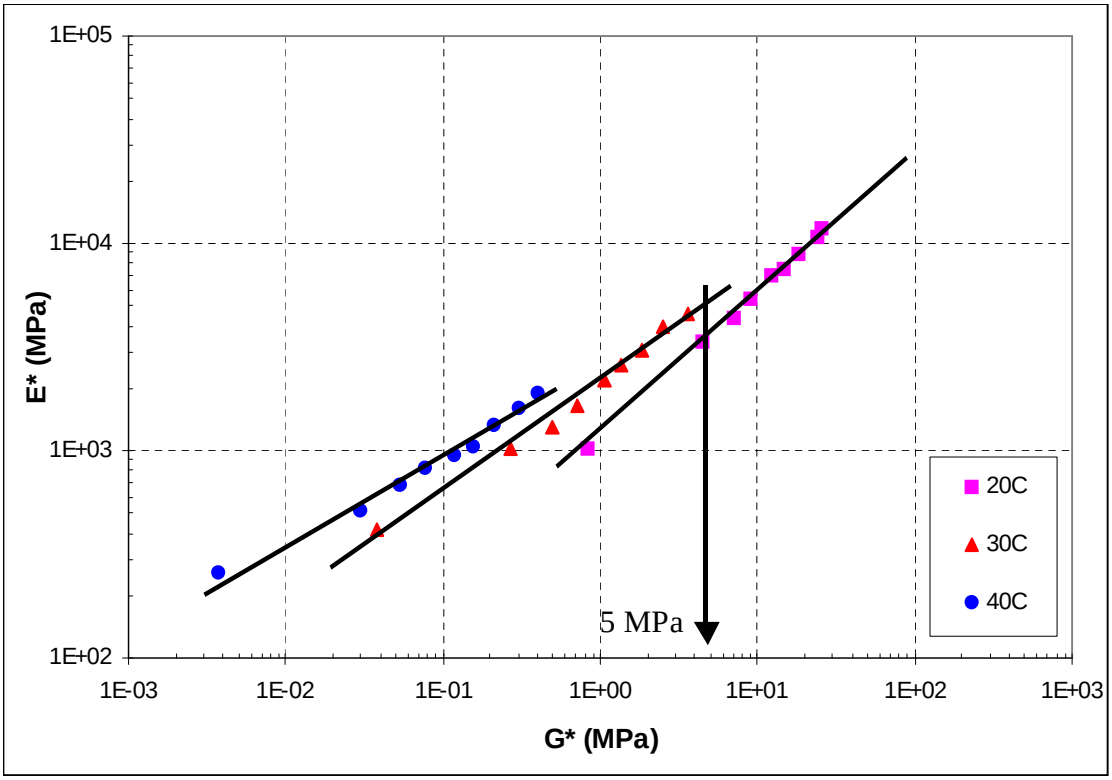

Figure 6.11: Temperature relationship between bitumen-mixture complex modulus for DBM mixture with EVA PMB

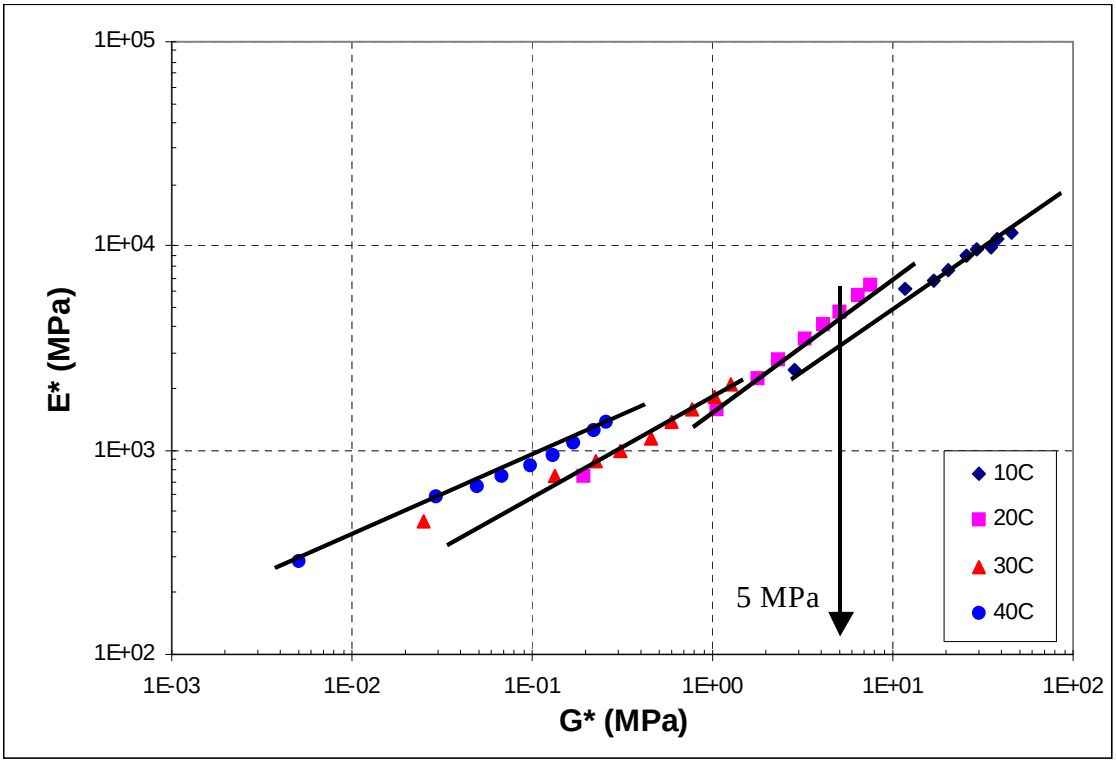

Figure 6.12: Temperature relationship between bitumen-mixture complex modulus for DBM mixture with linear SBS PMB

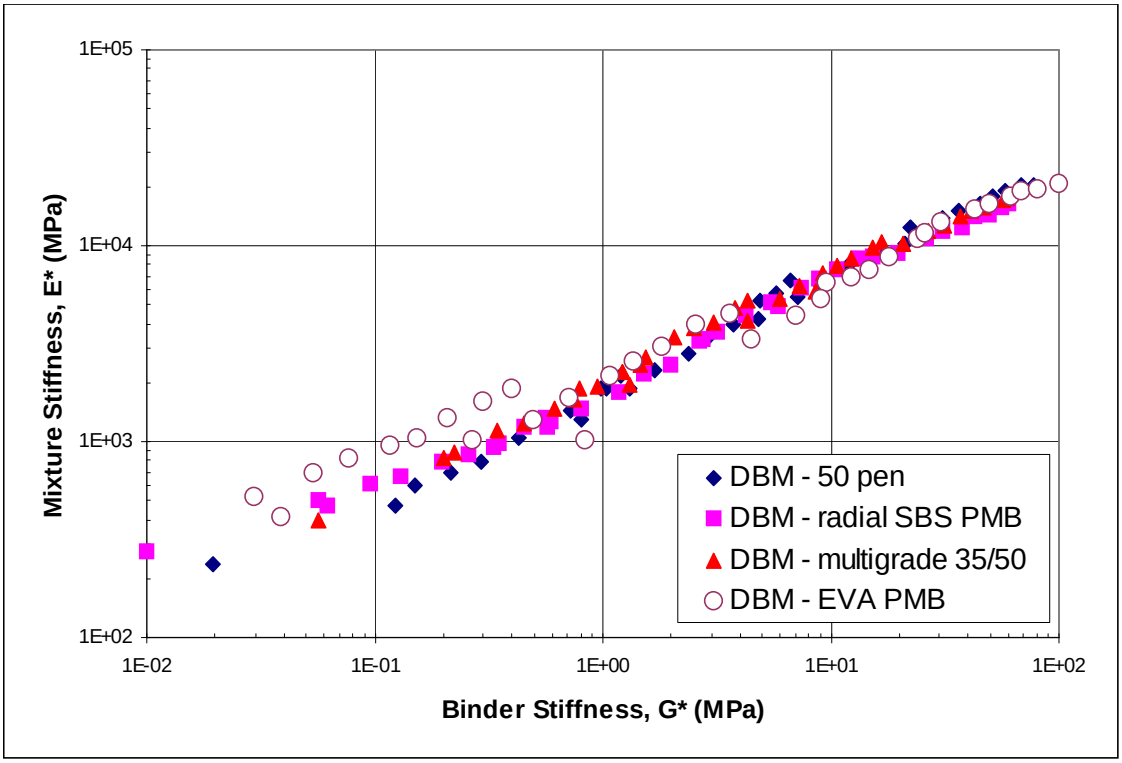

Figure 6.13: Comparison of Mixture to Binder Stiffness for DBM with EVA PMB with other DBM mixtures

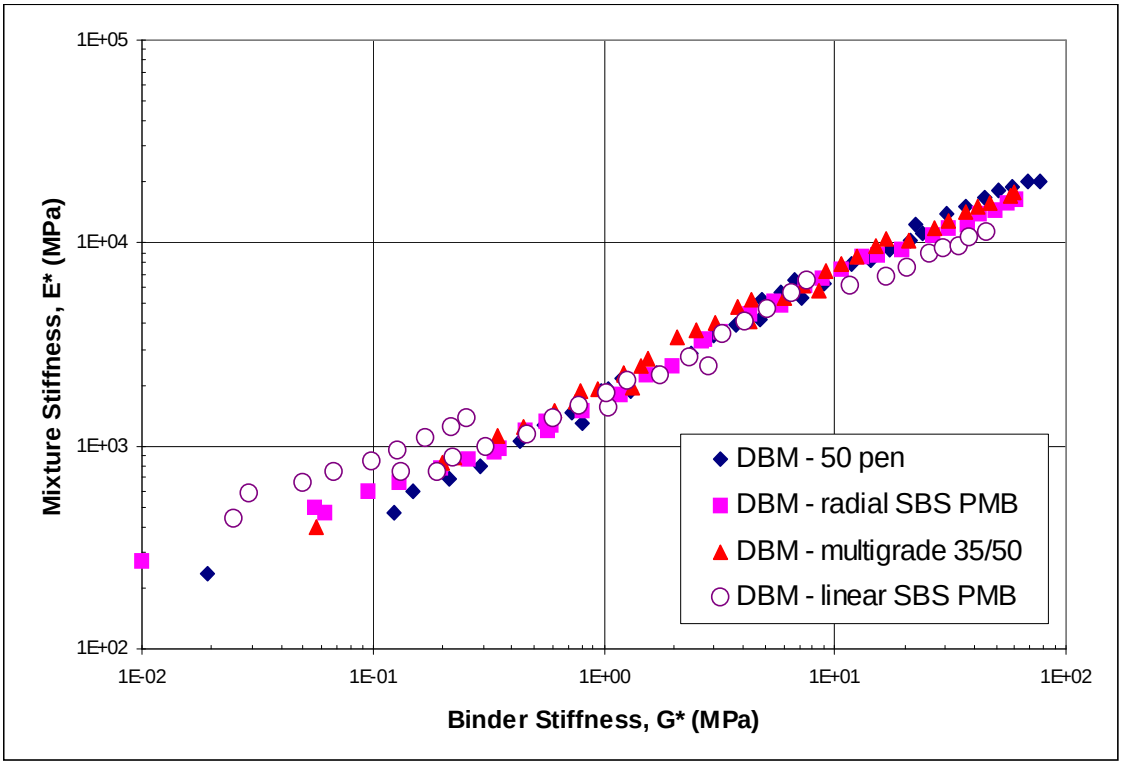

Figure 6.14: Comparison of Mixture to Binder Stiffness for DBM with linear SBS PMB with other DBM mixtures

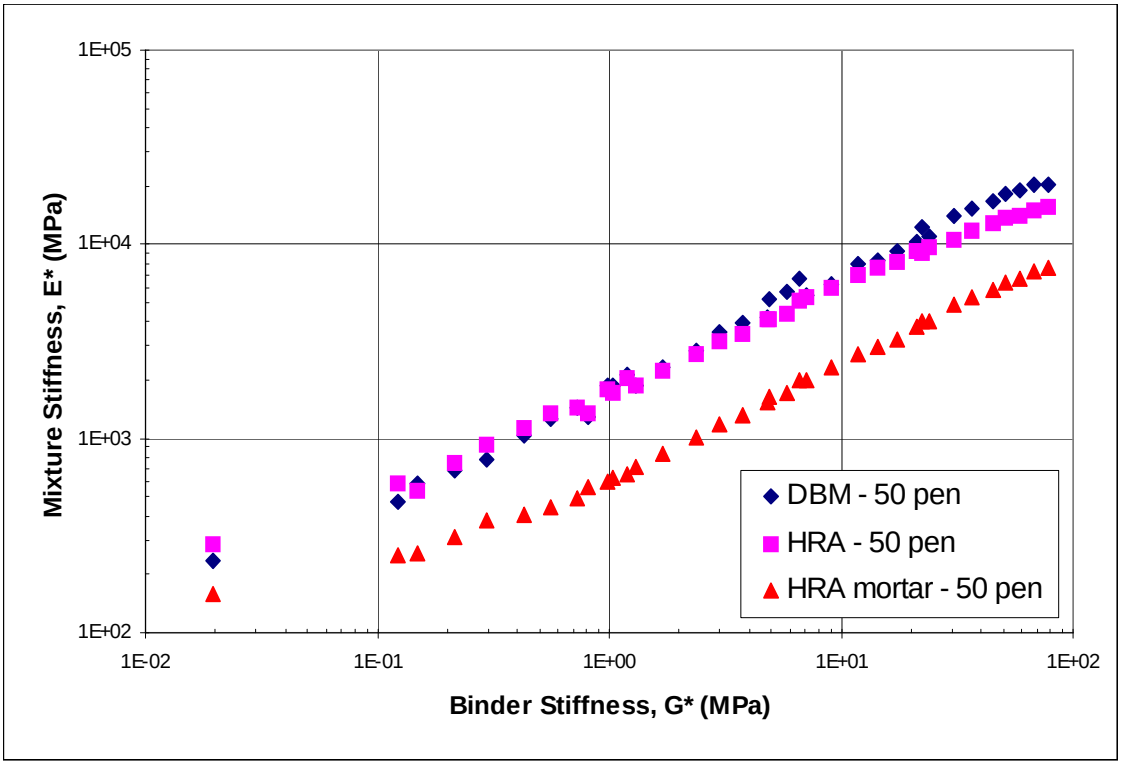

Figure 6.15: Comparison of DBM, HRA and HRA mortar mixtures with 50 pen bitumen

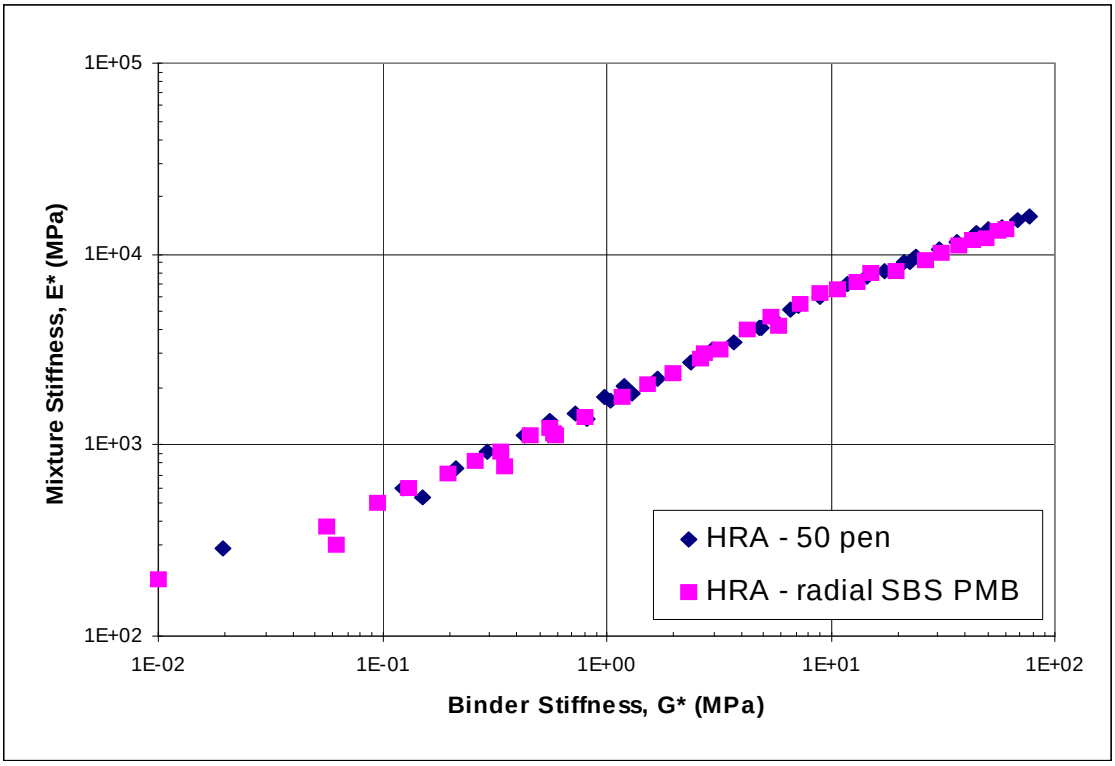

Figure 6.16: Comparison of HRA mixtures with 50 pen bitumen and radial SBS PMB

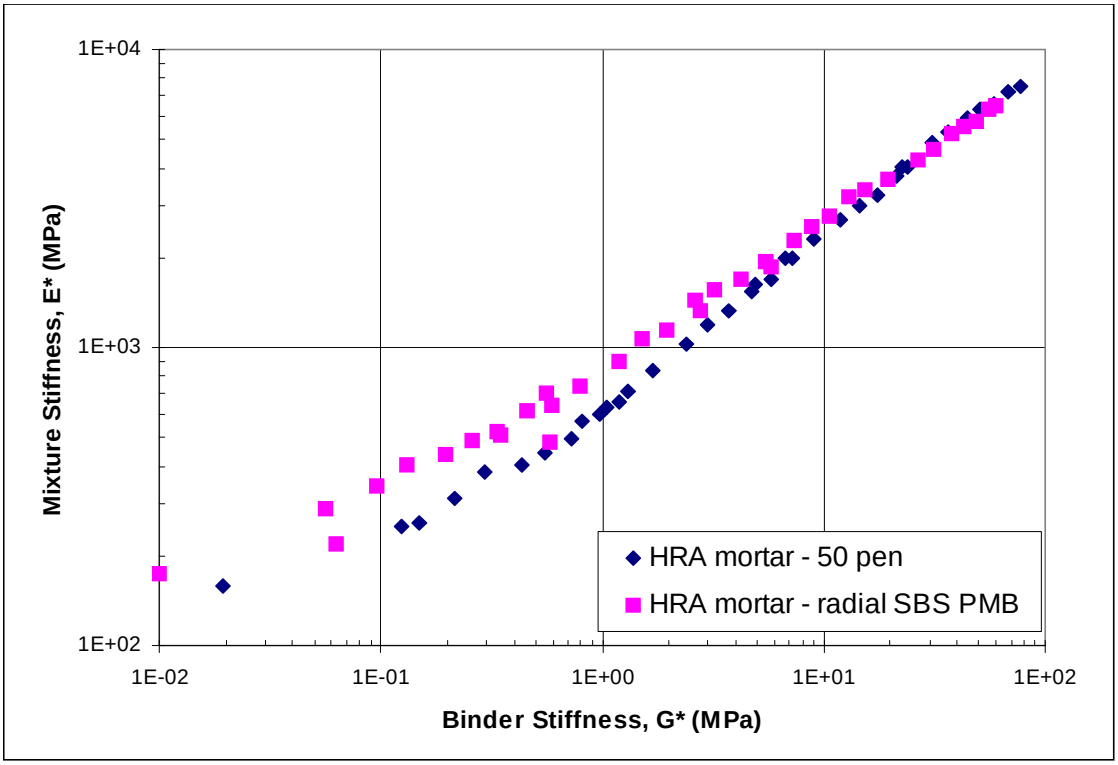

Figure 6.17: Comparison of HRA mixtures with 50 pen bitumen and radial SBS PMB

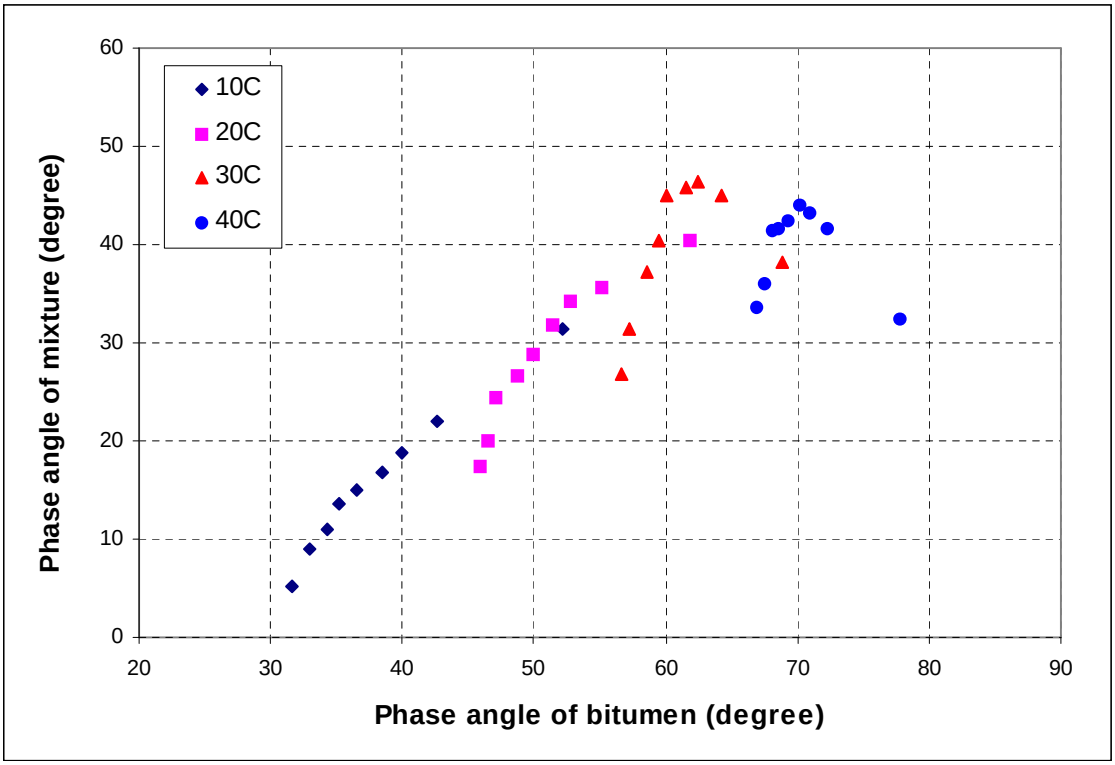

Figure 6.18: Relationship between phase angle of bitumen and DBM asphalt mixture with 50 pen bitumen

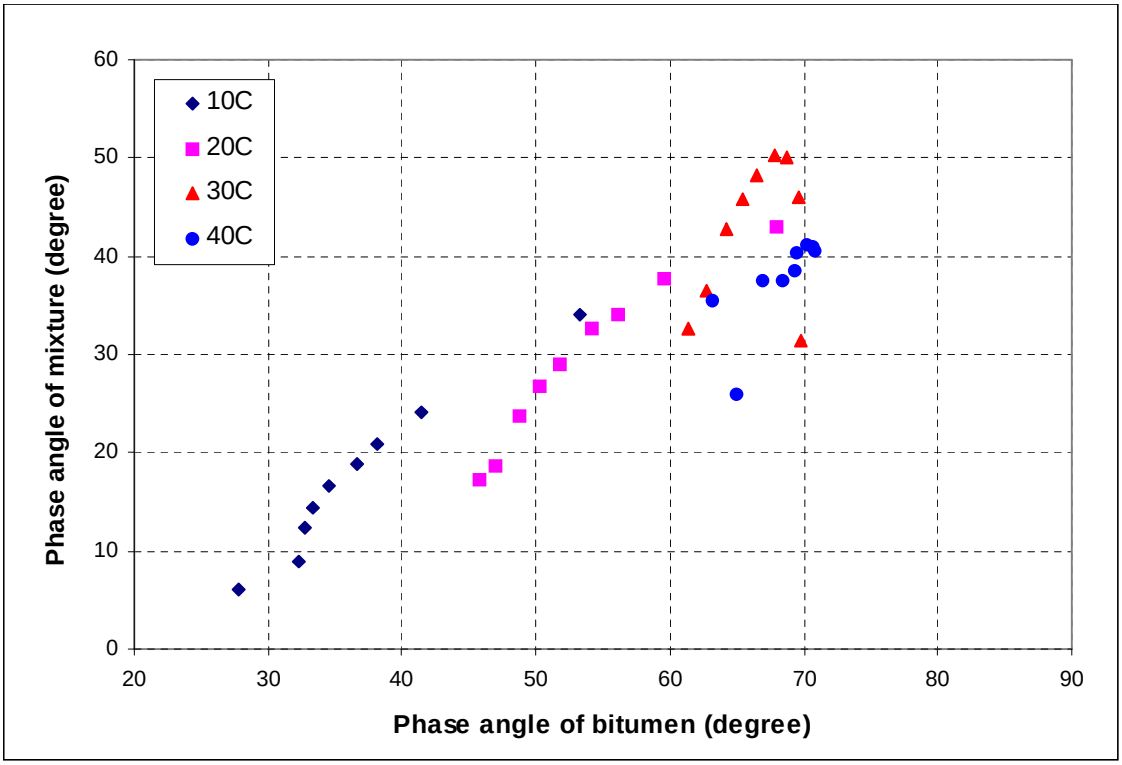

Figure 6.19: Relationship between phase angle of bitumen and DBM asphalt mixture with radial SBS PMB

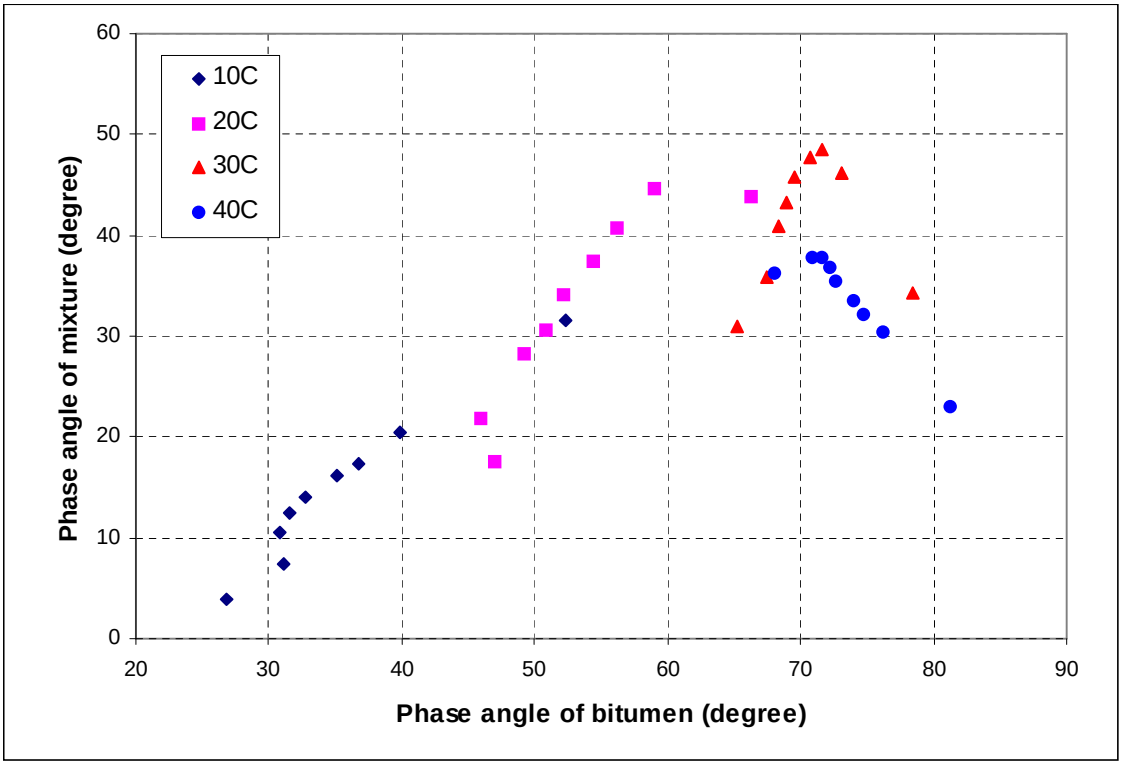

Figure 6.20: Relationship between phase angle of bitumen and DBM asphalt mixture with EVA PMB

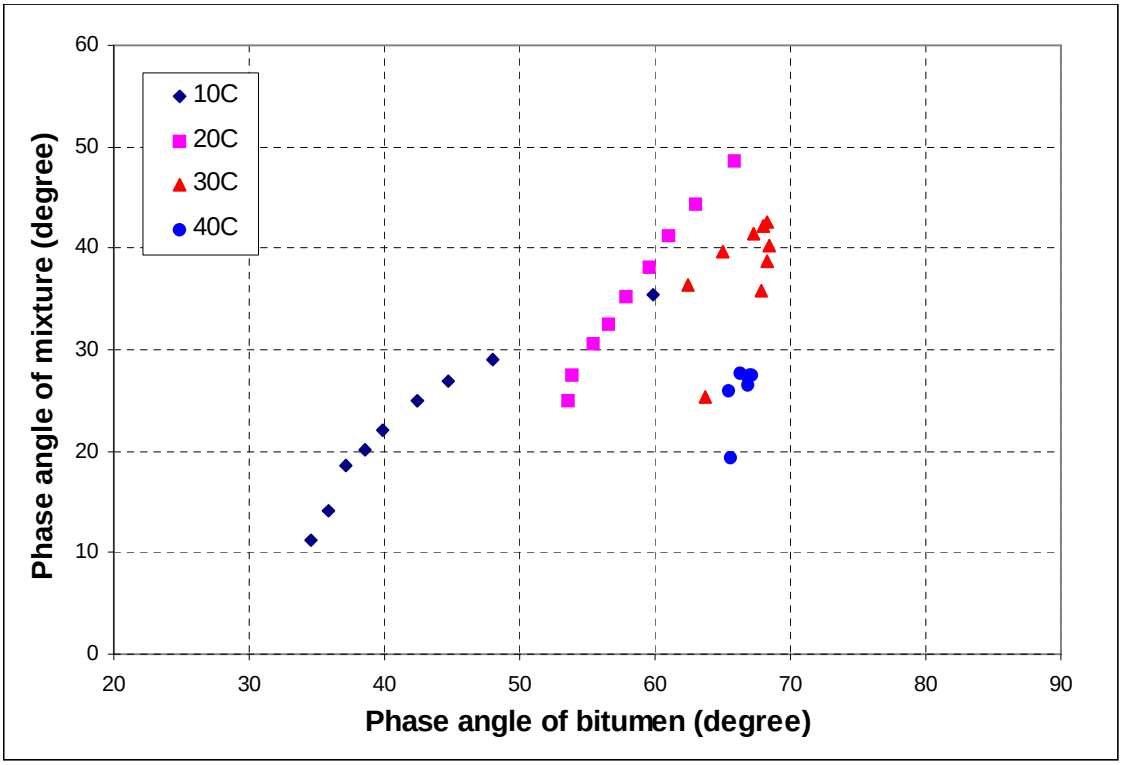

Figure 6.21: Relationship between phase angle of bitumen and DBM asphalt mixture with linear SBS PMB

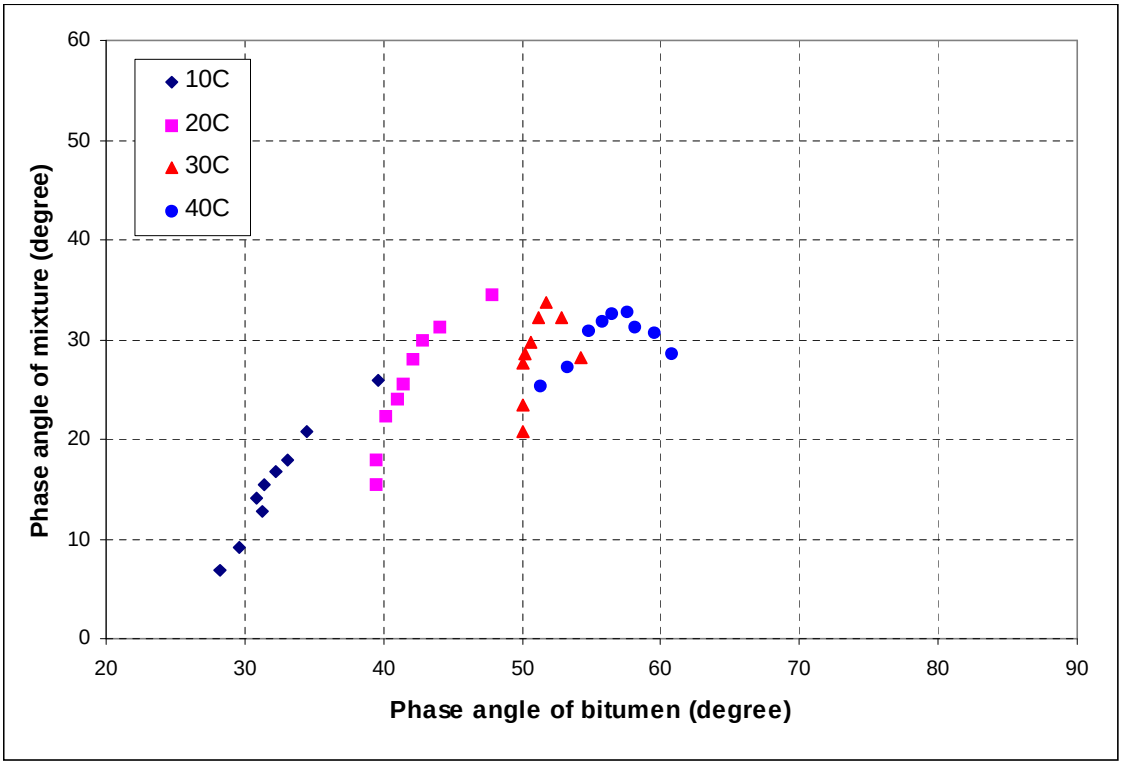

Figure 6.22: Relationship between phase angle of bitumen and DBM asphalt mixture with multigrade 35/50 bitumen

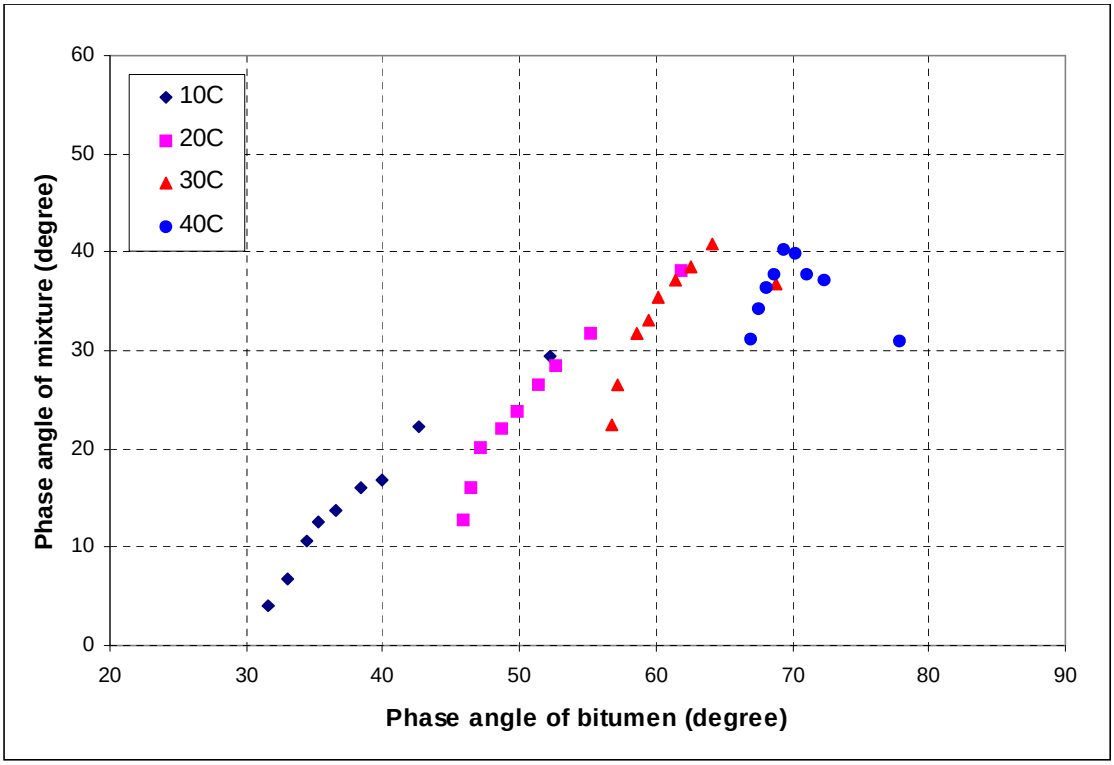

Figure 6.23: Relationship between phase angle of bitumen and HRA asphalt mixture with 50 pen bitumen

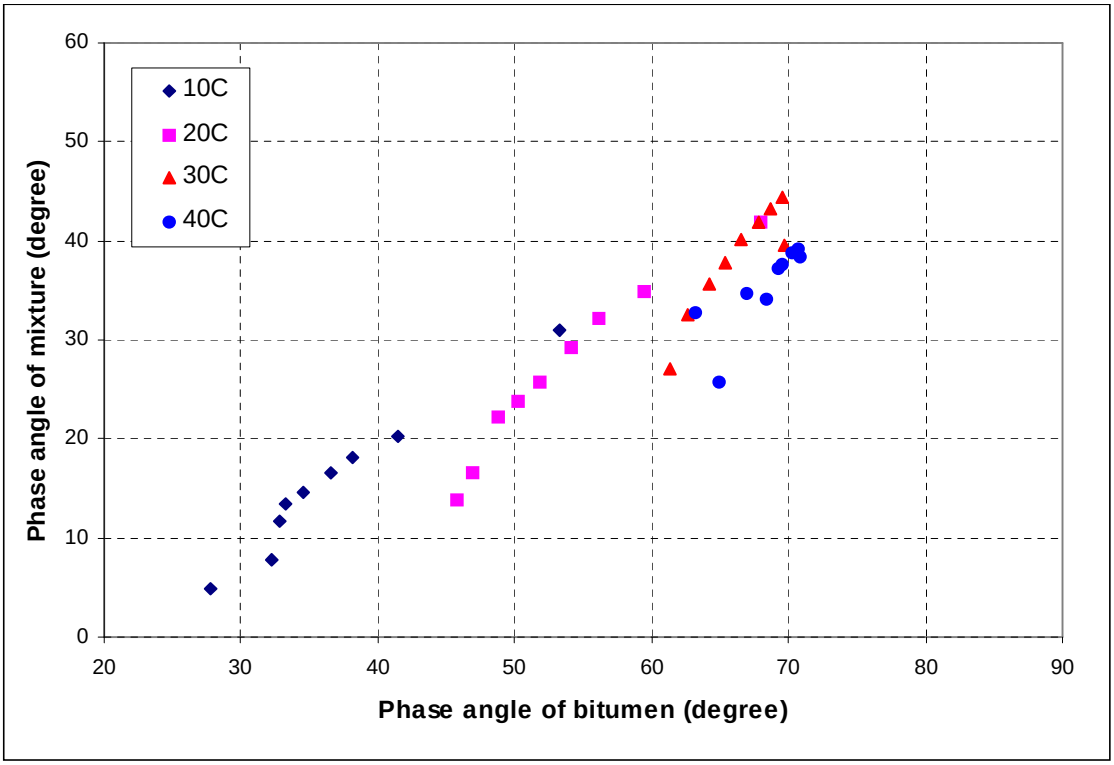

Figure 6.24: Relationship between phase angle of bitumen and HRA asphalt mixture with radial SBS PMB

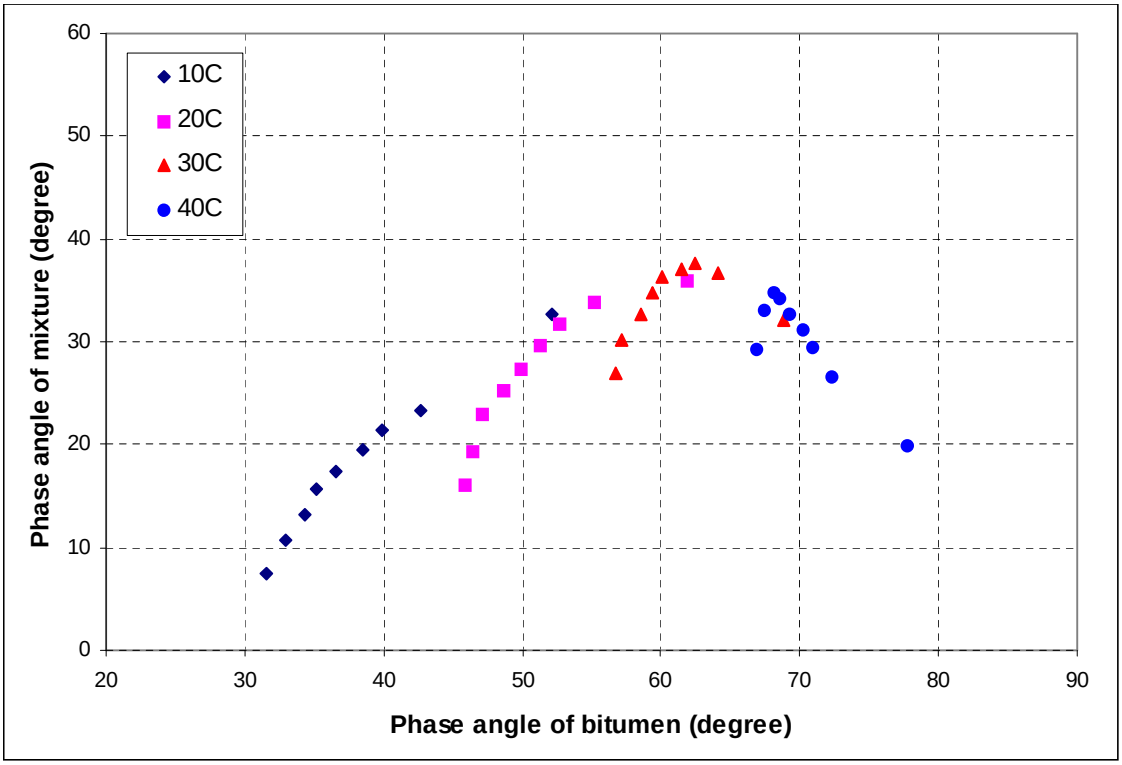

Figure 6.25: Relationship between phase angle of bitumen and HRA mortar asphalt mixture with 50 pen bitumen

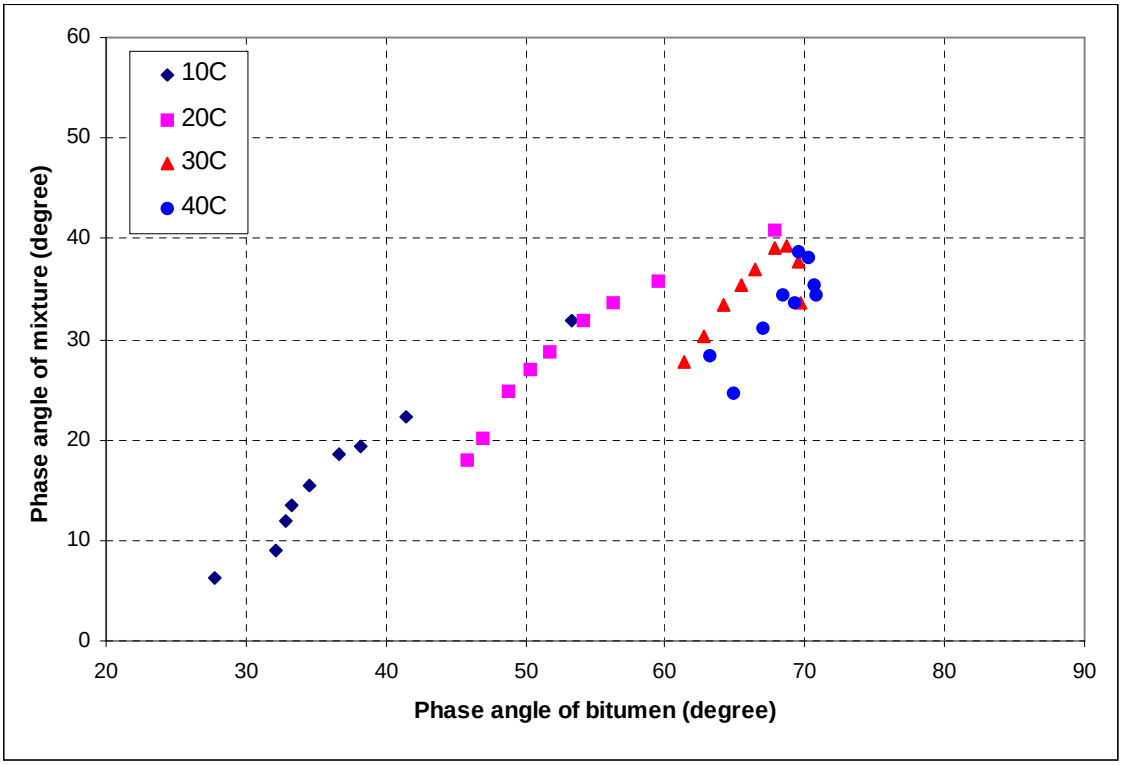

Figure 6.26: Relationship between phase angle of bitumen and HRA mortar asphalt mixture with radial SBS PMB

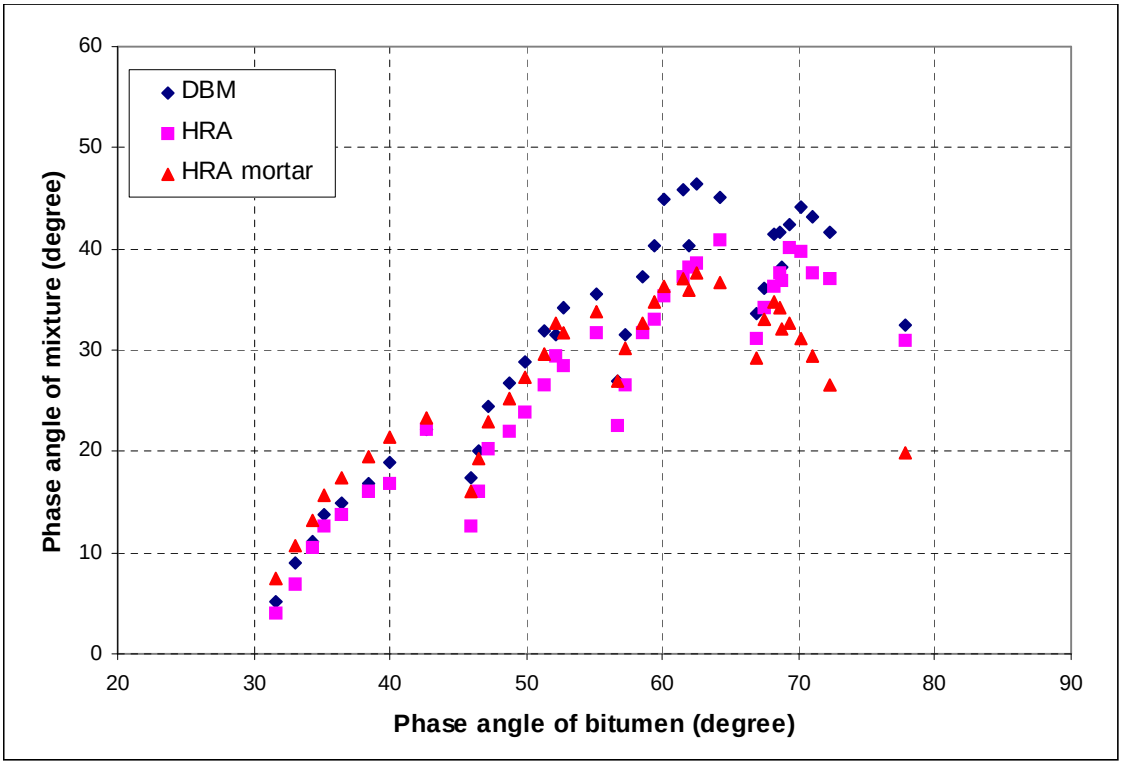

Figure 6.27: Relationship between phase angle of bitumen and all asphalt mixtures with 50 pen bitumen

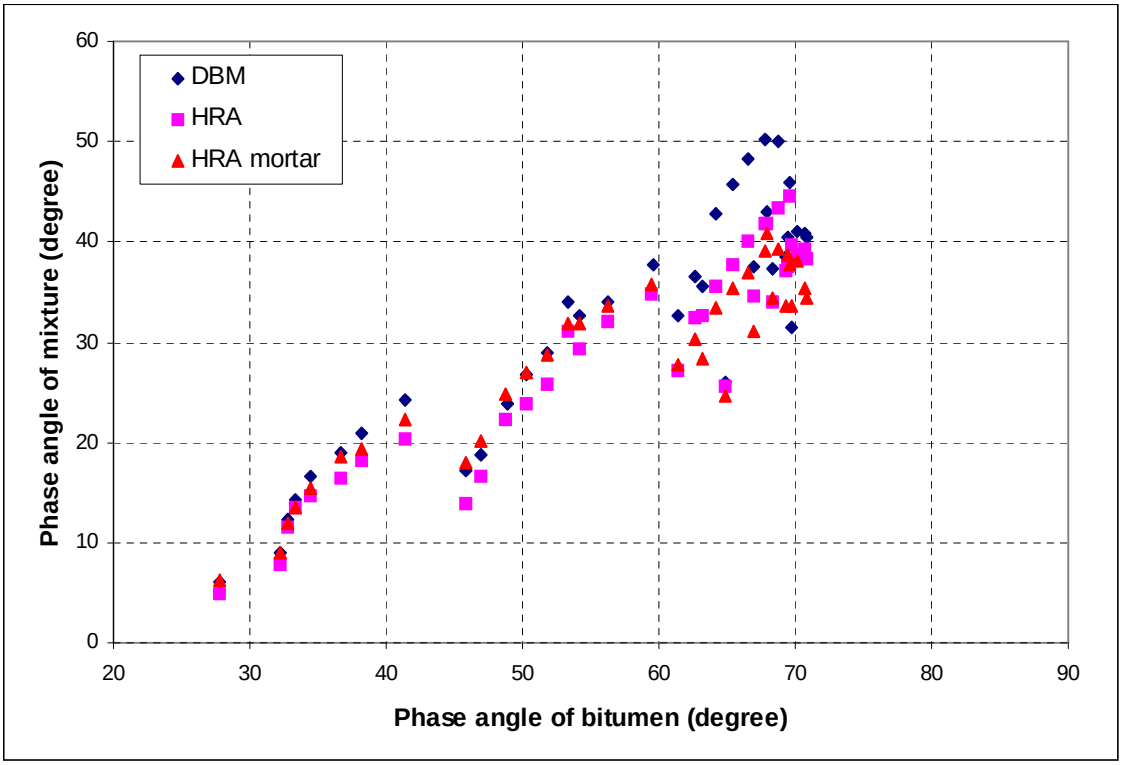

Figure 6.28: Relationship between phase angle of bitumen and all asphalt mixtures with radial SBS PMB

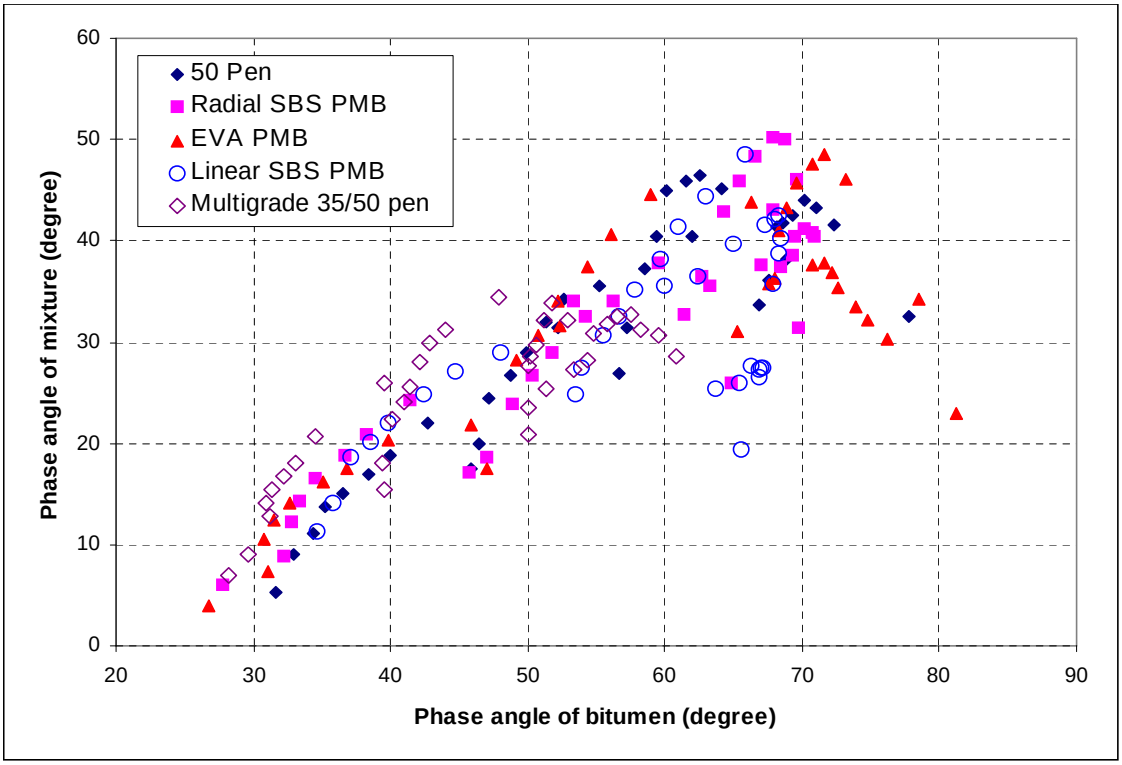

Figure 6.29: Relationship between phase angle of bitumen and DBM asphalt mixtures

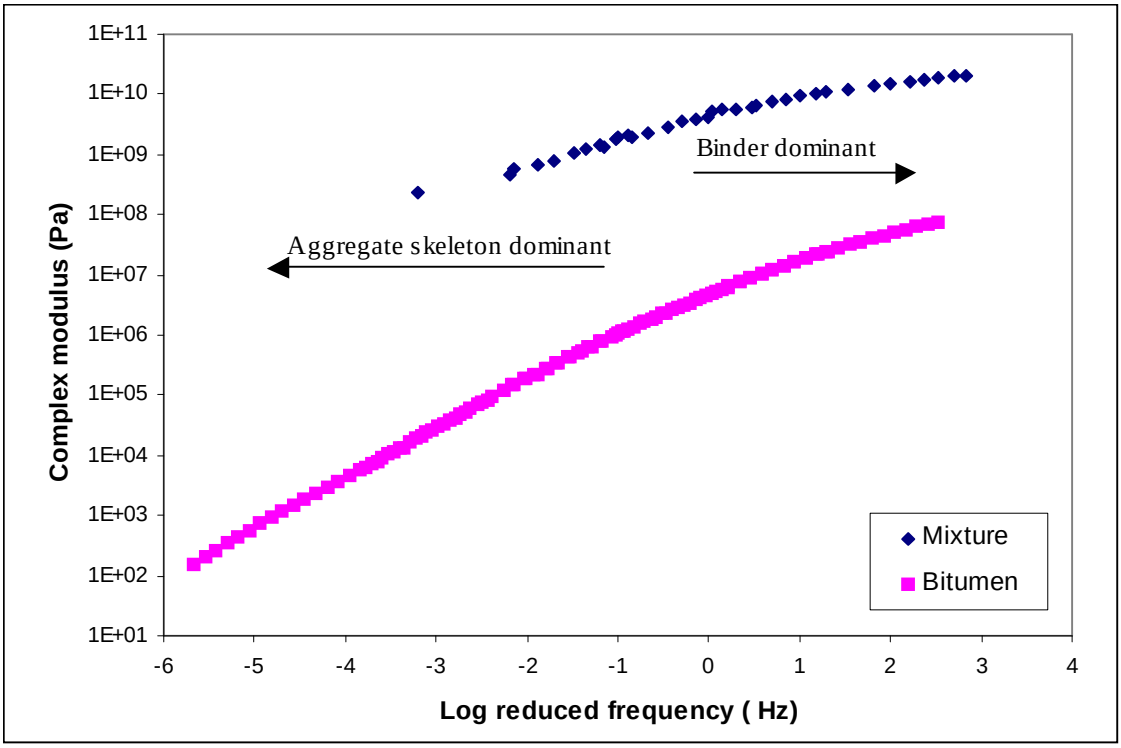

Figure 6.30: Complex modulus master curves for 50 pen bitumen and DBM mixture with 50 pen bitumen

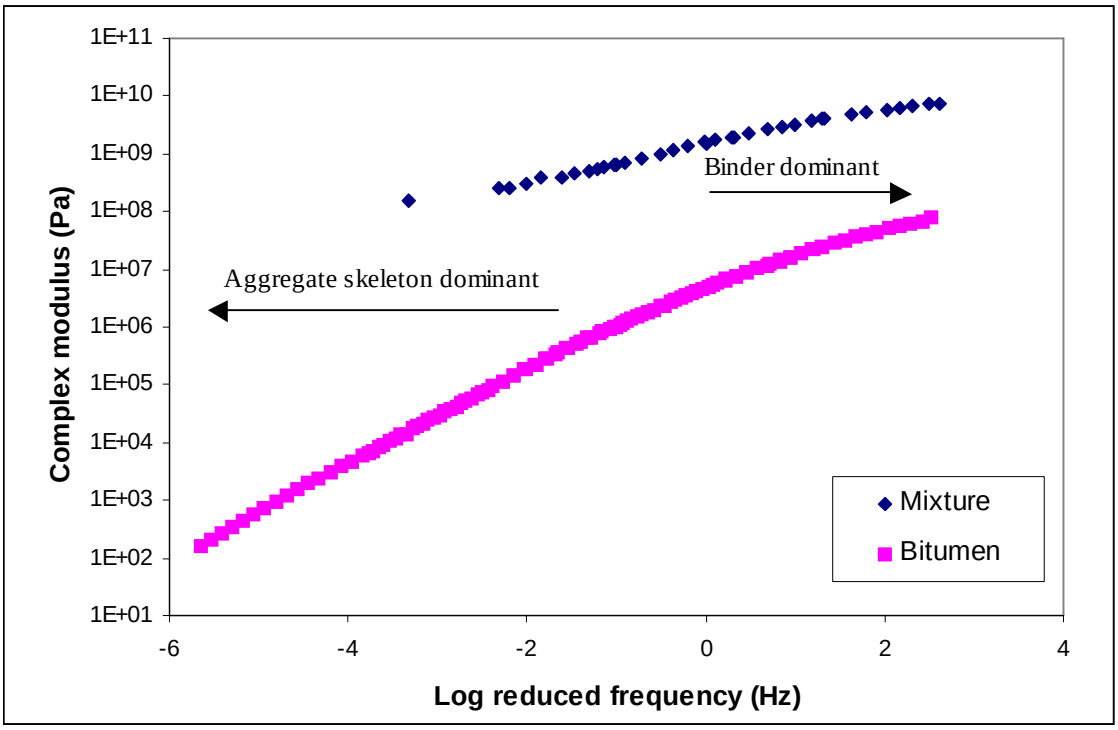

Figure 6.31: Complex modulus master curves for 50 pen bitumen and HRA mortar mixture with 50 pen bitumen

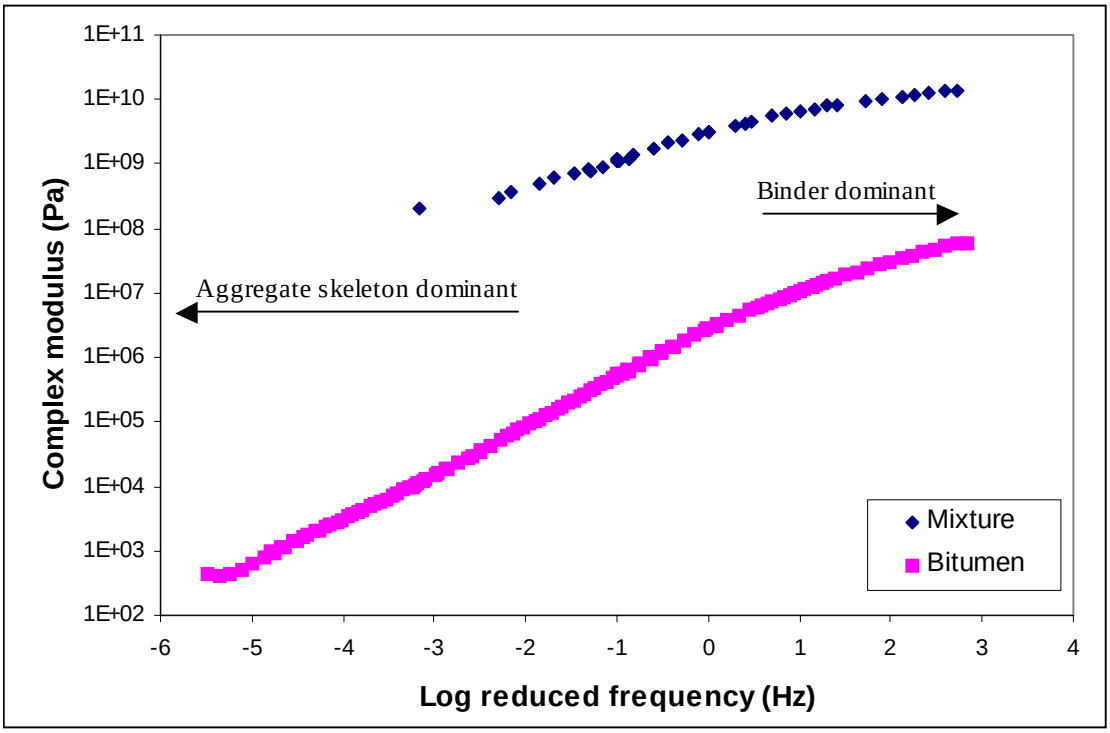

Figure 6.32: Complex modulus master curves for radial SBS PMB bitumen and HRA mixture with radial SBS PMB bitumen

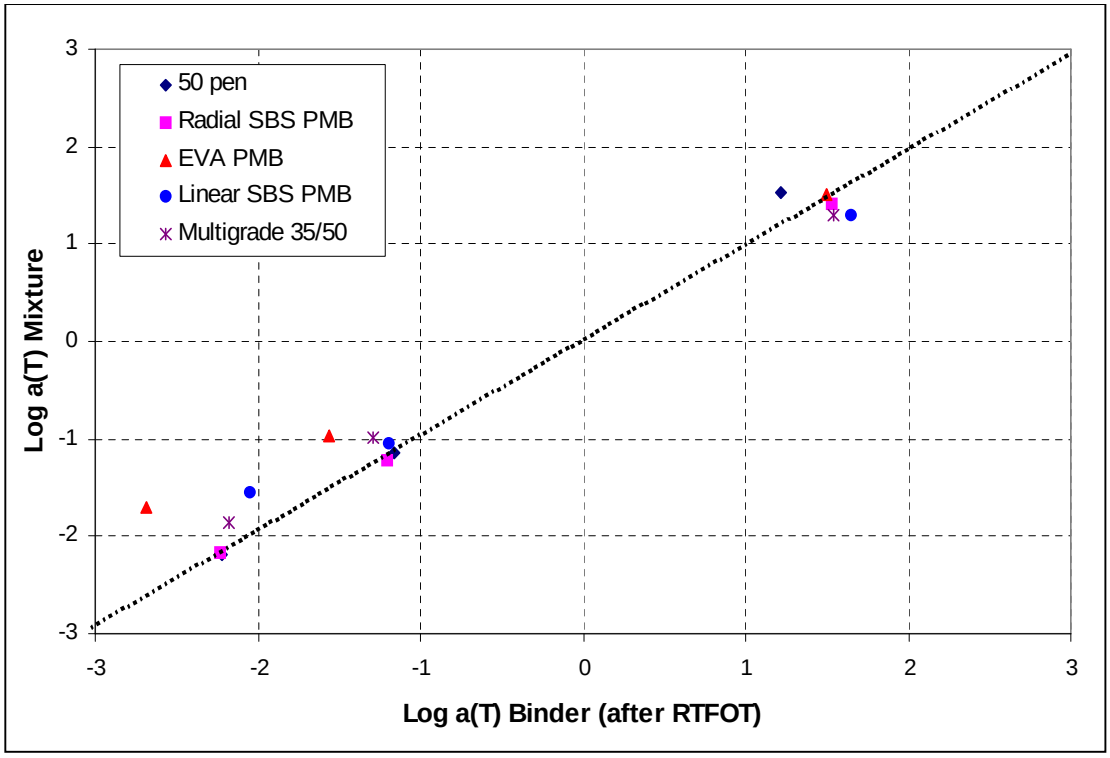

Figure 6.33: Relationship between mixture and binder shift factors

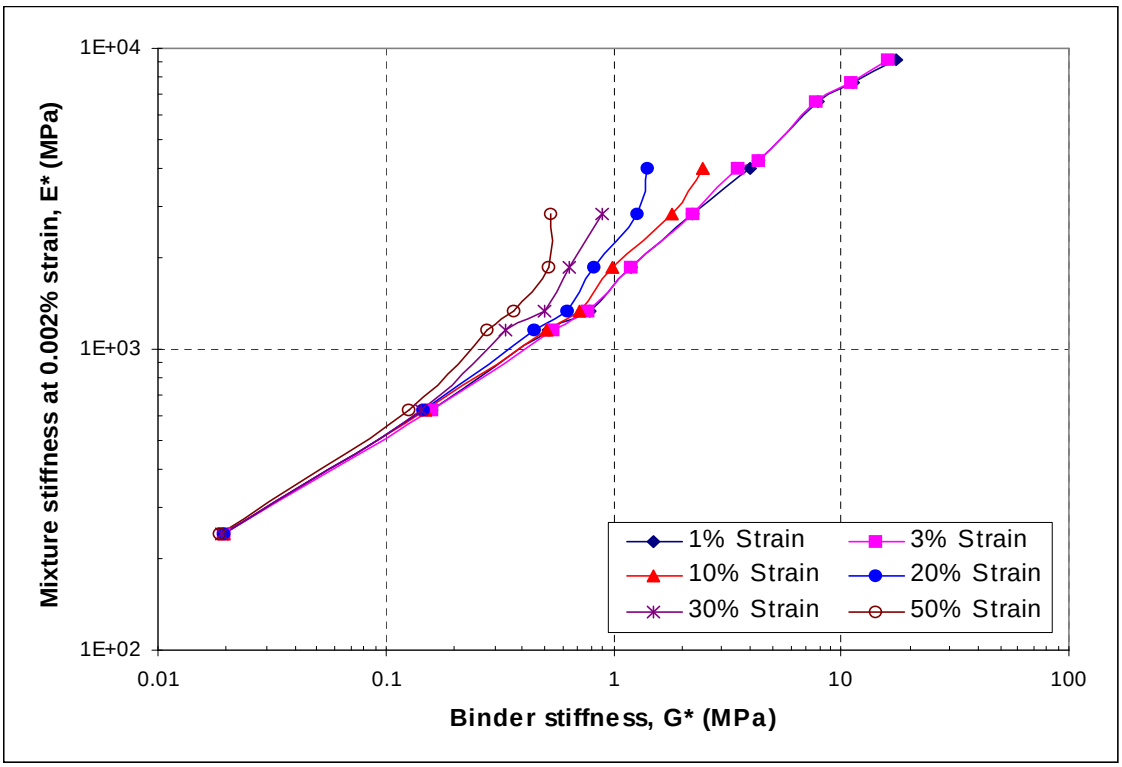

Figure 6.34: Complex modulus of DBM mixture with 50 pen bitumen at a strain level of 0.002 percent versus complex modulus of 50 pen aged bitumen at different strain levels

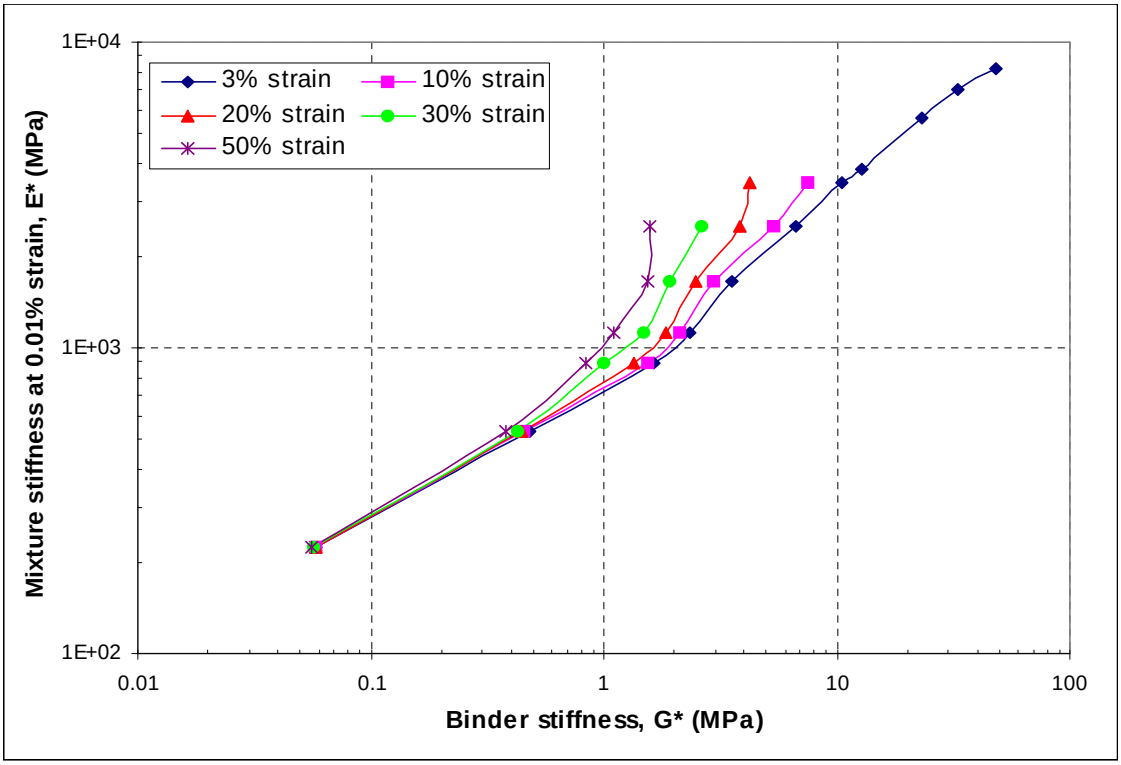

Figure 6.35: Complex modulus of DBM mixture with 50 pen bitumen at a strain level of 0.01 percent versus complex modulus of 50 pen aged bitumen at different strain levels

Chapter 7

MODELLING

7.1 Introduction

The performance of an asphalt pavement structure is significantly influenced by the stiffness modulus of the asphalt mixture layers. Therefore measurement of stiffness modulus is a fundamental part of pavement design. The stiffness modulus of asphalt mixtures can be evaluated by several direct testing procedures, for example the dynamic stiffness modulus of an asphalt mixtures can be determined by direct tension-compression, flexural, and diametral (resilient or indirect) modulus tests. However, undertaking these tests requires time and is also expensive. Therefore in order to save time and cost, several empirical and theoretical indirect predictive techniques have been produced to calculate asphalt mixture stiffness modulus. A literature review of a selective list of empirical and theoretical binder to mixture stiffness relationships were presented in Chapter Two.

The objective of this chapter is to compare asphalt mixture stiffness measured by direct tension-compression tests with selected empirical and theoretical binder to mixture stiffness relationships.

7.2 Empirical Binder to Mixture Stiffness Relationships

As mentioned in Chapter Two, empirical models of binder to mixture stiffness relationships generally involve the calculation of mixture stiffness from binder stiffness as a function of variables such as the volume concentration of the aggregate, and air voids. From the different empirical models described in Chapter Two, the Heukelom and Klomp [60], Brown [33] and Bonnaure [30] models were selected because of their relatively widespread use. Figures 7.1 to 7.3 present a comparison of mixture complex modulus computed using the binder to mixture stiffness relationships of Heukelom and Klomp, Brown, and Bonnaure to those obtained from complex modulus testing of the DBM mixture with 50 pen bitumen, HRA mixture

with radial SBS PMB and the HRA mortar with radial SBS PMB respectively. It can be seen from these figures that there is a large difference between the stiffnesses predicted by empirical methods and the experimental data. As mentioned previously, the Heukelom and Klomp model and Brown's model, which is a modification of the Heukelom and Klomp model, are based on mixture stiffnesses obtained from dynamic bending beam tests and bitumen stiffnesses obtained with conventional binder tests such as penetration and ring and ball softening point. The Bonnaure model is based on mixture stiffnesses obtained from dynamic trapezoidal tests and bitumen stiffnesses obtained with conventional binder tests such as penetration and ring and ball softening point. In terms of the experimental data, the asphalt mixture stiffnesses were obtained from direct tension-compression testing and bitumen stiffnesses using the DSR. Therefore, the differences between stiffness predicted by empirical models and that measured by the experimental method may be due to differences in the type of tests that have been used to determine binder and mixture stiffness.

7.3 Theoretical Binder to Mixture Stiffness Relationships

In the theoretical methods, mixture stiffness is calculated from binder stiffness and the volumetric proportions of asphalt mixtures through micromechanical analysis. As mentioned in Chapter Two, micromechanics is a method by which properties of composite materials, such as the stiffness modulus, can be obtained from known properties of the constituents that make up the composite. The Weng [109] and Christensen and Lo [41] models were selected from the different micromechanical models explained in Chapter Two to evaluate whether or not micromechanical models are a viable alternative to compute mixture stiffnesses from the properties of the mixture constituents. Weng developed a model of an elastic sphere isotropically dispersed in an elastic matrix and based on the Mori-Tanaka theory [75]. In this model, the mixture stiffness moduli are calculated from equations 2.74, 2.85 and 2.86 presented in Chapter Two. The Christensen and Lo model consists of an isotropic elastic spherical inclusion of radius r, which is overlapped by a concentric shell of external radius r+e. The composite sphere is embedded in an equivalent homogeneous medium whose bulk modulus (K*) and shear modulus (G*) are calculated using equations 2.80 and 2.81 presented in Chapter Two. Similar to the Weng model, the composite stiffness modulus can be calculated using equation 2.74.

The following elastic constants were selected for the two models for calculating stiffnesses of asphalt mixtures:

- (Poisson's ratio of bitumen) $\nu_b = 0.48$
- (Elastic modulus of aggregate) $E_{agg} = 100$ GPa
- (Poisson's ratio of aggregate) $\nu_{agg} = 0.15$

In addition to the above elastic constants, the parameter c has an important effect on asphalt mixture stiffnesses as calculated by Christensen and Lo model. Parameter c for each grain can be calculated from the following formula:

$$c = \frac{r}{r + e} \qquad \textbf{(7.1)}$$

Where r = radius of grain
e = binder film thickness

It can be seen from equation 7.1 that parameter c depends on the size of aggregate and binder film thickness. Therefore, an accurate prediction of mixture stiffness is definitely dependant on an accurate prediction of the thickness of the binder film over the various aggregate sizes. Duriez's [46] method was used for predicting the binder film thickness in this investigation. Duriez showed that the variation in binder thickness, e, (expressed in microns) is approximately linear in logarithmic co-ordinates with the size of grains. In this method, the thickness of the binder film coating the aggregate is derived from the following formula:

$$e = \frac{10\alpha}{S^{0.8}} \qquad \textbf{(7.2)}$$

Where: e = film thickness in microns,
α = the rich factor (dimensionless), and
S = the specific surface (in m^2)

The rich factor and the specific surface can be calculated from following formula:

$$\alpha = \frac{BC}{\sqrt[5]{S}} \quad \textbf{(7.3)}$$

$$S = \frac{6}{\rho \times d} \quad \textbf{(7.4)}$$

Where: BC = the binder content (percent)

ρ = the specific gravity of the aggregate (in kg/m^3)

d = diameter of aggregate (in mm)

Table 7.1 shows the results of film thickness and parameter c based on different aggregate sizes for different asphalt mixtures.

Table 7.1: Bitumen film thickness and parameter c for different asphalt mixtures according to aggregate size

	DBM		**HRA**		**HRA Mortar**	
d	e	c	e	c	e	c
10 mm	243	0.93	310	0.91	-	-
6 mm	146	0.93	186	0.91	-	-
Dust or Sand	81	0.93	104	0.91	148	0.88
Filler	2	0.92	2.3	0.91	3.3	0.88

Figures 7.4 to 7.6 present a comparison of mixture stiffnesses computed using the micromechanical models to the experimental results obtained from the direct tension-compression tests. It can be seen from these figures that the micromechanical models greatly underpredict measured mixture stiffnesses. The poor predictions obtained with the micromechanical models raise some questions as to the sensitivity of these models to certain input properties. Therefore, asphalt mixture stiffnesses were calculated using different input properties such as aggregate stiffness and Poisson's ratio. Figures 7.7 and 7.8 show the results of asphalt stiffnesses with different values of the aggregate stiffness and Poisson's ratio in Weng's model. It can be seen from these figures that the aggregate stiffness and Poisson's ratio of bitumen do not have a significant influence on mixture stiffness prediction using Weng's model. Therefore,

differences in stiffness prediction by this model cannot be attributed to estimations in aggregate stiffness and Poisson's ratio of bitumen. Variation of the Poisson's ratio of the aggregate were also investigated, but were not found to provide a rational explanation for the observed differences in predicted stiffness of the Weng's micromechanical model and experimental data.

Similar sensitivity analysis was conducted for the Christensen and Lo model. As shown in Figures 7.9 and 7.10, similar to Weng model, the aggregate stiffness and Poisson's ratio of bitumen do not have a significant influence on predicted stiffness. However, Figure 7.11 shows that parameter c has a significant influence on predicted stiffness using Christensen and Lo model. It can be seen from this figure that the stiffnesses computed for larger values of c are closer to the experimental results especially for high stiffness values. This indicates that the Christensen and Lo model is very sensitive to the bitumen film thickness and therefore greater accuracy in predicting the binder film thickness may improve the ability of the model to predict mixture stiffness.

Variations in aggregate stiffness, Poisson's ratio and parameter c do not explain the differences in stiffness prediction using the micromechanical models. A possible reason may be due to the large differences between bitumen and aggregate stiffness. Shapery [94] recognised that micromechanical models underpredict mixture stiffnesses and that the models were very sensitive to matrix stiffness. Buttlar and Roque [35] also observed similar discrepancies between the stiffnesses calculated by micromechanical models and those found by experimental work. They stated that the lack of modelling complexity to adequately portray interacting inclusions was a major source of the observed discrepancies.

7.4 Summary

The stiffnesses of asphalt mixtures tested in this investigation were predicted through a selection of empirical and theoretical binder to mixture stiffness relationships and compared to the mixture stiffnesses measured by direct tension-compression tests. From the different empirical models described in Chapter Two, the models of Heukelom and Klomp, Brown and Bonnaure, because of their relatively widespread

use, were selected. The results showed that there were a large differences between the stiffnesses predicted by the empirical methods and those measured experimentally.

The Weng and Christensen and Lo models were selected from the different micromechanical models described in Chapter Two to evaluate whether or not micromechanical models are a viable method to compute mixture stiffnesses from the properties of the mixture constituents. The micromechanical models greatly underpredicted measured mixture stiffnesses. The poor predictions obtained with the micromechanical models raised some concerns as to the sensitivity of these models to certain input properties. Therefore, asphalt mixture stiffnesses were calculated using different aggregate stiffnesses and Poisson's ratio values. However, there was still a large difference between the experiment results and what were predicted and calculated using these models.

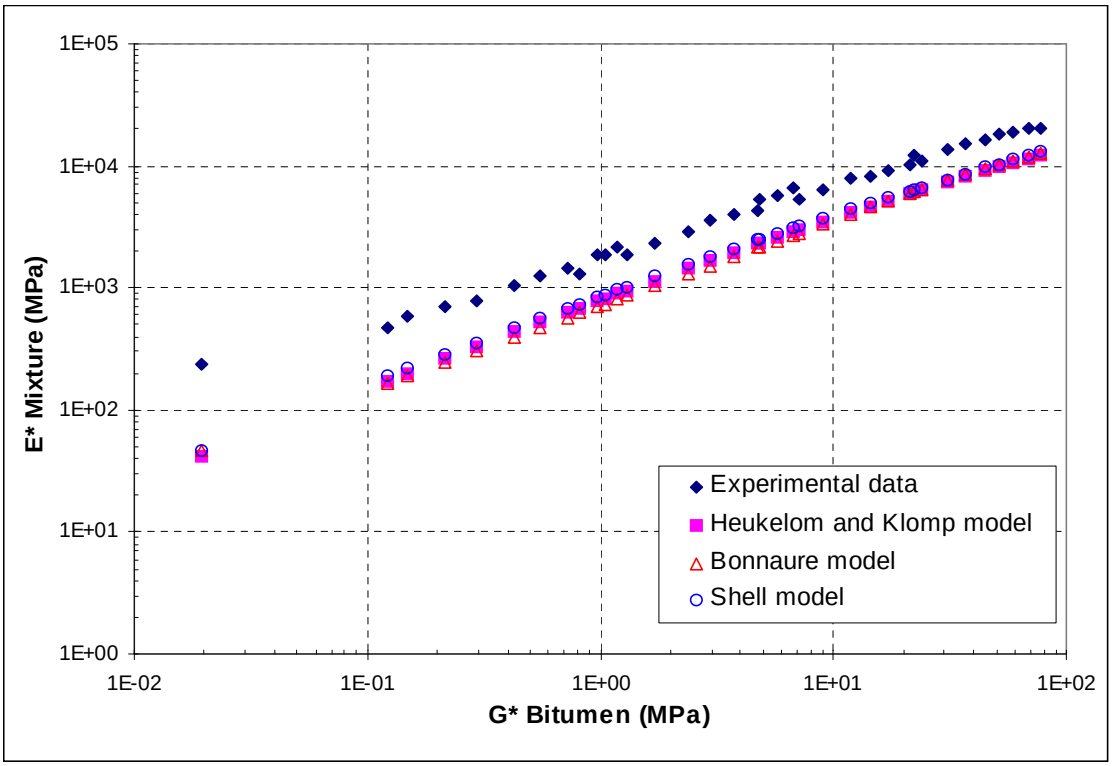

Figure 7.1: Relationship between complex modulus of bitumen and DBM mixture with 50 pen bitumen using different empirical models

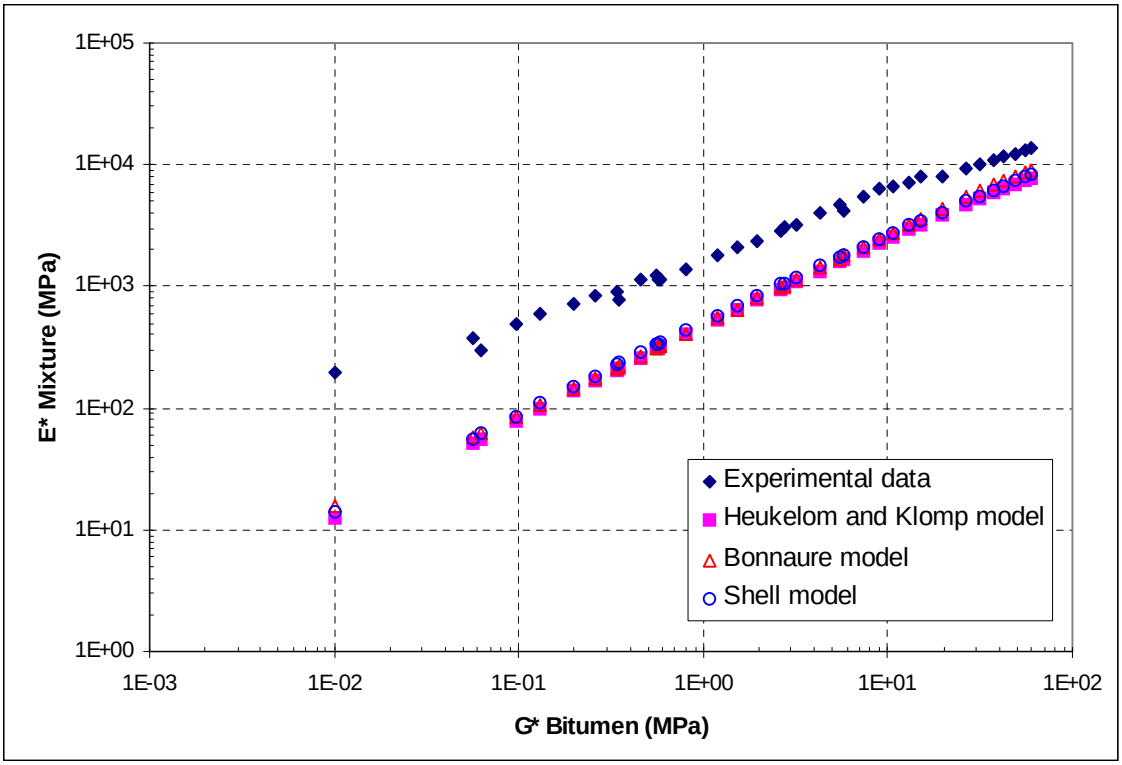

Figure 7.2: Relationship between complex modulus of bitumen and HRA mixture with radial SBS PMB using different empirical models

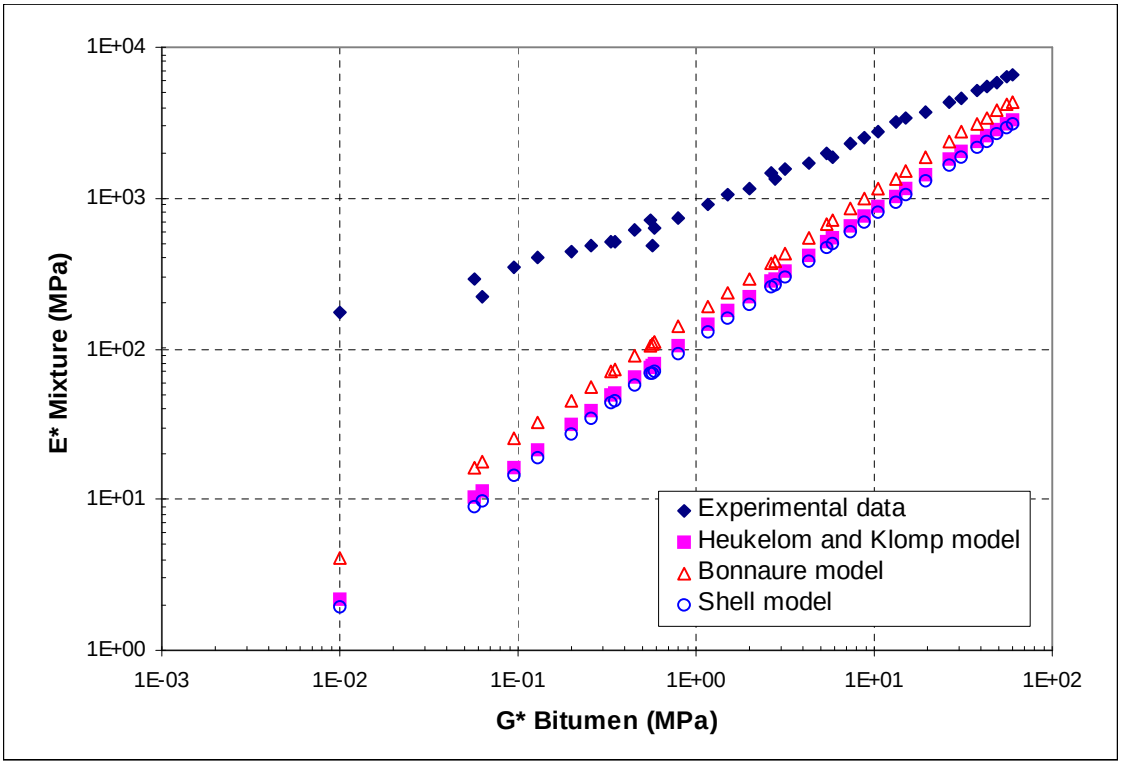

Figure 7.3: Relationship between complex modulus of bitumen and HRA mortar mixture with radial SBS PMB using different empirical models

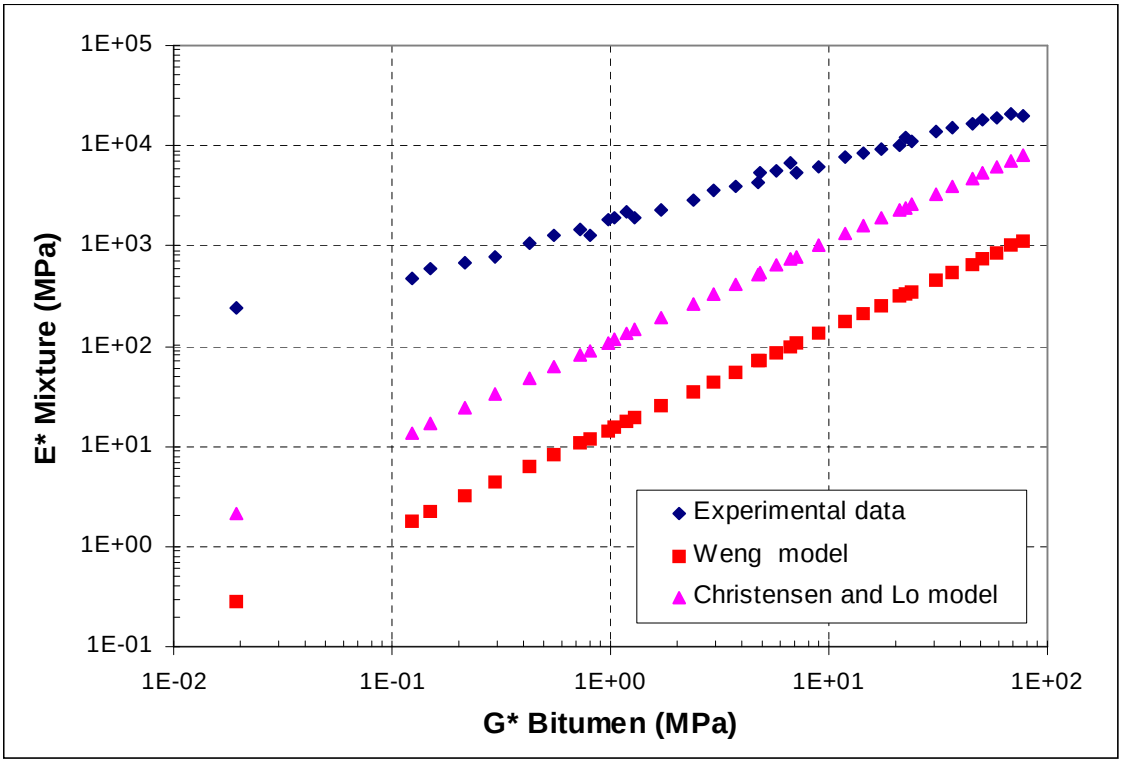

Figure 7.4: Relationship between complex modulus of bitumen and DBM mixture with 50 pen bitumen using different micromechanical models

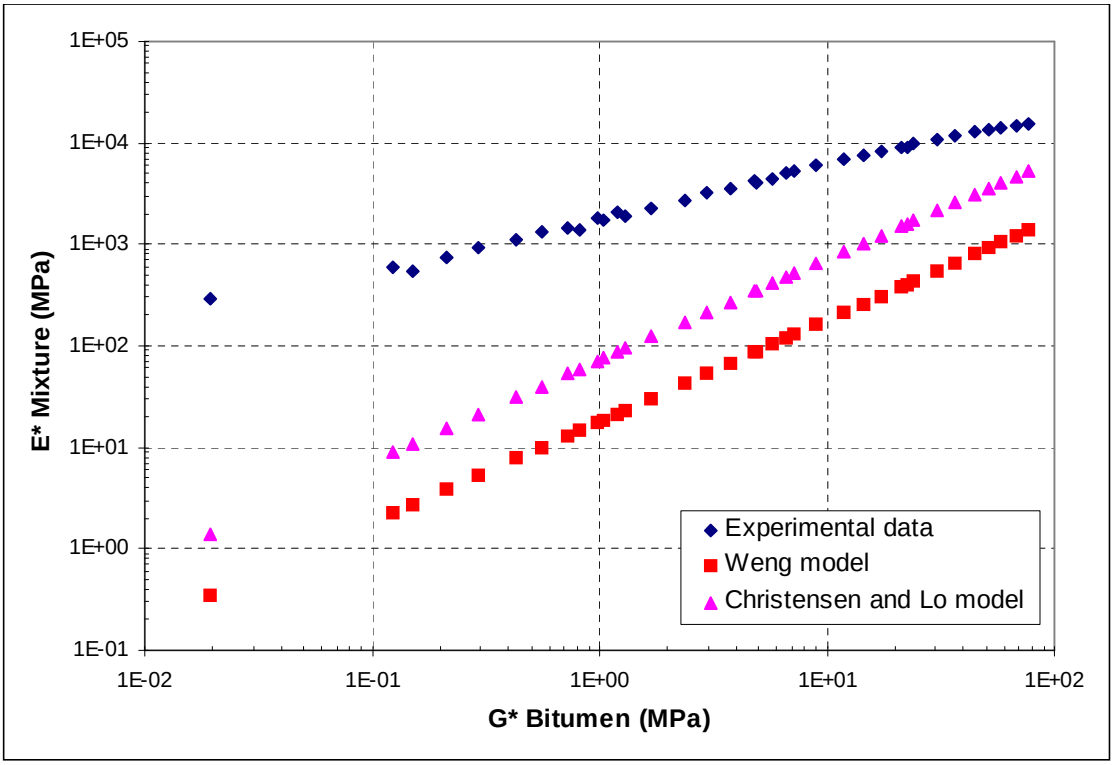

Figure 7.5: Relationship between complex modulus of bitumen and HRA mixture with 50 pen bitumen using different micromechanical models

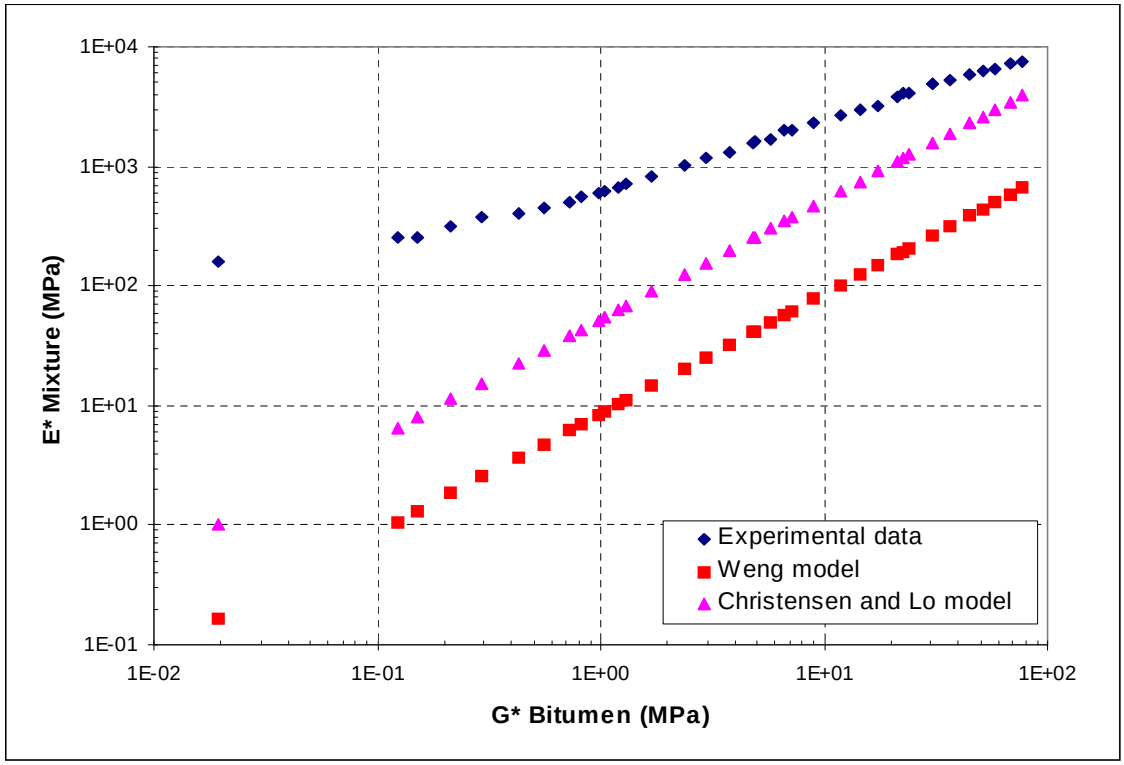

Figure 7.6: Relationship between complex modulus of bitumen and HRA mortar with 50 pen bitumen using different micromechanical models

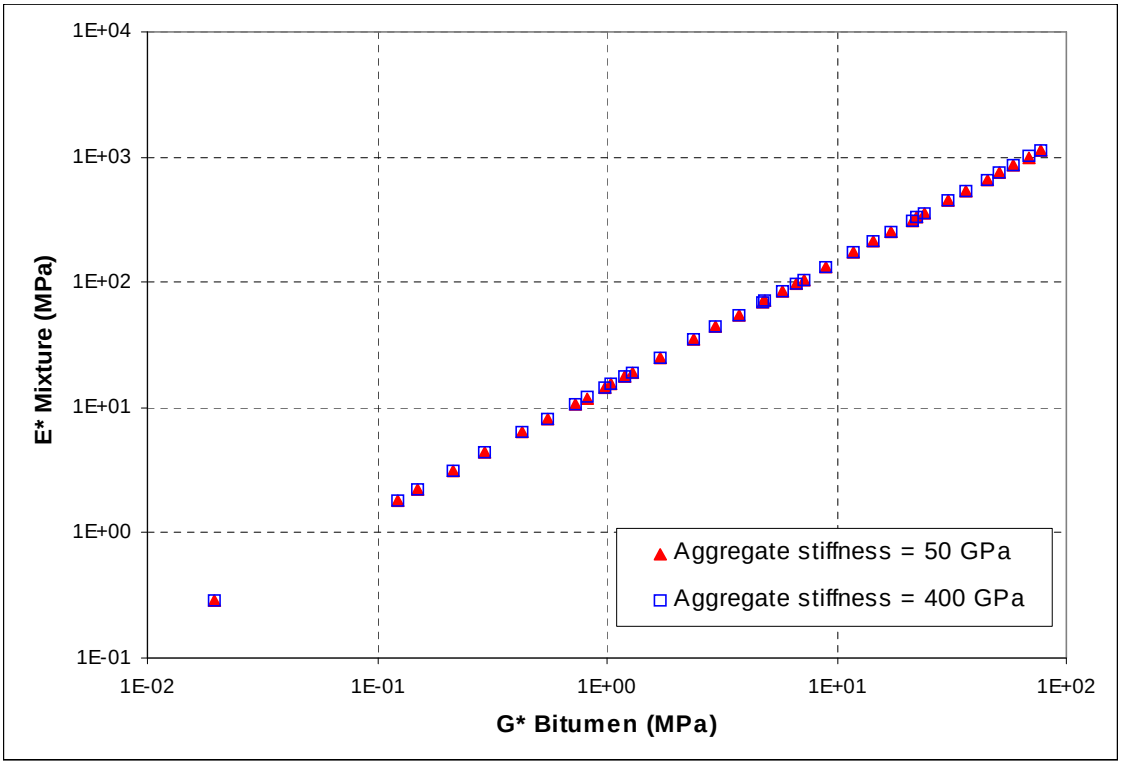

Figure 7.7: Sensitivity of Weng's model to variations in aggregate stiffness

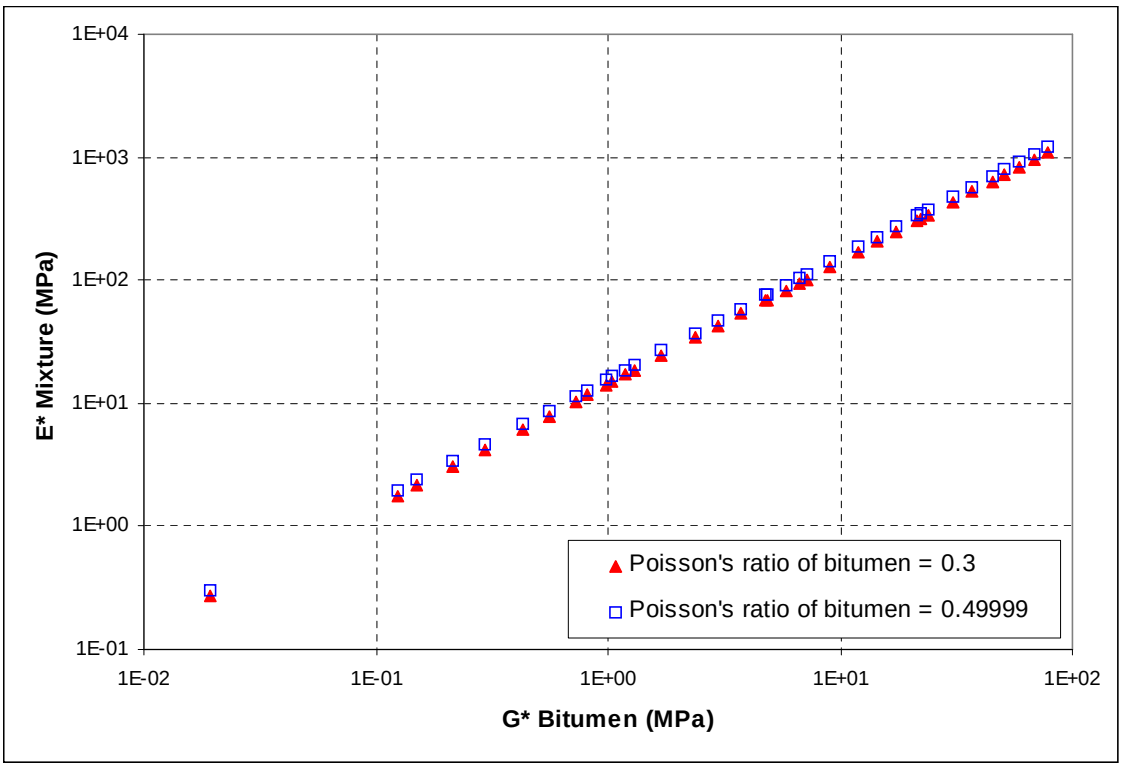

Figure 7.8: Sensitivity of Weng's model to variations in Poisson's ratio of bitumen

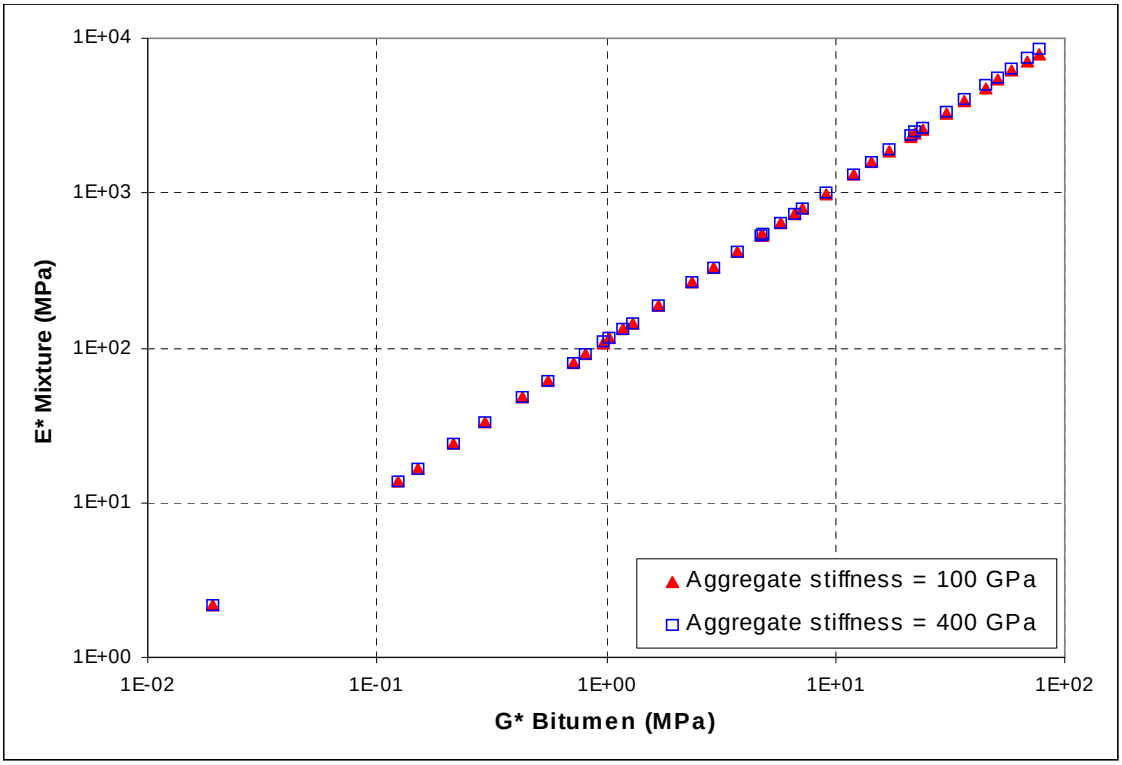

Figure 7.9: Sensitivity of Christensen and Lo model to variations in aggregate stiffness

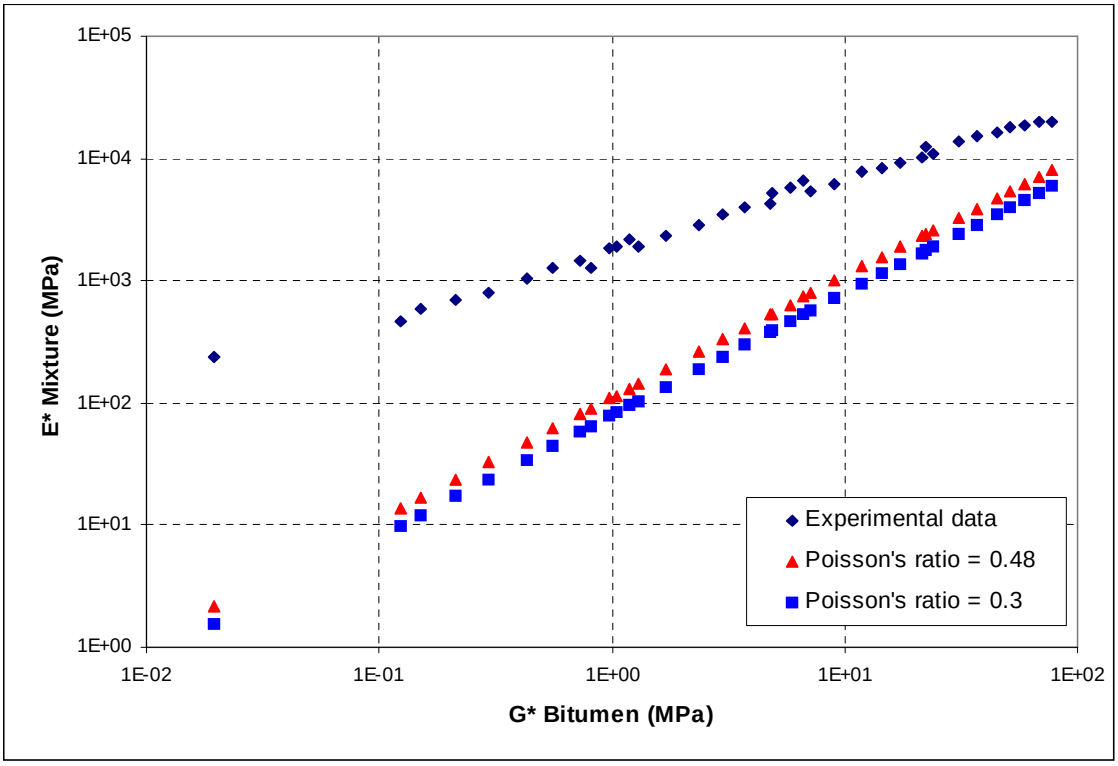

Figure 7.10: Sensitivity of Christensen and Lo's model to variations in Poisson's ratio of bitumen

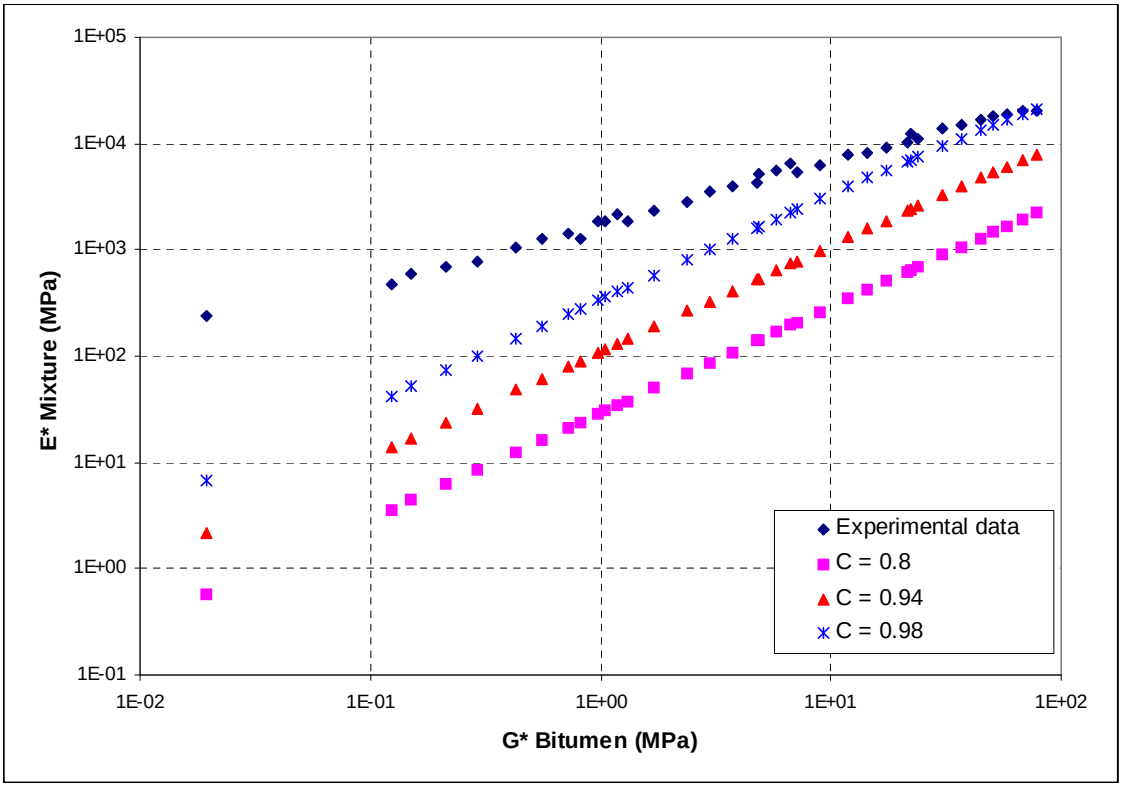

Figure 7.11: Sensitivity of Christensen and Lo model to variations in c values

Chapter 8

CONCLUSIONS AND RECOMMENDATIONS FOR FUTURE WORK

8.1 Conclusions

The conclusions presented in this chapter were drawn from the literature and experimental work undertaken in this study.

8.1.1 Experimental Investigation into DSR Limitations and Sample Preparation Methods

The following conclusions were drawn from Chapter Three dealing with the study of the limitations of the DSR and the sample preparation methods used with the DSR:

- DSR operational limitations correspond to the lower and upper limits of torque or angular deflection. Because of these limitations, the DSR cannot apply torque values below the minimum and above the maximum torque level of the instrument.
- The operational limitations of the DSR can be addressed by changing either the plate diameter or the target percentage strain amplitude. To prevent the maximum torque being exceeded, the plate diameter and strain amplitude should be reduced. To prevent the minimum torque limit being exceeded, the plate diameter and strain amplitude should be increased.
- Among the three sample preparation methods, the weighing (mass) preparation method, in general, produced specimens with the lowest G* values. In addition, this method showed a lower repeatability compared to the other two methods.
- In terms of the possible errors associated with inaccurate temperature control during DSR testing, the repeatability of each of the three sample preparation methods can be considered to be acceptable.
- For the particular DSR used in this study (Bohlin DSR50) a temperature equilibrium time of 600 seconds was found to be sufficient prior to testing. This equilibrium time should also be sufficient to allow the dissipation of any internal stresses in the sample that may have been generated during sample preparation.

- In general the silicone mould preparation method produced specimens with the highest G* values.

8.1.2 Binder Testing

The following conclusion were drawn from the binder testing investigation:

- The effect of stress level on different unmodified and modified binders was evaluated by means of stress sweep tests conducted with the DSR at different temperatures and frequencies. The results showed non-linear behaviour for all the binders.
- There was no significant narrowing of the linearity range for the modified bitumens, although the strain and stress LVE limits for Multigrade 35/50 bitumen were marginally lower than that found for the other four bitumens.
- Although, there was generally an increase in the LVE strain limit with temperature for all the bitumens, the LVE strain limit at low temperatures (10˚C and 20˚C) was relatively stable for all bitumens. Also there was a relatively stable LVE strain limit at high temperatures (60˚C and 70˚C) for the SBS PMBs.
- The process modified, plastomeric and conventional binders showed a strain dependent LVE criteria between 2% and 6% at low temperatures (high stiffness and intermediate to low phase angles) as well as a stress dependent LVE criteria between 1.5 and 7 kPa at high temperatures (low stiffness and high phase angles).
- The thermoplastic rubbers (SBS PMBs) showed, in addition to the low temperature strain criteria, a high temperature (low stiffness) polymeric-based strain dependent LVE criteria between 50% and 150%.
- The strain dependent LVE criteria for the SBS PMBs at high temperatures did translate to a narrowing of the linear range and a reduction in linearity limit over the range where the elastomeric polymer was dominant.
- In respect to the LVE strain limits as functions of phase angle, there was a strain dependent LVE criterion between 2% and 6% at intermediate to low phase angle (<55˚) (corresponding to bitumen tested at low temperatures), where bitumen behaviour is more elastic. However, at high phase angles (>55˚), there was a steady increase of the LVE strain limits for all the bitumens except for the SBS PMBs, which showed a second LVE strain criterion between 50% and 150%. In

addition all the bitumens, except for SBS PMBs, showed a stress dependent LVE criterion between 1.5 and 7 kPa at high phase angles (>80˚), where bitumen behaviour is more viscous.

- The LVE stress and strain limits were greater than the stress and strain levels recommended by the SHRP equations.
- The effect of bitumen ageing did not alter the linear limits and linearity behaviour of the unmodified bitumen and radial SBS PMB.
- Within the low frequency region (corresponding to high temperatures), the rheological behaviour of the SBS PMBs differed from that of the other bitumens. These two bitumens showed a second crossover point for G' and G" at low frequencies (stiffness values below approximately 10^3 Pa), which indicated that these bitumens began to display a dominant elastic behaviour at low frequencies due to the SBS polymer.
- Three viscoelastic regions were observed from the master curves of the five bitumens. These three regions were related to high, intermediate and low frequency domains (corresponding to low, intermediate and high temperatures). In the first region, all the binders exhibited dominant elastic behaviour with minor differences between the viscoelastic properties of the bitumens. As frequency decreased or temperature increased, the SBS PMBs started to show differences in viscoelastic behaviour compared to the other binders. This was extremely noticeable in the phase angle master curves where the SBS polymers begin to significantly improve the elasticity of the modified binders at intermediate frequencies. The results also showed that there was a plateau in the loss tangent master curves for the SBS PMBs in the intermediate frequency range (between 0.01 and 1 Hz). At very low frequencies (corresponding to high temperatures), all the bitumens, except for the SBS PMBs, started to lose their elasticity and approach a viscous state. This was seen as a dramatic increase in the loss tangent for these bitumens at low frequencies.

8.1.3 Mixture Testing

The following conclusions were drawn from the asphalt mixture tests presented in Chapter Five:

- Non-linear behaviour was evident for all the DBM, HRA and HRA mortar mixtures studied at all test temperatures and frequencies.
- The LVE limits of the asphalt mixtures were found to be strain dependent rather than stress dependent.
- The linear viscoelastic strain limit was found to be between 20 and 100 microstrain for all the DBM and HRA mixtures and between 50 and 150 microstrain for all the HRA mortar mixtures.
- Isochronal plots of the asphalt mixtures showed that there was not a continuous increase in phase angle with increasing temperature, but rather an increase up to a peak phase angle followed by a subsequent decrease. This behaviour highlights the increased dominance of the aggregate skeleton at high temperatures resulting in lower phase angles and increased elastic response compared to higher phase angles and increased viscous response found for bituminous binders.
- The isochronal plots of phase angle for the different asphalt mixtures were similar, although the HRA mortar demonstrated greater elastic response (lower phase angles) at high temperatures compared to the larger aggregate sized DBM and HRA mixtures.
- The complex modulus values for the HRA mortar were approximately 50% less than those found for the DBM and HRA mixtures. This was due to the lower aggregate volume and higher air voids content of the mortar compared to the DBM and HRA asphalt mixtures.
- In terms of binder type, there were differences in complex modulus and phase angle for the asphalt mixtures incorporating these binders, particularly at intermediate temperatures and loading frequencies where the binder's unique rheological properties are evident and to a certain extend at low temperatures where the stiffness of the base bitumen is important.
- All the asphalt mixtures tended to converge towards the same phase angle versus loading frequency relationship at high frequencies (low temperatures). This can be attributed to the high elastic response of both bituminous binders and asphalt

mixtures at low temperatures and high frequencies irrespective of binder type. Over the central frequency region, the phase angle master curves of the five DBM mixtures differed considerably. It was within this central region that the unique rheological properties of the conventional, process and polymer modified bitumens have the greatest influence on the rheological properties of the asphalt mixtures. Finally, although the testing was limited to a maximum temperature of 40°C, there is an indication that at low frequencies (high temperatures) the master curves of the different mixtures start to converge to a second unique phase angle versus frequency relationship as the viscoelastic response of the mixtures become dominated by the aggregate structure.

8.1.4 Relation between Bitumen and Asphalt Mixture Rheology

The following conclusions were drawn from the investigation of the relationship between bitumen and asphalt mixture rheological parameters in Chapter Six:

- The bitumen to mixture complex modulus relationship in the linear region was found to be independence of temperature. In other words, for a given bitumen stiffness, there is a unique corresponding mixture stiffness.
- The bitumen to mixture complex modulus relationship for the EVA PMB and linear SBS PMB binders was found to be temperature dependence. In other word, for a given binder stiffness, there was not a unique corresponding mixture stiffness.
- The HRA mortar with 50 pen bitumen and radial SBS PMB showed similar binder to mixture stiffness relationships at high binder stiffnesses (corresponding to low temperatures) but the HRA mortar with radial SBS PMB had higher stiffnesses at low binder stiffnesses (corresponding to high temperatures).
- Similar bitumen to asphalt mixture phase angle relationships were observed at low bitumen phase angles ($\leq 45^{o}$) for all the bitumens. This can be attributed to the properties of the asphalt mixtures being solely dependent on bitumen properties and volumetric proportions of the asphalt mixture. However, dispersions were seen in the bitumen-asphalt mixtures phase angle relationships at high bitumen phase angles ($> 45^{o}$). This indicates that other parameters, such as aggregate grading, shape, texture and degree of interlock, and the method and degree of

compaction, become significant in addition to the binder and the volumetric proportions of the asphalt mixture. Asphalt mixture phase angles started to decrease at bitumen phase angles between 55 and 70º due to the increased influence of the aggregate skeleton on asphalt mixture properties at high temperatures and low frequencies resulting in increased elastic behaviour of the asphalt mixtures.

- A comparison of asphalt mixture and bitumen master curves showed that the relationship between the rheological behaviour of the asphalt mixtures and bitumens could be divided into three regions. At high frequencies (corresponding to low temperatures) all the binders and asphalt mixtures begin to approach an asymptotic behaviour corresponding to the glassy limiting stiffness modulus of the bitumen. As frequency decreases (corresponding to increasing temperature) both the bitumen and asphalt mixture stiffness decreases. As the frequency decreases further (corresponding to high temperatures $\geq$ 40ºC), the complex modulus of the bitumens continue to decrease, however the complex modulus of the asphalt mixtures approach a plateau due to the effect of aggregate interlock.
- A direct relationship between binder and asphalt mixture shift factors was identified for the DBM, HRA and HRA mortar mixtures.
- The relationship between bitumen and asphalt mixture complex modulus in the non-linear region was found to be a function of the non-linear behaviour of both the bitumen and asphalt mixture.

8.1.5 Modelling

The following conclusions were drawn from Chapter Seven dealing with the evaluation of some empirical and theoretical models relating binder and asphalt mixture stiffness:

- There was a large difference between the stiffness predicted by empirical methods and that generated experimentally.
- The micromechanical models greatly underpredicted asphalt mixture stiffnesses.
- The sensitivity analysis of the micromechanical models to input parameters such as aggregate stiffness and Poison's ratio was found to be minimal.

8.2 Recommendation for Future Research

Based upon the findings and conclusions of this study, the following recommendations for future work are made:

- In this investigation, the DSR testing was performed with the parallel plate geometry. Using the parallel plate geometry results in a change of shear stress and strain at distances from the centre of the testing geometry. It is, therefore, recommended that a cone and plate geometry be used for DSR linearity testing.
- Although different kinds of unmodified and modified bitumens were tested in this study, it is recommended that bitumens with different percentages of modifier with the same base bitumen be tested to investigate the effects of the modification on the LVE limits of modified binders.
- The research in this thesis concentrated on linear and non-linear viscoelastic behaviour of bitumens at moderate and high temperatures. It is, therefore, recommended to investigate the non-linear properties of different bitumens, especially PMBs, at low temperatures using the Direct Tension Tester (DTT).
- Evaluation of long term ageing and a further evaluation of short term ageing effects on the LVE limits of unmodified and modified binders is recommended. This can be accomplished by an experimental study of PAV aged bitumens.
- The investigation described in this thesis involved dynamic modulus testing of asphalt mixtures in tension-compression using sinusoidal axial loading. In order to investigate the effect of tension or compression loading on asphalt mixture linearity, dynamic tension and compression tests are recommended.
- Since there are large differences in stiffness between the binder and aggregate in an asphalt mixture, most of the bulk strain will be in the binder domain. Therefore, by accurately estimating the strain in the binder using image analysis and finite element methods, an accurate relationship between the stiffness of binders and asphalt mixtures may be established.
- At low asphalt mixture stiffness values there is an indication that there may be a stress dependent LVE criterion similar to that found for the binders. Unfortunately, the asphalt mixture linearity study was limited to a maximum temperature of 40°C and further tests at higher temperatures would be required to substantiate this possible stress dependent LVE behaviour.

- The temperature dependent binder to mixture relationship for asphalt mixtures produced with EVA and linear SBS PMBs may be due to an interaction between the filler and binder in these asphalt mixtures. It is therefore recommended that the effect of fillers on different unmodified and modified binders at different temperatures be investigated. This could be done by performing DSR tests on binders before and after mixing with fillers to find the effect of fillers on binder stiffness at different temperatures.

References

[1] Annual Book of ASTM Standards, ASTM D 1754-87, Standard Test Method for Effect of Heat and Air on Asphaltic Materials (Thin-Film Oven Test), Vol. 04.03, Philadelphia, pp. 231-233, 1991.

[2] Annual Book of ASTM Standards, ASTM D 2170-85, Standard Test Method for Kinematic Viscosity of Asphalt (Bitumens), Philadelphia, pp. 260-268, 1991.

[3] Annual Book of ASTM Standards, ASTM D 2171-88, Standard Test Method for Viscosity of Asphalt by Vacuum Capillary Viscometer", Philadelphia, pp. 269-275, 1991.

[4] Annual Book of ASTM Standards, ASTM D 2872-88, Standard Test Method for Effect of Heat and Air on a Moving Film of Asphalt (Rolling Film Oven Test), Vol. 04.03, Philadelphia, pp. 315-318, 1991.

[5] British Standard 2000: Part 49, Penetration of Bituminous Materials, 1983.

[6] British Standard 2000: Part 58, Softening Point of Bitumen (Ring and Ball), 1983.

[7] Coated Macadam for Roads and other Paved Area, British Standard Institution, BS 4987: Part 1, 1988.

[8] Determination of the complex Shear Modulus and Phase Angle of Bituminous Binders - Dynamic Shear Rheometer (DSR) Method, Institute of Petroleum, IP PM CM/99, 1999.

[9] Glossary of Rheological Terms - A Practical Summary of the Most Common Concepts, Rheology of Bituminous Binders, Edited by Eurobitumen, 1996.

[10] Hot Rolled Asphalt for Roads and other Paved Areas, British Standard Institution, BS 594: Part 1, 1992.

[11] Manual of Contract Documents for Highway Works: Volume 1, Specification for Highway Works, 1998.

[12] Methods for Determination of the Indirect Stiffness Modulus of Bituminous Materials, British Standard Institution, DD213, 1993.

[13] Standard Method of Test for Determining the Rheological Properties of Asphalt Binder Using a Dynamic Shear Rheometer (DSR), AASHTO Designation: TP5, Washington, D. C., 1994.

[14] Standard Practice for Long-Term Ageing of Asphalt Concrete Mixtures, SHRP No. 1030, Strategic Highway Research Program, National Research Council, Washington, D. C., 1992.

[15] Standard Practice for Short-Term Ageing of Asphalt Concrete Mixtures, SHRP No. 1030, Strategic Highway Research Program, National Research Council, Washington, D. C., 1992.

[16] Airey, G. D., Rheological Characteristics of Polymer Modified and Aged Bitumens, University of Nottingham, PhD Thesis, 1997.

[17] Airey, G. D., and Brown, S. F., "Rheological Performance of aged Polymer Modified Bitumens" *Journal of the Association of Asphalt Paving Technologists*, vol. 67, pp. 66-100, 1998.

[18] Anderson, D. A., and Kennedy, T. W., "Development of SHRP binder Specification" *Journal of the Association of Asphalt Paving Technologists*, vol. 62, pp. 481-507, 1993.

[19] Anderson, D. A., Christenson, D. W., and Bahia, H. U., "Physical Properties of Asphalt Cement and the Development of Performance-Related

Specifications" *Journal of the Association of Asphalt Paving Technologists*, vol. 60, pp. 437-475, 1991.

[20] Anderson, D. A., Christenson, D. W., Bahia, H. U., Dongre, R., Sharma, M. G., Antle, C. E., and Button, j., "Binder Characterization and Evaluation, Volume 3: Physical Characterization" Strategic Highways Research Program, National Research Council, Washington, D. C., SHRP-A-369, 1994.

[21] Bahia, H. U., "Critical Evaluation of Asphalt Modification Using Strategic Highway Research Program Concepts" Transportation Research Record, Washington, D.C., 1488 (Materials and Construction), pp. 82-88, 1995.

[22] Bahia, H. U., and Anderson, D. A., "The Development of the Bending Beam Rheometer; Basic and Critical Evaluation of the Rheometer" American Society for Testing and Materials, Philadelphia, Physical Properties of Asphalt Cement Binders: ASTM STP 1241, pp. 28-50, 1995.

[23] Bahia, H. U., and Anderson, D. A., "The New Proposed Rheological Properties of Asphalt Binders: Why are they Required and how do they Compare to Conventional Properties", Physical Properties of Asphalt Cement Binders: ASTM STP 1241, Philadelphia, pp. 1-27, 1995.

[24] Bahia, H. U., and Anderson, D. A., "The Pressure Aging Vessel (PAV): A Test to Simulate Rheological Changes Due to Field Aging", Physical Properties of Asphalt Cement Binders: ASTM STP 1241, Philadelphia, pp. 67-88, 1995.

[25] Bahia, H. U., Anderson, D. A., and Christensen, D. W., "The Bending Beam Rheometer; A Simple Device for Measuring Low Temperature Rheology of Asphalt Binders" *Journal of the Association of Asphalt Paving Technologists*, vol. 61, pp. 117-153, 1992.

[26] Bahia, H. U., Hislop, W. P., Zhai, H., and Rangel, A., "Classification of Asphalt Binders Into Simple and Complex Binders" *Journal of the Association of Asphalt Paving Technologists*, vol. 67, pp. 1-41, 1998.

[27] Bahia, H. U., Perdomo, D., and Turner, P., "Applicability of Superpave Binder Testing Protocols to Modified Binders" *Transportation Research Record, No. 1586*, pp. 16-23, 1995.

[28] Bahia, H. U., Zhai, H., Bonnetti, K., and Kose, S., "Non-Linear Viscoelastic and Fatigue Properties of Asphalt Binders" *Journal of the Association of Asphalt Paving Technologists*, vol. 68, pp. 1-34, 1999.

[29] Bell, C. A., AbWahab, Y., and Cristi, M. E., "Investigation of Laboratory Ageing Procedure for Asphalt-Aggregate Mixtures" Transportation Research Record, TRB, National Research Council, Washington, D.C., No. 1323 (Materials and Construction), pp. 32-46, 1991.

[30] Bonnaure, F., Gest, G., Gravois, A., and Uge, P., "A New Method of Predicting the Stiffness of Asphalt Paving Mixtures" *Journal of the Association of Asphalt Paving Technologists*, vol. 46, pp. 64-104, 1977.

[31] Bouldin, M., "Discussion to California Desert Test Road-A Step Closer to Performance Based Specifications" By Reese R. E. and Goodrich, J. L." *Proceedings of Association of Asphalt Paving Technologists*, vol. 62, pp. 294-297, 1993.

[32] Boussad, N., Croix, P. D., and Dony, A., "Prediction of Mix Modulus and Fatigue Law from Binder Rheological Properties" *Journal of the Association of Asphalt Paving Technologists*, pp. 40-72, 1996.

[33] Brown, S. F., "Bituminous Pavements: Materials, Design and Evaluation" Department of Civil Engineering, University of Nottingham, Nottingham, U.K., 1992.

[34] Brown, S. F., Cooper, K. E., Gibb, J. M., Read, J. M., and Scholz, T. V., "Practical Tests for Mechanical Properties of Hot Mix Asphalt" presented at Proceedings of the 6th Conference on asphalt Pavement for Southern Africa, Cape Town, South Africa, pp. 29-45, 1994.

[35] Buttlar, W. G., and Roque, R., "Evaluation of Empirical and Theoretical Models to Determine Asphalt Mixture Stiffnesses at Low Temperatures" *Journal of the Association of Asphalt Paving Technologists*, vol. 65, pp. 99-141, 1996.

[36] Button, J. W., and Epps, J. A., "Identifying Tender Asphalt Mixtures in the Laboratory" *Transportation Research Record 1034*, pp. 20-26, 1985.

[37] Carswell, J., Claxton, M. J., and Green, P. J., "Dynamic Shear Rheometers: Making Accurate Measurements on Bitumens" Institute of Asphalt Technology, Proceedings of the Asphalt Yearbook 1997, pp. 79-84, 1997.

[38] Cheung, C. Y., and Cebon, D., "Experimental Study of Pure Bitumens in Tension, Compression, and Shear" *Journal of Rheology*, vol. 41, pp. 45-73, Jan/Feb 1997.

[39] Cheung, C. Y., and Cebon, D., "Thin Film Deformation Behaviour of Power-Law Creeping Materials" *ASCE Journal of Engineering Mechanics*, vol. 123(11), pp. 1138-1152, July/ Dec 1997.

[40] Christensen, D. W., and Anderson, D. A., "Interpretation of Dynamic Mechanical Test Data for Paving Grade asphalt Cements" *Journal of the Association of Asphalt Paving Technologists*, vol. 61, pp. 67-116, 1992.

[41] Christenson, R. M., and Lo, K. H., "Solutions for Effective Shear Properties in Three Phase Sphere and Cylinder Models" *Journal of the Mechanics and Physics of Solids*, vol. 27, pp. 315-330, 1979.

[42] Collins, J. H., Bouldin, M. G., Gelles, R., and Berker, A., "Improved Performance of Paving Asphalts by Polymer Modification" *Journal of the Association of Asphalt Paving Technologists*, vol. 60, pp. 43-79, 1991.

[43] Dickinson, E. J., and Witt, H. P., "The Dynamic Shear Modulus of Paving Asphalts as a Function of Frequency" *Transportations of the Society of Rheology*, vol. 18, No. 4, pp. 591-606, 1974.

[44] Dobson, G. R., "The Dynamic Mechanical Properties of Bitumen" *Journal of the Association of Asphalt Paving Technologists*, vol. 38, pp. 123-139, 1969.

[45] Dongre, R., Ramaiah, S., and Dangelo, J., "Use of Viscosity Standard Fluid to Control Quality of Rheological Measurements for Characterizing Asphalt Binders" *Transportation Research Record, No. 1586*, pp. 24-31, 1996.

[46] Duriez, M., "Traite de materiaux de construction" presented at Ed. Dunod, Paris, 1950.

[47] Ferry, J. D., *Viscoelastic Properties of Polymers*. New York: Joun Wiley & Sons Inc., Third Edition, 1980.

[48] Flugge, W., *Viscoelasticity*, Second Revised Edition ed., New York: Springer-Verlang, 1975.

[49] Francken, L., Vanelstraete, A., and Verhasselt, A., "Long Term Ageing of Pure and Modified Bitumen : Influence on the Rheological Properties and Relation with the Mechanical Performance of Asphalt Mixtures" pp. 1259-1278, 1996.

[50] Gahvari, F., "Effects of Thermoplastic Block Copolymers on Rheology of Asphalt" *Journal of Materials in Civil Engineering*, vol. 9, No. 3, pp. 111-116, Aug. 1997.

[51] Gardner, L. J., and Skok, E. L., "Use of Viscoelatic Concepts to Evaluate Laboratory Test results and Field Performance of Some Minnesota Asphalt Mixtures" presented at Proceedings, Second International Conference on the Structural Design of Asphalt Pavements, Ann Arbor, Michigan, pp. 1018, 1967.

[52] Goodrich, J. L., "Asphalt and Polymer Modified asphalt Properties Related to the Performance of Asphalt Concrete Mixes" *Proceedings of the Association of Asphalt Paving Technologists*, vol. 55, pp. 116-175, 1988.

[53] Goodrich, J. L., "Asphaltic Binder Rheology, Asphalt Concrete Rheology and Asphalt Concrete Mix Properties" *Journal of the Association of Asphalt Pavings Technologists*, vol. 60, pp. 80-120, 1991.

[54] Grandiner, M. S., and Newcomb, D., "Evaluation of Rheological Measurements for Unmodified and Modified Asphalt Cements" *Journal of Transportation Research Record, No. 1488*, pp. 72-81, 1995.

[55] Gregg, L. E., and Alcocke, W. H., "Investigation of Rubber Additives in Asphalt Paving Mixtures" *Proceedings of Association of Asphalt Paving Technologists*, vol. 23, pp. 28, 1954.

[56] Hashin, Z., and Shtrikman, S., "A Variational Approach to the Theory of the Elastic Behaviour of Multiphase Materials" *Journal of Mechanics and Physics of Solids*, vol. 11, pp. 126-140, 1963.

[57] Hastead, W. J., "Relation of Asphalt Chemistry to Physical Properties and Specifications" *Proceedings of the Association of Asphalt Paving Technologists*, vol. 54, pp. 91-117, 1985.

[58] Hayton, B., "Bitumen Rheology and the Bohlin Dynamic Shear Rheometer" Scott Wilson Pavement Engineering, pp. 1-13, 1998.

[59] Herve, A., and Zaoui, a., "Modelling the Effective Behaviour of Non-linear Matrix-inclution Composites" *European Journal of Mechanics, A/Solids*, vol. 9, No. 6, pp. 505-515, 1990.

[60] Heukelom, W., and Klomp, A. J. G., "Road Design and Dynamic Loading" *Journal of the Association of Asphalt Paving Technologists*, vol. 33, pp. 92-125, 1964.

[61] Hicks, R. G., Finne, F. N., Monismith, C. L., and Leahy, R. B., "Validation of SHRP Binder Specification Through Mix Testing" *Journal of the Association of Asphalt Paving Technologists*, vol. 62, 1993.

[62] Hoban, T., "Modified Bitumen Binders for Surface Dressing" *Chimistry and Industry*, pp. 538-542, 1990.

[63] Jongepier, R., and Kuilman, B., "Characteristics of the Rheology of Bitumens" *Journal of the Association of Asphalt Paving Technologists*, vol. 38, pp. 98-121, 1968.

[64] Kallas, B. F., "Dynamic Modulus of Asphalt Concrete in Tension and Tension-Compression" *Proceedings of the Association of Asphalt Paving Technologists*, vol. 39, pp. 1-23, 1970.

[65] Kandhal, P. S., and Chakraborty, S., "Effect of Asphalt Film Thickness on Short- and Long-Term Ageing of Asphalt Paving Mixtures" Transportation Research Record, Washington, D.C., No. 1535 (Materials and Construction), pp. 83-90, 1996.

[66] Kerbs, R. D., and Walker, R. D., *Highway Materials*, New York: Mc-Graw Hill, 1971.

[67] Kerner, K. W., "The Elastic and Thermoelastic Properties of Composite Media" *Proceedings of the Physical Society (B)*, vol. 69, pp. 808, 1956.

[68] Kim, Y. R., and Lee, Y. C., "Interrelationships Among Stiffnesses of Asphalt-Aggregate Mixtures" *Journal of the Association of Asphalt Paving Technologists*, vol. 64, pp. 575-606, 1995.

[69] King, G. N., and King, H. W., "Polymer Asphalt Overview, Solution for Pavement Rehabilitation Problem" ASCE, New York, pp. 240-254, 1986.

[70] Lancaster, I., "Polymer Chemistry and Polymerisation" Nynas Network, Issue No. 3, Summer 1996.

[71] Louis, A. R., "Limits of Linear Viscoelastic Behaviour of an Asphalt Concrete in Tension nd Compression" Civil Engineering, University of California, Berkeley, PhD Thesis, 1973.

[72] Mcleod, N. W., "A 4 Year Survey of Low Temperature Transverse Pavement Cracking on Three Ontario Test Roads" *Proceedings of the Association of Asphalt Paving Technologists*, vol. 41, pp. 424-493, 1972.

[73] Monismith, C. L., and Secor, K. E., "Viscoelastic Behaviour of Asphalt Concrete Pavements" presented at International Conference of the Structural Design of Asphalt Pavements Proceedings, University of Michigan, USA, pp. 476-498, August 1963.

[74] Monsmith, C. L., Alexander, R. L., and Secor, K. E., "Rheological Behaviour of Asphalt Concrete" *Proceedings of Association of Asphalt Paving Technologists*, vol. 35, pp. 400-450, 1966.

[75] Mori, T., and Tanaka, K., Average Stress in Matrix and Average Elastic Energy of Materials with Misfitting Inclusions, *Acta Metallurgica*, vol. 21, pp. 571, 1973.

[76] Mortazavi, M., and Moulthrop, J. S., "The SHRP Materials Reference Library, Report SHRP-A-64" Strategic Highway Research Program, National Reserch Council, Washington, D. C., 1993.

[77] Nellensteyn, F. J., "Bereiding en Constitutie van Asphalt (Manufacture and Constitution of Asphalt Bitumen)" *Dissertatie Technische Hoogesshool, Delft*, 1923.

[78] Newman, J. K., "Dynamic Shear Rheological Properties of Polymer-Modified Asphalt Binders" *Journal of Elastomers and Plastics*, vol. 5, No. 4, pp. 245-263, 1998.

[79] Pagan, C. A., "Size and Thermological Relationships of Asphaltic Concrete" *Proceedings of the Association of Asphalt Paving Technologists*, vol. 37, pp. 228, 1968.

[80] Pagan, C. A., and Ku, B., "Effect of Asphalt Viscosity on Rheological Properties of Bituminous Concrete" Highway Research Record, No. 104, Highway Research Board, Washington, D. C., pp. 17, 1965.

[81] Pagen, C. A., "Rheological Response of Bituminous Concrete" Highway Research Record, No. 67, Highway Research Board, Washington, D.C., pp. 1-26, 1965.

[82] Paul, B., "Prediction of Elastic Constants of Multiphase Materials" *Journal of Applied Mechanics*, vol. 36, pp. 218, 1960.

[83] Pell, P. S., "Discussion, Session IV" presented at Proceedings, International Conference on the Structural Design of Asphalt Pavements, Ann Arbor, Michigan, pp. 386-387, 1962.

[84] Pell, P. S., and Taylor, I. F., "Asphaltic Road Materials in Fatigue" *Proceeding of the Association of Asphalt Paving Technologists*, vol. 38, pp. 371-422, 1969.

[85] Petersen, J. C., Robertson, R. E., Branthaver, J. F., Harnsberger, P. M., Duvall, J. J. , Kim, S. S., Anderson, D. A., Christenson, D. W., Bahia, H. U., Dongre,

R., Sharma, M. G., Antle, C. E. , Button, J. W., and Glover, C. J., "Binder Characterization and Evaluation, Volume 4: Test Methods" Strategic Highways Research Program, Washington, D. C., SHRP-A-370, 1994.

[86] Pfeiffer, J. P., and Saal, R. N. J., "Asphaltic Bitumen as Colloid System" *Journal of Physical Chemistry*, vol. 44, pp. 139-149, 1940.

[87] Phromsorn, C. J., and Kennedy, T. W., "Evaluation of Laboratory Methods Simulating Aging Effects of asphalt Binder" Transportation Research Record, Washington, D.C., 1488 (Materials and Construction), pp. 13-20, 1995.

[88] Ramond, G., Pastor, M., and Such, C., "Determination of Performance of a Binder from its Complex Modulus" presented at Proceedings of 5th Eurobitume Congress, Stockholm, pp. 81-85, June 1993.

[89] Roberts, F. L., Kandhal, P. S., Brown, E. R., Lee, D., and Kennedy, T. W., *Hot Mix Asphalt Materials, Mixture Design and Construction*: National Centre for Asphalt Technology (NCAT), NAPA Education Foundation, Lanham, MD, 1991.

[90] Roque, R. D., Hiltunen, R., Buttlar, W. G., and Farwanna, T., "Development of the SHRP SUPERPAVE Mixture Specification Test Method to Control Thermal Cracking Performance of Pavements" American Society for Testing and Materials, Philadelphia, PA, Symposium on Engineering Properties of Asphalt Mixtures and Relation to Performance, ASTM STP 1265, Huber, G. A., and Decker, D. S., Eds, American Society for Testing and Materials, Philadelphia, 1994.

[91] Rowe, G. M., "Performance of Asphalt Mixtures in the Trapezoidal Fatigue Test" *Proceedings of the Association of Asphalt Paving Technologists*, vol. 62, pp. 344-384, 1993.

[92] Rowlett, R. D., "Performance of Asphalt Modifiers: Classification of Modifiers and Literature Review" Centre for Construction Materials Technology, SWL, Houston, April 1990.

[93] Sayegh, G., "Determination of the Viscoelastic Properties of Bituminous Concrete by Longitudinal Vibrations" presented at Conference of the British Rheology Society, 1967.

[94] Scharpery, R. A., "Extension and Replacement of Asphalt Cement with Sulphur" Final Report to the Federal Highway Administration, Report No. FHWA-RD-78-95, Washington, D. C., pp. 115-125, 1978.

[95] Schmidt, R. J., and Santucci, L. E., "A Practical Method for Determining the Glass Transition Temperature of Asphalt and Calculation of their Low Temperature Viscosities" *Proceedings of the Association of Asphalt Paving Technologists*, vol. 38, pp. 61-90, 1966.

[96] Shashidhar, N., Needham, S. P., and Chollar, B. H., "Rheological Properties of Chemically Modified Asphalts" Transportation Research Record, Washington, D.C., 1488 (Materials and Construction), pp. 89-95, 1995.

[97] Shook, J. F., and Kallas, B. F., "Factors Influencing Dynamic Modulus of Asphalt Concrete" *Proceedings of the Association of Asphalt Paving Technologists*, vol. 38, pp. 141-177, 1969.

[98] Sousa, J. B., Harvey, J., Painter, L., Deacon, J. A., and Monismith, C. L., "Evaluation of Laboratory Procedures for Compacting Asphalt-Aggregate Mixtures" Report No. SHRP-A/UWP-91-523, Strategic Highway Research Program, National Research Council, Washington, D. C., 1991.

[99] Stastna, J., Zanzotto, L., and Ho, K., "Fractional Complex Modulus Manifested in Asphalts" *Rheol Acta*, vol. 33, pp. 344-354, 1994.

[100] Taylor, I. F., "Asphaltic Road Materials in Fatigue" Scool of Civil Engineering, University of Nottingham, Ph.D. Thesis, 1968.

[101] Tchir, W. J., and Saucier, P. C., *Society of Plastic Engineers (SPE) ANTEC Papers*, vol. 37, pp. 2321, 1991.

[102] Thompson, D. C., "Rubber Modified in Bituminous Material (Holberg, A., ed.)" *Interscience*, vol. 1, pp. 375, 1964.

[103] Usmani, A. M., "Polymer Network Formation in Asphalt Modification" *Asphalt Science and Technology*, pp. 369-383, 1997.

[104] Van Der Poel, C., "A General System Describing the Visco-Elastic Properties of Bitumens and its Relation to Routine Test Data" *Journal of Applied Chimistry*, vol. 4, pp. 221-236, 1954.

[105] Van Der Poel, C., "Time and Temperature Effects on the Deformation of Asphaltic Bitumens and Bitumen-Mineral Mixtures" *Society of Petrolium Energies*, pp. 47-53, 1955.

[106] Van Draat, W. E. F., and Sommer, P., "Ein Gerat zur Bestimmung der Dynamichen Elastizitasmoduln von Asphalt" *Strasse und Autobahn*, vol. 6, 1965.

[107] Von Quintus, H. L., and Scherocman, J. A., Hughes, C. S., and Kennedy, T. W., "Asphalt-Aggregate Mixture Analysis System" National Cooperative Highway Research Program Report 338, Transportation Research Board, National Research Council, Washington, D. C., March 1991.

[108] Walker, P. M. B., *Chambers Materials Science and Technology Dictionary*: Chambers Harrap Publishers, 1993.

[109] Weng, G. J., "Some Elastic Properties of Rainforced Solids, with Special Reference to Isotropic ones Containing Spherical Inclusions" *International Journal of Engineering Science*, vol. 22, pp. 845-856, 1984.

[110] Whiteoak, C. D., *The Shell Bitumen Handbook*. Surrey, UK: Shell Bitumen, 1990.

[111] Whitmoyer, S. L., and Kim, Y. R., "Determination of Elastic Properties of Asphalt Concrete Using Vibration Analysis" *ASTM Journal of Testing and Evaluation*, vol. 22, No. 2, pp. 139-148, 1994.

[112] Williams, M. L., Landel, R. F., and Ferry, J. D., "The Temperature-Dependence of Relaxation Mechanisms in Amorphous Polymer and other Glass-Forming Liquids" *Journal of the American Chemical Society*, vol. 77, pp. 3701-3706, 1955.

[113] Witczak, M. W., Leahy, R. B., Caves, J., and Uzan, J., "The Universal Airport Pavement Design System, Report II: Asphaltic Mixture Material Characterisation" University of Maryland, May 1989.

[114] Zakar, P., *Asphalt*. New York: Chemical Publishing Company, 1971.

[115] Zanzotto, L., Stastna, J., and Ho, K., "Characterization of Regular and Modified Bitumens via their Complex Moduli" *Journal of Applied Polymer Science*, vol. 59, pp. 1897-1905, 1996.

[116] Zielinski, J., "Factors Influencing Compounding of Constituents in Bitumen-Polymer Compositions" *Asphalt Science and Technology*, pp. 337-347, 1997.